UNIVERSIDADE FEDERAL DE SANTA MARIA
GRADUATE PROGRAM IN SOIL SCIENCE

UNIVERSITÉ DE POITIERS
ÉCOLE DOCTORALE GAY LUSSAC

FINGERPRINTING SEDIMENT SOURCES IN AGRICULTURAL CATCHMENTS IN SOUTHERN BRAZIL

DOCTORAL THESIS IN JOINT SUPERVISION

Tales Tiecher

Santa Maria, RS, Brasil

2015

FINGERPRINTING SEDIMENT SOURCES IN AGRICULTURAL CATCHMENTS IN SOUTHERN BRAZIL

Tales Tiecher

Thesis submitted to the Doctoral Program of the Graduate Program in Soil Science, Concentration Area in Chemical Processes and Elements Cycling, at the Federal University of Santa Maria, Brazil, as a partial requirement for the degree of **Doctor in Soil Science**, and to the Doctoral School in Science for Environment Gay Lussac, at University of Poitiers, France, as a partial requirement for the degree of **Doctor in Sciences of the Earth and the Universe, Space**, research area in Solid Earth and Superficial Envelopes.

Advisor at UFSM: Prof. Dr. Danilo Rheinheimer dos Santos
Advisor at University of Poitiers: Prof. Dr. Laurent Caner

Santa Maria, RS, Brazil

2015

Ficha catalográfica elaborada através do Programa de Geração Automática
da Biblioteca Central da UFSM, com os dados fornecidos pelo(a) autor(a).

Tiecher, Tales
Fingerprinting sediment sources in agricultural catchments in Southern Brazil / Tales Tiecher.-2015.
307 p.; 30cm

Orientador: Danilo dos Santos Rheinheimer
Coorientadores: Laurent Caner, Jean Paolo Gomes Minella
Tese (doutorado) - Universidade Federal de Santa Maria, Centro de Ciências Rurais, Programa de Pós-Graduação em Ciência do Solo, RS, 2015

1. soil erosion 2. source of diffuse pollution 3. tracers 4. spectroscopy 5. fingerprinting I. Rheinheimer, Danilo dos Santos II. Caner, Laurent III. Minella, Jean Paolo Gomes IV. Título.

Address: Universidade Federal de Santa Maria/Centro de Ciências Rurais/Departamento de Solos/Roraima Avenue, n. 1000, Cidade Universitária, Camobi, Santa Maria, RS, 97105-900
Phone/Fax +55 (055) 3220-8108; E-mail: tales.t@hotmail.com

Universidade Federal de Santa Maria
Graduate Program in Soil Science

Université de Poitiers
École Doctorale Gay Lussac

The Examining Committee, undersigned,
approved the Doctoral Thesis

FINGERPRINTING SEDIMENT SOURCES IN AGRICULTURAL CATCHMENTS IN SOUTHERN BRAZIL

elaborated by
Tales Tiecher

as a partial requirement for the degree of
Doctor in Soil Science by the Federal University of Santa Maria and **Doctor in Sciences of the Earth and the Universe, Space,** research area in Solid Earth and Superficial Envelopes, by the University of Poitiers

EXAMINING COMMITTEE:

Dr. Danilo Rheinheimer dos Santos
Universidade Federal de Santa Maria, Brazil (President/Advisor/Examiner)

Dr. Laurent Caner
Université de Poitiers, France (Advisor/Examiner)

Dr. Jean Paolo Gomes Minella
Universidade Federal de Santa Maria, Brazil (Examiner)

Dr. Olivier Evrard
Commissariat à l'Energie Atomique et aux Energies Alternatives, France (Examiner/Rapporteur)

Dr. Jérôme Labanowski
Université de Poitiers, France (Examiner)

Dr. Gustavo Henrique Merten
University of Minnesota Duluth, USA (Examiner/Rapporteur)

Santa Maria, March 5, 2015.

Dedico aos meus pais Ernani e Singlair, pelo amor e carinho,
À minha irmã Talise, por ser meu exemplo de dedicação aos estudos desde criança,
Ao meu irmão Tadeu, pelo companheirismo nessa longa jornada acadêmica...

...e à Silvana Ceolin, por tudo!

ACKNOWLEDGEMENT
AGRADECIMENTOS
REMERCIEMENTS

À Universidade Federal de Santa Maria pelos 10 anos de ensino público, gratuito e de extrema qualidade.

Ao Programa de Pós-Graduação em Ciência do Solo pela formação científica durante meu curso de doutorado.

À l'Université de Poitiers, à l'École Doctorale Gay Lussac, et à l'équipe HydrASA, pour la formation scientifique.

À Coordenação de Aperfeiçoamento de Pessoal de Nível Superior pela concessão da bolsa de doutorado no Brasil, e ao programa CAPES/COFECUB pela concessão da bolsa de doutorado na França.

Ao mestre e amigo Danilo Rheinheimer dos Santos pela orientação desde a iniciação científica em 2005, pela formação política, pelos conselhos e pelo exemplo de dedicação à pesquisa.

À Laurent CANER pour la confiance, les conseils, pour les voyages et la bonne humeur habituelle pendant ma thèse, aussi bien qu'à Sandrine, Julien, Clémence et Roman, ma famille en France, pour me faire sentir comme chez-moi, même de l'autre côté de l'Atlantique.

Ao professor Jean Paolo Gomes Minella pelo incentivo e amparo intelectual na aplicação e desenvolvimento da abordagem *fingerprinting* nas bacias estudadas.

À professora Maria Alice Santanna e ao professor Carlos Alberto Ceretta pela ajuda nos trâmites da documentação do acordo de co-tutela de tese.

Ao Edson Campanhola Bortoluzzi pelas conversas e ensinamentos durante o período de convivência no laboratório HydrASA.

Ao professor João Kaminski pela amizade e pelos sábios ensinamentos.

Ao Marcos Antonio Bender e Lucas Henrique Ciotti pela ajuda indispensável na coleta, processamento e análise das amostras de solo e sedimento.

To my friend Mohsin Zafar by his hard work in sampling sediment samples at Guapore catchment while I have been outside of Brazil.

Aos bolsistas de iniciação científica do Laboratório de Química e Fertilidade dos Solos, em especial à Daniela Herzog e Mayara Fornari.

À Melissa Berguemaier (*in memoriam*) e ao Matheus Librelotto (*in memoriam*), que trabalharam incansavelmente no processamento das amostras de solo e sedimento, mas que infelizmente nos deixaram muito cedo.

À Viviane Capoane pela ajuda na confecção de todos os mapas.

Ao André Pellegrini, Jimmy Rasche e Gilmar Luiz Schaefer, pela ajuda na coleta das amostras de solo e sedimento nas bacias hidrográficas de Júlio de Castilhos.

Ao Elizeu Didoné pela companhia e ajuda durante os longos dias de coleta de solo na bacia hidrográfica do Conceição.

Ao Leandro Dalbianco, Rafael Ramon e Cláudia Alessandra Peixoto de Barros pela ajuda na coleta de solo e instalação dos coletores na bacia hidrográfica do Guaporé.

Ao Clamarion Maier por ceder as amostras de solo e de sedimento da bacia hidrográfica de Arvorezinha.

Aos colegas de Pós-Graduação em Ciência do Solo, pela amizade e convívio, especialmente ao Leandro Bittencourt de Oliveira, Fábio Joel Kochem Mallmann, Cledimar Rogério Lourenzi, Rogério Piccin, Carlos Alberto Casali, Paulo Ademar Avelar Ferreira Renan Gonzatto, Elci Gubiani, Marília Camotti Bastos, José Augusto Monteiro de Castro Lima e Márcia Luciane Kochem.

Ao Alexandre Troian e Alex Giuliani pela amizade, disposição e presteza de sempre.

À Marie-France HUBERT, pour l'accueil, les balades et les repas.

À Alain MEUNIER et Paul SARDINI pour l'amitié et pour la bonne humeur habituelle, surtout au cours de petites pauses café.

À Lucile BRUNAUD, que malgré avoir râlé tout le temps, m'a beaucoup aidé dans l'analyse d'infrarouge et diffraction des rayons X.

À Leslie MONDAMERT, Jérôme LABANOWSKI et Elodie LAURENT pour m'avoir reçu dans l'Equipe Eaux, Géochimie, Santé, et avoir permis la réalisation d'analyses de pyrolyse de carbone.

À Nadia GUIGNARD, Pierre CHANSIGAUD, Claude FONTAINE et Nathalie DAUGER pour l'aide au laboratoire et avec les équipements.

A mi gran amigo hermano Mauricio León Velásquez Márquez por el buen humor y la alegría contagiosa.

À mes chers amis de l'Université de Poitiers, Valentin ROBIN, Jean-Christophe VIENNET, Fabien BARON, Thomas RIEGLER, Genia SOLDATENKO, Liva DZENE, Sahar SEIFI, Héloïse VERRON, Vanessa BERTOLAZI, Benoît MERCKX, Sophie Van MEYEL, Thomas ICHON, Anthony RODRIGUES, Ahmed ELKHIAL, Axel ANGILERI, Marie

COLLARD, Alice TAWK, Florien LAPALUS, Benoît HEBERT, Sophie BILLON, pour la très agréable compagnie pendant les innombrables déjeuners au RU, dîners et cafés.

As agricultores Raul Santo, Celso Zardin, João da Silva Almeida, Nei Musselin, Roberto Grisa, Zeferino e Isabel Tomazi, Claudir Santin Zanchin, Fiorindo Dassi, Gilberto Somavilla, Deise Roy e família, pela presteza e pelo zelo dos amostradores de sedimentos.

Enfim, a todos que estiveram presentes direta ou indiretamente nesta etapa da minha vida e que contribuíram para a realização deste trabalho.

“Porque eu não quero deixar pro meu filho
a pampa pobre que herdei de meu pai”

Humberto Gessinger

RESUMO

Tese de Doutorado em Co-tutela
Programa de Pós-Graduação em Ciência do Solo – Universidade Federal de Santa Maria, Brasil
Escola Doutoral Ciência pelo Ambiente Gay Lussac – Universidade de Poitiers, França

IDENTIFICAÇÃO DE FONTES DE SEDIMENTO EM BACIAS HIDROGRÁFICAS RURAIS DO SUL DO BRASIL

AUTOR: TALES TIECHER
ORIENTADOR NA UFSM: DANILO RHEINHEIMER DOS SANTOS
ORIENTADOR NA UNIVERSIDADE DE POITIERS: LAURENT CANER
Data e Local da Defesa: Santa Maria, 05 de março de 2015.

O conhecimento das principais fontes difusas de sedimentos pode aumentar a eficiência de utilização dos recursos investidos em estratégias de gestão que visem mitigar a transferência de sedimentos aos cursos d'água. Métodos convencionais baseados na composição geoquímica ainda tem alto custo, são onerosos e demandam preparação preliminar crítica das amostras. Dessa forma, métodos espectroscópicos podem ser uma alternativa menos trabalhosa, mais rápida e viável para esse propósito. Objetivou-se com o presente trabalho avaliar a contribuição das fontes de sedimentos em bacias hidrográficas agrícolas do estado do Rio Grande do Sul, e avaliar o potencial uso da espectroscopia como uma alternativa para traçar a origem dos sedimentos. As áreas de estudo são representativas dos principais impactos da agricultura nos recursos hídricos no estado. A área total das bacias hidrográficas de Arvorezinha, Júlio de Castilhos 1, Júlio de Castilhos 2, Conceição e Guaporé é de 1,19, 0,80, 1,43, 804,3 e 2.031 km^2, respectivamente. As fontes de sedimento avaliadas foram lavouras, pastagens, estradas e canais da rede de drenagem. A estratégia de amostragem de sedimentos incluiu coleta com amostradores do tipo integrador no tempo, sedimento de fundo e sedimento coletado durante eventos pluviométricos. A concentração de vários traçadores geoquímicos foram estimados nas amostras de sedimento e das fontes. Análises espectroscópicas foram realizadas na região do ultravioleta-visível, infravermelho próximo e infravermelho médio na bacia hidrográfica de Arvorezinha. A contribuição das fontes estimadas pelos métodos espectroscópicos foram similares às obtidas com traçadores geoquímicos. Além disso, a combinação de parâmetros de cor derivados da faixa espectral do visível pode ser uma alternativa rápida e de baixo custo para melhorar a discriminação das fontes e aumentar a precisão das predições. Os resultados demonstram que outros fatores além da proporção do uso do solo são importantes na produção do sedimento, como a distribuição das lavouras, florestas e estradas na paisagem. As florestas ripárias exercem um fator chave na erosão dos canais de drenagem. As estradas parecem ser fortemente dependentes da escala e do número de pontos em que cruzam os canais de drenagem. As lavouras, mesmo cultivadas sob plantio direto, ainda são as principais fontes de sedimentos nas bacias hidrográficas rurais do sul do Brasil. A produção específica de sedimentos das áreas de lavoura variou de 0.06 a 3.95 ton ha^{-1} de lavoura ano^{-1}. Essa variação é devida em parte às condições naturais intrínsecas de relevo e fortemente influenciada pelo uso e manejo do solo. A quantidade de sedimento erodida das lavouras ainda são muito elevadas para áreas de baixa susceptibilidade à erosão manejadas sob plantio direto, como na bacia hidrográfica do Conceição (1.30 ton ha^{-1} de lavoura ano^{-1}), indicando que maiores esforços ainda são necessários para reduzir a erosão do solo. Existe uma necessidade urgente de planejar a utilização e ocupação da terra nessas bacias, uma vez que os sistemas de manejo do solo utilizados pelos agricultores são ineficientes para reduzir a erosão nas lavouras no sul do Brasil.
Palavras-chave: erosão do solo, fontes de poluição difusa, traçadores, espectroscopia, *fingerprinting*.

RÉSUMÉ

Thèse de Doctorat en Cotutelle
Programme de Graduation en Science du Sol - Université Fédérale de Santa Maria, Brésil
École Doctorale Science pour l'Environnement Gay Lussac - Université de Poitiers, France

TRAÇAGE DES SOURCES DE SÉDIMENTS DANS DES BASSINS VERSANTS AGRICOLES DU SUD DU BRÉSIL

AUTEUR : TALES TIECHER
DIRECTEUR THESE A L'UFSM : DANILO RHEINHEIMER DOS SANTOS
DIRECTEUR THESE A L'UNIVERSITE DE POITIERS : LAURENT CANER
Lieu et Date de la Soutenance : Santa Maria, le 5 Mars 2015.

La connaissance des principales sources diffuses de sédiments permettrait d'améliorer l'utilisation des ressources publiques investies dans les stratégies de gestion des sols. Les méthodes de traçage (*fingerprinting*) conventionnelles basées sur la composition géochimique sont laborieuses et nécessitent une préparation importante des échantillons. Cette étude visait à rechercher les sources de sédiments dans des bassins versants agricoles du Rio Grande do Sul (sud du Brésil) et évaluer l'utilisation des outils spectroscopiques comme technique alternative. La superficie des bassins versants étudiés est comprise entre 0,80 et 2027 km^2. Les sources de sédiments correspondent aux terres cultivées, aux prairies, aux chemins agricoles et aux berges des cours d'eau. L'échantillonnage des sédiments est basé sur des préleveurs automatiques pendant un suivi temporel, des prélèvements de sédiments fins du lit de la rivière, et lors d'événements de pluvieux. La concentration totale des traceurs géochimiques a été mesurée dans les échantillons de sédiments et de sols. Les mesures spectrales ont été faites dans les gammes ultraviolet-visible, infrarouge proche et infrarouge moyen pour le bassin versant d'Arvorezinha. Les deux méthodes, classiques et spectroscopiques, permettent de discriminer et de fournir la contribution des sources de sédiments. L'information spectrale peut être aussi précise que les traceurs géochimiques. En outre, la combinaison de paramètres de couleur dérivés du spectre dans le visible avec les traceurs géochimiques était une façon rapide et peu coûteuse pour améliorer la discrimination entre les sources et la précision des prédictions. La contribution des sources de sédiments démontrent que d'autres facteurs que les proportions de l'utilisation des terres, comme la distribution de terres agricoles, les forêts et les chemins agricoles dans le paysage, jouent un rôle important dans la production de sédiments. Forêt riparienne semble être un facteur clé de l'érosion des berges des cours d'eau. L'érosion due aux chemins agricoles semble être fortement liée échelle d'observation et dépend du nombre de points où les routes traversent le réseau hydrographique. Les terres cultivées, même lorsque cultivées sans labour (semis direct), sont encore la principale source de sédiments dans les bassins versants agricoles dans le sud du Brésil. La quantité de sédiments produite par les terres cultivées et par unité de surface qui atteint efficacement le réseau de drainage variait de 0,06 à 3,95 tonnes ha^{-1} an^{-1}. Ces variations sont partiellement liées au relief et à la pente, mais elles sont essentiellement influencées par l'utilisation des terres et la gestion des sols. La quantité de sédiments provenant des terres cultivées est encore trop élevée pour des zones de faible érosivité et cultivées sans labour du sol, comme le bassin versant de Conceição (1,30 tonnes ha^{-1} an^{-1}). Ceci indique que des efforts supplémentaires sont encore nécessaires pour réduire l'érosion du sol. Par conséquent, il est urgent de mieux planifier l'utilisation et l'occupation des terres dans ces bassins versants, dans la mesure où les systèmes de gestion des sols utilisés par les agriculteurs sont encore inefficaces pour réduire le ruissellement et l'érosion dans les zones cultivées dans le sud du Brésil.
Mots-clés : érosion des sols, source de pollution diffuse, traceurs, spectroscopie, *fingerprinting*.

ABSTRACT

Doctoral Thesis in Joint Supervision
Graduation Program in Soil Science – Federal University of Santa Maria, Brazil
Doctoral School in Science for Environment Gay Lussac – University of Poitiers, France

FINGERPRINTING SEDIMENT SOURCES IN AGRICULTURAL CATCHMENTS IN SOUTHERN BRAZIL

AUTHOR: TALES TIECHER
ADVISOR AT UFSM: DANILO RHEINHEIMER DOS SANTOS
ADVISOR AT UNIVERSITY OF POITIERS: LAURENT CANER
Place and Date of the Defense: Santa Maria, March 5, 2015.

Knowledge of the main diffuse sources of sediment can enhance efficiency in the use of public resources invested in soil conservation management strategies. Conventional fingerprinting methods based on geochemical composition are time-consuming and require critical preliminary sample preparation. In this context, spectroscopic methods can be less labor-intensive, cheap, and viable alternative for this purpose. The present study aimed to quantify the sediment sources supplied to rivers in agricultural catchments of Rio Grande do Sul State, Brazil, and to evaluate the potential use of spectroscopy measurements as a low cost and easy alternative to fingerprint sediment sources. Five study areas with increased size (Arvorezinha, Júlio de Castilhos 1, Júlio de Castilhos 2, Conceição, and Guaporé, with areas of 1.19, 0.80, 1.43, 804.3, and 2,027.2 km^2, respectively) were evaluated. Sediment sources evaluated were crop fields, grasslands, unpaved roads, and stream channels. Sediment sampling strategies included time-integrated samplers, fine-bed sediments, and storm-event sediments. The total concentrations of several geochemical tracers were measured in both sediment and source samples. Spectral measurements were made for ultraviolet-visible, near-infrared, and mid-infrared ranges only for the Arvorezinha catchment. Source ascriptions obtained by alternative methods based on spectroscopy analysis were in agreement with ascriptions from classical fingerprinting method based on geochemical composition. Spectral information can provide as relevant information as the geochemical tracers. Furthermore, combining visible-based-colour with geochemical tracers was a rapid and cheap way to enhance discrimination between source types and to improve the precision of sediment sources apportionment. Results of sediment source apportionment demonstrate that other factors than proportion of land use, such as distribution of croplands, forests, and unpaved roads across the landscape play an important role in sediment production. Riparian forests seems to be a key factor to control stream channel erosion. The sediment yielded from unpaved roads seems to be strongly scale-related and it depends on the number of intersections between roads the stream network. Crop fields, even when cultivated with no-tillage, are still the main source of sediment to rivers in agricultural catchments in Southern Brazil. The amount of cropland specific sediment yield ranged from 0.06 to 3.95 ton ha^{-1} yr^{-1}. These variations are partly attributed to the relief and slope, but land use and soil management are also important control factors. The cropland specific sediment yield remains too high for areas with low sensitivity to erosion where no-tillage is applied, as in Conceição catchment (1.30 ton ha^{-1} of cropland yr^{-1}), indicating that additional efforts are necessary to further reduce soil erosion. Therefore, there is an urgent need to better plan land use and cover in these catchments, inasmuch as the soil management systems used by farmers proved to be inefficient to reduce runoff and erosion in cultivated areas of Southern Brazil.

Keywords: soil erosion, source of diffuse pollution, tracers, spectroscopy, fingerprinting.

RESUMO LONGO

1 Introdução e justificativa

A degradação dos recursos naturais causados pela produção de alimentos tem se intensificado nas recentes décadas. Cerca da metade da superfície terrestre livre de gelo tem sido convertida ou substancialmente modificada pelas atividades humanas nos últimos 10.000 anos (LAMBIN; GEIST; LEPERS, 2003). As práticas agrícolas modernas e intensivas expõem o solo à erosão e aceleram a transferência de sedimentos para as partes baixas da paisagem (MINELLA; WALLING; MERTEN, 2014) e aos corpos de água, juntamente com vários contaminantes como pesticidas (MAGNUSSON et al., 2013; YAHIA; ELSHARKAWY, 2014) e fósforo (DODD; MCDOWELL; CONDRON, 2014; GUO et al., 2014). Isto é particularmente preocupante, pois os seres humanos obtém mais de 99,7% de seus alimentos (calorias) a partir da terra e menos de 0,3% dos oceanos e outros ecossistemas aquáticos (PIMENTEL, 2006), ainda mais tendo em vista que o crescimento contínuo da população e do consumo significa que a demanda mundial por alimentos vai aumentar por pelo menos mais 40 anos (GODFRAY et al., 2010).

Em bacias hidrográficas agrícolas com alta produção de sedimentos e alto coeficiente de escoamento, como no sul do Brasil, o processo de erosão precisa ser controlada para evitar a degradação irreversível dos solos e da qualidade da água. Embora reconhecendo que o conhecimento das principais fontes difusas de produção de sedimentos pode melhorar a eficiência no uso dos recursos públicos investidos em estratégias de gestão que visam mitigar a transferência de sedimentos para cursos de água em bacias hidrográficas, somente alguns estudos tem sido desenvolvidos para identificar as fontes de sedimentos no sul do Brasil. Os estudos anteriores de contribuição das fontes de sedimentos em bacias brasileiras são promissores e indicam que a essa abordagem é uma ferramenta adequada para estudar fontes de sedimentos em nossas condições ambientais (bacia hidrográfica do Vacacaí Mirim, RS, 20 km^2 - MIGUEL et al., 2014a, 2014b; bacia hidrográfica de Arvorezinha, RS, 1,19 km^2 - MINELLA; MERTEN; CLARKE, 2009; MINELLA; WALLING; MERTEN, 2008; MINELLA et al., 2009; bacia hidrográfica de Agudo, RS, 1,68 km^2 - MINELLA et al., 2007; bacia hidrográfica de Júlio de Castilhos, RS, 0,8 km^2 - TIECHER et al., 2014). Embora muitos desses estudos indicam que as áreas de lavoura são uma das principais fontes de sedimentos, e

que as estradas têm contribuição não negligenciável, a magnitude dos valores obtidos para as bacias hidrográficas menores pode não necessariamente ser extrapolados para bacias maiores. Além disso, outras fontes potenciais além das lavouras, estradas e canais de drenagem, devem ser investigadas, tais como as áreas de pastagem.

Estudos adicionais de identificação de fontes de sedimentos devem incorporar a conectividade hidrogeomorfológica da bacia hidrográfica, para entender como e quão eficiente ocorre o transporte de sedimentos em toda a bacia hidrográfica, desde as cabeceiras até o exutório da bacia hidrográfica (KOITER et al., 2013b). Não obstante, há uma necessidade de gerar resultados com alta resolução espacial e temporal da contribuição das fontes de sedimento, especialmente durante os eventos de chuva-vazão ao longo de todo o ano hidrológico, a fim de melhorar a compreensão dos processos erosivos no sul do Brasil. Além disso, ainda há a necessidade de gerar resultados convincentes para promover a conscientização dos agricultores sobre o impacto das atividades agrícolas sobre os recursos hídricos, quando as práticas de conservação do solo são parcialmente ou utilizados incorretamente.

O uso da abordagem fingerprinting convencional baseado em traçadores geoquímicos para identificar fontes de sedimentos como ferramenta de gestão no sul do Brasil é dificultado porque são metodologias demoradas, caras, destrutivas e exigem grandes quantidades de amostra. Além disso, o acesso aos equipamentos utilizados para essas análises (ICP-OES, ICP-MES, espectrômetros γ) também é um obstáculo para o desenvolvimento desta abordagem no Brasil, assim como em outros países subtropicais. Portanto, é importante e necessário (i) desenvolver diretrizes para pré-selecionar traçadores relevantes e conservativos e (ii) desenvolver e validar métodos facilmente aplicáveis a um grande número de amostras que envolvam preparação mínima e que sejam da mesma forma eficazes para discriminar as fontes potenciais de sedimento.

1.1 Contexto

A presente tese é o resultado de dois projetos de pesquisa que permitiram desenvolver os trabalhos de campo e de laboratório necessários para a execução do presente estudo. O primeiro projeto "*Água e poluentes, das lavouras às cidades: avaliação e tecnologias melhoradas de manejo em rede de bacias hidrográfica - Edital FAPERGS nº 008/2009, Processo nº 10/0034-0*) foi financiado pelo Programa de Apoio a Núcleos de Excelência –

PRONEX da Fundação de Amparo à Pesquisa do Estado do Rio Grande do Sul – FAPERGS. O projeto foi coordenado e executado pelos professores da UFSM Dr. Danilo Rheinheimer dos Santos, Dr. Jean Paolo Gomes Minella e Dr. José Miguel Reichert, de maio de 2010 à maio de 2014. Este projeto possibilitou realizar o monitoramento hidrossedimentológico das bacias estudadas e as análises geoquímicas das amostras de solo e sedimento no Laboratório de Química e Fertilidade de Solos da UFSM.

O segundo é um projeto internacional financiado pelo programa CAPES/COFECUB. COFECUB é a sigla em francês para o Comitê Francês de Avaliação das Cooperações Acadêmicas e Científicas com o Brasil (*Comité Français d'Evaluation de la Coopération Universitaire avec le Brésil*). O projeto "*Evolução mineralógica dos solos do sul do Brasil: caracterização dos processos de alteração e de impacto antrópico"* começou em Janeiro de 2012 sob coordenação do Professor Dr. Danilo Rheinheimer dos Santos (UFSM) no Brasil, e do Professor Dr. Laurent Caner (Universidade de Poitiers) na França. Esse projeto de cooperação foi baseado em características que são comuns entre as instituições envolvidas: histórico de colaboração e perspectivas de aplicação semelhantes, em termos de formação e transferência dos resultados da pesquisa. Esse projeto envolve três universidades brasileiras (UFSM, UPF e UFRGS) e dois grupos de pesquisa da Universidade de Poitiers, da França: a equipe *HydrASA* (acrônimo Francês para Hidrogeologia, Argilas, Solos e Alterações), e a equipe *Eaux Géochimie Santé* (Água, Geoquímica, Saúde), ambos pertencentes ao *Institut de Chimie des Milieux et Matériaux de Poitiers - IC2MP* (Instituto de Química de Meios e Materiais de Poitiers).

Com o projeto CAPES/COFECUB foi possível fazer a tese no regime de co-tutela entre a UFSM, no Brasil (de março de 2011 a março de 2013, e de setembro de 2014 a fevereiro de 2015), e a Universidade de Poitiers, na França (de abril de 2013 a agosto de 2014). Além disso, a cooperação com a Universidade de Poitiers tornou possível avançar no desenvolvimento e validação de métodos alternativos para identificar as fontes de sedimentos usando análises espectroscópicas, bem como a realização de outras análises como difração de raios-X e a pirólise de carbono com cromatografia gasosa acoplada à espectrometria de massa, que serviram para compreender as propriedades físicas e químicas que permitem a utilização de métodos espectroscópicos para identificar a fonte de sedimentos.

1.2 Hipótese

As áreas de lavoura, mesmo cultivadas sob plantio direto, ainda são a principal fonte de sedimentos em bacias hidrográficas agrícolas do sul do Brasil, e a condição atual dos sistemas de conservação, bem como o impacto das atividades agrícolas sobre os recursos hídricos quando as práticas de conservação do solo são parcialmente ou incorretamente utilizados, pode ser avaliado utilizando a abordagem *fingerprinting* para identificação das fontes de sedimentos.

1.3 Objetivos

O objetivo geral deste trabalho é gerar informações que possam contribuir para a recomendação de práticas de conservação do solo para a redução dos problemas ambientais associados ao escoamento superficial e erosão em bacias hidrográficas que incluem alguns dos principais problemas relacionados ao impacto da agricultura sobre os recursos hídricos no sul do Brasil. Os objetivos específicos foram:

(i) Gerar recomendação ou orientações para pré-seleção de traçadores no sul do Brasil.

(ii) Validar métodos espectroscópicos alternativos para identificação de fontes de sedimentos, comparando os resultados com uma abordagem mais clássica, baseada em traçadores geoquímicos, e melhorar a erros de discriminação de origem e de previsão através da combinação de parâmetros de cor com traçadores geoquímicos em um único linear misto modelo.

(iii) Melhorar a compreensão do processo de erosão no sul do Brasil por meio da geração de informações de contribuição de fontes de sedimentos em alta resolução temporal e espacial, especialmente durante eventos chuva-vazão ao longo do ano hidrológico.

(iv) Estimar a mobilização de sedimentos das áreas de lavoura, a fim de gerar resultados convincentes para promover a conscientização dos agricultores sobre o impacto das atividades agrícolas nos recursos hídricos, quando as práticas de conservação do solo são parcialmente ou incorretamente utilizadas.

2 Material e métodos

O presente estudo foi realizado no Estado do Rio Grande do Sul. A escolha das bacias hidrográficas de estudo foi guiada pela necessidade de caracterizar a magnitude de processos erosivos e hidrológicos em condições distintas de uso da terra, que fossem representativas do solo e da paisagem da região. Três pequenas (0,802–1,426 km^2) e duas grandes (804,3–2.031,9 km^2) bacias hidrográficas foram escolhidas de forma a gerar resultados que refletem condições e processos regionais mais amplos, ao invés de condições e processos específicos. As bacias hidrográficas selecionadas são representativos das condições mais importantes do impacto da agricultura sobre os recursos hídricos no Estado do Rio Grande do Sul. As bacias de Júlio de Castilhos estão localizadas sob solos arenosos onde a integração lavoura-pecuária sob plantio direto é o principal sistema de produção. A bacia do Conceição apresenta atividade agrícola intensiva, com a produção de grãos (principalmente soja, milho e cereais de inverno), sob plantio direto em solos profundos e argilosos ricos em óxidos de ferro. A bacia do Guaporé tem características fisiográficas que determinam fragilidade ambiental quando o solo é utilizado para agricultura sem levar em conta práticas conservacionistas. A bacia de Arvorezinha é uma bacia hidrográfica de cabeceira do terço inferior da bacia do Guaporé, onde a cultura principal é o tabaco cultivado por agricultores familiares em áreas declivosas em solos rasos frequentemente arados. Em comum, as cinco bacias hidrográficas apresentam elevada produção de sedimentos e desequilíbrio ambiental.

As fontes de sedimentos avaliadas foram as áreas de lavoura, pastagens, estradas não pavimentadas e as margens dos rios e riachos. A amostragem de sedimentos foi baseada em amostradores de modo contínuo de sedimentos em suspensão, as amostras de sedimento fino do leito do rio, e amostras de sedimento em suspensão coletados durante os eventos pluviométricos. Todas as amostras de solo e de sedimentos foram secas em estufa a 50ºC e levemente desagregados usando gral de ágata. Todas as amostras de solo e de sedimentos das cinco bacias hidrográficas foram analisados para um gama de traçadores geoquímicos. O

carbono orgânico total foi estimado pela oxidação úmida com $K_2Cr_2O_7$ e H_2SO_4. A concentração total de vários elementos (Ag, A, B, Ba, Be, Ca, Cd, Co, Cr, Cu, Fe, K, La, Li, Mg, Mn, Mo, Na, Ni, P, Pb, Sb, Se, Sr, Ti, Tl, V e Zn) foi estimada por ICP-OES após digestão assistida por micro-ondas por 9,5 min a 182°C com HCl e HNO_3 concentrado na proporção de 3:1 (água régia).

A granulometria das amostras de sedimento e solo foi analisada somente para as amostras da bacia de Arvorezinha após a oxidação da matéria orgânica com H_2O_2 e dispersão com NaOH, em um granulômetro à laser. A área superficial específica foi calculada a partir da distribuição de tamanho de partícula, considerando que as partículas são esféricas e cilíndricas. Outras análises adicionais nas amostras da bacia de Arvorezinha também foram realizadas para avaliar o potencial de utilização das análises espectroscópicas para identificar as fontes de sedimentos.

Os espectros de refletância difusa ótica na faixa do ultravioleta-visível (UV-VIS) das amostras foram obtidos à temperatura ambiente na faixa de 200–800 nm, a cada 1 nm, utilizando um espectrofotômetro Cary 5000 UV-VIS-NIR (Varian, Palo Alto, CA, USA). As amostras foram postas em um acessório de refletância difusa Mantis Harrick Rezar que usa espelhos elípticos. $BaSO_4$ foi usado como um padrão de 100% de reflexão. Vinte e quatro (24) parâmetros de cor foram derivados a partir do espectro do VIS utilizando vários modelos de colorimétricos descritos em detalhe por Viscarra Rossel et al. (2006). Os espectros de infravermelho próximo (NIR) foram registrados da faixa de 10000–4000 cm^{-1} utilizando um espectrômetro FTIR Nicolet 26700 (Waltham, Massachusetts, EUA) no modo de refletância difusa com uma esfera de integração e um detector InGaAs interoa com uma resolução de 2 cm^{-1} e 100 leituras por espectro. Os espectros de infravermelho médio (MIR) foram obtidos na faixa de 400–4000 cm^{-1} utilizando um espectrômetro Nicolet 510-FTIR (Thermo Electron Scientific, Madison, WI, EUA) no modo de reflexão com uma resolução de 2 cm^{-1} e 100 leituras por espectro. Os espectrômetros de infravermelho eram constantemente varridos com uma corrente de ar para eliminar o CO_2 afim de não perturbar as medições.

A fim de dar suporte à interpretação das análises espectroscópicas, algumas análise complementares foram realizadas em amostras compostas de cada fonte de sedimento que foram formadas por mistura de todas as amostras individuais de cada fonte em laboratório (e.g. mistura das 10 amostras das estradas para compor uma amostra composta, 10 amostras dos canais, e 20 das lavouras). Nessas três amostras compostas foram realizadas a pirólise de carbono com cromatografia gasosa acoplada à espectrometria de massa (Py-GC/MS) e a

difração de raios-X (XRD) para identificar os principais compostos orgânicos e minerais, respectivamente.

O procedimento estatístico utilizado para estimar a contribuição das fontes de sedimento utilizando o método clássico baseado nos traçadores geoquímicos e o método alternativo baseado nas análises espectroscópicas foi bem diferente. Resumidamente, as etapas utilizadas no método convencional, foram: *i*) seleção dos traçadores com base no teste de Kruskal-Wallis *H*, *ii*) seleção do melhor conjunto de traçadores utilizando análise discriminante e, finalmente, *iii*) a utilização de um modelo linear misto para calcular a contribuição das fontes de sedimentos. Os passos utilizados no método alternativo foram *i*) análise de componente principal para reduzir o número de variáveis, *ii*) análise discriminante para determinar o potencial traçador das análises espectroscópicas e, finalmente, *iii*) o uso da regressão do método dos mínimos quadrados (*Partial Least Squares Regression* – PLSR) com base em misturas das fontes de sedimentos em várias proporções para calcular a contribuição fontes de sedimentos.

3 Principais resultados

3.1 Diretrizes para pré-seleção de traçadores geoquímicos no sul do Brasil

Em relação à recomendação e orientações para pré-seleção de traçadores no sul do Brasil, verificou-se que um total de 18 diferentes traçadores geoquímicos foram selecionados pelo menos em uma bacia hidrográfica para estimar a contribuição das fontes de sedimentos no modelo linear misto (Ag, Al, As, Ba, Be, Co, Cr, Cu, Fe, La, Li, Mn, Mo, Ni, P, Ti, V e Zn). Os resultados sugerem que os metais de transição são os traçadores geoquímicos mais adequados para serem utilizados em bacias hidrográficas agrícolas do sul do Brasil, devido a sua conservatividade e potencial discriminante. Apesar do potencial de discriminar fontes de sedimentos em alguns casos, os metais alcalinos e metais alcalino-terrosos tendem a ser menos conservativos durante o processo de erosão e devem ser evitados.

Com exceção do carbono orgânico total e fósforo não houve consistência óbvia na relação de outros traçadores geoquímicos com as fontes de sedimentos. O fósforo foi consistentemente maior nas áreas de lavoura, enquanto o carbono orgânico total foi igualmente superior para as fontes superficiais, como as pastagens e lavouras. Isso destaca que a seleção

do traçador é altamente específica do local. Não obstante, deve-se tomar cuidado para avaliar a conservatividade do P e carbono orgânico total para cada bacia hidrográfica antes de sua utilização como traçador.

Nenhum traçador geoquímico foi capaz de classificar 100% das amostras nas respectivas fontes de origem em qualquer uma das bacias estudadas. Isso demonstra que é necessário um conjunto de propriedades traçadoras para discriminar várias fontes difusas de sedimentos a fim de fornecer estimativas confiáveis sobre a contribuição relativa dessas fontes em bacias hidrográficas agrícolas. Diferentes traçadores geoquímicos podem explicar diferentes processos erosivos. Dessa forma, o uso de vários traçadores geoquímicos podem reduzir as incertezas e aumentar a robustez dos modelos, bem como a confiabilidade dos resultados. Em geral, quanto menor bacia hidrográfica e quanto menor for o número de fontes estudadas, mais eficazes foram os traçadores em discriminar as fontes de sedimentos. A discriminação satisfatória das pastagens só foi possível nas pequenas bacias de Júlio de Castilhos. Nas bacias de Guaporé e Conceição não foi possível discriminar satisfatoriamente as áreas de pastagens das áreas de lavoura devido à sua composição geoquímica similar, bem como devido à alta variabilidade nos tipos de solo e litologia nessas bacias, o que dificultou a seleção de traçadores para tal. Uma possível explicação para isso pode ser a baixa densidade amostras nas bacias hidrográficas do Guaporé e Conceição (0.15 e 0.23 amostras por km^{-2}, respectivamente) comparado com as bacias hidrográficas de Júlio de Castilhos (variando de 21 a 37 amostras km^{-2}).

3.2 O potencial de uso de métodos alternativos baseados na espectroscopia

Os métodos alternativos baseados na espectroscopia na faixa do UV-VIS, NIR e MIR, foram validados para estimar as fontes de sedimentos na bacia hidrográfica de Arvorezinha pela comparação com resultados obtidos em uma abordagem mais clássica com base na composição geoquímica. A contribuição das fontes de sedimento obtido pelos dois métodos foram muito similares, especialmente os modelos baseados no NIR. Além disso, os resultados da identificação das fontes de sedimentos baseados nas informações espectrais podem ser tão precisos quanto aos resultados obtidos com traçadores geoquímicos, mesmo utilizando modelos independentes para cada fonte, obtidos pela regressão do método dos mínimos quadrados (*Partial Least Squares Regression* – PLSR), ou seja, cada modelo estimou a proporção de uma

fonte, de forma independente dos outros dois. Os modelos espectroscópicos obtidos pelo método PLSR são uma abordagem promissora por causa de seu baixo custo e rapidez, facilitando a realização de inúmeras medidas e, portanto, alta resolução, o que é essencial para compreender melhor o comportamento de bacias que apresentam respostas hidrossedimentológico rápidas. Além disso, combinando parâmetros de cor baseado no VIS com marcadores geoquímicos foi uma maneira rápida e barata para melhorar a discriminação e baixar os erros de precisão das fontes de sedimentos.

3.3 Alta resolução espacial e temporal da contribuição das fontes de sedimentos

A contribuição das fontes de sedimentos coletados em intervalos que variaram ao longo da ascensão e recessão do hidrograma em eventos chuva-vazão revelam uma alta variabilidade na contribuição das fontes de sedimentos tanto inter quanto intra-eventos. Tais variações refletem condições antecedentes e mudanças no uso do e da cobertura do solo entre os eventos, exaustão de fontes ao longo do evento, e do estágio do hidrograma em que a amostra é coletada. Os resultados da classificação das fontes de sedimentos durante os eventos chuva-vazão nas cinco bacias monitoradas indicam que os eventos pluviométricos estão associadas à um aumento da contribuição relativa de sedimento das fontes superficiais do solo, como as áreas de pastagem e de lavoura. A entrada atrasada do sedimento oriundo dos canais na fase de recessão dos hidrogramas nas grandes bacias hidrográficas indicam que existe colapso dos canais na medida que o nível da água retrocede. Para as estradas no entanto, nenhum padrão claro da variação da sua contribuição intra-eventos foi verificado em todas as bacias hidrográficas do estudo. As variações intra-eventos na origem dos sedimentos para bacias hidrográficas agrícolas do sul do Brasil demonstra a individualidade de cada evento em diferentes ambientes hidrossedimentológicos. Esses resultados reforçam a necessidade da alta frequência de amostragem para alcançar resultados satisfatórios que permite compreender os processos de erosão ao longo dos eventos pluviométricos, em especial nas pequenas bacias hidrográficas onde as respostas hidrológicas são mais rápidas.

Os resultados obtidos nas diferentes bacias e sub-bacias monitoradas demonstram que outros fatores além da proporção de uso do solo desempenham um papel importante na produção de sedimentos no sul do Brasil, como a distribuição das terras agrícolas, florestas e estradas não pavimentadas na paisagem. A vegetação ciliar preservada, as zonas úmidas e

açudes promovem interceptação dos sedimentos e reduzem a conectividade das áreas de lavoura com a rede de drenagem, diminuindo a quantidade de sedimentos transferidos para os corpos d'água. A mata ciliar parece ser um fator-chave para a erosão do canal. A presença de árvores adultas nas margens dos rios e riachos aumenta sua estabilidade das margens contra seu colapso através do reforço do sedimento das margens com raízes. Os resultados deste trabalho também demonstram que a contribuição das estradas é fortemente relacionada com a escala e depende do número de pontos em que elas cruzam a rede de drenagem. A contribuição das estradas não pavimentadas é relevante para a produção de sedimentos em todas bacias hidrográficas monitoradas, mas particularmente nas pequenas. A maioria das estradas nas bacias de estudo não são planejadas, construídas seguindo a linha de inclinação, e muitas vezes são danificadas por sulcos e voçorocas. Na bacia hidrográfica do Conceição, a contribuição das estradas foi a menor entre as bacias hidrográficas estudadas, o que foi particularmente surpreendente porque nessa bacia hidrográfica é possível verificar que o nível das estradas é significativamente mais baixo comparativamente ao nível original do terreno nas lavouras adjacentes e vários processos erosivos podem ser verificados ao longo das estradas. Apesar da baixa contribuição relativa de estradas comparativamente as áreas de lavoura nas grandes bacias hidrográficas, eles representam um componente estático da paisagem, o que torna primordial seu planejamento de alocação em programas que visam mitigar a transferência de sedimentos.

3.4 Efeito do manejo do solo na transferência de sedimentos das áreas de lavoura

Os resultados indicam que a quantidade de sedimentos gerados nas áreas de lavoura por unidade de área que realmente atinge a rede de drenagem fluvial (produção específica de sedimentos das áreas de lavoura) foi muito diferente entre as bacias estudadas, devido em parte às condições naturais intrínsecas de relevo, e foram fortemente influenciados pelo uso da terra e manejo do solo. Nas bacias de Júlio de Castilhos, a quantidade de sedimentos originada nas áreas de lavoura foi muito baixa (variando de 6 a 12 toneladas de sedimento por quilometro quadrado de lavoura por ano), devido ao relevo mais suave e, principalmente, devido à presença de áreas úmidas e açudes artificiais, que promovem a interceptação dos sedimentos que reduzem a conectividade das áreas de lavoura com rede de drenagem. Por outro lado, as encostas íngremes e solo rasos frequentemente arados, nas áreas de lavoura da bacia hidrográfica de Arvorezinha resultou na produção de sedimentos aproximadamente 20-35 vezes

maior do que nas bacias hidrográficas de Júlio de Castilhos, o que é particularmente preocupante, uma vez que o sistema de produção dessas áreas envolve altas doses de fertilizantes fosfatados e pesticidas, aumentando o risco ambiental de eutrofização dos corpos d'água.

Embora as bacias hidrográficas do Guaporé e do Conceição apresentam produção de sedimentos muito semelhante, a produção de sedimentos oriundo das áreas de lavoura é cerca de três vezes menor na bacia do Conceição do que na bacia do Guaporé. A bacia Guaporé tem características naturais que favorecem a erosão e a transferência de sedimentos para os corpos d'água, especialmente no seu terço médio e inferior, onde o relevo é montanhoso e os solos são rasos. Mesmo assim, em muitas áreas, as culturas e o manejo do solo não levam em conta a fragilidade dos solos, resultando em alta erosão das áreas de lavoura. A menor produção de sedimento nas áreas de lavoura da bacia do Conceição em comparação com a do Guaporé, estão de acordo com o seu principal manejo do solo (> 80% das áreas de lavoura são cultivadas sob plantio direto) e com as características naturais de solo e paisagem que indicam baixa suscetibilidade à erosão. No entanto, a quantidade de sedimentos gerados nas áreas de lavoura que atinge a rede fluvial ainda é muito elevada para uma área considera de baixa susceptibilidade à erosão sem revolvimento do solo, indicando que novos esforços ainda são necessários para reduzir a erosão do solo. As principais causas disso são o abandono das práticas mecânicas para o controle de escoamento (i.e. utilização de terrações), a monocultura de soja negligenciando o sistema de rotação de culturas, o baixo aporte de biomassa resultando em redução da cobertura do solo, e o tráfego excessivo e descontrolado de máquinas agrícolas pesadas muitas vezes sob condições de umidade desfavoráveis.

4 Conclusão

As áreas de lavoura, mesmo cultivadas sob plantio direto, ainda são a principal fonte de sedimentos em bacias hidrográficas agrícolas do sul do Brasil. O estado atual dos sistemas de conservação, bem como os impactos das atividades agrícolas nos corpos d'água podem ser avaliados utilizando a abordagem *fingerprinting* para a identificação de fontes de sedimentos. Os resultados mostram que as atuais práticas de conservação do solo utilizados pelos agricultores ainda não são suficientes para reduzir a produção de sedimentos nas áreas de lavoura para taxas aceitáveis. Por isso, existe uma necessidade urgente de planejar melhor o

uso e ocupação do solo nessas bacias hidrográficas, na medida em que os sistemas de manejo do solo utilizados pelos agricultores são ineficazes na redução do escoamento superficial e erosão nas áreas de lavoura do sul do Brasil.

RÉSUMÉ LONG

1 Introduction et justification de l'étude

La dégradation des ressources naturelles due à l'érosion de terres cultivées s'est intensifiée au cours des dernières décennies. Environ la moitié de la surface des terres émergées a été convertie ou sensiblement modifiée par les activités humaines au cours des 10 000 dernières années (LAMBIN; GEIST; LEPERS, 2003). Les pratiques agricoles modernes et intensives exposent le sol à l'érosion et accélèrent le transfert des sédiments de versant vers les plaines (MINELLA; WALLING; MERTEN, 2014) et les cours d'eau. Elles transfèrent aussi les contaminants associés aux particules comme les pesticides (MAGNUSSON et al., 2013; YAHIA; ELSHARKAWY, 2014) et le phosphore (DODD; MCDOWELL; CONDRON, 2014; GUO et al., 2014). Cette situation est particulièrement inquiétante car des estimations montrent que les hommes extraient plus de 99,7% de leurs ressources alimentaires de la terre mais moins de 0,3% de celles-ci dans les océans et les autres écosystèmes aquatiques (PIMENTEL, 2006). De plus, la population humaine et la consommation alimentaire continuent de croître, ce qui signifie que la demande alimentaire mondiale va continuer à augmenter pendant au moins 40 ans (GODFRAY et al., 2010).

Dans les bassins versants agricoles où les taux de production de sédiments et les coefficients de ruissellement sont élevés, comme dans le sud du Brésil, les processus d'érosion doivent être contrôlés pour éviter une dégradation irréversible des sols et de la qualité de l'eau. La connaissance des principales sources de sédiments diffuses permettrait d'améliorer l'utilisation des ressources publiques investies dans les stratégies de gestion qui visent à atténuer le transfert de sédiments des versants vers les cours d'eau. Pourtant, seules quelques études ont tenté de quantifier l'origine des sédiments dans les bassins versants du sud du Brésil. Les études actuellement menées à cette fin sont donc prometteuses et indiquent que cette approche est appropriée pour étudier les sources de sédiments dans ce type de conditions environnementales. Bien que des études antérieures aient montré que les terres cultivées soient la principale source de sédiments, et que les chemins agricoles génèrent une contribution sédimentaire non négligeable dans les petits bassins versants agricoles (<10 km^2), ces résultats ne peuvent pas être directement extrapolés aux grands bassins versants (>100 km^2). Par ailleurs, d'autres

sources potentielles que les terres cultivées, les chemins agricoles, et les berges des cours d'eau, comme les prairies, doivent être étudiées.

D'autres études sur la contribution des sources de sédiments ont montré qu'il fallait prendre en compte la connectivité hydro-géomorphologique du bassin versant pour mieux comprendre le transport des sédiments de l'amont vers l'exutoire du bassin versant (KOITER et al., 2013b). Cependant, il est nécessaire d'obtenir des informations sur la contribution des sources de sédiments avec une résolution spatiale et temporelle élevée, en particulier pendant des événements pluvieux au cours de l'ensemble de l'année hydrologique, afin d'améliorer la compréhension des processus d'érosion dans le sud du Brésil. En outre, il est indispensable d'obtenir des résultats fiables pour sensibiliser les agriculteurs quant à l'impact de leurs pratiques sur les ressources en eau.

L'approche classique du *fingerprinting* pour identifier les sources de sédiments est difficile à mettre en œuvre en routine dans le sud du Brésil car elle est basée sur l'emploi de traceurs géochimiques dont la détermination nécessite une masse importante d'échantillons, ainsi qu'une préparation laborieuse, destructive et coûteuse. L'accès aux appareils de mesure (ICP-OES, ICP-MES, spectromètres γ) constitue également un frein au développement de cette approche au Brésil comme dans d'autres pays subtropicaux. En conséquence, il est nécessaire (i) d'adopter une méthodologie permettant de présélectionner les traceurs pertinents et conservatifs et (ii) de développer et de valider des méthodes facilement applicables et efficaces à un grand nombre d'échantillons, nécessitant une préparation minimale de ces derniers.

1.1 Contexte

La présente thèse est le résultat de deux projets de recherche qui ont permis de réaliser des échantillonnages sur le terrain et de réaliser des analyses géochimiques du ceux-ci au laboratoire. Le premier projet intitulé « Eau et polluants, des terres cultivées vers les villes : évaluation de technologies améliorées de gestion en réseau dans des bassins versants » (*Água e poluentes, das lavouras às cidades: avaliação e tecnologias melhoradas de manejo em rede de bacias hidrográfica - Edital FAPERGS nº 008/2009, Processo nº 10/0034-0*) a été financé par le Programme de Soutien aux Centres d'Excellence de la Fondation de Soutien à la Recherche de l'État du Rio Grande do Sul (*Programa de Apoio a Núcleos de Excelência – PRONEX da Fundação de Amparo à Pesquisa do Estado do Rio Grande do Sul – FAPERGS*).

Le projet a été coordonné par le professeur Dr. Danilo RHEINHEIMER dos Santos, le Dr Jean Paolo Gomes MINELLA, et le Dr. José Miguel REICHERT, de mai 2010 à mai 2014. Ce projet a rendu possible le suivi hydro-sédimentaire des bassins versants étudiés et les analyses géochimiques des échantillons de sol et de sédiments au Laboratoire de Chimie et de Fertilité des Sols de l'UFSM.

Le second projet est un projet international Franco-Brésilien soutenu par le programme CAPES / COFECUB. COFECUB est l'acronyme du Comité Français d'Evaluation de la Coopération Universitaire avec le Brésil, et CAPES est l'acronyme portugais de l'Agence Fédérale de Soutien et de l'Évaluation du Personnel de l'Enseignement Supérieur (*Coordenação de Aperfeiçoamento do Pessoal de Nível Superior*). Le projet « Evolution minéralogique des sols du sud du Brésil : caractérisation des processus d'altération et de l'impact anthropique » a débuté en janvier 2012 et est coordonné par le Professeur Dr. Danilo RHEINHEIMER dos Santos pour la partie brésilienne (UFSM, Brésil), et Laurent CANER pour la partie française (Université de Poitiers, France). Le projet de coopération tire profit des caractéristiques qui sont communes entre les institutions concernées : l'historique de la collaboration et les perspectives d'application similaires en termes de formation et de transfert des résultats de recherche. Le projet comprend trois universités brésiliennes (UFSM, Université de Passo Fundo – UPF et l'Université Fédérale du Rio Grande do Sul – UFRGS) et deux groupes de recherche de l'Université de Poitiers, à savoir : l'équipe *HydrASA* (Hydrogéologie, Argiles, Sols et Altérations) et l'Équipe Eaux Géochimie Santé, les derniers appartient à l'Institut de Chimie des Milieux et Matériaux de Poitiers (IC2MP), UMR 7285.

Le projet CAPES / COFECUB a rendu possible la réalisation de la thèse en cotutelle entre l'UFSM, au Brésil, et l'Université de Poitiers, en France. Par ailleurs, la coopération avec l'Université de Poitiers a permis le développement et la validation de méthodes alternatives pour l'identification des sources de sédiments. Des analyses spectroscopiques (IR et UV-VIS), de diffraction des rayons X et de pyrolyse-chromatographie en phase gazeuse couplée à le spectrométrie de masse ont permis d'étudier les propriétés physico-chimiques et leur utilisation pour identifier les sources de sédiments.

1.2 Hypothèse

Même lorsque les terres sont cultivées avec des techniques culturales simplifiées sans labour du sol et en semis-direct (ce qui est commun au sud du Brésil), elles constituent encore la principale source de sédiments dans les bassins versants agricoles du sud du Brésil. L'impact des pressions agricoles sur les ressources en sol et en eau ainsi que l'état actuel des systèmes de conservation (plus ou moins bien utilisés) peut être évaluée en utilisant l'approche d'identification des sources de sédiments par *fingerprinting*.

1.3 But et objectifs

L'objectif général de cette étude est de comprendre les processus de production et de transfert des sédiments à l'échelle des bassins versants cultivés dans le sud du Brésil, en vue de contribuer à la recommandation de pratiques de conservation des sols permettant de réduire le ruissellement et l'érosion ainsi que les transferts de polluants associés. Les objectifs spécifiques sont déroulés ci-après :

(i) Affiner la procédure de sélection des traceurs et proposition de lignes directrices pour la pré-sélection des traceurs.

(ii) Valider les méthodes spectroscopiques alternatives pour l'identification des sources de sédiments en comparant leurs résultats avec ceux de l'approche classique basée sur les traceurs géochimiques.

(iii) Améliorer la compréhension des processus d'érosion dans le sud du Brésil en obtenant des informations sur la contribution des sources de sédiments avec une résolution spatiale et temporelle importante, en particulier lors d'événements pluvieux.

(iv) Estimer l'apport de sédiments provenant des terres cultivées vers le réseau hydrologique afin d'obtenir des résultats probants pour sensibiliser les agriculteurs sur l'impact de leurs pratiques sur les ressources en eau.

2 Matériel et méthodes

L'étude a été réalisée dans l'état du Rio Grande do Sul, plus méridional du Brésil. Le choix des bassins versants a été guidé par la nécessité de caractériser l'impact des processus hydrologiques et d'érosion dans diverses conditions d'utilisation des terres, du sol et du paysage représentatives de cette région. Trois petits bassins versants (de 0,802 à 1,426 km^2) et deux grands bassins (804,3-2.031,9 km^2) ont été choisis pour refléter les principaux systèmes agricoles et les processus d'érosion derrières. Les bassins versants choisis subissent les impacts typiques les plus importants qu'induit l'agriculture sur les ressources en eau dans l'État de Rio Grande do Sul. Les bassins versants de Júlio de Castilhos (0,802 et 1,426 km^2) sont situés sur des sols sableux et le système de production qui y est pratiqué correspond à une agriculture intensive intégrée combinent culture du soja en été et pâturage ou prairies temporaires pour l'élevage en hiver, on y pratique un système sans labour (semis direct). Le bassin versant de la rivière Conceição (804,3 km^2) présente une activité agricole intensive avec la production de céréales (principalement le soja, le maïs et les céréales d'hiver) sans travail du sol (semis-direct) sur des sols profonds, argileux et riches en oxydes de fer. Le bassin versant de la rivière Guaporé (2.031,9 km^2) a des caractéristiques physiographiques telles que les sols y sont fragiles, lorsqu'ils sont utilisés pour l'agriculture. Le bassin versant d'Arvorezinha (1,19 km^2) est un petit bassin versant situé dans la partie inférieure du bassin versant de Guaporé. On y pratique une agriculture familiale produisant majoritairement du tabac sur des versants en pente avec labour du sol. Les cinq bassins versants ont comme point commun une production importante de sédiments et ont, de ce fait, un impact important sur l'environnement.

Les sources de sédiments correspondent aux terres cultivées, aux prairies, aux chemins agricoles et aux berges des cours d'eau. L'échantillonnage des sédiments est réalisé par des préleveurs automatiques pour permettre un suivi temporel, dérouillé des prélèvements de sédiments fins du lit de la rivière, et lors d'événements pluvieux. Les échantillons de sédiments et de sols ont été séchés à l'étuve à 50°C et désagrégés délicatement avec un mortier et un pilon. Les traceurs géochimiques ont été déterminés sur les échantillons des cinq bassins versants. Le

carbone organique total a été estimé par oxydation en voie humide avec du dichromate de potassium (K_2Cr_2O7) et de l'acide sulfurique concentré (H_2SO_4). Les concentrations totales en éléments chimiques (Ag, As, B, Ba, Be, Ca, Cd, Co, Cr, Cu, Fe, K, La, Li, Mg, Mn, Mo, Na, Ni, P, Pb, Sb, Se, Sr, Ti, Tl, V et Zn) ont été mesurées par ICP-OES après digestion au four micro-ondes pendant 9,5 min à 182ºC avec ajout de HCl et HNO_3 concentré selon un rapport 3/1 (eau régale).

La granulométrie a uniquement été analysée par granulométrie laser pour les échantillons d'Arvorezinha après oxydation de la matière organique avec H_2O_2 et dispersion avec NaOH (pH < 9). La surface spécifique a été calculée à partir de la distribution de taille de particules en considérant que les particules sont sphériques et cylindriques. D'autres analyses ont également été effectuées pour évaluer la pertinence de l'analyse spectroscopique pour tracer les sources de sédiments.

Les spectres de réflectance diffuse dans la gamme ultraviolet-visible (UV-VIS) ont été enregistrés à la température ambiante entre 200 et 800 nm avec un pas de 1 nm en utilisant un spectrophotomètre Cary 5000 UV-VIS-NIR (Varian, Palo Alto, CA, USA). Les échantillons ont été broyés et chargés dans un accessoire de réflectance diffuse « Mantis Harrick Prier » qui utilise des miroirs elliptiques. L'appareil est calibré en utilisant du $BaSO_4$ comme standard de 100 % de réflectance. Vingt-quatre (24) paramètres ont été dérivés des spectres VIS avec l'aide de divers modèles de colorimétrie décrits en détail par Viscarra Rossel et al. (2006). Les proche spectres infrarouge (NIR) en mode de réflectance diffuse ont été enregistrés dans le domaine 10000–4000 cm^{-1} en utilisant un spectromètre FTIR Nicolet 26700 (Waltham, Massachusetts, USA) équipé d'une sphère d'intégration d'un détecteur InGaAs interne avec une résolution 2 cm^{-1}. Les spectres moyen infrarouge (MIR) en mode de réflexion diffuse ont été enregistrés dans la gamme spectrale 400–4000 cm^{-1} en utilisant un spectromètre FTIR Nicolet 510 (Thermo Electron scientifique, Madison, WI, USA) avec une résolution de 2 cm^{-1}. Les spectromètres infrarouges sont balayés par un flux d'air dont le CO_2 a été éliminé pour ne pas perturber les mesures.

Afin de faciliter l'interprétation des analyses de spectroscopie, des analyses complémentaires ont été effectuées sur des échantillons composites générés en mélangeant tous les échantillons de chaque source de sédiment (10 pour les sources des chemins agricoles et des berges de cours d'eau, et 20 pour les terres cultivées). Ces trois types d'échantillons composites ont été analysés par pyrolyse-chromatographie en phase gazeuse couplée avec la spectrométrie de masse (Py-GC / MS) et par diffraction des rayons X (XRD) pour identifier les principaux composés organiques et minéraux.

L’analyse statistique utilisée pour la méthode alternative basée sur l'analyse spectroscopique est très différente de l’analyse statistique conventionnelle utilisée pour l’approche basée sur la composition géochimique. Les étapes utilisées dans la méthode conventionnelle sont décrites comme suit : *i*) la sélection du traceur potentiel avec le test de Kruskal-Wallis *H, ii*) la sélection de la meilleure combinaison de traceurs permettons la discrimination et, enfin, *iii*) l'utilisation d'un modèle linéaire mixte pour calculer la contribution de chaque source de sédiments. Les étapes utilisées dans le cadre de la méthode alternative sont *i*) une analyse en composantes principales pour réduire le nombre de variables, *ii*) l’analyse discriminante pour déterminer le potentiel de traceur de la spectroscopie et, enfin, *iii*) l'utilisation de la régression partielle par les moindres carrés (PLSR) à base de mélanges des sources de sédiments composites dans des proportions massiques variables pour calculer la contribution des sources de sédiments.

3 Principaux résultats

3.1 Lignes directrices pour la pré-sélection des traceurs de sédiments dans le sud du Brésil

Les analyses préliminaires montrent que 18 traceurs géochimiques (Ag, Al, As, Ba, Be, Co, Cr, Cu, Fe, La, Li, Mn, Mo, Ni, P, Ti, V et Zn) ont été présélectionnés comme traceurs potentiels pour estimer la proportion des sources de sédiments avec le modèle linéaire mixte dans au moins l’un des bassins versants étudiés. Les résultats révèlent que les métaux de transition sont les traceurs géochimiques à privilégier dans les bassins versants agricoles du sud du Brésil en raison de leur conservativité et de leur pouvoir de discrimination. En dépit de leur potentiel de discrimination des sources de sédiments, les alcalins et les alcalino-terreux sont moins conservatifs pendant le processus d'érosion et doivent, de ce fait, être évités. Cette première étape permet de proposer des lignes directrices pour la présélection des traceurs en n’analysant pas les éléments inefficaces.

Le phosphate et le carbone organique total sont systématiquement présents en concentrations plus élevées dans les sources superficielles, c’est à dire les prairies et les terres cultivées. Cet exemple souligne que la sélection des traceurs est spécifique de chaque bassin

versant. Cependant, il convient d'évaluer la conservativité du P et du carbone organique total dans chaque bassin versant cible avant leur utilisation comme traceurs.

Les résultats démontrent clairement qu'aucun traceur géochimique ne permet seul de classer 100% des échantillons dans les catégories de sources correctes, quel que soit le bassin versant étudié. Plusieurs traceurs doivent donc être combinés pour distinguer plusieurs sources diffuses et fournir des estimations fiables de la contribution relative de ces sources dans les bassins versants agricoles. En règle générale, plus le bassin versant est petit et plus le nombre de sources potentielles de sédiments est faible, meilleure est la discrimination des sources au moyen des traceurs. La discrimination des prairies n'a été possible que dans les petits bassins versants de Júlio de Castilhos. Pour les bassins versants de Guaporé et de Conceição, il n'a pas été possible de différencier la contribution des prairies de celles des terres cultivées en raison de leur composition géochimique similaire et la grande variabilité des types de sol et de lithologie rencontrés dans ces bassins.

3.2 L'utilisation potentielle de méthodes alternatives basées sur l'analyse spectroscopique

L'utilisation des méthodes spectroscopiques alternatives dans les gammes spectrales UV-VIS, NIR et MIR a été validée pour estimer les contributions des sources de sédiments dans le petit bassin d'Arvorezinha en comparant les résultats avec ceux de l'approche classique basée sur la composition géochimique. La contribution des sources obtenue par des méthodes alternatives basées sur des modèles de spectroscopie-PLSR est en accord avec les résultats obtenus par la méthode classique, en particulier l'approche NIR-PLSR. De plus, les méthodes alternatives basées sur l'analyse spectroscopique peuvent être aussi précises que les méthodes basées sur les traceurs géochimiques pour ce même bassin, y compris en utilisant des modèles de PLSR indépendants pour chaque source. Dans ce dernier cas, chaque modèle estime alors la proportion d'une source, indépendamment des deux autres. Le modèle par spectroscopie-PLSR constitue une approche prometteuse en raison de son faible coût et de sa rapidité d'exécution. Cette méthode permet donc l'obtention de prévisions à haute résolution qui sont essentielles pour mieux comprendre le comportement érosif des bassins versants qui présentent des réponses hydro-sédimentaires rapides. Enfin, la combinaison des paramètres de couleur dérivés du spectre VIS avec des traceurs géochimiques s'est révélée être une méthode rapide et peu coûteuse pour améliorer la discrimination entre les sources et la précision des prédictions.

3.3 Haute résolution spatiale et temporelle des contributions de sources de sédiments

Les résultats de la contribution des sources pour les échantillons de sédiments prélevés en divers points de l'hydrogramme lors d'événements pluie-débit révèlent une grande variabilité des contributions des sources au sein d'un même événement ainsi que d'un événement à l'autre. Ces variations reflètent les conditions antécédentes d'utilisation des terres et de couverture végétale entre les événements, l'épuisement des sources, et le choix du moment de l'échantillonnage par rapport au pic de l'hydrogramme. Les résultats obtenus pour les cinq bassins étudiés confirment que les événements de précipitations sont associés à une augmentation quantitative du transfert des sédiments des sources superficielles vers les cours d'eau. Les résultats obtenus au cours des crues étudiés montrent que les sédiments provenant des berges des cours d'eau arrivent après les autres sources. Les précipitations et l'élévation du niveau d'eau induisent un alourdissement de la teneur en eau et une augmentation de poids des berges des cours d'eau. Ceux-ci réduisent la cohésion entre les particules et diminuent la stabilité des berges. Si les précipitations se poursuivent, la formation d'une nappe superficielle induit une pression hydrostatique qui diminue la résistance et la cohésion du matériau. De plus, la hauteur des berges et leur inclinaison peut être modifiée au fur et à mesure de l'érosion liée aux crues. Enfin, la combinaison de ces effets et la diminution rapide de la pression hydrostatique lors de la décrue peut induire un effondrement des berges.

Par contre, aucune tendance n'apparait clairement en ce qui concerne la contribution sédimentaire des chemins agricoles dans les bassins versants étudiés. Les variations de cette source au cours des crues dans les zones agricoles du sud du Brésil illustrent la particularité de chaque évènement dans différents environnements hydro sédimentaires. Ces résultats soulignent la nécessité d'atteindre une fréquence d'échantillonnage plus élevée pour permettre la compréhension des processus d'érosion au cours des événements pluvieux. Ceci est d'autant plus important pour les petits bassins versants où les réponses hydrologiques sont plus rapides. Les résultats obtenus dans les différents bassins et sous-bassins versants étudiés démontrent que des facteurs autres que la proportion des différents types d'utilisation des terres, comme la distribution spatiale des terres cultivées, des forêts et des chemins agricoles à travers le paysage, jouent un rôle important dans la production de sédiments au sud du Brésil. La préservations de végétation riparienne, des zones humides, et des étangs artificiels favorise le piégeage des sédiments et réduit la connectivité entre les terres cultivées et le réseau de drainage, diminuant la quantité de sédiments transférés dans les cours d'eau. En outre, la forêt riveraine semble être

un facteur clé limitant l'érosion des berges des cours d'eau. La présence d'arbres adultes sur les berges augmente leur stabilité et évite leur effondrement, du fait de la présence de nombreuses racines. Les résultats de ce travail montrent également que la contribution des chemins agricoles est fortement liée à l'échelle d'observation et qu'elle dépend du nombre de points où les chemins croisent le réseau hydrographique. La contribution des chemins agricoles est significative pour la production de sédiments dans tous les bassins versants, mais elle l'est particulièrement dans les plus petits. La plupart des chemins agricoles des bassins versants étudiés ne sont pas construits en tenant compte de la topographie de site. Ils sont souvent construits dans le sens de la plus grande pente et sont souvent endommagés par des rigoles et des ravines. Malgré la faible contribution des chemins agricoles par rapport à celles des terres cultivées dans les grands bassins versants, ils représentent une composante pérenne du paysage, ce qui rend primordial leur planification et leur prix en compte dans les programmes visant à atténuer le transfert des sédiments.

3.4 Effet des pratiques de conservation sur l'exportation de sédiments depuis les terres cultivées

Les résultats indiquent que la quantité de sédiments produits par les terres cultivées par unité de surface et qui atteignent effectivement l'exutoire des bassins versants est très différente dans les cinq bassins versants étudiés. Ce résultat est en partie lié au relief et à la pente caractéristique de chaque bassin versant, mais il l'est aussi lié à l'utilisation des terres et la gestion des sols. Dans les bassins versants de Júlio de Castilhos, la quantité de sédiments provenant de terres cultivées est très faible (6–12 tones km^2 an^{-1}) en raison d'un relief moins accidenté, de la présence de zones humides et d'étangs artificiels, qui favorisent le piégeage des sédiments en réduisant la connectivité entre les terres cultivées et le réseau de drainage. Par contre, les pentes abruptes et le labour des sols peu profonds du bassin versant d'Arvorezinha génèrent des apports de sédiments environ 20 à 35 fois plus élevés que dans le bassin versant de Júlio de Castilhos. C'est particulièrement inquiétant, car le système de production agricole de ce bassin versant emploie des doses élevées d'engrais phosphatés et de pesticides, ce qui augmente le risque environnemental d'eutrophisation des plans d'eau situés à l'aval.

Bien que les bassins versants de Guaporé et Conceição présentent des taux de production de sédiments très similaires, l'apport de sédiments provenant de terres cultivées est presque trois fois inférieur dans le bassin versant Conceição par rapport à celui de Guaporé. Le bassin versant

de Guaporé présente des caractéristiques naturelles qui favorisent l'érosion et le transfert de sédiments vers les cours d'eau, en particulier dans les parties intermédiaire et inférieure du bassin, où le relief est accidenté et les sols sont peu profonds. Même si, dans de nombreux domaines, les cultures et la gestion des sols ne tiennent pas compte de la fragilité des sols, entraînant l'érosion élevé de terres cultivées. Le taux de production de sédiments inférieurs provenant des terres cultivées dans le bassin de Conceição par rapport à celui de Guaporé reflètent les différences de gestion des sols dans ces deux sites. Dans le bassin versant de Conceição, au moins 80% de la superficie des terres agricoles est cultivée sans labour du sol (semis direct) et les caractéristiques naturelles du paysages (relief – pente) induisent une faible sensibilité des sols à l'érosion. Pourtant, la quantité de sédiments issus des terres cultivées qui atteignent le réseau fluvial reste élevée pour une zone de faible sensibilité à l'érosion où le semis direct est appliqué. Ce résultat indique que des efforts supplémentaires sont nécessaires pour réduire l'érosion du sol. Cette situation est le résultat de la monoculture intensive du soja qui implique l'abandon des rotations de cultures habituellement réalisés dans cette région et celui des pratiques mécaniques visent à limiter le ruissellement. La monoculture du soja se traduit aussi par de faibles retours de biomasse (résidus de culture) au sol et une plus faible couverture du sol par la végétation. Enfin, cette culture est associée à un passage important de machines agricoles lourdes, souvent dans des conditions d'humidité défavorables, ce qui a pour effet d'augmenter la sensibilité des sols à l'érosion.

4 Conclusion générale

Les parcelles agricoles, même lorsqu'elles sont cultivées sans labour du sol, constituent encore la principale source de sédiments dans les bassins versants agricoles du sud du Brésil. L'érosion générée par les systèmes de conservation réels, ainsi que l'impact des pressions agricoles sur les ressources en eau, peuvent être évalués en utilisant l'approche *fingerprinting* pour l'identification de source de sédiments. Les résultats montrent que les pratiques de conservation des sols telles qu'elles sont utilisée soit mal employées aujourd'hui n'ont pas permis de diminuer de façon significative l'érosion des sols. Il y a donc un besoin urgent de mieux planifier l'utilisation et l'occupation des terres dans ces bassins versants, dans la mesure où les systèmes de gestion des sols utilisés par les agriculteurs sont aujourd'hui insuffisants pour réduire le ruissellement et l'érosion du les terres cultivées du sud du Brésil.

LIST OF FIGURES

LIST OF TABLES

LIST OF ABBREVIATIONS

A1	Single electron transition of Fe in goethite
A2	Electron pair transition for Fe in goethite
A3	Electron pair transition for Fe in hematite
CF	Crop fields
CIE	Commission Internationale de l'Eclairage
CSSI	Compound specific stable isotope
DFA	Discriminant function analysis
E_2/E_3	Ratio between absorption bands at 254 and 365 nm
E_4/E_6	Ratio between absorption bands at 465 and 665 nm
EI30	Erosivity index
FBS	Fine-bed sediment
Gb	Gibbsite
Geoch	Geochemical approach
GIS	Geographical information system
GR	Grasslands
Gt	Goethite
HI	Hysteresis index
HIV	Hydroxy-interlayered vermiculite
Hr	Proportion of hematite in the pool of Fe-oxides
ICP-OES	Inductively coupled plasma optical emission spectrometry
JC140	Catchment of 1.426 km^2 from Júlio de Castilhos
JC80	Catchment of 0.802 km^2 from Júlio de Castilhos
Kt	Kaolinite
KW	Kruskal-Wallis
Mc	Mica
MIR	Mid-infrared
NIR	Near-infrared
NT	No-till
NTS	No-tillage system
OC	Organic compounds
PC	Principal component
PCA	Principal component analysis
PLSR	Partial least squares regression
Py-GC/MS	Pyrolysis-gas chromatography/mass spectrometry
Qz	Quartz
RME	Relative mean error
RMSEC	Root mean square error of calibration
RMSECV	Root mean square error of cross-validation
RMSEP	root mean square error of prediction
RPD	Ratio RMSECV/SD
SC	Stream channels
SCM	Soil clay minerals
SD	Standard deviation
SE	Standard error
SESS	Storm-event suspended sediments
SESS-U59	Storm-event suspended sediment collected by US U-59 trap
Sm	Smectite
SSA	Specific superficial area
SSY	Specific sediment yield
SWIR	Shortwave-infrared
TISS	Time-integrated suspended sediments
TOC	Total organic carbon
UR	Unpaved roads
UV	Ultraviolet
VIS	Visible
XRD	X-ray diffraction

LIST OF SYMBOLS

R	Red
G	Green
B	Blue
H_{RGB}	Hue
I_{RGB}	Light intensity
S_{RGB}	Chromatic information
x	Chromatic coordinate x
y	Chromatic coordinate y
Y	Brightness
X	Virtual component X
Z	Virtual component Z
L	Metric lightness function
u*	Chromatic coordinate opponent red–green scales
v*	Chromatic coordinate opponent blue–yellow scales
a*	Chromatic coordinate opponent red–green scales
b*	Chromatic coordinate opponent blue–yellow scales
c*	CIE hue
h*	CIE chroma
H	Hue
V	Value
C	Chroma
λ_d (nm)	Dominant wavelength
p	Probability
P_e	Purity of excitation
RI	Redness Index
Λ*	Wilks' Lambda value
8	Eight-shaped form hysteresis
C	Clockwise hysteresis
R_{adj}	Coefficient of determination

LIST OF CONTENTS

1 INTRODUCTION

Degradation of natural resources caused by agriculture for food production has been intensified in recent decades. About half of the ice-free land surface has been converted or substantially modified by human activities over the last 10,000 years (LAMBIN; GEIST; LEPERS, 2003). Modern and intensive agricultural practices expose the soil to the erosion and accelerate the transfer of sediment to low parts of landscape (MINELLA; WALLING; MERTEN, 2014) and into water bodies, along with several contaminants like pesticides (MAGNUSSON et al., 2013; YAHIA; ELSHARKAWY, 2014) and phosphorus (DODD; MCDOWELL; CONDRON, 2014; GUO et al., 2014). This is particularly worrisome since estimates shows that humans obtain more than 99.7% of their food (calories) from the land and less than 0.3% from the oceans and other aquatic ecosystems (PIMENTEL, 2006), and that continuing population and consumption growth will induce an increase of global demand for food for at least another 40 years (GODFRAY et al., 2010).

In agricultural catchments with high runoff coefficients and sediment yields, as in Southern Brazil, erosion process needs to be controlled to prevent an irreversible degradation of soil and water quality. In this regard, the study group in watersheds of the Department of Soil Science, Federal University of Santa Maria (UFSM), composed by professors, technicians, graduate and undergraduate students, has been intensively monitoring some catchments that are representative of the most conditions of agriculture impact on water resources in the State of Rio Grande do Sul. The Júlio de Castilhos catchments are covered with sandy soils where mixed crop-livestock farms under no-till takes place as the main production system. The Conceição catchment presents intensive agricultural activity with grain production (mainly soybean, maize and winter cereals) under no-till on deep and clayey soils enriched in iron oxides. The Guaporé catchment has physiographic characteristics that determine the environmental fragility when the soil is used for agriculture. The Arvorezinha catchment is a headwater catchment from the lower third of the Guapore catchment, where the main crop is tobacco cultivated by family farmers on sloping areas with soil plowing. In common, the five catchments present high sediment yields and environmental imbalance.

Table 1 displays the main studies carried out in the studied catchments. By far, most of studies were performed in Arvorezinha catchment due to the long-term monitoring records since 2002. Few of them integrated two or more catchments together (DIDONÉ et al., 2014;

KOCHEM, 2014). Most works were related to water and sediment modelling, certain on large catchments (DIDONÉ, 2013; DIDONÉ et al., 2014) and most of them in small ones (BARROS, 2012; BARROS et al., 2014a, 2014b; DALBIANCO, 2009, 2013; MERTEN; MINELLA, 2006; MERTEN et al., 2010; MINELLA; MERTEN; MAGNAGO, 2011; MINELLA; MERTEN; RUHOFF, 2010; MINELLA; MERTEN, 2012; MINELLA et al., 2008; MORO, 2011; OLIVEIRA, 2010; OLIVEIRA et al., 2012; PELLEGRINI A., 2013; UZEIKA, 2009; UZEIKA et al., 2012). The remaining were attempts to understand the dynamics of carbon, phosphorus, and other nutrients (ALVAREZ, 2014; JANSEEN, 2011; KOCHEM, 2014; LOPES, 2006; MELLO, 2006; SCOTTO, 2014), the influence of agricultural pressures on water quality (CAPOANE, 2011; CAPOANE et al., 2011), and on land use and cover (CAPOANE; RHEINHEIMER, 2012, 2013).

Although recognizing that the knowledge of the main diffuse sources of sediment production can enhance efficiency in use of public resources invested in management strategies to mitigate sediment transfer from catchment areas to waterways, only few attempts were made to target sediment origin in these catchments. So far, one master dissertation and two theses have focused on sediment sources (MAIER, 2013; MINELLA, 2003, 2007), all of them at Arvorezinha catchment, leady to the publish of six research papers (CLARKE, 2014; MINELLA; MERTEN; CLARKE, 2009; MINELLA; WALLING; MERTEN, 2008, 2014; MINELLA et al., 2007, 2009) plus one review paper (MINELLA; MERTEN, 2011). Moreover, a first attempt to estimate the contribution of unpaved roads and crop fields in a 0.8 km^2 catchment in the Rio Grande do Sul plateau region was performed by Tiecher et al. (2014).

The previous fingerprinting studies in the monitored catchments, as well as in others Brazilian catchments (FRANZ et al., 2014; MIGUEL et al., 2014a, 2014b; POLETO; MERTEN; MINELLA, 2009) are promising and indicate that this approach provides a suitable tool to study sediment sources in our environmental conditions as well. Although sediment apportionments from many of the previous studies indicate that crop fields are the main sediment source, and that unpaved roads have non-negligible contribution, the magnitude of the values obtained for the smaller catchments might not be valid for larger catchments. Moreover, the contribution of other potential sources than crop fields, unpaved roads, and channel banks should be further investigated, i.e. grasslands.

Table 1 – Summary of the studies performed in the study catchments. Bold references indicate fingerprinting studies.

Publication	Catchment			
	Arvorezinha	Júlio de Castilhos	Conceição	Guaporé
Monitoring since	2002	2009	2010	2010
Master Dissertation	**Minella (2003)**	Capoane (2011)	Didoné (2013)	Scotto (2014)
	Lopes (2006)	Schaefer (2015)*	Kochem (2014)***	Kochem (2014)***
	Dalbianco (2009)	Bender (2016)*		
	Uzeika (2009)			
	Janseen (2011)			
	Barros (2012)			
	Kochem (2014)***			
	Ramon (2017)*			
Doctoral Thesis	Mello (2006)	Pellegrini A. (2013)	Didoné (2017)*	Zafar (2016)*
	Minella (2007)	Alvarez (2014)		Bastos (2017)*
	Oliveira (2010)	Capoane (2015)*		Lima (2018)*
	Moro (2011)			
	Maier (2013)			
	Dalbianco (2013)			
	Barros (2016)*			
Research articles	Merten; Minella (2006)	Capoane et al. (2011)	Didoné et al. (2014)**	Didoné et al. (2014)**
	Minella et al. (2007)	Capoane; Rheinheimer (2012)		
	Minella; Walling; Merten (2008)	Capoane; Rheinheimer (2013)		
	Minella et al. (2008)	**Tiecher et al. (2014)**		
	Minella et al. (2009)			
	Minella; Merten; Clarke (2009)			
	Minella; Merten; Ruhoff (2010)			
	Minella; Merten (2011)			
	Minella; Merten; Magnago (2011)			
	Minella; Merten (2012)			
	Uzeika et al. (2012)			
	Oliveira et al. (2012)			
	Barros et al. (2014a)			
	Barros et al. (2014b)			
	Clarke (2014)			
	Minella; Walling; Merten (2014)			

* Ongoing works with estimated year of ending.
** Study performed in Guaporé and Conceição catchments together.
*** Study performed in Arvorezinha, Guaporé, and Conceição catchments together.

Further fingerprinting studies must incorporate the sediment connectivity of the watershed, to understand how efficiently the transport of sediment occurs throughout the river basin, from the headwaters to the outlet (KOITER et al., 2013b). Notwithstanding, there is a need to generate high-spatial and -temporal resolution source apportionment, especially during storm-events occurring at different moments during the hydrological year, in order to improve our understanding of erosion processes in Southern Brazil. In addition, there is still a need to generate reliable results to promote awareness among farmers about the impact of inappropriate soil conservation practices on water resources.

The use of conventional fingerprinting approach based on geochemical tracers to identify sediment sources as a management tool in Southern Brazil is complicated because it is time-consuming, costly, destructive, and demanding high quantities of sample. Furthermore, the difficult access to measuring equipment (ICP-OES, ICP-MES, spectrometers γ) is preventing the development of this approach in Brazil as in other subtropical countries. Therefore, it is important and necessary (*i*) to develop guidelines to pre-select relevant and conservative tracers and (*ii*) to develop and validate methods that are effective for discriminating potential sources of sediment and easily applicable to a large number of samples with minimal preparation.

The present thesis is the result of two research projects that have funded the required field and laboratory works. The first project i.e. “Water and pollutants, from the cropfields to the cities: evaluation and improved management technologies in network watersheds” (*Água e poluentes, das lavouras às cidades: avaliação e tecnologias melhoradas de manejo em rede de bacias hidrográfica - Edital FAPERGS nº 008/2009, Processo nº 10/0034-0*) was funded by the Support Program for Centers of Excellence of the Research Support Foundation of the Rio Grande do Sul State (*Programa de Apoio a Núcleos de Excelência – PRONEX da Fundação de Amparo à Pesquisa do Estado do Rio Grande do Sul – FAPERGS*). The project was coordinated by the professors Dr. Danilo Rheinheimer dos Santos, Dr. Jean Paolo Gomes Minella, and Dr. José Miguel Reichert from May 2010 to May 2014, at UFSM. This project made possible the hydrosedimentological monitoring of the studied catchments and the geochemical analyzes of soil and sediment samples at the Laboratory of Chemical and Fertility of Soils of the UFSM.

The second one is an international project supported by the CAPES/COFECUB program. COFECUB is the French acronym for French Committee for the Evaluation of Academic and Scientific Cooperation with Brazil (*Comité Français d'Evaluation de la Coopération Universitaire avec le Brésil*), and CAPES is the Portuguese acronym for the Federal Agency of Support and Evaluation of Postgraduate Education (*Coordenação de*

Aperfeiçoamento do Pessoal de Nível Superior). The project "Mineralogical evolution of soils from Southern Brazil: characterization of alteration processes and human impact" (*Evolution minéralogique des sols du sud du Brésil : caractérisation des processus d'altération et de l'impact anthropique/Evolução mineralógica dos solos do sul do Brasil: caracterização dos processos de alteração e de impacto antrópico*) started in January 2012 with coordination of the Professor Dr. Danilo Rheinheimer dos Santos (UFSM, Brazil), and the Professor Dr. Laurent Caner (University of Poitiers, France). The cooperation project is based on characteristics that are common among the institutions involved: history of collaboration and similar application prospects in terms of training and transfer of research results. The project involves three Brazilian universities (UFSM, University of Passo Fundo – UPF, and the Federal University of Rio Grande do Sul – UFRGS) and two research groups at the University of Poitiers, France, namely: the *HydrASA* team (the French acronym for Clays, Soils and Alterations – *Hydrogéologie, Argiles, Sols et Altérations*), and the *Eaux Géochimie Santé* team (Water, Geochemistry, Health), both from the Institute of Chemistry of Poitiers: Materials and Natural Resources – IC2MP, UMR 7285. The CAPES/COFECUB project made possible the joint supervision of the present thesis between the UFSM (from March 2011 to March 2013, and from September 2014 to February 2015), in Brazil, and the University of Poitiers (from April 2013 to August 2014), in France. Furthermore, the cooperation with the University of Poitiers made possible to advance in the development and validation of alternative methods for fingerprinting sediment sources using spectroscopic analysis, as well as some sophisticated analyses as X-ray diffraction and pyrolysis-gas chromatography/mass spectrometry, which served to understand the physical and chemical properties that allow the use of spectroscopic methods to identify the sources of sediment.

This thesis consists of five parts. The first is a literature review that addresses issues as (*i*) the soil erosion: a global issue getting worse in the "conservationist" agriculture context of Southern Brazil, (*ii*) the key issue: where does the sediment come from?, (*iii*) the Brazilian experience on sediment fingerprinting, and (*iv*) development of a rapid, timely, less expensive, non-destructive, and straightforward alternative to fingerprinting sediment sources. The second part describes in details the studied areas and presents the analytical methods employed to identify the sources of sediment.

The third part presents the results obtained for all study sites. The first part of this section presents the results from Arvorezinha catchment. Results from this catchment are separated in source discrimination for classical fingerprinting based on geochemical composition and for alternative methods based on spectroscopy analyses. Later are displayed results about the

building process of partial least-squares regression (PLSR) models based on spectroscopy analyses. Finally, the results of source apportionment for classical and alternative fingerprinting methods using PLSR models and colour parameters derived from visible reflectance measurements are presented. In the second part of this section the results of geochemical fingerprinting to trace sediment origin during rainfall-runoff events of the two catchments from Júlio de Castilhos together are presented. The third and the fourth parts show results of source discrimination and spatial, temporal, and intra-storm variability of sediment source contribution in Conceição and Guaporé catchments, respectively.

The fourth part presents a discussion of results. Unlike the results section, the discussion was not subdivided by study catchment. The discussion section was constructed around broader topics encompassing all the study catchments that are representative of the main geographical conditions found in the state of Rio Grande do Sul. Environmental problems arise from the misuse of natural resources by farmers, especially those related to water erosion. Thereby, first I present some insights on selection of geochemical tracers and source discrimination. Then, I discuss the applicability of spectrometry for fingerprinting sediment sources in Arvorezinha catchment. Later I discuss the inter and intra-storm variation in source apportionment for the five study catchments, while in the last part of discussion section I give an overview of sediment source apportionments in agricultural catchments from Southern Brazil.

Finally, the fifth section presents the conclusions, emphasizing four topics, namely: (*i*) the proposition of guidelines for tracer pre-selection, (*ii*) the use of alternative spectroscopic methods for fingerprinting sediment provenance, (*iii*) the source apportionment at high-spatial and -temporal resolutions, and (*iv*) the influence of soil conservation practices on sediment delivery from cultivated areas. Finally, some recommendations and perspectives for further investigations are provided.

2 HYPOTHESIS

The crop fields where no-tillage is implemented remain the main source of sediment in agricultural catchments of Southern Brazil. The impact of the current application of soil conservation measures in these catchments can be assessed by using the sediment fingerprinting approach.

3 AIM AND OBJECTIVES

3.1 Aim

The aim of this research is to generate new information that can contribute to recommend the improvement of soil conservation practices for reducing the environmental problems associated with runoff and erosion by understanding sediment generation and delivery in cultivated catchments representative of environmental conditions found in Southern Brazil.

3.2 Objectives

i) To refine the fingerprint property selection procedure and to generate recommendations or guidelines for tracer pre-selection in catchments of Southern Brazil.

ii) To validate alternative spectroscopic methods for fingerprinting sediment sources by comparing their results with a more classical fingerprinting based on geochemical tracers, and to improve source discrimination and prediction errors by combining spectroscopic-colour-based fingerprint parameters with geochemical tracers in a single mixed linear model.

iii) To improve understanding of erosion processes in Southern Brazil by generating high-spatial and -temporal resolution source apportionment results, especially during storm-events al throughout the hydrological year.

iv) To estimate sediment delivery from crop fields in order to generate reliable results to promote awareness among farmers on the impact of their soil conservation practices.

4 BACKGROUND: LITERATURE REVIEW

4.1 The soil erosion: a global issue getting worse in the "conservationist" agriculture context of Southern Brazil

Soil erosion is an important phenomenon of degradation of agricultural land worldwide. It is estimated that nearly 60% of current soil erosion is induced by human activity, and that the development of cropland in the last century has increased potential soil erosion by about 17% (YANG et al., 2003). Current estimates of global soil erosion rates by water erosion on agricultural land range from 28.3 Pg yr^{-1} (VAN OOST et al., 2007) to 73.5 Pg yr^{-1} (PIMENTEL et al., 1995). Overall, soil is being lost from land areas 10 to 40 times faster than the rate of soil renewal. As a consequence, about 10 million ha of cropland are lost each year due to soil erosion, thereby reducing the cropland available for food production, endangering future human food security and environmental quality (PIMENTEL, 2006). Growing competition for land, water, and energy resources will soon affect our ability to produce food. In this context , there is an urgent requirement to reduce the impact of the food production systems on the environment (GODFRAY et al., 2010). According to Telles; Guimarães; Dechen (2011), among the various estimates of soil erosion costs between 1933 a 2010, the highest figure was 45.5 billion dollars a year for the European Union, whereas in the United States, the highest figure was 44 billion dollars a year. The same authors found that in Brazil, estimates for the state of Paraná indicate a value of 242 million dollars a year, and for the state of São Paulo, 212 million dollars a year, highlighting that, above all, conservation measures must be implemented if crop and livestock farming production are to be sustainable.

In the entire Brazilian territory, the agricultural activities are among those that most disturb the environment, by increasing the soil exposition to erosion processes, accelerating the transfer of sediments and contaminants to water bodies. Soil erosion in Brazil is considered as the main factor of degradation of agricultural land (GUERRA et al., 2014). In the 1990s, Brazil was one of the few countries in the world that increased agricultural area, estimated to reach 250 million hectares by 2000, and it currently occupy 27.6% of its territory for agricultural activities, whilst protected areas currently cover about 55 million hectares (MANZATTO; JUNIOR; PERES, 2002). Moreover, according to Merten; Minella (2013), during the next 10

years Brazil's agricultural area will expand to meet increased domestic and worldwide demand for food, fuel, and fiber. These authors warn that the present choices regarding land use will determine to what degree this expansion will have adverse effects that include soil erosion, reservoir siltation, water quality problems, loss of biodiversity and social conflicts, especially around indigenous reservations. Nowadays, available studies compiled by Guerra et al. (2014) show that total soil loss often exceeds 50 t ha^{-1} yr^{-1} and can exceed 100 t ha^{-1} yr^{-1}, which makes Brazil one of the global erosion 'hotspots'.

In the modern era, the intensification of agriculture in Brazil was strongly influenced by the technologies used in Northern countries as a result of the various immigration phases experienced by the country (CASÃO JUNIOR; ARAÚJO; LLANILLO, 2012). In the 1950s and 1960s, conventional tillage with plowing and heavy harrowing were frequently preceded by residue burning to reduce biomass volume in order to facilitate mechanical operations. This production system caused soil erosion losses of up to 10 t ha^{-1} per ton of grain produced, resulting in huge environmental impacts and loss of cultivated land (CASÃO JUNIOR; ARAÚJO; LLANILLO, 2012). Consequently, in the 1970s, several separate initiatives arose in the south of Brazil seeking to modify the soil management system towards a more conservationist approach.

Nowadays, Brazil is a leader in the development of conservation agriculture practices and technology in South America. It has encouraged the dissemination of conservation agriculture throughout the region through an effective and innovative network of farmers and their associations, under the form of private and public partnerships (SPERATTI et al., 2015). The widespread adoption of no-till system (NTS) was one of the largest evolutions for Brazilian agriculture since the Green Revolution (which actually began at the end of 1940, but the term Green Revolution only appeared after 1966, in Washington). The NTS is based on some basic principles as the reduction or elimination of soil disturbance, the maintenance of permanent soil cover with plant residues or living plants as long as possible, the diversification of crops by growing multiple species, in rotation, succession and/or in intercropping, and the implementation of mechanical runoff control measures for soil conservation. This management system is sustainable and highly productive, it improves the structure, the aggregation and porosity of the soil, maximizes nutrient cycling and stimulates soil biological activity, thereby protecting the soil against erosion. Furthermore, NTS promotes soil carbon sequestration, and offers a strategy to achieve food security through the improvement of soil quality (GEBHARDT et al., 1985; LAL, 2004). The widespread adoption of NTS (no-tillage, crop rotations, soil cover/cover crops) was undoubtedly one of the factors responsible for the evolution of Brazilian

agriculture, especially in the last two decades, which has raised incomes and sustainability in the regions of intensive agriculture in Brazil (CASÃO JUNIOR; ARAÚJO; LLANILLO, 2012). In this regard, results obtained by Merten et al. (2015) in a 14-years experiment in Southern Brazil aiming to evaluate soil and surface runoff losses on small and large plots with differing slope lengths, cropping sequences, and tillage systems, shows that when compared with conventional soil tillage (disk plow + lighter off-set disk-harrow or heavy off-set disk-harrow + lighter off-set disk-harrow), soil losses under NTS were > 70% lower. However, the authors warn that the benefit of reduced surface runoff losses was less evident, suggesting the need to implement additional practices to control surface runoff to avoid transport of pollutants to waterways.

Unfortunately, only a small fraction of farmers in Brazil respect the fundamental principles of NTS, and, as a rule, the only principle broadly used by farmers is to avoid soil disturbance with plowing and harrowing because sowing without soil disturbance is less labor intensive. After the consolidation of the "no-till" (NT – note hereafter NT means not plowing, which is different than NT as a system) mechanization in Brazil, the area without soil disturbance (including areas with no soil disturbance cultivation or "NT" and areas under NTS) for crop production has exponentially increased from 1 million hectares in the beginning of the 1990's to 31.8 million hectares in 2011/12, representing approximately 25% of the area under NT in the world (FEBRAPDP, 2013).

The southern region has the highest percentage of area under high use intensity in Brazil (41% of total area) (MANZATTO; JUNIOR; PERES, 2002). In the state of Rio Grande do Sul, the area under NT for grain production covers approximately 90% of the cultivated area (DIDONÉ et al., 2014). Influenced by colonization of European immigrants, agrarian activity in the southern region is different from cultivation in other regions of the country, formed predominantly by small farms, usually organized in cooperatives (MANZATTO; JUNIOR; PERES, 2002). Notwithstanding, the agricultural traditionalism did not avoid problems such as loss of productivity due to soil erosion problems, even in these areas under NT. The primary reasons for these problems are the abandonment of mechanical practices for runoff control, the soybean monoculture neglecting crop rotation, the low biomass input reducing soil cover, and the excessive and uncontrolled traffic of heavy agricultural machinery (often under unfavorable moisture conditions). Even worse, local farmers interpret the use of mechanical practices for runoff control (e.g. terraces) as an obstacle to daily activities (e.g. planting, harvesting, and phytosanitary treatments) and as an additional cost due to longer time spent when driving between plots parallel to the contours of the terrain (DIDONÉ et al., 2014). Moreover, the

majority of rural roads are built without planning, following the main slope line, and many principal roads and secondary access paths are often damaged by rills and gullies which disturb agricultural activities and increase maintenance costs (THOMAZ; VESTENA; RAMOS SCHARRÓN, 2014).

In Rio Grande do Sul State, it is noticeable that most farmers neglect soil losses in crop areas under NT. This perception is even more strongly rooted for those who participated to the transition from conventional soil management with soil plowing to no-till system. For that time where soil was plowed, there are reports of soil loss of arable layer up to 20–30 cm during a single rainfall event after soil plowing, resulting in complete obstruction of local streams. Keeping these experiences and images in mind, soil losses under no-till conditions are erroneously considered by local farmers as insignificant. Indeed, as observed in Ethiopia by Moges; Holden (2007), the perception of soil degradation by farmers is mainly triggered by a reduction of crop yields. In this context, as satisfactory productions levels are obtained thanks to the large input of fertilizers, the general farmer's perception is that there is no soil degradation in areas with NT in RS state although soil losses remain significant. The soil degradation problem in Southern Brazil is complex and encompasses environmental, economic, social and political issues (PELLEGRINI J., 2011). However, to promote awareness among farmers, there is still a lack of consistent data to demonstrate the impact of their practices on water resources. A preliminary study on the impact of no-tillage agricultural systems on sediment yield in two large catchments in Southern Brazil was conducted by Didoné et al. (2014). Due to the responses during high magnitude events, the authors conclude that soil management systems used by farmers in both catchments are still inefficient to reduce (mitigate) runoff and erosion in areas with crops. However, the relative contribution of the potential sources of sediment under these conditions in Southern Brazil remains unknown.

4.2 The key issue: where does the sediment come from?

Soil erosion is a well-known problem that generates both on-site and off-site effects. On-sites problems are related to the decrease of soil fertility and water retention capacity which have direct effects on crop productivity (EVANS, 2005; LI et al., 2007; LI; SHAO, 2006; QUINTON et al., 2010; YAO et al., 2009; ZHANG; YANG; ZEPP, 2004). Off-site problems are related to the siltation of dams, reservoirs and channels (KONDOLF et al., 2014), as well

as to the degradation of aquatic environments caused by the accelerated transport of nutrients (MARTÍNEZ-CARRERAS et al., 2012) and pollutants to the water bodies. The link between sediment produced on hillslopes and its impacts on the quality of watercourses is not straightforward, as it is controlled by complex mechanisms resulting from the specific hydrosedimentological behavior of each river catchment (MINELLA; MERTEN, 2011). Therefore, a major limitation of most studies on sediment transfer, whether quantitative or qualitative, is the lack of information about the origin of the sediments (COLLINS; WALLING, 2004). Information on sediment sources is required to design effective sediment control strategies, to understand nutrient and pollutant transport, and to develop soil erosion models (NOSRATI et al., 2014; WALLING; COLLINS, 2008). Recently, there has been a growing interest in studies aiming to understand spatial patterns of suspended sediment sources in order to have a better description of the connection processes between sediment sources and sinks as well as the planning of natural resources (WALLING, 2013b).

The contribution of sediment sources can be assessed by direct and indirect methods. Traditional methods employ indirect approaches as visual observations and erosive activity measurements. Aerial photographs can provide evidence of the impact of channel and gully erosion and rill and interrill erosion (DAY et al., 2013). Geographical Information Systems (GIS) and remote sensing can also be used to assess vulnerability to soil erosion risk (DENGIZ; YAKUPOGLU; BASKAN, 2009). Erosion plots can be used to determine soil loss rates from surface sources (ANH et al., 2014). However, according to Collins; Walling (2004) the use of indirect methods to investigate the contribution of sediment sources to river suspended matter usually face two main limitations: *i*) practical, logistical and sampling constraints due to the large spatial and temporal variability of sediment sources; and *ii*) economic constraints, since the cost of using several methods limited the spatial and temporal coverage duration of monitoring programs.

Direct methods for estimating sediment origin are based on the fact that physicochemical properties of suspended sediment in the river are related to those from the main sediment sources. A wide range of tracer properties have been employed for this purpose, such as color (ERSKINE, 2013; KREIN; PETTICREW; UDELHOVEN, 2003; MARTÍNEZ-CARRERAS et al., 2010b, 2010c), magnetic susceptibility (BLAKE et al., 2006; CAITCHEON, 1998, 1993; LIU et al., 2010; QUARANTA et al., 2014), plant pollen content (CLARK, 1986), rare earth oxides (DEASY; QUINTON, 2010), soil enzymes (NOSRATI et al., 2011), organic carbon (BEN SLIMANE et al., 2013), stable isotopes of nitrogen and carbon ($\delta^{15}N$ and $\delta^{13}C$) (MCKINLEY; RADCLIFFE; MUKUNDAN, 2013), compound-specific

isotope analysis (BLAKE et al., 2012; HANCOCK; REVILL, 2013), natural radionuclides, such as ^{238}U, ^{232}Th, ^{40}K (ZEBRACKI et al., 2015), isotopes ratios ($^{208}Pb/^{206}Pb$ and $^{207}Pb/^{206}Pb$ - BIRD et al., 2010), mineralogy (DE BOER; CROSBY, 1995; FRYIRS; GORE, 2013; KOUHPEIMA et al., 2012; MIGUEL et al., 2014b; PRIZOMWALA; BHATT; BASAVAIAH, 2014; RAVAIOLI; ALVISI; VITTURI, 2003), geochemical composition (STONE et al., 2014), fallout radionuclides ^{137}Cs, ^{210}Pb, and ^{7}Be (BELYAEV et al., 2013; GOLOSOV; BELYAEV; MARKELOV, 2013; HUGHES et al., 2009; LIM et al., 2014; MATISOFF, 2014; OLLEY et al., 2013; PORTO; WALLING; CALLEGARI, 2013; WALLING, 2013a).

The most widespread and successful tracers are fallout radionuclides (^{137}Cs, ^{210}Pb, ^{7}Be), and the geochemical composition (D'HAEN; VERSTRAETEN; DEGRYSE, 2012; DAVIS; FOX, 2009; GUZMÁN et al., 2013; HADDADCHI et al., 2013; KOITER et al., 2013a; MUKUNDAN et al., 2012). According to Haddadchi et al. (2013), physical tracers, as color, density, and fine sediment dimensions, are less expensive and can be measured easily, but they are not conservative and may lead to ambiguity in interpretation of results. Geochemical tracers are favored due to the large number of elements available for sediment fingerprinting; and radionuclide tracers are the most powerful tracers to distinguish soils from different land uses, but need expensive instruments. Moreover, fallout radionuclide tracers are well-suited for use in heterogeneous watersheds since their concentrations are effectively independent of soil type and underlying geology (WALLING, 2005). Tracers like C, N, C/N, P, and fallout radionuclides are recognized to provide a clear distinction between subsoil and topsoil sources (NAZARI SAMANI; WASSON; MALEKIAN, 2011). In addition, Belmont et al. (2014) demonstrated that differences in sediment apportionment from ^{10}Be, $^{210}Pbex$, and ^{137}Cs measurements can be used to estimate the fraction of suspended sediment transported during the observed storm event that participates in channel–floodplain exchange.

The use of only one tracer characteristic is often not sufficient to discriminate the sources, especially in studies involving a large number of potential sediment sources. Yu; Oldfield (1989) demonstrated that the quantitative resolution of multiple sediment sources can be achieved by using composite signatures ("fingerprints") involving multiple tracers that are statistically different among the sediment sources. Thereby, over the past three decades, an approach known as "fingerprinting" has been developed, applied, and improved by researchers worldwide to address the sediment origin. The growth of sediment source fingerprinting studies since their beginning in the mid-1970s up to 2012 indicates that there has been a near exponential increase in sediment source fingerprinting studies (WALLING, 2013b). Today, this approach is a consolidated technique widely used to quantify the contribution of non-point

sediment sources through the use of a range of natural tracers combined with rigorous statistical modeling techniques, becoming a valuable tool to assist in developing strategies for effective remediation of pollution in watersheds (D'HAEN; VERSTRAETEN; DEGRYSE, 2012; DAVIS; FOX, 2009; HADDADCHI et al., 2013; KOITER et al., 2013a; MUKUNDAN et al., 2012). Nevertheless, according to Laceby et al. (2015), although an underlying premise of the composite fingerprinting technique is that the inclusion of more elements is beneficial to sediment tracing research, it may be as important to understand the utility of a few meaningful elements and their geological foundation for discrimination rather than solely relying on statistical techniques for determining elemental discrimination.

In a recent review, Walling (2013b) listed the seven key advances and developments achieved in sediment source fingerprinting investigations over the past 30 years. Firstly, he mentioned the use of composite fingerprints and an expanding range of fingerprint properties to improve the discrimination between potential sources. This was essential for increasing the number of potential sources to be considered in fingerprinting investigations. Secondly, he reported the use of statistical tests to confirm the ability of particular fingerprint properties to discriminate between potential sediment sources and to assist in the selection of the 'best' properties to include in a composite fingerprint. Thirdly, he referred to the use of numerical mixing (or unmixing) models to provide quantitative assessments of the relative contribution of different potential sources. The fourth advance was the recognition of the need to ensure that fingerprint properties behave conservatively and to take account of grain size and organic matter enrichment/depletion effects when comparing the properties of target samples with those of potential sources. The fifth was the extension of the approach to consider an increased range of 'targets', in addition to discrete samples of suspended sediment collected from a sampling site, and to include a greater range of potential sources. The sixth was addition of a temporal dimension, in order to study changes in sediment source through time. Finally, the seventh was the assessment of the uncertainty associated with source apportionment results.

In fingerprinting studies, sediment provenance can be defined as spatial sources or source type (COLLINS; WALLING, 2004; WALLING, 2005, 2013b). Spatial source can be different sub-basins or areas characterized by different rock types or land use types in a catchment or river basin. Source types are independent of spatial location. It involves consideration of the processes responsible for mobilizing sediment, as sheet erosion, rill erosion, gully erosion, channel erosion, mass movements and mobilization of sediment from unpaved roads and urban surfaces. Because spatial source information can be obtained by measuring and comparing the sediment loads of individual sub-basins or tributaries, it is

investigated to a much lower extent than source types in fingerprinting studies. Information on source type, however, is very difficult to obtain using traditional monitoring techniques and, has therefore been targeted more often in studies for identifying sediment provenance.

4.3 The Brazilian experience on sediment fingerprinting

Although studies of identification of sediment sources are important for understanding the diffuse pollution processes, most of the hydrosedimentological research developed at the watershed scale in Brazil was focused primarily on the interpretation of sediment yield data in terms of magnitude of erosion rates and water quality (MINELLA; MERTEN, 2011). Most sedimentological studies in Brazil aims to estimate the silting of reservoirs on major rivers (ARAÚJO, 2003; BRONSTERT et al., 2014; DE ARAÚJO; GÜNTNER; BRONSTERT, 2006). These studies are usually based on a weak monitoring program. In Brazil, there has never been major interest in studying erosion processes, and in a minor extent, the fine erosion processes. In addition, there is no requests or interest in quantifying water quality problems due to agricultural activities because the perception of the off-site effects is still unclear for the Brazilian decision makers.

So far, studies on the identification of sediment sources have been published for only six Brazilian catchments, five of them in the state of Rio Grande do Sul. Besides, all of them are very recent (published after 2007). The surprisingly low number of studies on identification of sediment sources in Brazil (especially outside of the Rio Grande do Sul state) when compared to their massive use around the world rises some questions, such as follow: is the method less widespread due to a lack of knowledge or due to a distrust about the approach? Due to indisposition of researchers or a lack of resources and infrastructure to go through? A wider search in the rest of South America reveals that the use of fingerprinting approach is even more incipient. So far, only one fingerprinting study was found to document suspended sediment sources in small forested catchments in south-central Chile (SCHULLER et al., 2013). The main reason for this is unclear. Notwithstanding, despite recognizing the importance of knowledge on spatial patterns of the main diffuse sources of pollution, such as sediment, it seems that there is general lack of interest for fingerprinting sediment sources in fluvial systems in South America.

Four of the six target catchments for fingerprinting studies in Brazil are small rural watersheds (Table 2). Namely: Agudo catchment (1.68 km^2 – MINELLA et al., 2007), Arvorezinha catchment (in the entire catchment, covering an area of 1.19 km^2 - CLARKE, 2014; MAIER, 2013; MINELLA; WALLING; MERTEN, 2008, 2014; MINELLA et al., 2007, 2009, and in a sub-catchment of 0.57 m^2 - MINELLA; MERTEN; CLARKE, 2009), Júlio de Castilhos catchment (0.80 km^2 – TIECHER et al., 2014), and Vacacaí-Mirim catchment (20 km^2 – MIGUEL et al., 2014a, 2014b). The two other catchments are located in urban areas (Table 2). Poleto; Merten; Minella (2009) evaluated the main sediment sources in a small residential urban watershed (0.83 km^2) in the suburbs of Porto Alegre, the capital of Rio Grande do Sul state, in Southern Brazil. Franz et al. (2014) studied the sediment sources deposited in the artificial Lago Paranoá in the capital of Brazil, Brasília, in Central Brazil (total catchment area of 950 km^2), as well as in the sub-catchment of Riacho Fundo (224 km^2).

The small rural catchments from the municipalities of Agudo and Arvorezinha are both located in steep areas where the dominant activity is small-scale tobacco cultivation with soil plowing. The two catchments showed a similar pattern of sediment sources contributions (Table 2): in Agudo catchment, the contribution of crop land topsoil was 68%; unpaved roads 28%, and river drainage network 4%; in Arvorezinha catchment, the contribution of crop land topsoil was 55%; unpaved roads 38%, and channel bank 7% (MINELLA et al., 2007). Minella et al. (2009) also found that the fingerprinting approach was effective in detecting changes in the contribution of sediment sources due to the adoption of conservation practices in the crop land areas at Arvorezinha catchment, such as cultivation of winter cover crops and implementation of minimum tillage. After the adoption of these practices, the contribution of crop land areas in sediment yield decreased from 62 to 54%, and the contribution of unpaved roads decreased from 36 to 24%. On the other hand, the contribution of channel banks increased from 2 to 22%. Thus, whilst demonstrating the value of introducing mini- mum-till practices to reduce sediment mobilization and delivery, the results of the study also demonstrated the need to take a wider view of catchment management and to also target stream channels if further reductions in sediment yield were required. The authors showed that after introduction of improved soil management practices, up to more than 40% of the sediment mobilized from the catchment during individual storm events was derived from stream channels, whereas previously the maximum contribution from stream channels was an order of magnitude less.

Table 2 – Summary results of sediment source apportionment obtained in fingerprinting studies conducted in Brazil. RS, Rio Grande do Sul. DF, Distrito Federal.

Catchment	State	Area (km^2)	Period	Sediment source contribution (%)								Reference
				Crop field	Unpaved road	Stream channel	Topsoil	Urban areas	Agricultural areas	Natural areas	Paved roads	
Agricultural catchments												
Agudo	RS	1.68	Apr/2003–Jun/2004	68	28	4	-	-	-	-	-	Minella et al. (2007)
Arvorezinha	RS	1.19	Apr/2003–Jun/2004	55	38	7	-	-	-	-	-	Minella et al. (2007)
Arvorezinha sub-catchment	RS	0.57	Apr/2002–Oct/2002	64	36	-	-	-	-	-	-	Minella; Merten; Clarke (2009)
Arvorezinha pre-treatment period	RS	1.19	May/2002–Jul/2003	61	37	2	-	-	-	-	-	Minella; Walling; Merten (2008), Minella et al. (2009)
Arvorezinha post-treatment period	RS	1.19	Oct/2003–Mar/2006	53	29	18	-	-	-	-	-	Minella; Walling; Merten (2008), Minella et al. (2009)
Arvorezinha	RS	1.19	May/2002–Jul/2003	63	36	2	-	-	-	-	-	Minella; Walling; Merten (2014)
Vacacaí-Mirim	RS	20.0	May/2011–Dec/2011	-	35	3	62	-	-	-	-	Miguel et al. (2014a)
Vacacaí-Mirim	RS	20.0	May/2011–Dec/2011	-	31	35	34	-	-	-	-	Miguel et al. (2014b)
Júlio de Castilhos	RS	0.80	May/2009–Apr/2011	44	56	-	-	-	-	-	-	Tiecher et al. (2014)
Urban catchments												
Arroio Mãe d'Água	RS	0.83	Jan/2003–Dec/2006	-	23	31	-	-	-	-	46	Poleto; Merten; Minella et al. (2009)
Lago Paranoá	DF	950.0	2011	-	-	-	-	85	5	10	-	Franz et al. (2014)
Riacho Fundo	DF	224.0	2011	10	7	-	-	78	-	5	-	Franz et al. (2014)

According to Minella; Walling; Merten (2008), the coupling of sediment source tracing and more traditional monitoring techniques must be seen as providing both an improved understanding of improved management practices on the sediment response of a catchment as well as important information to inform the design and implementation of effective sediment management and control measures.

More recently, Minella; Walling; Merten (2014) combined ^{137}Cs measurements with monitoring of sediment yield to fingerprint the sources of the fine sediment export to establish a provisional sediment budget for Arvorezinha catchment. The information provided by the three primary data sources has been integrated to establish the sediment budget for the catchment over the past 57 years. The budget calculations indicate that the Arvorezinha catchment has a sediment delivery ratio of about 15%. In another recent fingerprinting study in Arvorezinha catchment, Clarke (2014) found that it is more appropriate to use the inequality constraint $0 < P_s < 1$ instead of the more commonly used constraint $0 \leq P_s \leq 1$, as a watershed region identified as a potential sediment source will always make some contribution to suspended sediment load but will never contribute all of it.

Miguel et al. (2014a) evaluated the contribution of the major sources of sediment production from a hillside catchment area with the predominance of shallow soils and family farming. The catchment is located in the central region of Rio Grande do Sul, and the dominant land use is native forest, followed by native grassland, shrubland, annual crops, and a few plantation of *Eucalyptus* spp. and urban settlements. Overall the four monitoring periods, the main contribution to sediment production originated from topsoil. However, in the second monitoring period, unpaved roads contribution significantly increased up to 81% in the middle portion of the catchment. Moreover, Miguel et al (2014b) demonstrated that mineralogical variables, such as kaolinite and hematite contents, showed potential to discriminate sediment sources in the same catchment, increasing the predictive power of their model.

Tiecher et al. (2014) have studied the relative contribution of roads and croplands to the overall production of sediments in a rural catchment with the dominance of soybean cultivation under no-tillage in the Rio Grande do Sul plateau region. The authors showed that inadequate soil management in croplands, the lack of planning of access roads, and the absence of mechanical practices for surface runoff control combined with the natural fragility of the soils, have caused the acceleration of erosion processes with negative effects for farmers and society. Roads represented a high percentage of contribution to sediment transfer, but the contribution of cropland increased during heavy rainfall. Comparing the first (from May 2009 to October 2009) and the second sampling period (from October 2009 to July 2010) the amount of rainfall was

much higher than the 30 years average (1.76 times higher), especially during the months of November and December 2009 and January 2010, because of the manifestations of the climate phenomenon El Niño. The authors affirm that the higher rainfall, the soil of crop fields may have reached high humidity conditions over a longer period of time than normal. Thus, during the most intense events, soil infiltration capacity in the crop fields may have been exceeded. This effect combined with low adoption of conservation tillage systems, the lack of crop rotation, and the low soil cover resulted in an increased contribution of crop fields from 30.8% in the first period to 47.8% in the second one. These findings show that the magnitude of rainfall events modifies the proportion of sediment source contributions throughout the year in the catchment area, affecting the process of mobilization of sediments and nutrients towards the river system

Poleto; Merten; Minella (2009) found that paved and unpaved roads and the stream channel itself contribute, on average, 46, 23, and 31%, respectively, to the suspended sediment flux in a small residential urban watershed in Southern Brazil (*Table 2*). Furthermore, they demonstrated variations in source contributions at both inter-event and intra-event scales, depending on local precipitation patterns. Moreover, the authors indicated that the level of uncertainty in source apportionments tends to decline with increasing numbers of tracers; hence, successful sediment fingerprinting and source apportionment in complex hydrologic environments, such as urban watersheds, may require the use of a larger number of chemical and/or physical tracers.

Franz et al. (2014) derived valuable information on the response of the main sediment sources in a fast growing agglomeration with an emphasis on specific land uses and human activities. They found that construction sites and sparse residential areas around Brasilia city were the major sources (74±3%) of the sediment deposited in the Lago Paranoá, while areas with (semi-) natural vegetation and natural gullies contributed 10±2%, and agricultural sites have only provided a minor sediment contribution of about 5±4% within at the entire catchment scale. However, as the proportion of the total area with agricultural land and farm tracks is very low, their contribution of sediment to the Lago Paranoá emphasize that topsoils of crop land and farm tracks are strongly connected to erosion and sediment generation. Moreover, the authors stated that the model results confirmed the hypothesis that natural areas are less vulnerable for sediment mobilization, and that a dense vegetation cover might be one of the most effective strategies to reduce sediment mobilization.

Although most of Brazilian watersheds where fingerprinting approaches were conducted are located in different environments, with regard to relief, steepness, lithology, soil type, land use, and soil management, some general findings demonstrate that:

(i) The fingerprinting approach is a suitable tool to study sediment sources in Brazilian environmental conditions;

(ii) The unpaved roads provide a relevant contribution to the total sediment yield (20– 80%), even in urban areas, although the contribution found in the smaller catchments might not necessarily be extrapolated to larger catchments;

(iii) Crop fields are the main source of sediment in steep areas under tobacco cultivation with soil plowing. However, there is still a need to generate reliable results to promote farmers awareness about the impact of their practices on water resources.

4.4 Development of a rapid, timely, less expensive, non-destructive, and straightforward alternative to fingerprinting sediment sources

The wider use of the fingerprinting approach as a management tool is hampered for several reasons. The main cause is the absence of universal recommendation or guidelines for tracer pre-selection because successful fingerprint properties are highly site-specific, making parameter selection time-consuming and costly (COLLINS; WALLING, 2002), i.e. source material properties that provide good discrimination between potential sources in one catchment may not prove successful in an adjacent catchment. Moreover, traditional analysis such as loss-on-ignition, colorimetry, and total chemical analysis, tend to be expensive, time consuming, and destructive. In addition, these techniques demand large quantities of samples, complicating the comparison with suspended sediment samples that are often available in low quantities (COOPER et al., 2014; GUZMÁN et al., 2013). Thus, there is a challenge to develop methods easily applicable to a large number of samples involving minimal sample preparation remaining efficient in detecting potential sediment sources.

In this sense, Poulenard et al. (2009) developed a first attempt to use spectroscopy to directly fingerprint sediment sources in watersheds. They demonstrated that spectroscopy analysis coupled with chemometric multivariate analysis methods, provided a way to quantify the contribution of different sources to river sediment, and developed an effective property capable of differentiating between potential sources. Fingerprint sediment sources using spectroscopy analysis was successfully used to discriminate and predict sediment origin of both source types (POULENARD et al., 2009) and spatial sources (POULENARD et al., 2012). Spectroscopy has been largely employed during the last decade as a rapid, timely, less expensive, non-destructive, and straightforward alternative to quantify physicochemical soil properties (CAÑASVERAS SÁNCHEZ et al., 2012; VISCARRA ROSSEL; MCGLYNN; MCBRATNEY, 2006; VISCARRA ROSSEL et al., 2006a, 2006b, 2009). The wavelengths frequently used for this purpose correspond to the ranges of ultra-violet (UV – from 10 to 400 nm), visible (VIS – from 400 to 700 nm), near-infrared (NIR – from 700 to 2,500 nm, also subdivided into short wave infrared - SWIR from 1,100 to 2,500 nm), and mid-infrared (MIR – from 2500 to 2,5000 nm). Recently, MIR (COOPER et al., 2014; EVRARD et al., 2013; POULENARD et al., 2009, 2012) and VIS-NIR (BROSINSKY et al., 2014a, 2014b; MARTÍNEZ-CARRERAS et al., 2010a, 2010b, 2010c; VERHEYEN et al., 2014) spectroscopy has been applied to trace suspended sediment sources.

The electromagnetic radiation interacts with soil in macroscopic and microscopic ways. The first interaction is related to the phenomena of refraction, diffraction, and scattering of the incident energy. Macroscopic interactions are responsible for the variations of reflectance and are affected by the physical and textural characteristics of the soil (particle size distribution, shape, size, structure, roundness, and grain packaging). However, the microscopic interaction is the main aspect to be considered in reflectance spectroscopy because it occurs on the soil functional groups, both organic and mineral. These functional groups are responsible of chemical processes such as adsorption, desorption, cation and anion exchange, and of physical processes such as water retention and micro aggregation. They also control biological processes such as enzymatic activity, decomposition and mineralization.

Soil microscopic absorption of electromagnetic energy occurs in two ways depending on the energy level of each wavelength: atomic level (or electronic level) or molecular level. The atomic level, there is a change in energy level of the electrons, which is related to transitional processes and electronic rearrangement of valence electrons (Figure 1). This process occurs in short waves (shorter than 1000 nm), because it requires a greater amount of energy. The absorption or reflectance in the visible range directly affects the perceived color of

soil. Because the energy of the UV-VIS radiation is high, electronic excitations are the main processes in this spectral region. Therefore, due to the broad and overlapping bands, UV-VIS spectra contain fewer absorptions features than the MIR region, which may hinder interpretation (STENBERG, 2010). Nevertheless, this region contains useful information on organic and inorganic soil constituents, such as the absorptions at 400–780 nm associated to iron oxides (e.g., haematite, goethite), and broad absorption bands assigned to chromophores of organic matter (STENBERG, 2010).

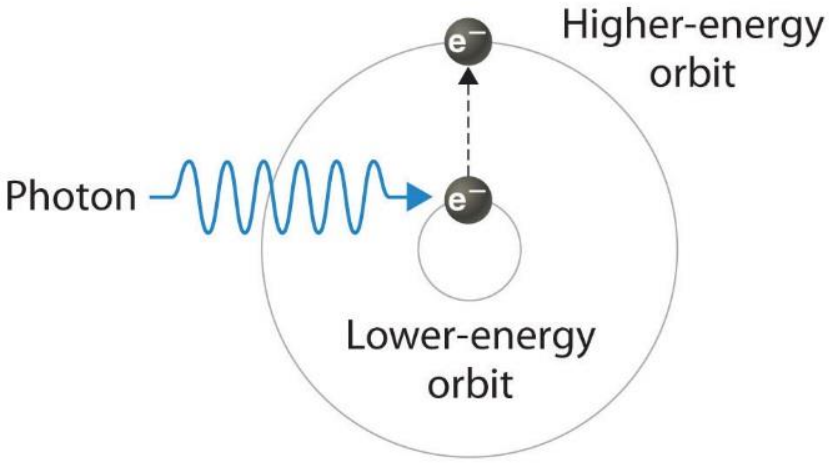

Figure 1 – The emission of light by a hydrogen atom in an excited state (AVERILL; ELDREDGE, 2015).

At the molecular level, the electromagnetic radiation is related to the vibration of molecules from functional groups of soil constituents. This process requires less energy and occurs at wavelengths higher than 1000 nm, producing more intense, defined and pronounced absorption features. The molecular vibrations can be stretching, caused by alterations in charge of the ligands atoms, or deformation, resulting from the dipole moment originated by induction of electric field of the molecule (Figure 2). The molecular vibrations can be divided into fundamental and non-fundamental vibrations. The fundamental vibrations occur between 2500 and 25000 nm, and are the most useful vibrational frequencies. They are intense and well defined, and result from the association of Fe, Al, Si and Mn with O in the oxides. The non-fundamental vibrations occur between 1100 and 2500 nm and are considered to be a

propagation of fundamental vibrations. These are secondary vibrations of lower intensity and are not as well defined. The non-fundamental vibrations can be further divided into *overtones* (2 ν) when a molecule is excited twice or more, and *combination-tones* (ν + δ), when the molecule is excited by the sum of two or more fundamental vibrations.

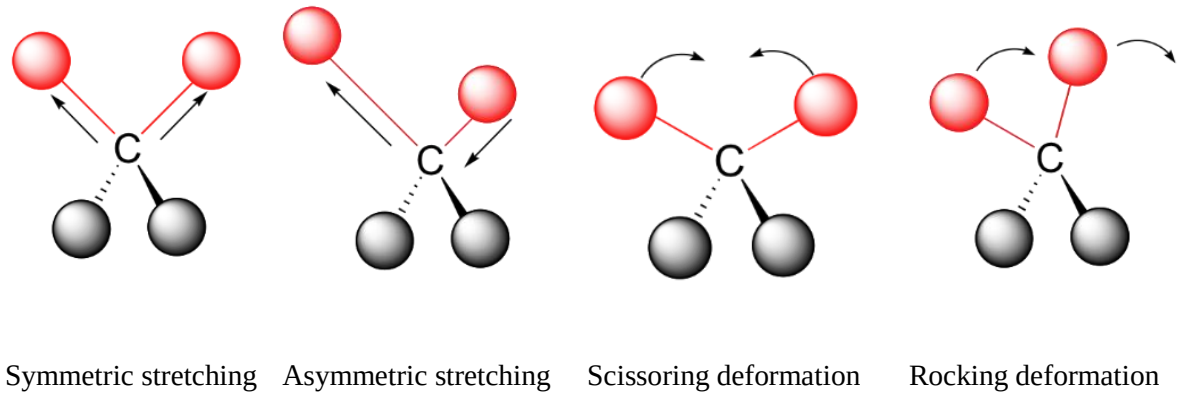

Figure 2 – Examples of vibrational modes. Adapted from Larsen (2015).

As a prerequisite for the inclusion of tracer properties in sediment fingerprinting using tracer mixing models, they must have conservative and linear additive behaviors. In this sense, Poulenard et al. (2009, 2012) have demonstrated that MIR spectra remain at least temporarily (i.e. min. 1 month) conservative in the river, while Legout et al. (2013) have demonstrated the same result for VIS-based colour parameters (i.e. min. 2 month). Furthermore, Martínez-Carreras et al. (2010b) conducted an experiment using laboratory mixtures and confirmed that linearity for VIS-based-colour parameters was achieved.

Overall, source fingerprinting studies using diffuse reflectance measurements have been conducted in four different ways. First, there were several attempts using VIS-based-colour parameters and spectral features to trace sediment origin directly in an optimized mixing model. In brief, Martínez-Carreras et al. (2010b, 2010c) have shown the potential of colour parameters as fingerprint properties for discriminating sediment origin in small catchments from Luxemburg with areas ranging from 0.7 to 4.4 km^2, as well as in larger ones with areas ranging from 19.4 to 247 km^2. In the same way, Brosinsky et al. (2014a, 2014b) used both VIS-based-colour parameters and additional 77 spectral features from VIS, NIR, and shortwave-infrared (SWIR) diffuse reflectance spectroscopy in a 445 km^2 catchment of the central Spanish

Pyrenees. Second, Martínez-Carreras et al. (2010a) combined VIS-NIR spectra with partial least-squares regression (PLSR) models to predict the concentrations of geochemical tracers which were then used in an optimized mixing model to trace sediment provenance. In the same way, Cooper et al. (2014) used a combined X-rayfluorescence spectroscopy and diffuse reflectance mid-infrared Fourier transform spectroscopy approach to estimate concentrations for a range of elements (Al, Ca, Ce, Fe, K, Mg, Mn, Na, P, Si, Ti) and compounds (organic carbon, $Al_{dithionate}$, $Al_{oxalate}$, $Fe_{dithionate}$, and $Fe_{oxalate}$) within SPM trapped on quartz fibred filters at masses as low as 3 mg. A third method consists of using directly the whole spectra to estimate the proportion of the different source materials in suspended sediment samples after developing a PLSR model calibrated using artificial source material mixtures (French Alps - Poulenard et al. (2009, 2012); Mexico - Evrard et al. (2013); Ethiopia - Verheyen et al. (2014)). The fourth attempt used by Legout et al. (2013) combined VIS spectra and deduced colorimetric parameters in PLSR models calibrated using artificial source material mixtures.

According to Poulenard et al. (2009), although the results clearly demonstrate the potential for using infrared spectroscopy to fingerprinting sediments in river basins, the results should also be compared with those provided by classic chemical and isotopic fingerprinting methods. Despite all the above-mentioned studies recognized this need, very few works performed this comparison. Evrard et al. (2013) have made a direct comparison of the MIR spectroscopy method and the traditional fingerprinting approach based on the use of geochemical and radionuclides tracers in three rural catchments from Mexico. They found similar results with both methods in only two of the three catchments studied, because the method was very sensitive to the high organic matter content in sediments from one catchment. In this context, the method still needs to be applied to other geological and land-use conditions in order to test the general applicability of MIR spectroscopy to sediment fingerprinting. When tracing primary source materials (geological sub-areas) in a headwater catchment from the French Alps, Legout et al. (2013) found a general good agreement between PLSR models based on visible reflectance and those obtained from a conventional geochemical fingerprinting method (NAVRATIL et al., 2012). Verheyen et al. (2014) proved that fingerprinting based on VIS-NIR spectra offers a great potential and the values obtained are comparable with the ones from more established techniques such as those based on geochemical fingerprints. Martínez-Carreras et al. (2010b) found a good consistency when comparing suspended sediment source apportionments based on color parameters obtained from visible reflectance and apportionments derived from classical fingerprinting parameters based on geochemistry and radionuclides in three small catchments from Luxembourg. They showed that 94% of the

centroids of suspended sediment source ascriptions estimated using the colour-based fingerprinting approach remained within the estimated confidence intervals of the values provided by the classical fingerprinting approach. However, so far, there has not been any attempt to combine VIS-based-colour parameters and geochemical tracers in a single mixed linear model, nor to compare the use of VIS-based-colour parameters and the whole spectra in PLSR for discriminating sediment sources.

5 MATERIALS AND METHODS

5.1 Study catchments

The study was carried out in Rio Grande do Sul, the southernmost state of Brazil. The choice of catchments was guided by the need to characterize the magnitude of erosive and hydrological processes in distinct and representative land use, soil and landscape conditions found in this region. Three small (0.8–1.4 km^2) and two large (804.3–2,031.9 km^2) catchments were chosen (Figure 3) in order to generate results that would reflect broader regional conditions and processes rather than local conditions and specific processes. Table 3 provides a comparison of the main characteristics of the studied catchments, while a more detailed description of each catchment is given in the subsequent sections.

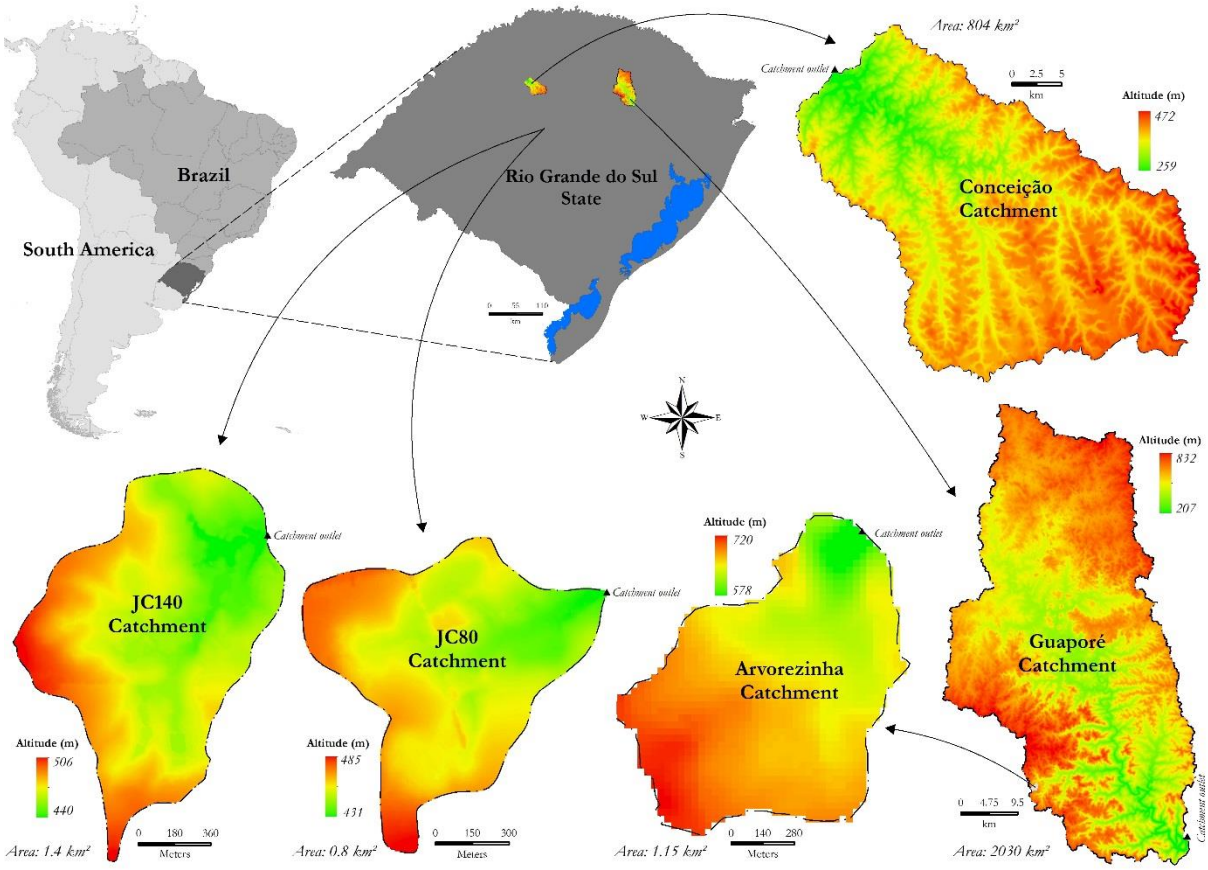

Figure 3 – Location and topography of the five study catchments.

Table 3 – Main characteristics of the monitored catchments.

Characteristic	Catchments				
	Arvorezinha	Júlio de Castilhos		Conceição	Guaporé
		JC80	JC140		
Start of the monitoring	2002	2009	2009	2010	2010
Drainage area	1,19 km^2	0.802 km^2	1.426 km^2	804.3 km^2	2,031.9 km^2
Coldest month	13ºC	11–14ºC		13.9ºC	13.1ºC
Hottest month	23ºC	23–26ºC		24.8ºC	23.0ºC
Annual rainfall	1,250–2,000 mm	1,500–1,700 mm		1,750–2,000 mm	1,400–2,000 mm
Sediment yield	156.0 t km^{-2} yr^{-1} [b]	24.6 t km^{-2} yr^{-1} [c]	66.7 t km^{-2} yr^{-1} [c]	139.7 t km^{-2} yr^{-1} [d]	139.8 t km^{-2} yr^{-1} [d]
Property size [a]	Small	Small		Medium to large	Small to medium
Soil types	Acrisol (57%) Cambisol (33%) Leptosol (10%)	Acrisol (>90%) Cambisol Gleysol Leptosol		Acrisol (2.1%) Ferralsol (83%) Nitosol (17.6 %)	Acrisol (16.6%) Ferralsol (31.2%) Luvisol (24.2%) Leptosol (6.6%) Nitosol (21.4%)
Land use	Crop fields (40.0%) Grasslands (7.0%) Forest (49.0%)	Crop fields (64.0%) Grasslands (29.9%) Forest (1.5%)	Crop fields (64.7%) Grasslands (18.0%) Forest (10.2%)	Crop fields (73.6%) Grasslands (18.2%) Forest (7.8%)	Crop fields (32.5%) Grasslands (9.7%) Forest (56.6%)
Landscape	Undulating relief (7% slope) on top of the catchment and strongly undulating (>15%) in the middle and lower sections, with short and steep hillslopes.	Relief of both catchments is homogeneous, formed generally by gentle and well-rounded hills.		Gentle slopes (6–9 %) on top and hillside slopes and higher steepness (10–14 %) near the drainage channels	Steep slopes in the middle and lower parts of the catchment and gentle slopes at the top of the catchment
Main crops	Tobacco (*Nicotiana tabacum*) in summer, maize (*Z. mays*) crops in spring, oats (*A. strigosa*) and ryegrass (*L. multiflorum*) in winter, and reforestation (*Eucalyptus* spp.)	Soybean (*Glycine max*) in summer and oats (*A. strigosa*) and ryegrass (*L. multiflorum*) in winter for cattle feeding		Soybean (*G. max*) in summer and wheat (*Triticum aestivum*), oats (*A. strigosa*) and ryegrass (*L. multiflorum*) in winter	Soybean (*G. max*) and tobacco (*N. tabacum*) in summer, maize (*Z. mays*) crops in spring, and oats (*A. strigosa*) and ryegrass (*L. multiflorum*) in winter, and reforestation (*Eucalyptus* spp.)
Soil management	Minimum tillage and conventional plow farming	Crop-livestock integration under no-tillage system		No-tillage system (approximately 80%)	No-tillage, minimum tillage, and conventional plow farming

[a] Small <25 ha, medium 25–100 ha, large >100 ha.
[b] Average of 10 years records from 2002 to 2011 (MINELLA; WALLING; MERTEN, 2014).
[c] Average of 2 years records from 2011 to 2012 (PELLEGRINI A., 2013).
[d] Estimative of 2 years records from 2011 to 2012 extended to 10 years series by the use of a discharge rating curve (DIDONÉ et al., 2014).

5.1.1 Arvorezinha catchment

The Arvorezinha catchment is located in the municipality of Arvorezinha, which is in the Central-North region of the state of Rio Grande do Sul (28°52′S and 52°05′W) in Southern Brazil (Figure 4). The Arvorezinha catchment covers an area of 1.19 km^2 within the Guaporé catchment. It represents the headwaters of the Taquari River, a tributary of the Jacuí River, a major river from RS, which supplies with water the metropolitan region of Porto Alegre City, the capital of RS, state where over 2 million people are living.

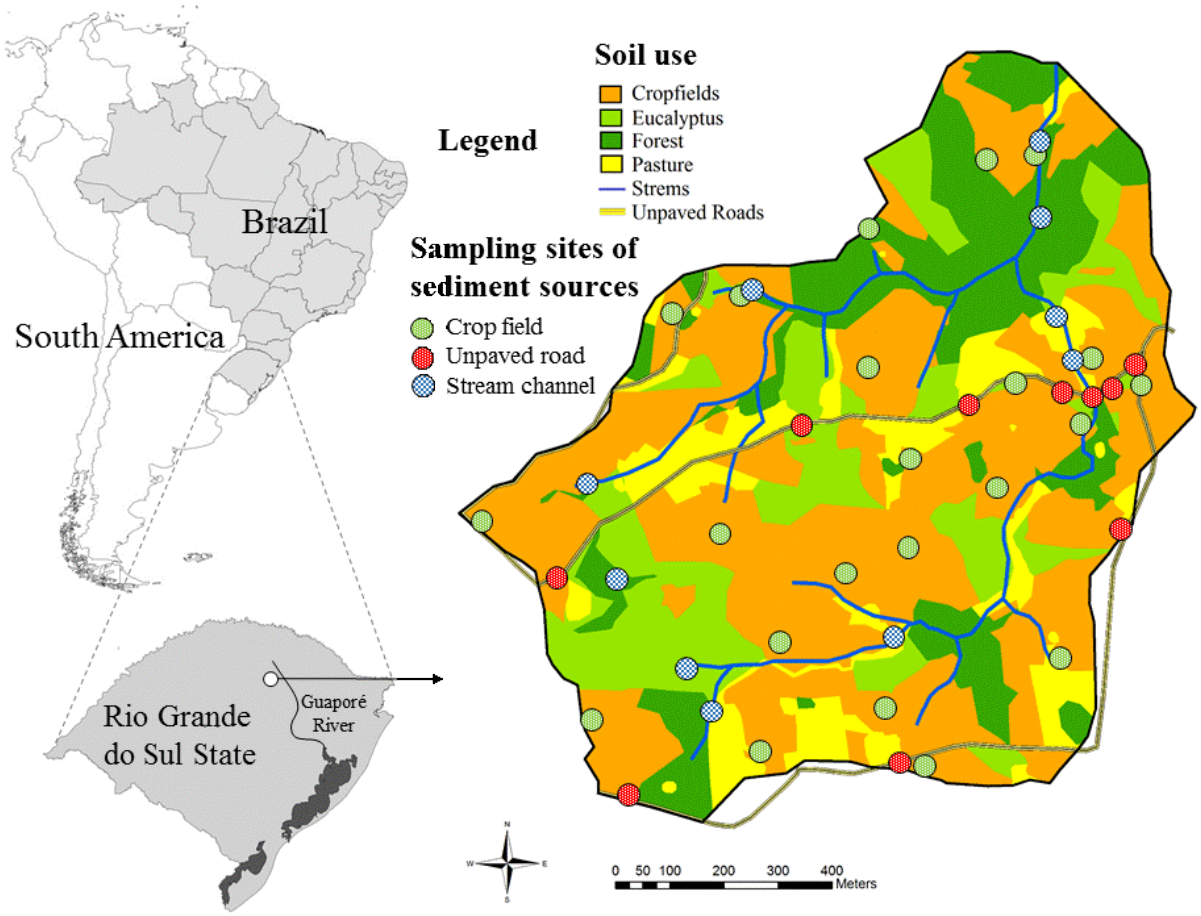

Figure 4 – The location of the Arvorezinha catchment, land use distribution and sampling sites.

The climate is subtropical super-humid meso-thermic (i.e. Cfb) according to the Köppen classification. There are four relatively well-marked seasons and the mean annual precipitation

ranges from 1250 to 2000 mm yr^{-1} well distributed throughout the year. The average annual rainfall is 1,605 mm. The erosivity index (EI30) calculated from 40 years of historical data is 6,540 MJ mm ha^{-1} yr^{-1}, which is considered as moderate to strong (ARGENTA; PANTE; MERTEN, 2001). The elevation ranges between 560 and 740 m a.s.l. and the relief on top of the catchment is undulating (7% slope), and the middle and lower sections is strongly undulating (>15%) with short and steep hillslopes. The time to peak for storm runoff hydrographs typically ranges from 20 to 50 min. The catchment is underlain by acid volcanic rocks (Rhyodacite) and the highly erodible nature of these rocks has resulted in terrain characterized by steep slopes and deep, narrow valleys. Rhyodacite is an extrusive volcanic rock intermediate in composition between dacite and rhyolite. It is a high silica rock containing 20 to 60% quartz with the remaining constituents being mostly feldspar.

The soils are moderately to highly weathered with average depths of about 50 cm (EMBRAPA, 1999). The soil types in the catchment according to World Reference Base for soil resources (WRB) (IUSS WORKING GROUP WRB, 2007) determined from a detailed soil classification survey (1:5000) are Acrisols (57%), Cambisols (33%) and Leptosols (10%). The Acrisols are mainly located in the upper portion of the catchment, which is characterized by an abrupt texture change between horizons A and argic B, and thus there is a discontinuity of water infiltration into the soil profile, due to the low permeability of the argic B horizon (higher clay content). Cambisols appear as specific spots in areas dominated by Acrisols and/or Leptosols. The Leptosols occur in the lower portion of the catchment, where the relief is steep and characterized by the absence of a subsurface horizon. The surface horizon is thus in direct contact with the rock, thereby affecting water flux into deeper layers.

The area is predominantly rural with well-developed agriculture. There is no urban settlement in Arvorezinha catchment. It is located in the rural community of Cândido Brum where 16 families involved in tobacco cultivation live. The agricultural development of the region started around 1925, with the exploitation of mate (*Ilex paraguariensis*) and wood, as well as the cultivation of subsistence crops. The agricultural exploitation of the region gradually intensified until the early 1960s. Aerial photographs from 1960s shows larger agriculture area than currently (LOPES, 2006). Over the past four decades, tobacco has been the dominant crop, although corn and wheat are also grown, both under conventional tillage system with plowing and harrowing. Tobacco crop is cultivated by family farmers following strictly the instructions established by the international tobacco industry, involving application of high doses of both phosphate fertilizers and pesticides. The area covered with cash crops is typically around 35%, varying according to the commodity prices. From 1960s to 1990s, soils were inadequately

managed and protected, causing serious and widespread soil erosion problems. As a result, large amounts of sediment were accumulated along the drainage lines and on the valley floors, changing both the longitudinal and cross-sectional profiles of the drainage channels.

Since the 1990s, there has been increasing concerns about rapid soil loss from agricultural land through the State of Rio Grande do Sul. Increased rates of soil loss resulted in depletion of soil fertility and reduction of crop yields, as well as high diffuse pollution levels in the local rivers and streams. Recognizing both the environmental and the socio-economic dimensions of these problems, the government promoted improved land management aiming to reduce soil erosion and sediment inputs to watercourses, as a key component of its program against rural poverty (PARP). This initiative aimed to promote sustainable use of natural resources, environmental protection, increase family incomes and improve local infrastructure. As in many other areas of the world where such erosion control and sediment management programs have been implemented, the State Government decided to document the impact of the proposed improved land management, in order to evaluate its success, its cost-effectiveness, and promote its wider and longer-term application (MERTEN; MINELLA, 2005).

The current land use and soil management are characterized by the cultivation of tobacco in minimum cultivation (23%), the cultivation of tobacco in the conventional system with plowing (17%), the native forest (20%), afforestation with eucalyptus (23%), grassland (7%), rural settlements (3%), water reservoirs (1%), and regenerating forest (6%) (BARROS et al., 2014b). Table 4 displays the percentage of different land use and management practices in relation to total area in Arvorezinha catchment from 2002 to 2011.

Table 4 – Percentage of different land use and management practices in relation to total area in Arvorezinha catchment from 2002 to 2011.

Year	Crop fields with soil conservation (%)	Crop fields without soil conservation (%)	Forest, fallow, pastures and other uses (%)
2002-2003[a]	0.0	44.1	55.9
2003-2004[a]	21.0	29.7	49.3
2004-2005[a]	19.1	42.3	38.6
2005-2006[a]	43.2	20.8	36.0
2010-2011[b]	31.2	13.5	55.3

[a] Minella; Walling; Merten (2008)
[b] Barros (2012)

5.1.2 Júlio de Castilhos catchments

Two catchments were monitored at Alvorada agrarian reform settlement in the municipality of Júlio de Castilhos, geomorphological region of Planalto das Missões, in Rio Grande do Sul State. The total area of Alvorada settlement is 1,569 ha (Figure 5). Land use has changed dramatically after the implementation of Alvorada settlement in 1996. Until then, the main production system was extensive cattle under natural pasture with small areas of crop for cattle feeding. After the implementation of the settlement, more than 90% of native pastures areas were converted into areas for grain production, mainly soybean and maize (CAPOANE; RHEINHEIMER, 2012). The area was expropriated in February 1996, and then divided into 72 lots (MOREIRA, 2008). The decision to perform these studies in the area was taken in agreement with the INCRA (National Institute of Colonization and Agrarian Reform of Brazil), MDA (Ministry of Agrarian Development), and the settled farmers.

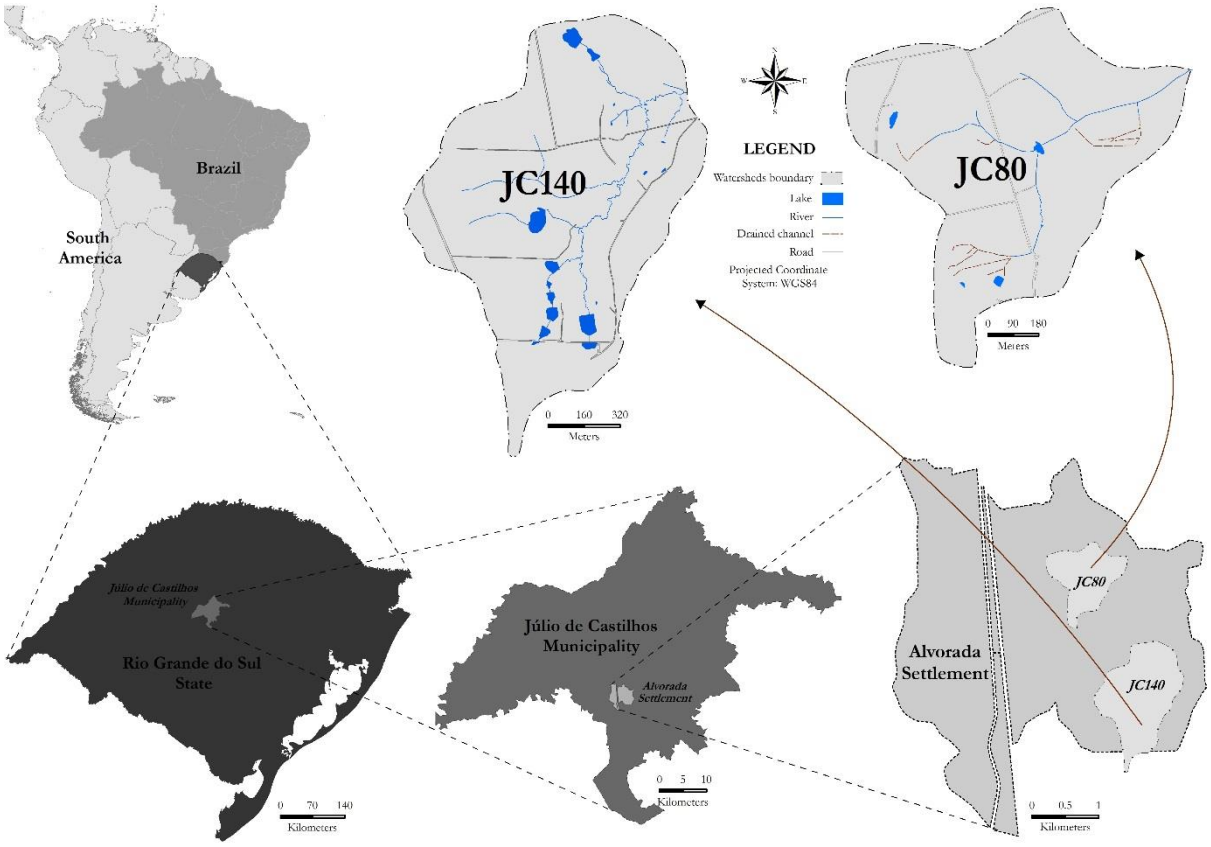

Figure 5 – Location of Alvorada agrarian reform settlement, Júlio de Castilhos, Rio Grande do Sul State.

In the area of Alvorada settlement two study catchments were chosen, for considering different aspects of water resources protection. The total area of the catchments were 80.2 and 142.6 ha, referred hereafter to as JC80 and JC140, respectively. The JC140 catchment is characterized by the larger presence of riparian forest (10.2%) and lower proportion of wetlands whereas the JC80 has lower proportion of riparian vegetation (1.5%), but it has a large wetlands area (Figure 6).

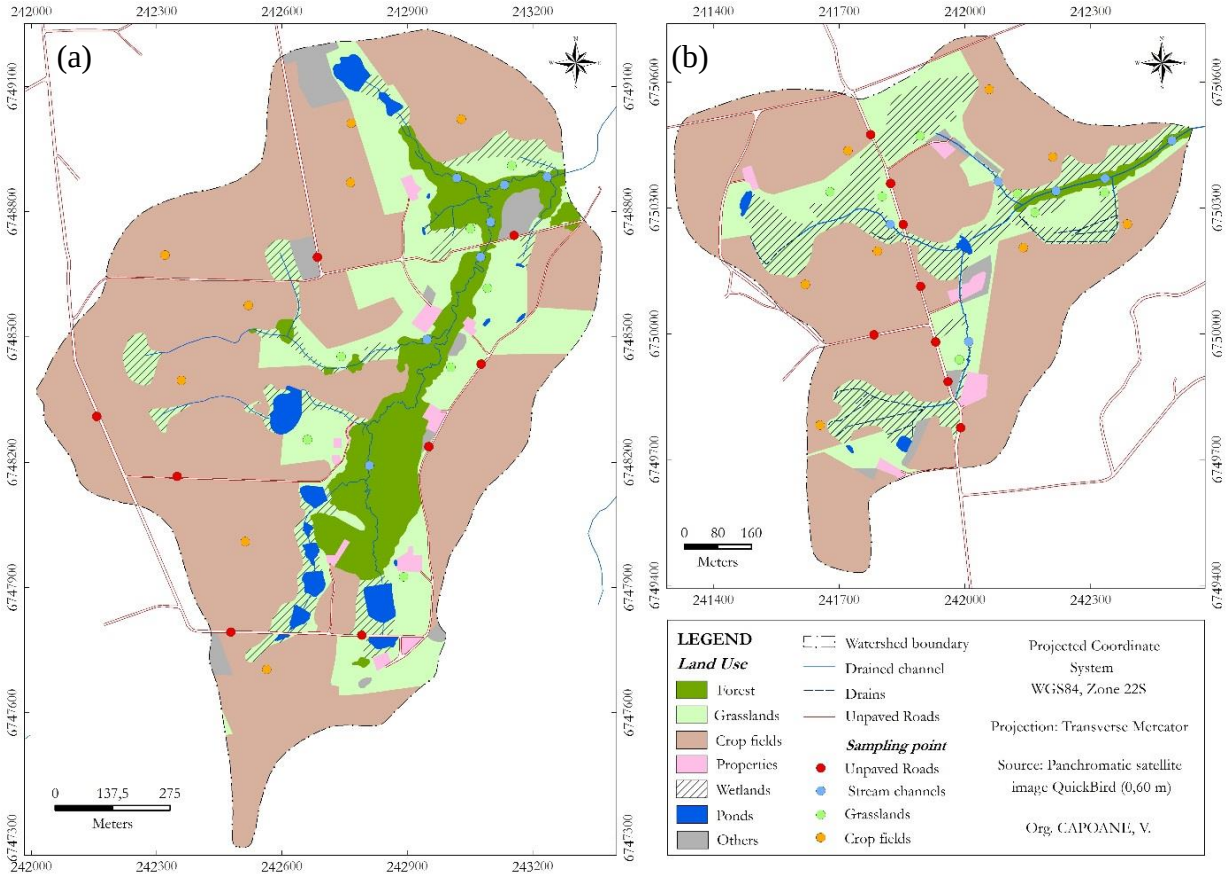

Figure 6 – The land use and the sampling sites in the (a) JC140 and (b) JC80 catchments.

Both catchments are drained by the Upper Jacuí River, which flows into the Jacuí River that supplies water to the metropolitan region of RS state where over 2 million people are living. These are third order catchments following the criteria introduced by Strahler (1957), i.e. channels that originate from the confluence of two second-order channels and can receive tributaries of second and first orders. According to Köppen, the climate is classified as Cfb subtropical humid with hot summers and winter with frequent frosts. The average annual

temperature ranges from 17 to 20ºC. The average temperature of the coldest month is between 11–14ºC and the mean temperature of the warmest month ranges from 23 to 26°C. The average rainfall is between 1,500–1,700 mm yr^{-1} well distributed throughout the year with 90–110 days of rain (ROSSATO, 2011).

The relief of both catchments is homogeneous, formed generally by well-rounded gentle hills, carved in basic volcanic rocks of the Serra Geral Formation and, to a lesser extent, in sedimentary rocks corresponding to Tupanciretã Formation. The soil types in the catchment according to World Reference Base for soil Resources (WRB) (IUSS WORKING GROUP WRB, 2007) are predominantly Acrisols, with some areas of Cambisols, Gleysols, and Leptosols. The main land use in both catchments is annual crops, representing about 64% of the total area (Table 5). The second most important land use is grasslands accounting for about 30 and 18% of the total area for the catchments JC80 and JC140, respectively. Unpaved roads cover about 1.4% of the catchment areas. In addition to the existing natural drainage network in the catchments, there are several artificial ponds that were built for supplying water to livestock as well as for fish farming, especially at JC140.

Table 5 – Land use in Júlio de Castilhos catchments.

Land use	Cacthment area (ha)		Cacthment area (%)	
	JC80	JC140	JC80	JC140
Rural facilities	1.1	1.5	1.4	1.1
Ponds	0.3	3.1	0.4	2.2
Forest	1.2	14.6	1.5	10.2
Others*	1.1	3.6	1.4	2.5
Crop fields	51.3	92.3	64.0	64.7
Grasslands	24.0	25.6	29.9	18.0
Unpaved roads	1.2	1.9	1.5	1.3
Stream channels	1.9 km	4.6 km	0.024 km ha^{-1}	0.032 km ha^{-1}
Total	80.2	142.6	100.0	100.0

* Other uses includes mainly subsistence farming.

5.1.3 Conceição catchment

The Conceição catchment is located in the northwest region of Rio Grande do Sul state, with a drainage area of approximately 804.3 km^2 (Figure 7). According to Köppen, the climate is Cfa type, subtropical humid without dry season, with an average annual rainfall between 1,750 and 2,000 mm and an average temperature of 18.6°C.

The predominant soil parent material is basic volcanic rocks of the Serra Geral Formation, Facies Gramado (93.9% of total area) and, to a lesser extent, sedimentary rocks corresponding to Tupanciretã Formation (6.1% – Figure 8a). The soils are deep, highly weathered, and rich in iron oxides and kaolinite. Ferralsols are the dominant soil class in the catchment (80.3% of total area – Figure 8b). Nitosols and Acrisols cover 17.6 and 2.1% of the total area, respectively. The topography of the region is characterized by gentle slopes (6–9%) in the top and middle parts of the slope, and higher slopes (10–14%) next to the drainage channels (Figure 9). The hillslopes are long and distinctive shapes.

Land use is very similar in the different subcatchments (Figure 10), but the size of farms tend to increase in the North-South direction. Figure 11 displays the land uses in the entire Conceição catchment. The main soil use is crop fields (73.1%). Grasslands and scrublands represent 18.1% of the total area. Forest cover only 7.7% of the total surface area in the catchment. Urbanization is not significant (0.7% of the total area) and include the municipalities of Augusto Pestana, Boa Vista do Cadeado, Ijuí, and Cruz Alta. Water bodies cover a very low surface (~0.4%). In summer, the areas are predominantly grown with soybean (Glycine max) under no-tillage system and on a smaller extent with corn, which is used to feed dairy cattle (silage). During winter, these areas are occupied by wheat (*Triticum aestivum*) for grain production, and cultivated with oats (*Avena strigosa*), and ryegrass (*Lolium multiflorum*) for the production of straw for mulching in the summer and for providing a pasture for dairy cattle in the winter. Soil management for grain production is based on no-tillage system on more than 80% of the crop-field area. However, these areas are devoid of additional measures to control runoff, such as terraces, strip cropping, vegetated ridges, or seeding perpendicular to the slope line.

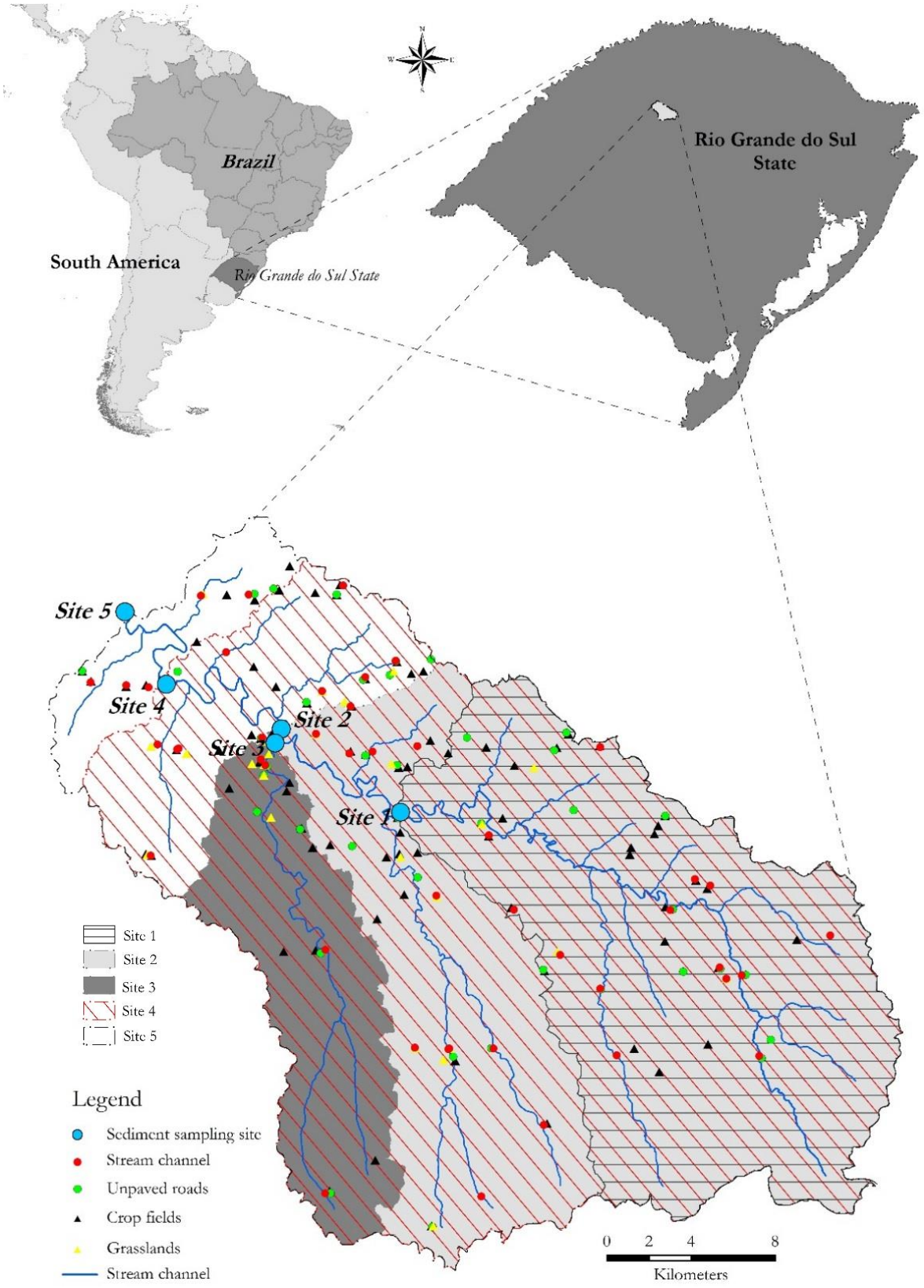

Figure 7 – The location of the Conceição catchment and sampling sites.

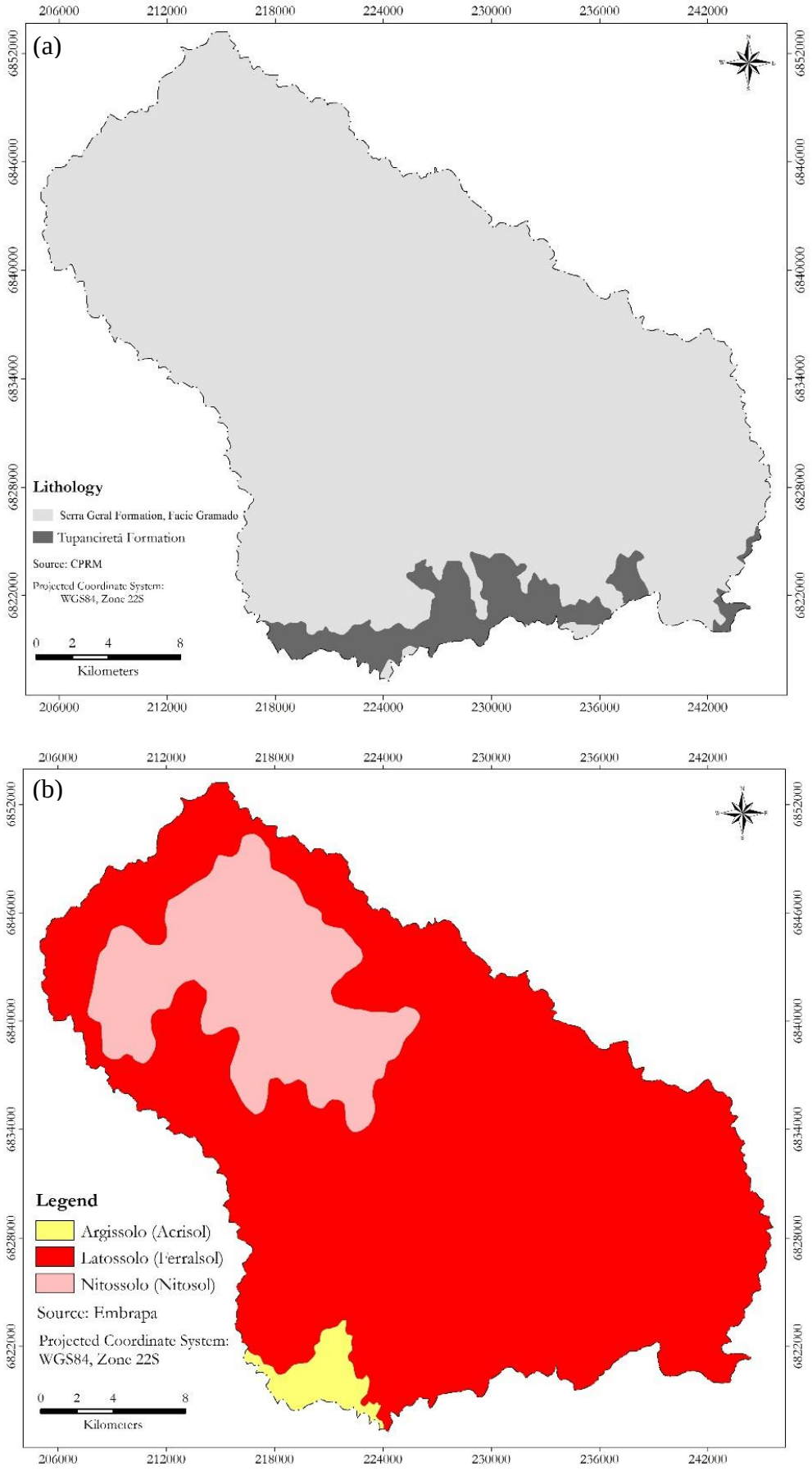

Figure 8 – Lithology (a) and soil types (b) of the Conceição catchment.

Figure 9 – Landscape in Conceição catchment.

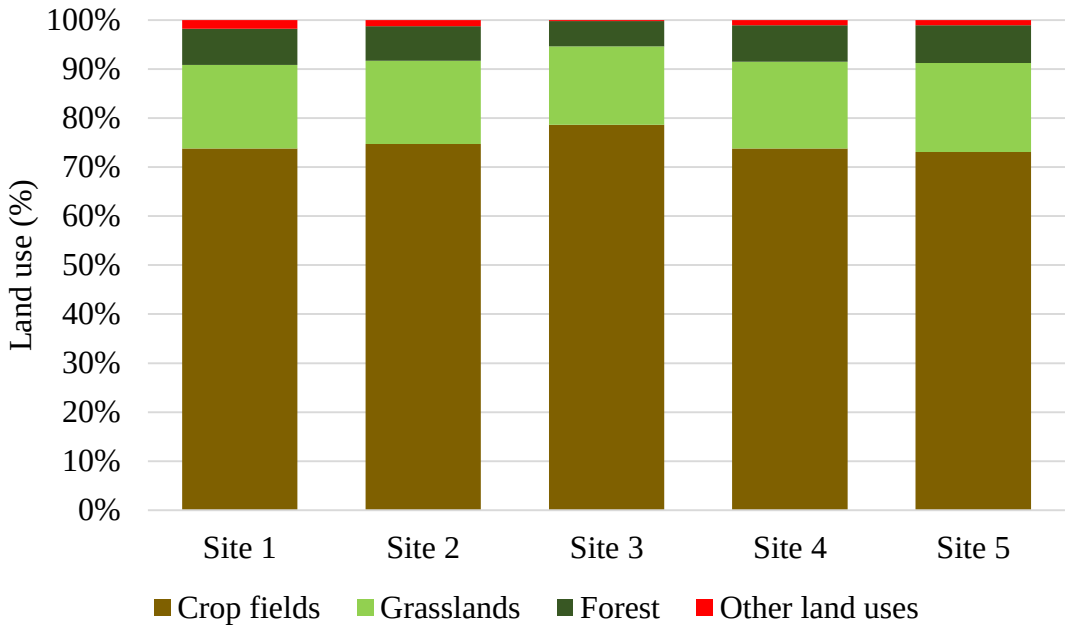

Figure 10 – Main land uses in the different sampling sites from Conceição catchment.

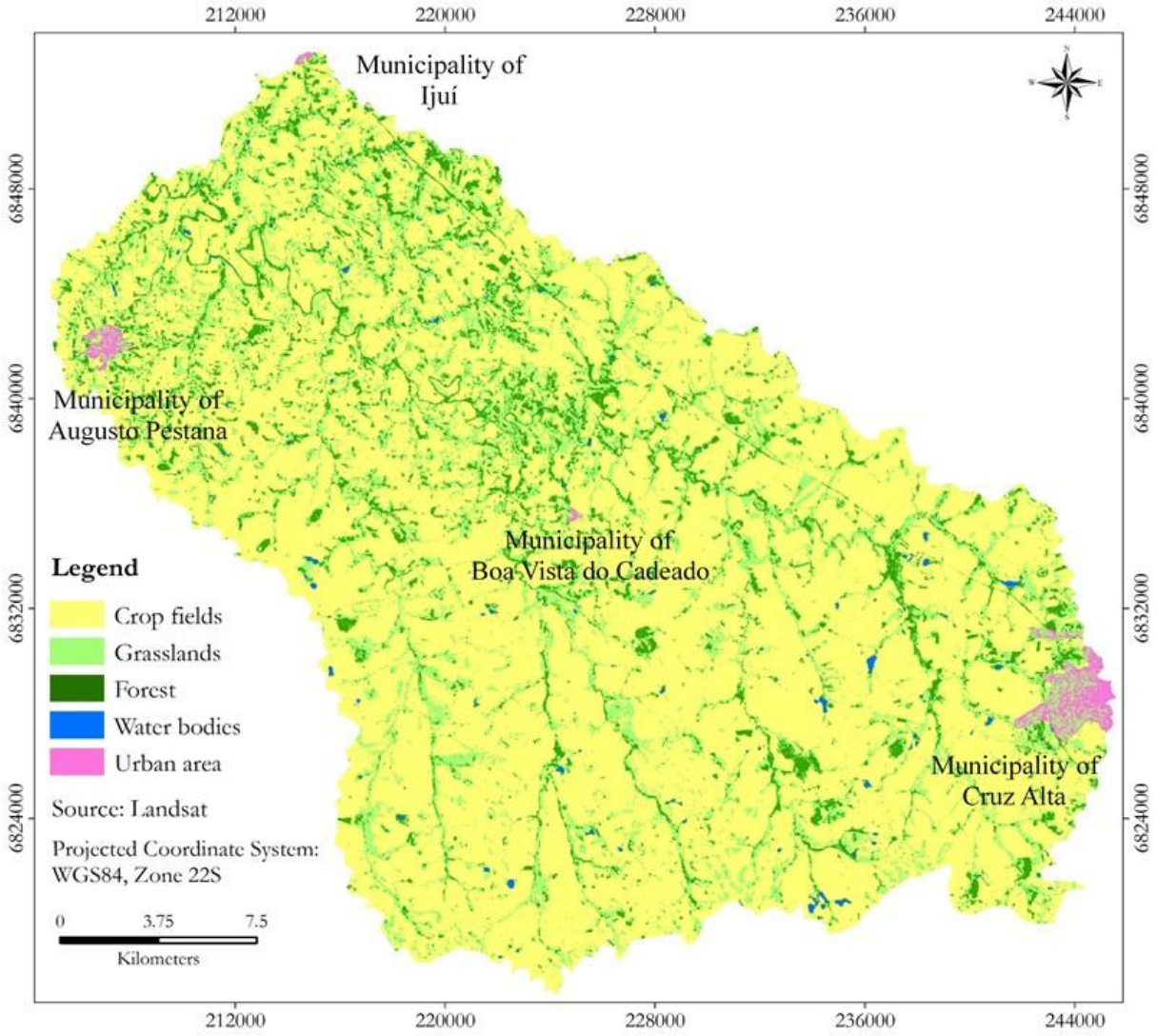

Figure 11 – Land use in Conceição catchment.

5.1.4 Guaporé catchment

The Guapore catchment is situated in the northeastern region of Rio Grande do Sul state and drains an area of 2,031.9 km^2 (Figure 12). It covers part of the physiographic regions of the middle plateau (upper third of the basin) and the lower northeastern slope (intermediate and lower thirds of the basin). Arvorezinha is a headwater catchment of Guaporé catchment (Figure 12). Climate is Cfa according to the Köppen climate classification, with average annual rainfall ranging from 1,400 to 2,000 mm, and an average annual temperature of 17.4°C. Geology is characterized by volcanic lava flows (Rhyodacite basalt) of Serra Geral Formation, Facies

Caxias, Gramado, and Paranapanema, covering 72.2, 26.1, and 1.7% of total area, respectively (Figure 13a). Topography is undulating to hilly. Due to variations in landscape and parent material, several classes of soils are found in the catchment. Acrisols, Ferralsols, Luvisols, Leptosols, and Nitosols correspond to 16.6, 31.2, 24.2, 6.6, and 21.4% of the total catchment area, respectively (Figure 13b). Ferralsols and Nitosols are predominant in the north part of the catchment, where the altitude is higher (Figure 3), while Leptosols predominate in the southern part of the catchment, where topography is hilly (Figure 3).

Land use is highly heterogeneous in Guaporé catchment (Figure 14). In the upper third of the catchment where the terrain is characterized by gentle hillslopes, there is a clear predominance of soybean (*Glycine max*) and maize (*Zea mays*) cultivated in summer and wheat (*Triticum aestivum*) during winter under no-tillage system (Figure 15 a, b). In the other two-thirds of the catchment (middle and lower parts), land use and soil management are very heterogeneous. The main land uses are tobacco (*Nicotiana tabacum*) and maize crops, areas that have been reforested with Eucalyptus (*Eucalyptus* spp.), as well as pastures for dairy cattle (Figure 15 c, d). In these areas, soil management vary greatly and conventional and minimum tillage are the main soil management techniques. In areas of with steeper slopes, especially on riversides, there are large portions of native forest areas as well as small towns and urban areas. The urbanization is sparse (~ 0.60% of total area) and is composed by the municipalities of Guaporé, Marau, Soledade, Anta Gorda, Ilópolis, Arvorezinha, Itapuca, União da Serrra, Nova Alvorada, Montauri, Vila Maria, Camargo, Casca, Gentil, Santo Antônia da Palma, Serafina Correa, and Mato Castelhano. Water bodies cover approximately 0.57%. Forest is the main land use and occupy 58% of the total area, while crop fields and grasslands represent only about 31 and 10% of the total area, respectively.

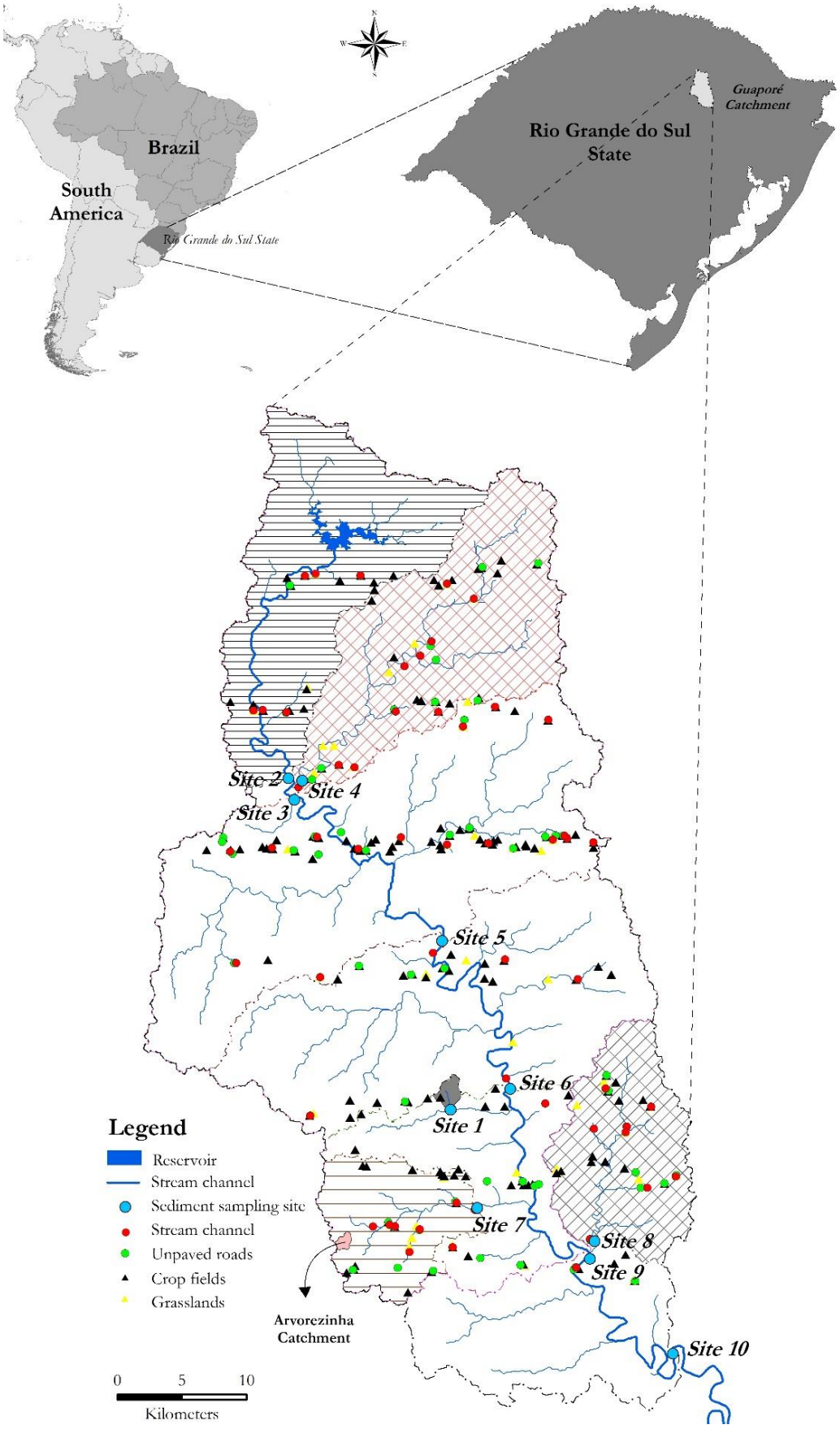

Figure 12 – The location of the Guaporé catchment and the sampling sites.

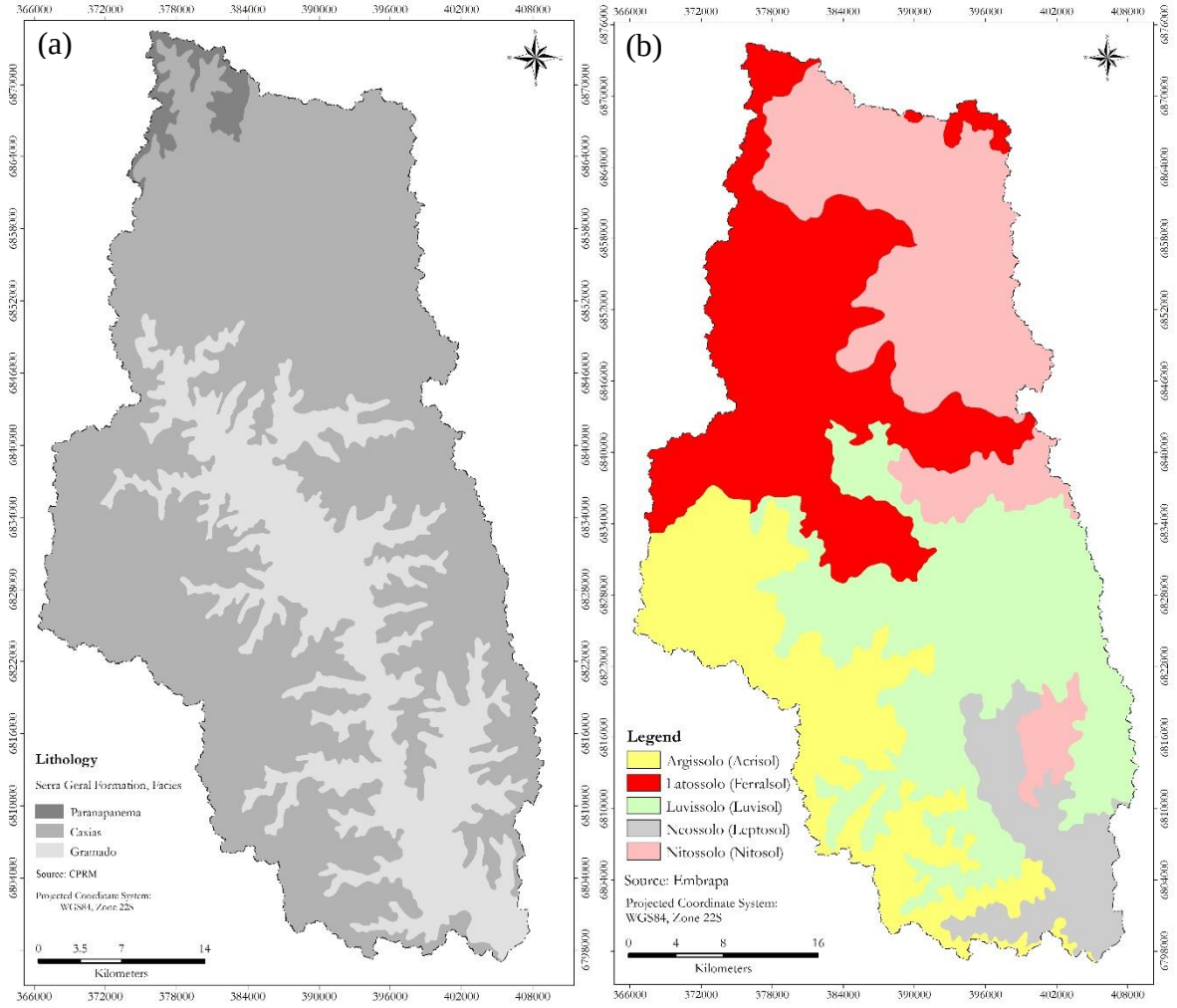

Figure 13 – Lithology (a) and soil types (b) of the Guaporé catchment.

Figure 14 was made using Landsat-TM image with a resolution of 30 m. This image gives an idea of the spatial distribution of land use in the Guaporé catchment, but it must be examined carefully. For example, Arvorezinha catchment, a detailed field survey of land use indicates that 40% of the total area are crops fields and 49% are forests (Figure 16). However, the land use for the same catchment using Landsat images indicates different proportion with only 10% of crops fields and 79% of forests. Figure 16 clearly demonstrates that the proportion of cropland decreases from the North to the South. Taking into account the sampling points along the main river, relative area of cropland decreases as follows: 2>3>5>6>9>10. However, the sites 1, 7, and 8, are situated in tributaries of the Guaporé River, in the lower part of the catchment and present a much lower proportion of cropland (8, 3, and 11% respectively) in their drainage area compared to the other sampling sites.

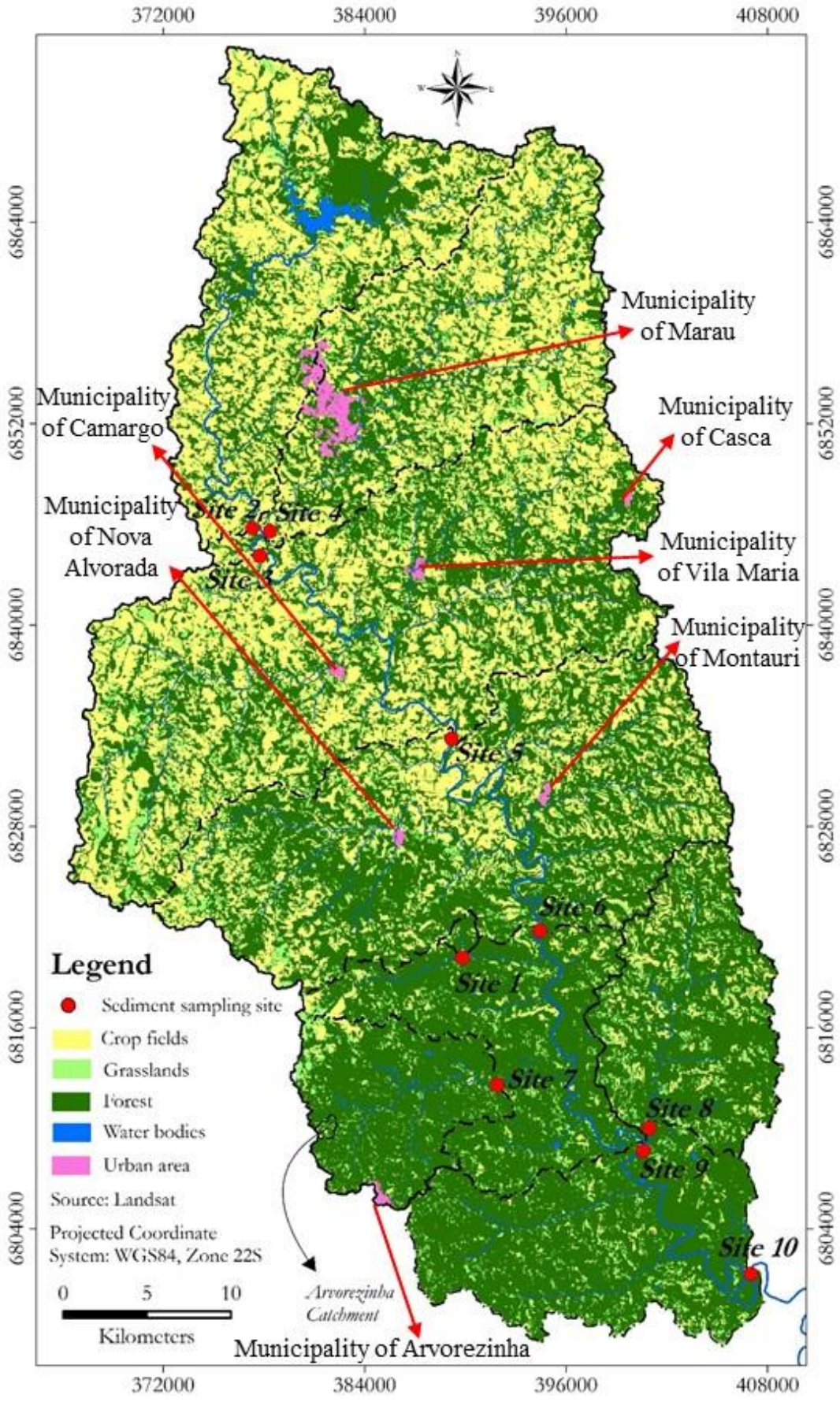

Figure 14 – Land use of the Guaporé catchment.

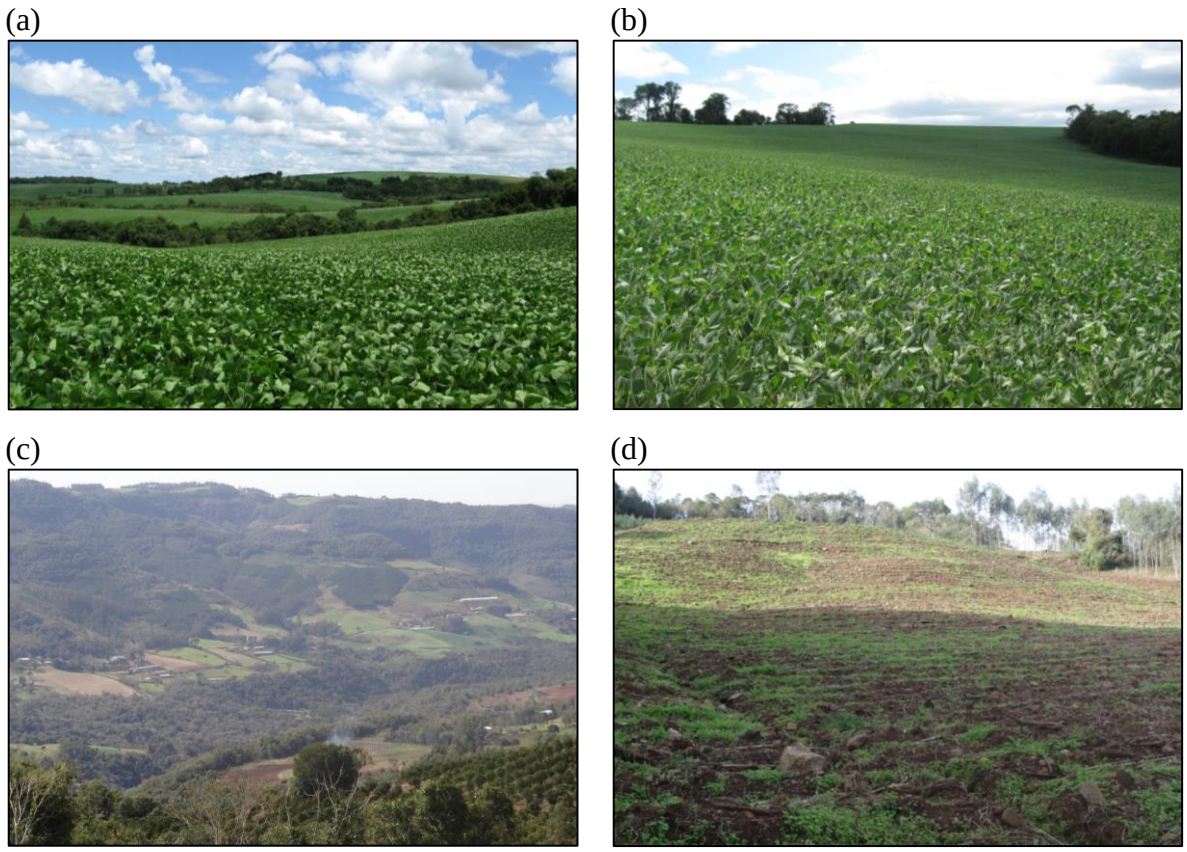

Figure 15 – Landscape (a) and tobacco field (b) in the upper Guaporé catchment, and landscape (c) and soybean field (d) in the lower and middle Guaporé catchment.

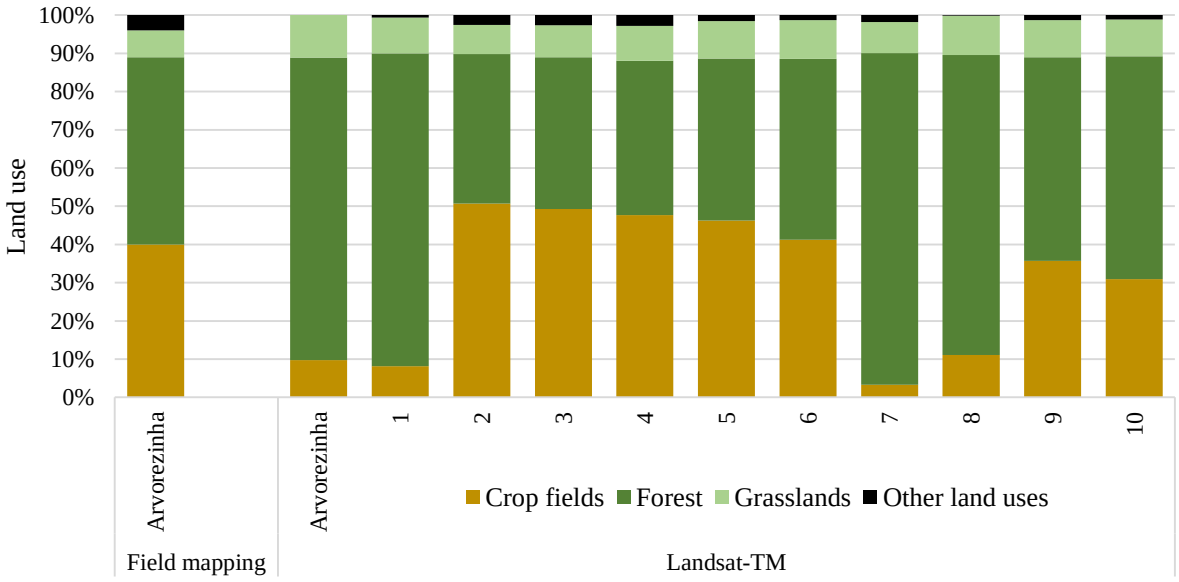

Figure 16 – Land use in Arvorezinha catchment (Arvorezinha is also a subcatchment of Guaporé catchment) estimated by field surveys and analysis of Landsat-TM images, and land use in the different subcatchments of Guaporé catchment estimated by Landsat-TM images.

5.2 Sediment source sampling

Potential sediment sources types were collected in areas where sediment mobilization and transport processes were visible in the study catchments during storm events. Four main sediment sources types were identified in JC80, JC140, Conceição, and Guaporé catchments, namely: (*i*) surface of cropland (CF), (*ii*) surface of grassland (GR), (*iii*) unpaved roads (UR), and (*iv*) stream channels (SC). Grasslands were not included in Arvorezinha catchment because it was considered of minor importance. The three main sediment source types in Arvorezinha catchment were identified and collected by Maier (2013). Areas under fallow and forest for all catchments were not evaluated because field observations indicated they were sediment sources of minor importance. In Guaporé and Conceição catchments were defined transects perpendicular to the main river to perform source sampling combining, therefore, the longitudinal and transversal variability in these catchments.

Table 6 shows the number and density of source samples collected in each catchment. Number of source samples collected for each source and in each catchment varies according to the catchment size and the proportion of land use of each sediment source. The sampling density in Guaporé was the lowest (0.15 sample km^{-2}, i.e., one sample each 6.58 km^{-2}). The sampling density in Conceição catchment was 1.5 times higher than in Guaporé catchment. The smaller catchments presented the highest sampling density, ranging from 21 to 37 samples km^{-2}. Compared to Guaporé catchment, the catchments from Arvorezinha, JC80, and JC140 presented sampling density approximately 221, 246, and 138 times higher.

Table 6 – Number and density of source samples collected in each catchment and sampling density relative to Guaporé catchment.

Catchment	Number of source samples										Sampling density relative to Guaporé catchment
	Cropland		Stream channel		Unpaved road		Grassland		Total		
	n	*n* km^{-2}	*n*	*n* km^{-2}	*n*	*n* km^{-2}	*n*	*n* km^{-2}	*n*	*n* km^{-2}	
Arvorezinha	20	16.81	10	8.40	10	8.40	-	-	40	33.61	221.0
JC80	8	9.98	6	7.48	8	9.98	8	9.98	30	37.41	246.0
JC140	8	5.61	7	4.91	8	5.61	7	4.91	30	21.04	138.3
Conceição	79	0.10	36	0.04	41	0.05	27	0.03	183	0.23	1.5
Guaporé	159	0.08	46	0.02	58	0.03	46	0.02	309	0.15	1.0
Total	274	-	105	-	125	-	88	-	592	-	-

A total of 592 composite sediment source samples were collected in the five catchments. The samples of potential source material were collected using nonmetallic trowel of the uppermost layer (0–0.05 m) of the CF, GR and UR, and on exposed sites located along the river channel network (SC). In order to obtain representative source material, each sample was composed by 10 sub-samples collected in the vicinity of the sampling point. Sampling points were concentrated in sites sensitive to erosion and potentially connected to the river network. Care was taken during sample collection to cover the entire range of soil types found in the catchment area (see Figure 4, Figure 6, Figure 7, Figure 12).

5.3 Sediment sampling

Sediment sampling strategy varied according to the studied catchment. For the small catchments of Arvorezinha and Júlio de Castilhos municipalities, only storm-event suspended sediments were collected, whereas in the two larger catchments (Conceição and Guaporé), sediment sampling was performed in three to four different ways. Below is given a detailed description of the four sediment-sampling strategies used in the present study:

i) *Storm-event suspended sediments (SESS)*: this sediment sampling strategy was employed in all the five catchments only at the outlet of the catchments. To this end, a large volume of water (50 to 200 liters) was collected manually at varying intervals along the rising and recession limb of the hydrograph during rainfall-runoff events to evaluate the intra-event variation of sediment source contributions. The Arvorezinha bulk water samples were centrifuged in continuous flow centrifuge (Alfie-500 Alfa Laval) to concentrate sediment samples for subsequent chemical and physical analyses (MAIER, 2013).

ii) *Time-integrated suspended sediments (TISS)*: this strategy was employed in the two larger catchments, i.e. Guaporé and Conceição. TISS were obtained employing a simple sediment sampler developed by Phillips; Russell; Walling (2000). At each point (5 and 10 in Conceição and

Guaporé catchments, respectively), two time-integrated trap samplers were installed to ensure that a sufficient quantity of sediment was collected for subsequent analyses. This collector has a small hole that allows the passage of water flow. It is based on the sedimentation principle: the material suspended in the water that pass through the collector will be accumulated at the bottom of the collector, integrating in a single sample the suspended sediment transported by water for a given period. These time-integrated trap samplers collect fine suspended sediment (<63μm) with particle size characteristics that are statistically representative of the ambient suspended sediment (PHILLIPS; RUSSELL; WALLING, 2000) and have been successfully used in previous studies (e.g., LAMBA; KARTHIKEYAN; THOMPSON, 2015; SMITH; BLAKE, 2014).

iii) *Fine-bed sediment (FBS)*: this strategy was only employed in the two larger catchments, Guaporé and Conceição, mainly because in these areas theft/vandalism made it impossible the use of equipment as time-integrating samplers. According to a study conducted by Horowitz et al. (2012) in 131 coastal river basins from Atlantic, Pacific and Gulf of Mexico coasts of the conterminous USA, the <63 μm fraction of near-surface (upper 1 cm) bed sediments does appear to serve as a useful surrogate for the estimation of suspended sediment-associated chemical concentrations. The authors affirm that it is particularly true for trace/major elements but less so for nutrients and carbon. Therefore, FBS were collected with a suction stainless sampler that allowed for collecting fine-bed surficial sediments without loss of the fine material at the sediment/water interface. Samples were composed of 20 to 30 subsamples collected along the river channel.

iv) *Storm-event suspended sediment US U-59 (SESS-U59)*: suspended sediment was also collected by using samplers that are an adaptation of the model US U-59 (CEW-EH-Y, 1995), installed at the streambed of the watercourse in 9 sampling sites only at Guaporé catchment.

A total of 320 sediment samples were collected in the present study. Table 7 summarizes the sampling strategy, the number of samples, and location of sediment samples collected in each catchment.

Table 7 – Sampling strategy, number, and location of sediment samples collected in each catchment.

Catchment	Time-integrated suspended sediments		Storm-event suspended sediments		Storm-event suspended sediments US U-59		Fine-bed sediment		Total
	n	Location	*n*	Location	*n*	Location	*n*	Location	*n*
Arvorezinha	-	-	29	Outlet	-	-	-	-	29
JC80	-	-	27	Outlet	-	-	-	-	27
JC140	-	-	27	Outlet	-	-	-	-	27
Conceição	33	Outlet + 4 sites	20	Outlet	-	-	34	Outlet + 4 sites	87
Guaporé	50	Outlet + 9 sites	12	Outlet	26	9 sites	62	Outlet + 9 sites	150
Total	83		115		26		96		320

5.4 Source materials and sediment analyses

5.4.1 Sample preparation

All the source materials and sediment samples were oven-dried at 50^{o}C, gently disaggregated using a pestle and mortar. Source materials and sediment samples from Arvorezinha, Guaporé and Conceição catchments were sieved to 63 µm prior to laboratory analyses to compare similar grain size-fractions for all the samples (sediments and sources). This limit was chosen to reduce uncertainties related to the effect of dilution of elements concentration effect of the sand particles (MICHELAKI; HANCOCK, 2013) and consider the clay aggregates which are suspended (MINELLA; WALLING; MERTEN, 2008). Due to

coarser soils (>60% sand) and sediments (ALVAREZ, 2014; TIECHER et al., 2014) from Júlio de Castilhos catchment, source materials and sediment samples were sieved to 150 µm prior to laboratory analyses.

5.4.2 Geochemical analyses

All source material and fine sediment samples of the five catchments were analyzed for a range of geochemical fingerprinting properties. Total organic carbon (TOC) was estimated by wet oxidation with $K_2Cr_2O_7$ and H_2SO_4 (WALKLEY; BLACK, 1934). The total concentration of several elements was estimated by ICP-OES after microwave assisted digestion for 9.5 min at 182ºC with concentrated HCl and HNO_3 in the ratio 3:1 (*aqua regia*). For Arvorezinha catchment samples the following elements were measured: Ag, As, B, Ba, Be, Ca, Cd, Co, Cr, Cu, Fe, K, La, Li, Mg, Mn, Mo, Na, Ni, P, Pb, Sb, Se, Sr, Ti, Tl, V, and Zn. For Júlio de Castilhos, Conceição, and Guaporé catchments samples concentration of Al, Ba, Be, Ca, Co, Cr, Cu, Fe, K, La, Li, Mg, Mn, Na, Ni, P, Pb, Sr, Ti, V, and Zn were analysed.

5.4.3 Additional analyses of samples from Arvorezinha catchment

Grain size distribution was analyzed with a laser granulometer for Arvorezinha catchment samples, after oxidation of organic matter with H_2O_2 and dispersion with NaOH in (MUGGLER; PAPE; BUURMAN, 1997). As surface specific area (SSA) depends largely on grain size distribution (FOOLADMAND, 2011; SEPASKHAH; TAFTEH, 2013), we estimated SSA from the particle size distribution considering that particles are spherical and cylindrical. Additional analyses of source and sediment samples in Arvorezinha catchment were also performed to evaluate the potential use of spectroscopy analyses for fingerprinting sediment sources.

5.4.3.1 Ultra-violet-visible diffuse reflectance analyses

Ultra-violet-visible (UV-VIS) diffuse reflectance spectra of powered samples were recorded at room temperature from 200 to 800 nm with a 1-nm step using a Cary 5000 UV-VIS-NIR spectrophotometer (Varian, Palo Alto, CA, USA). Samples were ground and loaded into a Harrick Praying Mantis diffuse reflectance accessory that uses elliptical mirrors. $BaSO_4$ was used as a 100% reflectance standard. Care was taken when adding the samples into the sample port to avoid differences in sample packing and smoothness of the surface.

5.4.3.1.1 VIS-based-colour parameters calculation

Twenty-four (24) components were derived from the UV-VIS spectra using various colorimetry models described in detail by Viscarra Rossel et al. (2006) (Table 8). The Commission Internationale de l'Eclairage (CIE) (1931) proposed the CIE models to facilitate visualization and standardize colour models. We calculated the XYZ tristimulus values based on the colour-matching functions defined in 1931 by the CIE (COMMISSION INTERNATIONALE DE L'ECLAIRAGE, 1931), where Y represents the brightness, and X and Z are virtual components of the primary spectra. The derived XYZ values were then transformed into eight other colour space models (i.e. RGB, decorrelated RGB, Munsell HVC, CIE xyY, CIE LAB, CIE LUV, CIE LHC and Helmholtz chromaticity coordinates) using ColoSol software developed by Viscarra Rossel (2004).

Later, the CIE introduced the CIE xyY system, where Y represents luminance and x and y represent colour variations from blue to red and blue to green, respectively. To overcome the non-linearity of the two previous colour models, CIE introduced later the CIE LAB and CIE LUV models, where L represents brightness or luminance, and a* and b* and u* and v* represent chromaticity coordinates as opponent red–green and blue–yellow scales. CIE LHC model represents a transformation of the CIE LAB spherical colour space into cylindrical coordinates, resulting in hue (h*) and chroma (c*) values. Helmholtz chromaticity coordinates describe luminescence (L), dominant wave-length (λ_d), and purity of excitation (P_e). RGB system forms a cube comprising orthogonal red (R), green (G) and blue (B) axes, from where every colour can be produced by a mixture of these three primary colours. Decorrelated RGB

is a transformation of highly correlated RGB values into three statistically independent components. Munsell HVC system is commonly used in soil science and describes the soil colour by the use of hue (H), value (V) and chroma (C). We also calculated the Redness Index (RI) introduced by Barron; Torrent (1986) to estimate the soil hematite content. Y is used in more than one colour space (e.g. CIE xyY, CIE XYZ and Helmholtz chromaticity) but it was used just once in our study. Table 8 presents a summary of the colour space models used in this study and the abbreviations for all 24 parameters calculated.

Table 8 – VIS-based-colour parameters derived from different colour space models calculated using ColoSol software (VISCARRA ROSSEL et al., 2006b). C.c., chromatic coordinate.

Colour space model	Colour parameter	Parameter abbreviation
RGB	Red	R
	Green	G
	Blue	B
Decorrelated RGB	Hue	H_{RGB}
	Light intensity	I_{RGB}
	Chromatic information	S_{RGB}
CIE xyY	Chromatic coordinate x	x
	Chromatic coordinate y	y
	Brightness	Y
CIE XYZ	Virtual component X	X
	Virtual component Z	Z
CIE Luv	Metric lightness function	L
	C.c. opponent red–green scales	u*
	C.c. opponent blue–yellow scales	v*
CIE Lab	C.c. opponent red–green scales	a*
	C.c. opponent blue–yellow scales	b*
CIE Lch	CIE hue	c*
	CIE chroma	h*
Munsell HVC	Hue	H
	Value	V
	Chroma	C
Helmholtz chromaticity	Dominant wavelength	λ_d (nm)
	Purity of excitation	P_e
Index	Redness Index	RI

5.4.3.1.2 Inferences in soil composition based on ratios of absorption bands in UV-VIS-spectra

Absorption in the VIS spectra (400-700 nm) is useful to discriminate iron oxides (e.g. hematite) and iron oxy-hydroxides (e.g. goethite) in soils (FRITSCH et al., 2005; KOSMAS et al., 1984; SCHEINOST, 1998). The proportions of hematite (Hr) and goethite (Gt) in the pool of Fe-oxides were estimated according to the methodology employed by Caner et al. (2011), Fritsch et al. (2005), Kosmas et al. (1984), and Scheinost (1998). Briefly, the remission function $f(R) = (1-R)^2/2R[(1-R)^2/2R]$, ($R$ being the measured diffuse reflectance) which is proportional to the concentration of the absorber, was calculated according to the Kubelka-Munk relationship (BARRON; TORRENT, 1986; SCHEINOST, 1998). The positions of the transitions were determined from second derivative functions after smoothing of the reflectance and remission functions using a cubic spline (KOSMAS et al., 1984) with the same parameters for all the samples. Goethite and hematite were determined from the position and intensities of absorption bands of second-derivative curves (CANER et al., 2011; FERNANDES et al., 2004; FRITSCH et al., 2005; KOSMAS et al., 1984; SCHEINOST, 1998)

Ratios between absorption bands in the UV-VIS-spectra at 254 and 365 nm (E_2/E_3), and between 465 and 665 nm (E_4/E_6), are considered as a measurement of aromaticity used widely to characterize the natural organic matter (RECIO-VAZQUEZ et al., 2014). These ratios will be obtained from the spectra of the solid samples to characterize the organic matter. Although these ratios tend to be robust, they are not linear additives and cannot therefore be used in linear mixing models (WALLING, 2005). Nonetheless, they can contribute to understand mineralogical and organic matter composition of soil and sediment samples.

5.4.3.2 Near-infrared diffuse reflectance analyses

Near-infrared (NIR) spectra were recorded in the 10000–4000 cm^{-1} range using a Nicolet 26700 FTIR spectrometer (Waltham, Massachusetts, USA) in diffuse reflectance mode with an integrating sphere with an internal InGaAs detector with 2 cm^{-1} resolution and with 100 co-added scans per spectrum.

5.4.3.3 Mid-infrared diffuse reflectance analyses

Mid-infrared (MIR) spectra were recorded in the 400–4000 cm^{-1} range using a Nicolet 510- FTIR spectrometer (Thermo Electron Scientific, Madison, WI, USA) in reflection mode with a 2 cm^{-1} resolution with 100 co-added scans per spectrum. The spectrometer was continuously purged with dry CO_2-depleted air. Care was taken when adding the samples into the sample port to avoid differences in sample packing and smoothness of the surface.

5.4.3.4 Complementary analysis of sediment sources

In order to support interpretation of spectroscopy analyses, complementary analyses were performed only for Arvorezinha catchment, in composed samples of each sediment source formed by mixing all the samples (10 for UR and SC, and 20 for CF) in laboratory. Thereby, we performed pyrolysis-gas chromatography/mass spectrometry (Py-GC/MS) and X-ray diffraction (XRD) to identify the major organic compounds and minerals, respectively.

Py-GC/MS analysis was performed following the methodology described by Julien et al. (2014) briefly described as follows: a quartz tube was packed with 40 mg of dry sample and quartz wool. The tube was then placed into the platinum filament of the Pyroprobe 2000 pyrolyzer (Chemical Data Systems, Oxford) and pyrolysis was performed upon rapid heating at high temperature (50–650ºC at a rate of 20ºC/ms). Thermal decomposition product analysis was performed on a Hewlett–Packard 5890 Series II gas chromatograph with mass spectrometry detector (HP G1800A operating at EI = 70 eV, scanning from 20 to 450 amu at 1 scan/s). The system is equipped with a DB-5 MS (J & W Scientific) fused-silica capillary column (30 × 0.25 mm i.d. with 0.25 µm film thickness). The injector temperature was 280ºC, and the detector temperature was 250ºC. The oven was programmed with an initial temperature of 50ºC, and the temperature was ramped to 300ºC at 7ºC min^{-1} and held for 10 min. Helium was used as the carrier gas at a constant flow rate of 1.0 mL min^{-1}. Forty-five major chromatogram peaks were selected and the respective pyrolytic fragments were identified after examining the NIST (National Institute of Standards and Technology) mass spectral library and results from previous works. Subsequently, these major peaks were then grouped in seven major organic

compound groups, namely: amino acids, amino sugars, alkyl benzene, protein, phenol, polysaccharides, and other compounds (BRUCHET; ROUSSEAU; MALLEVIALLE, 1990).

X-ray diffraction patterns (XRD) were recorded on powdered fine-earth samples on a Bruker D8 Advance diffractometer (Cu Kα radiation - 40 kV, 40 mA - Lynxeye detector) by scanning from 57-63º2θ in 0.02º2θ step at 96s/step (converted from scanning mode). To estimate the composition of the mineral assemblages, XRD patterns of the <63 µm fraction of the composed samples of each sediment source were decomposed in the range from 2 to 30°2θ to differentiate 2:1 clay minerals (undifferentiated ~ 14–15 Å), 1:1 clay minerals (kaolinite ~ 7.3 Å) and quartz (3.34 Å) at approximately 5.8, 12.1, and 26.6°2θ, respectively. We applied the procedure described by Lanson (1997) after background stripping using the Fityk 0.8.2 peak fitting software (WOJDYR, 2007), and introducing one curve for each one of the three main mineral components. The mineral abundance was estimated by comparing peak height and peak area of each composed sample of sediment source. It is admitted that the relative intensities or areas of each peak do not correspond to the relative mass percentage of the respective mineral. However, we assume that variations of relative intensities indicate variations in mineral quantities as the soils are developed from the same parent material (LANSON, 1997).

5.5 Sediment source discrimination and apportionment

The statistical procedure used for alternative method based on spectroscopy analysis greatly differs from the conventional fingerprinting approach based on geochemical composition. Figure 17 displays the main steps used for each approach. Briefly, the steps used in the conventional method were: i) tracer selection based on Kruskal-Wallis *H*-test, ii) selection of the best set of tracers using discriminant analyses and finally iii) the use of a mixed linear model to calculate the sediment source contributions. The steps used in the alternative method were i) principal component analyses to reduce the number of variables, ii) discriminant analyses to determine the tracer potential of the spectroscopic analysis, and finally iii) the use of partial least square regression based on mixtures of the sediment sources in several known weight proportions to calculate the sediment source contributions. It is important to highlight that in the first approach (conventional method) the subsequent steps are always dependent on the results of the first steps. However, for the alternative method, the first two steps are used only to verify if there is differences between source groups, but there is no selection of tracers.

Thus, in the third step of the alternative method, all the wavelength of each spectral range are entered again in the analysis to construct the partial leas squares regression (PLSR) models. In the subsequent items a more detailed description of each statistical step is provided for both approaches.

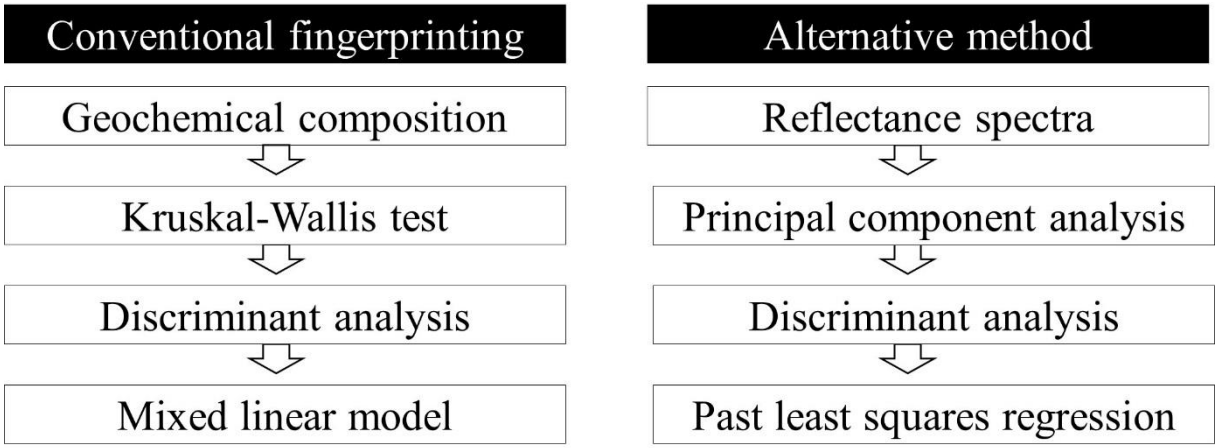

Figure 17 – The main statistical steps employed for conventional fingerprinting based on geochemical composition and for the alternative method based on spectroscopy analysis.

5.5.1 Sediment source discrimination for discrete variables

Sediment source discrimination for discrete variables (geochemical tracers, and VIS-based-colour parameters in the case of Arvorezinha catchment) was performed with some additional steps to identify outliers as suggested by Gellis; Noe (2013). In each source group, each tracer was tested to determine if it followed a normal distribution using the Shapiro-Wilk test (H_o=samples are random and come from a normal distribution). All variables not normally distributed were tested again for normality after transformation using log, power, square root, cube root, inverse, and inverse square root functions. The best transformation for normality was selected, and the variables were transformed accordingly. The average and standard deviation within each source group for each transformed variable were determined. If the value for a given source sample exceeded three times the standard deviation of the average value, this sample was considered to be an outlier and the entire sample was removed for all variables.

Additionally, the variables with sediment concentrations lying outside the range of sources were excluded from the next analyses hereafter, as recommended by Smith; Blake (2014) (known as "range test").

Subsequently, the two-stage procedure proposed by Collins; Walling; Leeks (1997) was used to identify composite fingerprints capable of discriminating the samples collected to represent individual sediment sources. The first step of the statistical analysis was performed to establish the set of properties with the ability to discriminate among the sediment sources by the application of two sequential tests: (a) a non-parametric Kruskal-Wallis (*H*) test and (b) a multivariate discriminant function. The *H* test allows to check the null hypothesis that the sources are from the same population. In this test soil properties that are statistically different among the sediment sources were defined. When one soil property is statistically different it can be used as tracer. The *H*-test is applied to each soil property, verifying its ability to discriminate individual sources, according to Equation 1:

$$H = \frac{12}{n(n+1)} \sum_{s=1}^{k} \frac{R_s^2}{n_1} - 3(n+1) \quad (1)$$

where R_s is the rank sum occupied by the source *s*, n_1 is the number of observations in each source; *n* is the sum of the n_1's; and *k* is the number of sources.

Subsequently, we performed a multivariate discriminant function analysis (DFA) in the backward mode to determine the minimum number of variables that maximizes the discrimination among the sources. The DFA analysis was performed only with variables showing differences among sources by the *H* test. The multivariate discriminant function is based on Wilks' Lambda (Λ*) value from the analysis of variance, where the criterion used by the statistical model is the minimization of Λ* (Equation 2). Λ* of 1 occurs if all the group means are the same, whilst a low Λ* value means that the variability within the groups is small compared to the total variability.

$$\Lambda^* = \frac{|W|}{|B+W|} \quad (2)$$

where |W| is the determinant of the matrix of sums of squares due to the error, while |B + W| represents the determinant of the matrix of the total sum of squares. At each step, the property which minimized the overall Wilks' Lambda was entered. Maximum significance of F to enter a property was 0.01. Minimum significance of F to remove a property was 0.05.

5.5.2 Sediment source apportionment for discrete variables

After defining the set of variables by minimizing Λ* the contribution of each sediment source in the composition of the sediment suspended was determined. Equation 3 describes the mathematical relationship between the proportions of contribution of each source and the variables in the sources and in the suspended sediment (WALLING; WOODWARD, 1995).

$$y_i = \sum_{s=1}^{n} a_{is} P_s \qquad (\mathrm{s} = 1, 2, \ldots, \mathrm{n}) \text{ and } (\mathrm{i} = 1, 2, \ldots, \mathrm{m}) \qquad (3)$$

where y_i is the value of the variable i obtained in the suspended sediment, a_{is} are the linear model coefficients (concentration of the soil property in the source s_i) and P_s is the proportion of mass from the source s, which may be presented as a set of linear functions of m variables and n sources.

To determine the P_s values an objective function was used (WALLING; WOODWARD, 1995). The solution was found by an iterative process aiming at minimizing the value of R (*f* min*con*) (Equation 4). The mixing model was run using Matlab® software. In the minimization process, P values are subject to two constraints: to be greater than or equal to zero and less than or equal to 1 (Equation 5) and the sum of P values must to be equal to 1 (Equation 6).

$$R = \sum_{i=1}^{m} \left\{ \frac{C_i - (\sum_{s=1}^{n} P_s C_{si})}{C_i} \right\}^2 \qquad (4)$$

$$0 \leq P_s \leq 1 \quad (5)$$

$$\sum_{s=1}^{g} P_s = 1 \quad (6)$$

where *m* is the number of soil properties selected as variable tracers; *n* is the number of sources, C_i is the concentration of the tracer *i* in the suspended sediment sample; P_s is the proportion of contribution of the source *s*, C_{si} is the average value of the tracer *i* obtained for the source *s*.

Subsequently, the optimization process of Equation 4 checked whether it provided acceptable results of the relative contributions of the sediment sources. The evaluation of the results was made by comparing the concentration of chemical property used (variables tracers) in the suspended sediments and the value predicted by the model based on the proportion calculated for each source. Then, with the values of the relative error of each variable an average (RME) was calculated to provide a unique value associated with each sample of suspended sediment (Equation 7). When values lower than 15% were obtained with Equation 7 it indicate that the model found a feasible solution of P_s values (relative contributions of each source) from the minimization procedure of Equation 4.

$$RME = \sum_{i=1}^{m} \left\{ \frac{C_i - (\sum_{s=1}^{n} P_s C_{si})}{m} \right\} \quad (7)$$

5.5.3 Sediment source discrimination for spectroscopy analyses

For spectroscopy approach, the sediment source discrimination was performed by using the whole spectra (UV-VIS, NIR, and MIR) of source samples from Arvorezinha catchment. Spectroscopy approach used the first-derivative of the UV-VIS, and the second-derivative of NIR, and MIR spectra to differentiate source apportionment. The derivative avoids differences in baseline positions and getting rid of the small differences due to uncontrolled sources of variation (e.g. sample packaging). In order to avoid any CO_2 (gas) interference in the MIR spectra, analyses were performed on wavelengths comprised in the ranges of 3800–2400 cm^{-1}

and 2300–650 cm^{-1}. Classical fingerprinting approach for source discrimination consists of a mean test (Kruskal-Wallis, Mann-Whitney or Tukey test) followed by a discriminant analysis based on the minimization of the parameter Wilk's Lambda (COLLINS; WALLING; LEEKS, 1997). However, this method can only discriminate discrete data (e.g. element concentrations), wherein the number of samples is greater than the number of variables. The data obtained from the UV-VIS, NIR, and MIR spectroscopy consists of a continuous spectrum with a large number of variables (UV-VIS: from 200 to 800 nm in intervals of 1 nm = 600 wavelengths; MIR: 3,800–2,400 cm^{-1} and 2,300–650 cm^{-1} in intervals of 2 cm^{-1} = 1583 wavelengths; NIR: from 10,000 to 4,000 cm^{-1} in intervals of 2 cm^{-1} = 3112 wavelengths) for a set of 40 sediment source samples. For this reason, we used the discriminant function analysis (DFA) based on scores from principal component analysis (PCA) (hereafter named PC-DFA model) proposed by Poulenard et al. (2009), briefly described as follows. PCA is a mathematical procedure which uses orthogonal transformation to convert a set of observations of variables possibly correlated into a set of values of linearly uncorrelated variables. PCA was performed in order to reduce the number of variables without losing any information of the data set. Subsequently, a DFA using the scores obtained from the PCA as input data was conducted. The DFA is based on comparing distances between samples in a wide space method. In the DFA the Mahalanobis distance was used because it takes into account the covariance between variables in the calculation of distances. It avoids problems due to changes in the overall intensity of the spectrum or the correlation between the loadings of the PCA (POULENARD et al., 2012).

5.5.4 Sediment source apportionment for spectroscopy analyzes

The samples of each sediment source from Arvorezinha catchment (i.e. CF, UR, SC) were mixed in equal proportions in the laboratory to constitute a unique reference sample for the corresponding source. Subsequently, those reference source samples were mixed in 48 composites with different weight proportions to obtain a range of different source material ratios as presented in the Figure 18 to calibrate the models.

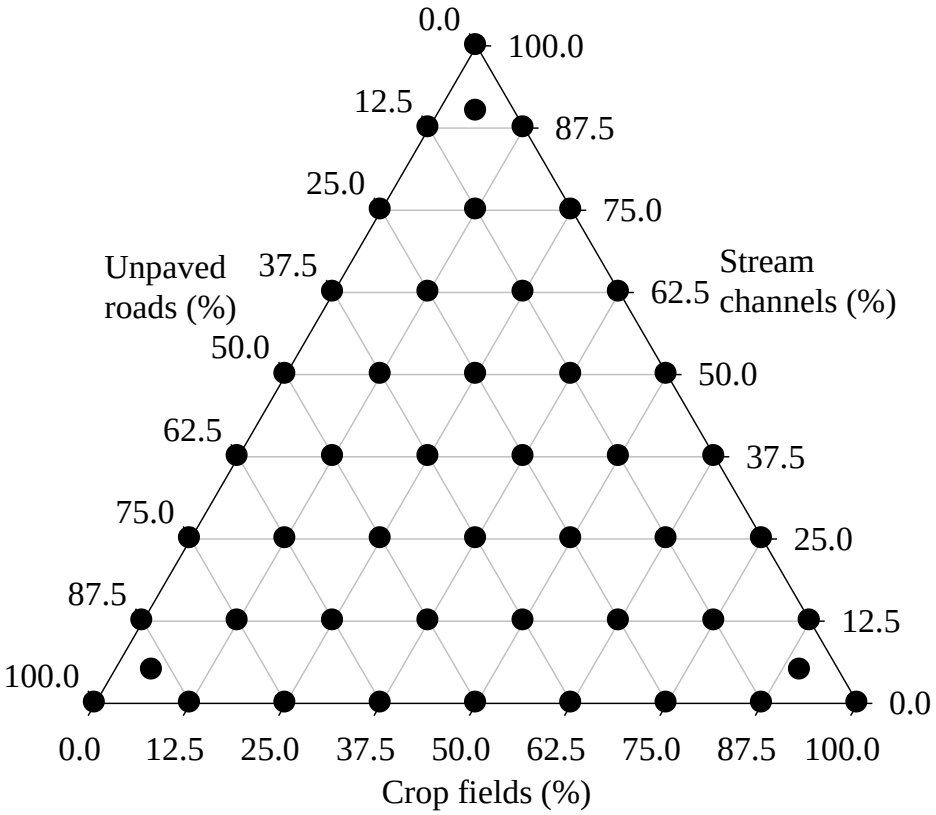

Figure 18 – Ternary diagram with the position of the experimental mixtures prepared for the PLSR models calibration.

UV-VIS, NIR, and MIR spectra were obtained for each mixture. Relationships between spectra (*x* variate) and the corresponding weight contribution of the sediment source datasets (*y* variate) were analyzed using partial least squares regression (PLSR). Partial least squares regression is an extension of the multiple linear regression model, were a linear model specifies the (linear) relationship between a dependent (response) variable *Y*, and a set of predictor variables, the *X*'s, so that:

$$Y = b_0 + b_1X_1 + b_2X_2 + \cdots + b_pX_p \quad (8)$$

where b_0 is the regression coefficient for the intercept and the b_i values are the regression coefficients for each wavelength computed from the data (*p* is equal 600 for UV-VIS, 1583 for MIR, and 3112 for NIR).

The composites samples were randomly picked to build the models (training set (s_t) = 33 composites samples - 69%), whereas the remaining (validation set (s_v) = 15 composites samples - 31%) were used for validation. Thus, the s_v:s_t ratio used was approximately 1:2, which is in agreement with recommendations in the literature (DASZYKOWSKI; WALCZAK; MASSART, 2002). The predictive performance of the models was evaluated by calculating several standard indicators such as the root mean square error of calibration (RMSEC), the root mean square error of cross-validation (RMSECV), the root mean square error of prediction (RMSEP), the ratio RMSECV to standard deviation (RPD) and the coefficient of determination (R_{adj}) of predicted values against reference data.

The procedure followed by Poulenard et al. (2009, 2012) was used to determine the number of components providing the best compromise between the description of the calibration set and the model predictive power, that is, the lowest predictive standard error. After define the best number of components to be used, all the 48 composites samples were used to generate the models.

Three independent PLSR models for each spectra range (UV-VIS, NIR, and MIR) were constructed to estimate the proportion of sediment originating from the three main potential sources. Unlike the mixed linear model used to estimate source ascription when using discrete variables (i.e. geochemical tracers and colour parameters), in the spectroscopy-PLSR models there is no boundary condition as the Equations 5 and 6. The uncertainty associated with the prediction was estimated by the confidence interval (95%) of prediction calculated by the regression of predicted values against reference data. UV-VIS, NIR, and MIR spectra of suspended sediment were then introduced into these PLSR models (e.g. Equation 8) to estimate the contribution of each sediment source and the associated uncertainty.

6 RESULTS

The results were presented specifically for each catchment. In the first part of this section, the results from Arvorezinha catchment are presented. Results from this catchment are subdivided as source discrimination by classical fingerprinting based on geochemical composition and by alternative methods based on spectroscopy analyses. Then, I present results regarding the building process of partial least-squares regression (PLSR) models based on spectroscopy analyses. Finally, results of source apportionment obtained with classical and alternative fingerprinting methods using PLSR models and colour parameters derived from visible reflectance are provided. In the second part of this section, I present the results of geochemical fingerprinting obtained for rainfall-runoff events that occurred in the two catchments of Júlio de Castilhos. The third and the fourth parts provide results of source discrimination with an emphasis on spatial, temporal, and intra-storm variations of sediment source contributions in Conceição and Guaporé catchments, respectively.

6.1 Arvorezinha catchment

6.2.1 Source discrimination

6.2.1.1 Classical fingerprinting based on geochemical composition

The scatterplot shows that differences in specific surface area (SSA) and total organic carbon (TOC) among the sources may have an effect on SSA and TOC of suspended sediments (Figure 19). Indeed, Kruskal-Wallis *H*-test demonstrated that the differences between sediment sources were significant for both SSA (H = 11.8; p = 0.003) and TOC (H = 13.4; p = 0.001). It means that the SSA and TOC could be used as sediment tracer properties. However, these properties have only been used to correct for particle sorting and the enrichment in fine particles and organic matter associated with downstream selective transport (e.g. COLLINS et al. 1997).

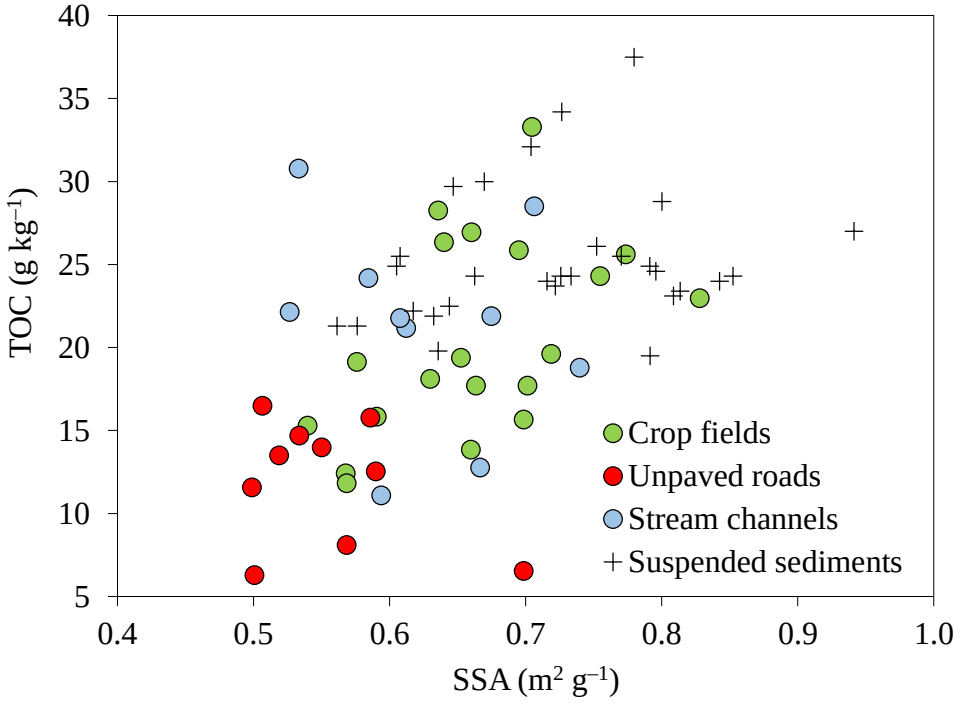

Figure 19 – Plots of specific surface area (SSA) versus total organic carbon (TOC) for suspended sediment samples and for source soil samples in Arvorezinha catchment.

According to Davis; Fox (2009), while cations and heavy metals show affinity towards fine sediments as a result of their high surface area for bonding, generalizing linearity is an assumption that could significantly change the estimated fraction of sediment from each source, if used erroneously. Thus, to further examine this phenomenon, the potential linear relationships with tracer property concentrations in source and sediment, Pearson's correlation coefficients were computed for SSA and TOC (Table 9). This table shows that the occurrence of significant correlations was variable across tracer properties and source categories for both SSA and TOC, similar to the findings of Smith; Blake (2014) and Pulley; Foster; Antunes (2015). No tracer properties showed significant correlations across all sources and sediment for either SSA or TOC. Only 20 and 13% of the possible pairs of SSA and TOC with tracer properties, respectively, were significant, and not all of them were positive correlated (Table 9), as it might have been expected, given that SSA and TOC tracer corrections are based on this assumption. Thereby, a positive linear relationship between SSA and TOC with geochemical tracer concentrations cannot not be assumed and applied uniformly to all the tracer properties examined in the present study. Besides, the particle size distribution of material sieved at 63 µm was very similar between sediment sources and suspended sediment (*Figure 20*). For this reason the tracer concentration were not corrected for SSA and TOC as the errors induced through inappropriate corrections could exceed those resulting from the use of uncorrected data.

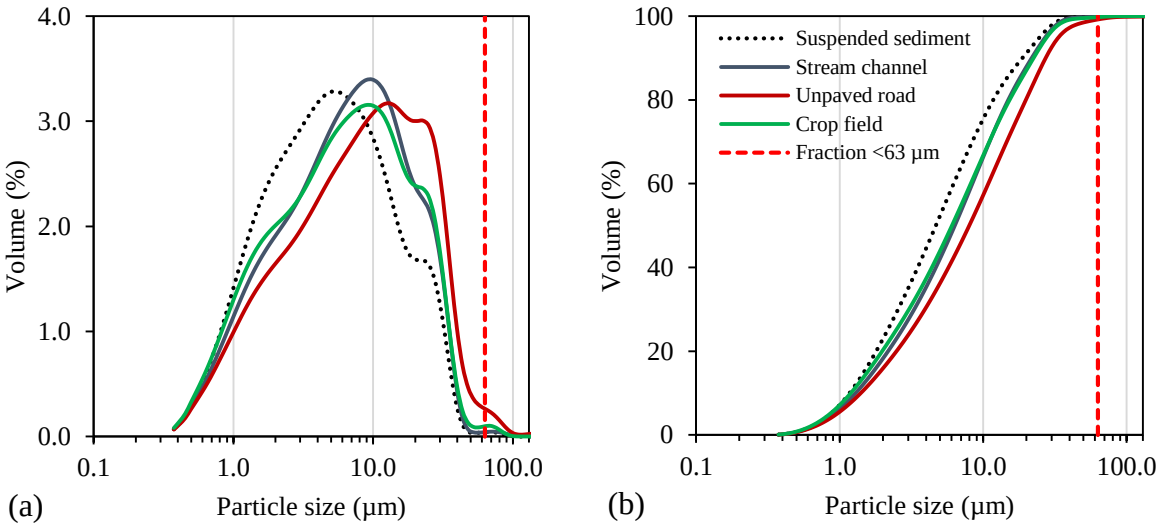

Figure 20 – Particle size distribution (a) and accumulated particle size distribution (b) of suspended sediment samples and sediment sources sieved at 63 µm in Arvorezinha catchment.

No outliers were detected in all tracers for all sediment sources (see Appendix 1). Ca, Be, Li, Ni, and TOC concentration of the 29 sediment samples were higher than the highest source concentration plus one standard deviation (Table 10). These elements were then considered as non-conservative (GELLIS; NOE, 2013) and were then excluded from the next steps. The sediments concentration in the remaining geochemical tracers laid well between the concentration ranges of the sources and were then kept.

Table 10 displays the Kruskal–Wallis *H*-values and the percentage of samples correctly classified for each tracer using discriminant function analysis (DFA). At this step, from the 24 remaining geochemical variables, 18 were selected as potential tracers by applying the Kruskal–Wallis *H*-test ($H>5.871$; $p<0.05$). No variable alone was able to correctly classify 100% of the source samples in their respective groups. The discriminatory power of individual variables ranged from 52.5 to 85%.

The 18 geochemical parameters identified as potential tracers were then entered into the stepwise multivariate DFA to select the optimum set for maximizing discrimination, whilst minimizing dimensionality. The progressive change of the Wilks' Lambda value (Λ^*) as the variables are introduced into the analysis are presented in Table 12. The final set of elements selected by DFA analyses was Mo, Ag, P, Fe, As, and Cr, resulting in a final value of the Λ^* parameter of 0.0126. This means that the set of selected variables explains approximately 98.7% of the differences between the sources, and only ~ 1.3% of the difference was due to intra source variation.

All the sediment source samples were correctly classified into their respective groups. Indeed, Mahalanobis distance shows the sediment sources were well separated by a significant distance of 48.1±5.5 from each other (Table 13 and Figure 21a). According to Minella; Walling; Merten (2008), even when a sample is correctly classified we need to consider the distance of each sample to the group central point, as shown in Figure 21a (i.e. the scatter within the group), because it represents the uncertainty associated with each source. The uncertainty associated with the discrimination of each source was very low, ranging from 0.002% for unpaved roads, to 0.024% for crop fields, with an average of 0.013%.

Table 9 – Pearson's correlation coefficients (*r*) and associated *p* values for correlations between total organic carbon (TOC) and specific surface area (SSA) with tracer property concentrations for source soil and suspended sediment samples. Bold values indicate significant correlation at $p<0.05$.

Fingerprint property	Crop fields				Unpaved roads				Stream channels				Suspended sediments			
	SSA		TOC		SSA		TOC		SSA		TOC		SSA		TOC	
	r	*p*	*r*	*p*	*r*	*p*	*r*	*p*	*r*	*p*	*r*	*p*	*r*	*p*	*r*	*p*
Ag	0.22	0.360	–0.34	0.139	0.15	0.688	0.03	0.942	–0.77	**0.010**	0.17	0.645	–0.05	0.793	0.21	0.268
As	0.15	0.520	–0.41	0.073	0.29	0.413	–0.53	0.114	–0.64	**0.049**	0.22	0.545	–0.19	0.312	–0.16	0.389
B	–0.14	0.564	–0.19	0.427	0.48	0.161	–0.07	0.849	0.42	0.231	0.08	0.831	–0.20	0.301	0.26	0.168
Ba	0.22	0.346	0.02	0.934	0.28	0.429	0.35	0.318	0.13	0.724	0.64	**0.048**	0.19	0.319	0.66	**0.000**
Be	–0.43	0.057	–0.11	0.631	0.42	0.228	0.30	0.401	–0.60	0.068	–0.26	0.473	0.15	0.430	0.61	**0.000**
Ca	0.33	0.158	0.38	0.096	0.00	0.994	0.11	0.769	0.65	**0.042**	0.37	0.297	0.01	0.951	0.75	**0.000**
Cd	0.41	0.074	0.18	0.437	–0.46	0.176	0.43	0.214	–0.12	0.747	0.70	**0.024**	–0.26	0.173	0.10	0.582
Co	–0.09	0.698	–0.18	0.437	–0.26	0.466	0.31	0.385	0.75	**0.012**	0.08	0.817	0.22	0.236	0.18	0.352
Cr	0.04	0.864	0.19	0.434	0.01	0.971	0.32	0.373	0.07	0.857	–0.74	**0.015**	–0.04	0.852	–0.12	0.542
Cu	0.04	0.852	0.56	**0.010**	–0.49	0.154	0.62	0.056	0.87	**0.001**	–0.18	0.628	0.48	**0.008**	0.07	0.718
Fe	–0.22	0.362	0.33	0.150	–0.05	0.887	0.07	0.850	0.79	**0.007**	–0.19	0.601	0.16	0.411	0.00	0.991
K	0.01	0.968	0.38	0.103	0.02	0.957	0.40	0.250	0.11	0.761	0.38	0.273	–0.24	0.192	–0.13	0.488
La	–0.12	0.611	0.21	0.378	–0.26	0.460	0.57	0.085	–0.35	0.326	0.33	0.351	0.16	0.385	0.33	0.079
Li	0.07	0.757	0.62	**0.003**	–0.43	0.212	0.42	0.229	0.63	0.053	–0.24	0.512	0.75	**0.000**	0.44	**0.014**
Mg	–0.25	0.279	0.12	0.604	–0.49	0.151	–0.10	0.783	0.63	0.050	–0.41	0.241	0.19	0.308	0.26	0.174
Mn	–0.29	0.219	–0.26	0.271	–0.25	0.489	0.17	0.647	0.76	**0.010**	0.15	0.678	–0.47	**0.008**	0.02	0.908
Mo	0.13	0.595	–0.25	0.284	0.10	0.786	0.30	0.399	–0.83	**0.003**	0.20	0.581	–0.42	**0.022**	–0.17	0.376
Na	0.29	0.211	0.06	0.805	0.28	0.425	–0.18	0.627	0.27	0.458	–0.17	0.636	0.45	**0.013**	0.49	**0.006**
Ni	0.05	0.846	0.35	0.125	0.06	0.872	0.44	0.202	0.76	**0.010**	–0.05	0.888	0.13	0.482	–0.02	0.910
P	–0.31	0.177	–0.02	0.919	–0.45	0.194	0.18	0.614	0.64	**0.048**	0.38	0.284	0.17	0.369	–0.17	0.358
Pb	–0.06	0.801	0.06	0.806	0.10	0.787	0.36	0.302	0.04	0.921	0.28	0.441	0.40	**0.030**	0.58	**0.001**
Sb	0.30	0.196	–0.40	0.079	–0.12	0.744	0.45	0.187	–0.43	0.220	0.38	0.276	0.18	0.346	–0.09	0.637
Se	–0.01	0.960	–0.32	0.172	–0.05	0.889	0.43	0.220	–0.80	**0.005**	0.34	0.331	0.04	0.818	–0.23	0.232
Sr	0.45	**0.044**	0.41	0.069	0.09	0.805	0.35	0.316	–0.12	0.737	0.25	0.486	0.25	0.184	0.79	**0.000**
Ti	–0.20	0.403	–0.29	0.218	–0.07	0.853	0.38	0.279	0.71	**0.022**	–0.02	0.957	0.67	**0.000**	0.42	**0.020**
Tl	0.30	0.196	0.31	0.182	0.09	0.796	–0.52	0.123	–0.55	0.101	–0.06	0.864	0.07	0.727	0.45	**0.012**
V	–0.12	0.619	0.09	0.709	0.09	0.796	0.22	0.539	0.73	**0.016**	–0.23	0.531	0.00	0.991	0.08	0.659
Zn	0.00	0.990	0.41	0.072	–0.47	0.167	0.50	0.142	0.75	**0.013**	0.28	0.427	0.29	0.122	0.16	0.404
Sign. correl.	1		2		0		0		14		3		7		9	
Pos. sign. correl.	1		2		0		0		10		2		5		9	

Table 10 – Test of sediment source range ("*range test*") of individual geochemical fingerprints for suspended sediments in Arvorezinha catchment. SD, standard deviation. Max+SD, maximum source concentration plus one standard deviation. Min+SD, minimum source concentration minus one standard deviation.

Fingerprint property	Crop fields (n = 20)		Unpaved roads (n = 10)		Stream channels (n = 10)		Suspended sediments (n = 29)	Source range		Sediment samples out of source range (%)	
	Mean	SD	Mean	SD	Mean	SD	Mean	Max+SD	Min+SD	Higher	Lower
Ag (mg kg^{-1})	8.77	1.99	2.36	2.07	6.37	2.18	6.97	10.8	0.3	0	0
As (mg kg^{-1})	68.91	8.12	39.02	20.97	42.20	14.53	51.37	77.0	18.1	0	0
B (mg kg^{-1})	2.60	1.08	6.37	1.69	3.81	1.65	5.69	8.1	1.5	4	0
Ba (mg kg^{-1})	143.05	41.91	159.55	48.20	268.82	57.31	328.20	326.1	101.1	10	0
Be (mg kg^{-1})	1.40	0.22	1.53	0.42	1.33	0.42	3.86	2.0	0.9	**29**	0
Ca (mg kg^{-1})	1514.14	323.95	1287.88	482.12	1985.76	333.70	2836.17	2319.5	805.8	**29**	0
Cd (mg kg^{-1})	0.29	0.03	0.14	0.06	0.38	0.04	0.47	0.4	0.1	24	0
Co (mg kg^{-1})	9.45	3.35	9.18	3.05	12.09	2.31	11.28	14.4	6.1	3	0
Cr (mg kg^{-1})	10.78	2.40	19.40	17.01	15.25	5.27	28.47	36.4	2.4	6	0
Cu (mg kg^{-1})	19.79	2.73	17.03	5.01	30.77	3.60	26.66	34.4	12.0	5	0
Fe (mg kg^{-1})	27376.06	4602.43	40011.04	4754.83	33388.90	4875.86	32505.82	44765.9	22773.6	0	0
K (mg kg^{-1})	1562.83	261.36	1846.68	629.78	1654.73	407.84	2093.77	2476.5	1216.9	1	0
La (mg kg^{-1})	27.27	8.02	53.68	11.35	38.46	5.48	48.91	65.0	19.2	0	0
Li (mg kg^{-1})	16.43	2.27	12.85	4.07	14.81	3.42	22.57	18.7	8.8	**29**	0
Mg (mg kg^{-1})	2319.94	490.03	3314.74	374.77	2135.38	536.49	3406.51	3689.5	1598.9	8	0
Mn (mg kg^{-1})	836.22	224.91	795.33	297.14	1318.99	289.17	1164.57	1608.2	498.2	0	0
Mo (mg kg^{-1})	48.76	9.06	11.20	10.50	10.70	10.48	43.84	57.8	0.2	1	0
Na (mg kg^{-1})	66.21	26.22	90.97	26.98	80.48	15.23	117.06	117.9	40.0	11	0
Ni (mg kg^{-1})	3.01	0.57	3.51	1.47	4.02	0.37	15.78	5.0	2.0	29	0
P (mg kg^{-1})	369.62	101.50	95.41	30.36	240.53	78.16	492.47	471.1	65.1	16	0
Pb (mg kg^{-1})	26.49	7.81	30.79	12.39	32.69	2.83	40.91	43.2	18.4	9	0
Sb (mg kg^{-1})	2.28	0.79	0.69	0.77	1.99	0.80	1.81	3.1	-0.1	2	0
Se (mg kg^{-1})	5.92	2.49	3.69	3.55	5.07	0.94	4.96	8.4	0.1	1	0
Sr (mg kg^{-1})	19.17	6.89	21.74	9.56	35.22	20.45	46.63	55.7	12.2	3	0
Ti (mg kg^{-1})	2822.99	684.99	3275.92	761.70	2453.56	647.21	3199.31	4037.6	1806.4	1	0
Tl (mg kg^{-1})	4.95	1.46	4.35	2.04	7.17	1.21	2.91	8.4	2.3	0	8
V (mg kg^{-1})	28.79	6.59	35.36	8.79	34.27	2.39	37.58	44.1	22.2	3	0
Zn (mg kg^{-1})	28.15	5.28	37.34	5.95	32.97	4.09	64.42	43.3	22.9	20	0
TOC (g kg^{-1})	20.51	5.88	11.95	3.74	21.31	6.09	28.80	27.4	8.2	**29**	0

Table 11 – The ability of individual geochemical fingerprints to distinguish sediment source type, assessing the Kruskal−Wallis *H*-test and discriminant function analysis (DFA). Bold values indicate significant differences between the sediment sources at $p<0.1$. Means followed by the same letter in the row are not different by the Kruskal–Wallis *H*-test at $p<0.05$. ns, not significant. *$p<0.1$, **$p<0.05$, ***$p<0.01$, ****$p<0.001$, *****$p<0.0001$.

Fingerprint property	Kruskal-Wallis test			DFA - correctly classified samples (%)	Crop fields	Unpaved roads	Stream channels
	p-value	*H*-value	Signif.		(*n* = 20)	(*n* = 10)	(*n* = 10)
Ag (mg kg^{-1})	**7.5E-04**	20.4	****	77.5	8.8 ±3.7 a	2.3 ±2.1 b	9.7 ±3.0 a
As (mg kg^{-1})	**2.8E-06**	23.2	*****	72.5	68.9 ±19.7 a	38.9 ±21.2 b	42.2 ±14.5 b
B (mg kg^{-1})	0.1081	4.4	ns	-	2.6 ±1.5 a	3.1 ±2.3 a	3.8 ±1.7 a
Ba (mg kg^{-1})	**0.0013**	13.2	***	57.5	143 ±44.0 b	159.6 ±48.2 ab	241.6 ±74.2 a
Be (mg kg^{-1})	**0.0535**	5.9	*	62.5	1.4 ±0.3 a	1.5 ±0.4 a	1.9 ±0.6 a
Ca (mg kg^{-1})	0.1023	4.6	ns	-	1514 ±391 a	1288 ±482 a	1539 ±432 a
Cd (mg kg^{-1})	**4.5E-05**	27.0	*****	85.0	0.27 ±0.08 b	0.13 ±0.07 c	0.36 ±0.06 a
Co (mg kg^{-1})	0.8219	0.4	ns	-	9.5 ±3.2 a	9.2 ±3.1 a	8.5 ±3.2 a
Cr (mg kg^{-1})	**0.0043**	10.9	***	55.0	10.8 ±10.5 b	19.4 ±17.0 a	18.6 ±7.8 a
Cu (mg kg^{-1})	**0.0001**	18.9	****	65.0	18.4 ±7.4 b	29.8 ±7.6 a	23.2 ±5.9 a
Fe (mg kg^{-1})	**0.0001**	19.8	****	77.5	27376 ±6957 b	40011 ±4755 a	25329 ±6957 b
K (mg kg^{-1})	0.2479	2.8	ns	-	1563 ±432 a	1847 ±630 a	1655 ±408 a
La (mg kg^{-1})	**8.0E-08**	26.6	*****	75.0	27.3 ±15.6 b	53.7 ±11.4 a	38.5 ±5.5 a
Li (mg kg^{-1})	**0.0068**	10.0	***	57.5	15.1 ±4.8 b	21.1 ±5.5 a	14.8 ±3.4 b
Mg (mg kg^{-1})	**0.0001**	18.6	****	65.0	2320 ±655 b	3315 ±375 a	2135 ±536 b
Mn (mg kg^{-1})	0.9317	0.1	ns	-	836.2 ±246.8 a	795.3 ±297.1 a	838.2 ±413.8 a
Mo (mg kg^{-1})	**2.3E-05**	22.0	*****	80.0	48.8 ±20.3 a	11.2 ±10.5 b	34.5 ±20.5 ab
Na (mg kg^{-1})	**0.0122**	8.8	**	52.5	66.2 ±28.6 b	91.0 ±27.0 a	80.5 ±15.2 ab
Ni (mg kg^{-1})	0.3301	2.2	ns	-	3.0 ±1.0 a	3.5 ±1.5 a	3.3 ±0.6 a
P (mg kg^{-1})	**2.3E-05**	23.7	*****	72.5	369.6 ±129.4 a	167.7 ±44.2 b	240.5 ±78.2 b
Pb (mg kg^{-1})	0.1133	4.4	ns	-	26.5 ±9.6 a	30.8 ±12.4 a	32.7 ±2.8 a
Sb (mg kg^{-1})	**0.0006**	14.8	****	67.5	2.3 ±1.1 a	0.7 ±0.8 b	2.0 ±0.8 a
Se (mg kg^{-1})	**0.0088**	9.5	***	55.0	5.9 ±3.1 a	3.6 ±3.7 b	6.8 ±1.4 a
Sr (mg kg^{-1})	**0.0012**	13.4	***	55.0	19.2 ±7.8 b	21.7 ±9.6 b	35.2 ±20.5 a
Ti (mg kg^{-1})	**0.0452**	6.2	**	55.0	2823 ±731 ab	3276 ±762 a	2454 ±647 b
Tl (mg kg^{-1})	**0.0024**	12.1	***	60.0	4.9 ±1.7 b	4.4 ±2.0 b	7.2 ±1.2 a
V (mg kg^{-1})	0.1239	4.2	ns	-	28.8 ±7.9 a	35.4 ±8.8 a	30.8 ±3.2 a
Zn (mg kg^{-1})	**0.0009**	14.0	****	65.0	28.1 ±7.0 b	37.3 ±6.0 a	25.7 ±6.1 b
TOC (g kg^{-1})	**0.0012**	13.4	***	60.0	20.5 ±6.6 a	12.0 ±3.7 b	21.3 ±3.1 a
SSA (m^2 g^{-1})	**0.0027**	11.8	***	60.0	0.663 ±0.086 a	0.555 ±0.061 b	0.625 ±0.071 ab

Table 12 – Results of the stepwise discriminant function analysis as indicated by the Wilks' Lambda values for the different fingerprinting approaches in Arvorezinha catchment.

Step	Fingerprint property selected	Wilks' Lambda	*p* to remove	Cumulative % of source type samples classified correctly
Geochemical				
1	Mo	0.4014	8.2E-07	72.5
2	Ag	0.0988	2.1E-06	97.5
3	P	0.0485	2.9E-05	100.0
4	Fe	0.0266	3.3E-05	100.0
5	As	0.0181	1.3E-03	100.0
6	Cr	0.0126	3.3E-03	100.0
NIR-spectroscopy				
1	PC2	0.3277	3.9E-14	77.5
2	PC1	0.1641	2.0E-09	90.0
3	PC5	0.0917	3.1E-06	95.0
4	PC3	0.0633	1.6E-04	97.5
5	PC14	0.0475	4.9E-04	97.5
6	PC4	0.0345	1.5E-03	97.5
7	PC10	0.0242	4.6E-03	97.5
8	PC21	0.0177	9.7E-03	100.0
MIR-spectroscopy				
1	PC2	0.5832	6.0E-10	60.0
2	PC1	0.2283	8.0E-10	75.0
3	PC4	0.1612	4.0E-06	87.5
4	PC5	0.0912	8.0E-06	95.0
5	PC10	0.0540	6.0E-05	97.5
6	PC8	0.0342	7.0E-04	97.5
VIS-based-colour parameters				
1	x	0.8533	4.59E-04	57.5
2	v*	0.7425	5.38E-04	57.5
3	c*	0.6712	6.46E-04	57.5
4	u*	0.4311	3.91E-03	62.5
Geochemical tracers + VIS-based-colour parameters				
1	Mo	0.4014	1.07E-05	72.5
2	Cr	0.3605	6.66E-05	80.0
3	Ag	0.0714	8.19E-05	97.5
4	Fe	0.0379	3.24E-04	97.5
5	u*	0.0360	3.98E-03	97.5
6	c*	0.0344	4.52E-03	97.5
7	b*	0.0292	4.96E-03	97.5
8	P	0.0150	5.30E-03	100.0
9	As	0.0081	6.61E-03	100.0
10	La	0.0061	7.94E-03	100.0
11	v*	0.0043	8.00E-03	100.0

Table 13 – Discriminant analysis output for the different fingerprinting approaches in Arvorezinha catchment. Underlined values indicate significant distances between the sediment sources groups at $p<0.05$.

DFA parameters	Geoch.	NIR	MIR	UV-VIS	VIS-colour	Geoch. + Colour
DFA output						
Wilks' Lambda	0.0126	0.0177	0.0341	0.0485	0.4311	0.0043
Variance explained by the variables (%)	98.7	98.2	96.6	95.2	56.9	99.6
Degrees of freedom	12;64	16;60	12;64	40;36	8;68	22;54
$F_{calculated}$	42.1	24.4	23.5	1.7	4.4	1.7
$F_{critical}$	1.9	1.82	1.9	7.7	2.1	35.1
p-value	<0.0001	<0.0001	<0.0001	0.0003	0.0002	<0.0001
F-values						
Degrees of freedom	6;32	8;30	6;32	20;18	4;34	11;27
$F_{critical}$	2.4	2.3	2.4	2.2	2.6	2.2
Stream channels vs. Unpaved roads	38.3	21.2	27.9	3.6	7.8	25.6
Stream channels vs. Crop fields	40.6	20.1	17.7	2.8	0.9	37.6
Unpaved roads vs. Crop fields	46.9	34.5	28.6	3.4	7.8	44.0
p-levels						
Stream channels vs. Unpaved roads	2.9E-13	2.4E-10	2.2E-11	0.0040	1.4E-04	1.9E-11
Stream channels vs. Crop fields	1.3E-13	4.4E-10	6.5E-09	0.0161	0.4802	1.7E-13
Unpaved roads vs. Crop fields	1.7E-14	4.5E-13	1.6E-11	0.0062	1.5E-04	2.4E-14
Squared Mahalanobis distances						
Stream channels vs. Unpaved roads	53.2	41.8	38.7	29.9	6.8	77.1
Stream channels vs. Crop fields	42.2	29.8	18.4	17.3	0.6	85.0
Unpaved roads vs. Crop fields	48.8	51.1	29.7	20.7	5.1	99.4
Average	48.1	40.9	28.9	22.6	4.2	87.2
Source type samples correctly classified (%)						
Stream channels	100.0	100.0	100.0	90.0	70.0	100.0
Unpaved roads	100.0	100.0	100.0	100.0	70.0	100.0
Crop fields	100.0	100.0	95.0	100.0	55.0	100.0
Total	100.0	100.0	97.5	97.5	62.5	100.0
Uncertainty associated with the discrimination of the source (%)						
Stream channels	0.005	0.094	0.311	11.170	45.693	9.9E-12
Unpaved roads	0.002	0.000	0.751	0.349	30.138	1.2E-12
Crop fields	0.024	1.772	6.322	2.933	52.596	2.5E-10
Average	0.013	0.910	3.426	4.346	45.256	1.3E-10

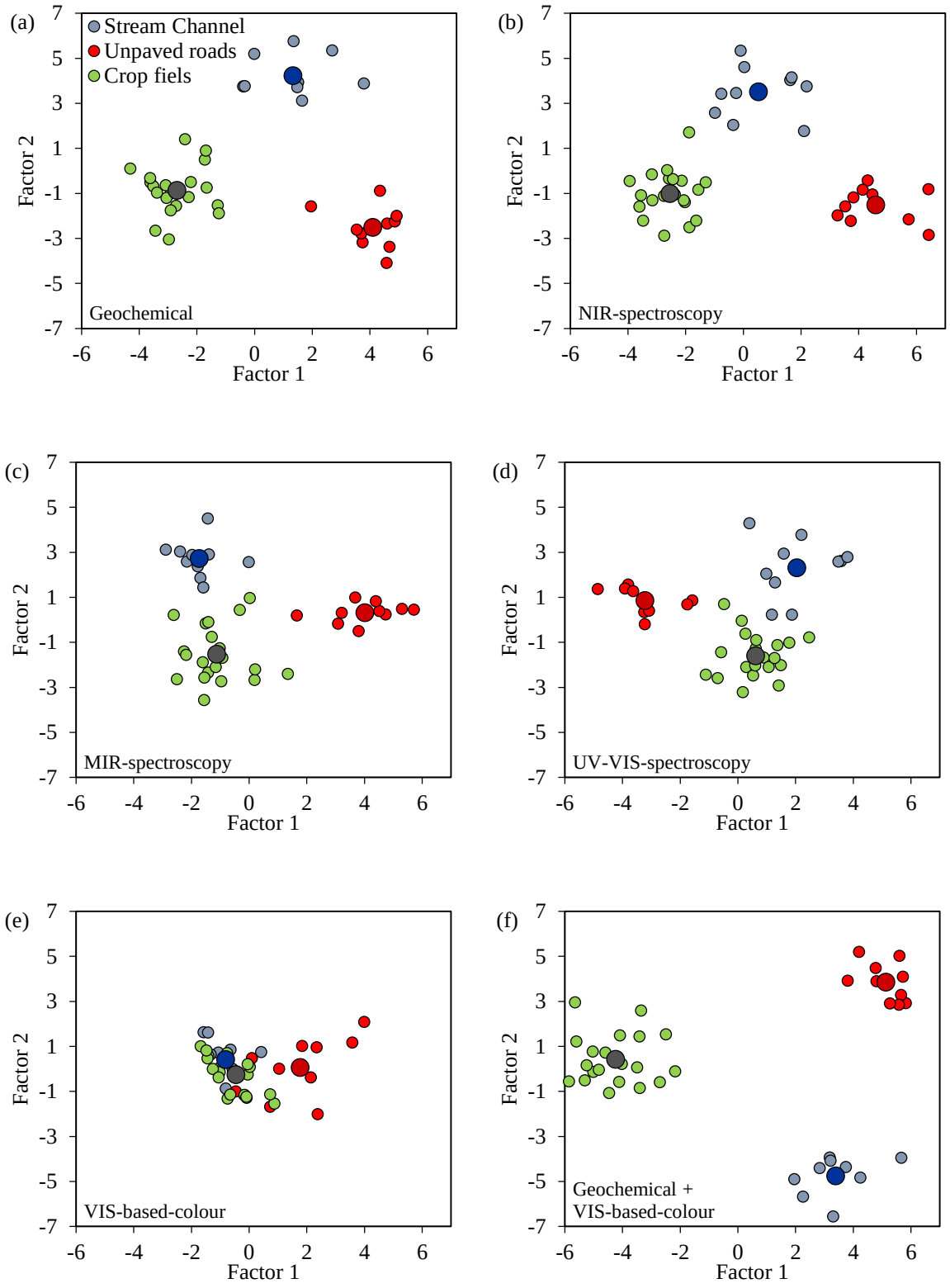

Figure 21 – Two-dimensional scatter plot of the first and second discriminant functions from stepwise discriminant function analysis (DFA) for geochemical composition (a), NIR-spectroscopy (b), MIR-spectroscopy (c), UV-VIS-spectroscopy (d), VIS-based-colour parameters (e), and geochemical composition coupled with VIS-based-colour parameters (f). Larger symbols represents the centroids of each source.

6.2.1.2 Alternative method based on NIR spectroscopy

NIR spectra of the <63 µm fraction of suspended sediments and each sediment source material were very similar (Figure 22), and 10 spectral features were observed (Table 14). To simplify the interpretation, the spectral features of NIR were grouped according to the main soil constituents, namely soil clay minerals (SCM – kaolinite [Kt], smectite [Sm], mica [Mc], and hydroxy-interlayered vermiculite [HIV]), and organic compounds (OC) (MADEJOVÁ; BALAN; PETIT, 2011; TERRA, 2011; VISCARRA ROSSEL; BEHRENS, 2010). The spectral features 1 and 3 at 7210 and 5243 cm^{-1} correspond to absorption bands of water. Spectral features 2 and 5 at 7072 and 4530 cm^{-1} correspond to the functional groups OH of SCM respectively. Spectral feature 4 at 4630 cm^{-1} correspond to $\nu_{1a}+\delta$ Al–OH of Kt. Spectral feature 8 and 10 at 4250 and 4095 cm^{-1} correspond to $\nu_{1b}+\delta$ (O–H)+(Al–OH) of Mc. Spectral feature 6 at 4467 cm^{-1} correspond to $\nu_1+\delta_b$ Al–OH of Sm. Finally, the spectral features 7 and 9 at 4331 and 4192 cm^{-1} correspond to OC, specifically to the stretching of C–H ($3\nu_4$) of methyl groups and stretching of C−O ($4\nu_1$) of carbohydrates, respectively.

The potential of discrimination of NIR spectroscopy was analyzed based on the scores obtained from the principal component analysis (PCA). The scores of 39 principal components (PC) obtained from PCA were entered into a DFA (PC-DFA model). DFA selected eight PCs (Table 12), resulting in a final Λ* value of 0.0177. It means 98.2% of variation in these eight PCs were due to differences between the sediment sources, i.e. only 1.8% of the variation was due to the intra-group variation. The PC-DFA model enables to correctly classify all (100%) the sediment source samples with an average uncertainty of 0.910% (Table 13). The square Mahalanobis distance between the sources was on average 40.9±10.7, and all the distances between sediment sources were highly significant (P<0.00001) (Figure 21b and Table 13).

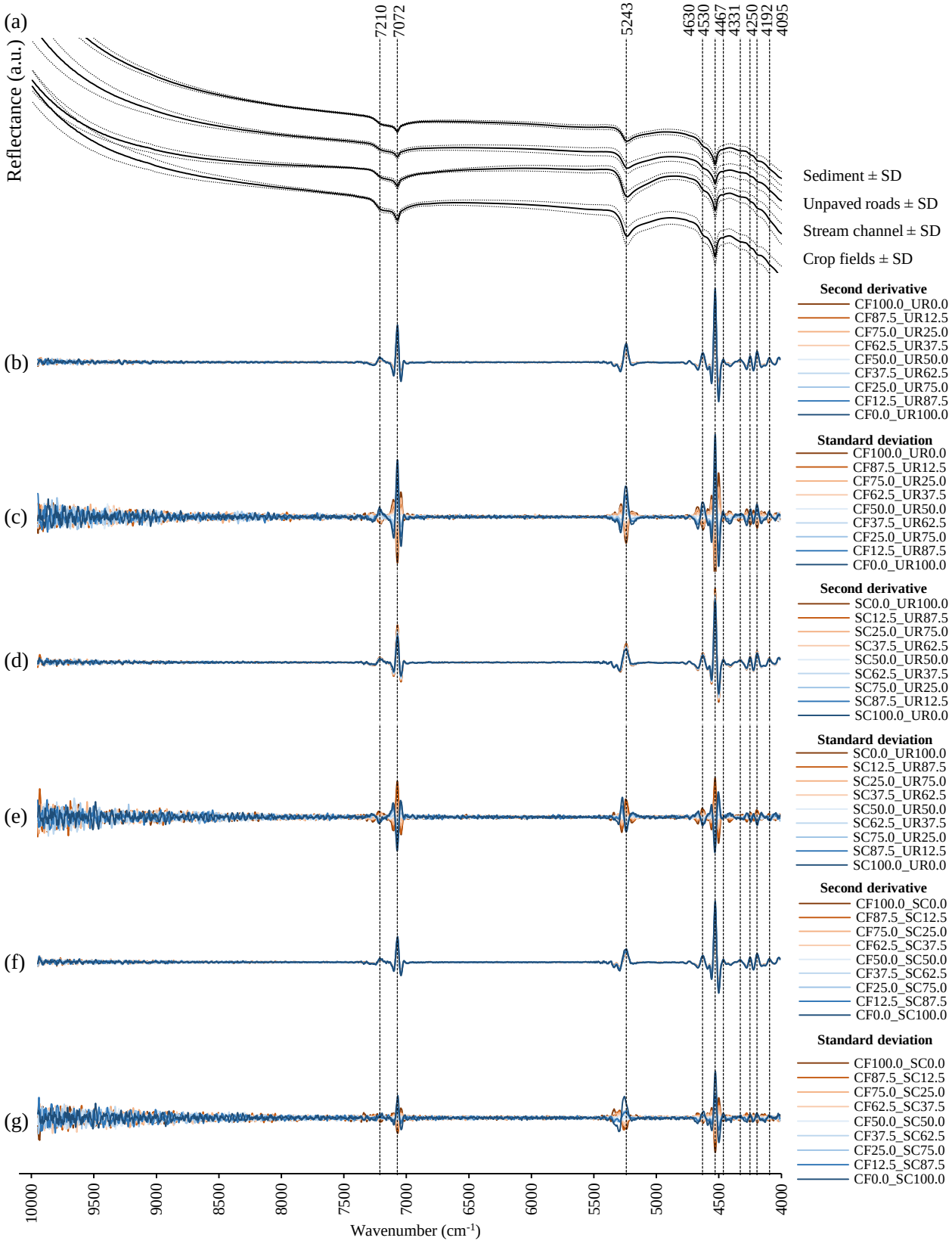

Figure 22 – Mean NIR reflectance spectra of the main sediment sources (unpaved road [UR], stream channel [SC], and crop field [CF]) and suspended sediment (a), and second-derivative of the simple mixtures used to calibrate NIR-PLSR models (b, d, f) and standard deviation of the simple mixtures (c, e, g). Values after the source abbreviation in the legend indicate the percentage of each source in the mixture. The standard deviation was calculated each 2 cm^{-1} by using the spectra of the 9 simple mixtures of each pair of sediment sources.

Table 14 – Characteristics of the absorption features detected by NIR spectroscopy. Kt, kaolinite; Sm, smectite; Mc, micas; HIV, hydroxy-interlayered vermiculite; OC, organic compounds.

Spectral feature	Wavenumber (cm^{-1})	Wavenumber from literature (cm^{-1})	Soil constituent	Functional group	NIR mode
1	7210	7246[a]	Water	O–H	$\nu_1+\nu_3$
2	7072	7067[b,c]	Kt, Sm, Mc, HIV	O–H	$2\nu_1$
3	5243	5422[a]	Water	(H–O–H)+(O–H)	$\nu_2+\nu_3$
4	4630	4630[a,c]	Kt	Al–OH	$\nu_{1a}+\delta$
5	4530	4529[a,c]	Kt	O–H	$\nu_{1b}+\delta$
		4533[a,c]	Sm	O–H	$\nu_1+\delta_a$
		4533[a,c]	Mc	O–H	$\nu_1+\delta$
6	4467	4484[a,c]	Sm	Al–OH	$\nu_1+\delta_b$
7	4331	4318[b]	OC (methyls)	C–H	$3\nu_4$
8	4250	4274[b,c]	Mc	(O–H)+(Al–OH)	$\nu_{1b}+\delta$
9	4192	4200[a]	OC (carbohydrates)	C–O	$4\nu_1$
10	4095	4082[b,c]	Mc	(O–H)+(Al–OH)	$\nu_{1b}+\delta$

[a] Viscarra Rossel; Behrens (2010)
[b] Terra (2011)
[c] Madejová; Balan; Petit (2011)

6.2.1.3 Alternative method based on MIR spectroscopy

MIR spectra of the fraction <63 µm for suspended sediments and sediment sources (Figure 23) were very similar, and 16 spectral features were observed in all spectra (Figure 23 and Table 15). In order to simplify the interpretation, the spectral features were grouped according to the main soil constituents, namely soil clay minerals (SCM – kaolinite [Kt], smectite [Sm], mica [Mc], hydroxy-interlayered vermiculite [HIV], gibbsite [Gb]), quartz (Qz), and organic compounds (OC) (TERRA, 2011; VISCARRA ROSSEL; BEHRENS, 2010; YANG; MOUAZEN, 2012). Spectral feature 1 at 3695 cm^{-1}corresponds to OH stretching (ν_{1a}) of Kt. Spectral features 2, 12, 13, 14 and 16 at 3620, 1115, 1020, 915 and 698 cm^{-1} respectively correspond to SCM. Spectral features 3 and 4, at 2930 and 2850 cm^{-1} correspond to CH stretching of aromatic and aliphatic organic compounds, respectively. Spectral features 5, 6, and 7 at 1990, 1870 and 1785 cm^{-1} correspond to SiO stretching bands of Qz. Spectral features 8 and 15 at 1630 and 808 cm^{-1} correspond to both SCM and Qz; features 9 and 10 at 1530 and 1340 cm^{-1} correspond to both OC and Qz; feature 11 at 1160 correspond to both OC and SCM.

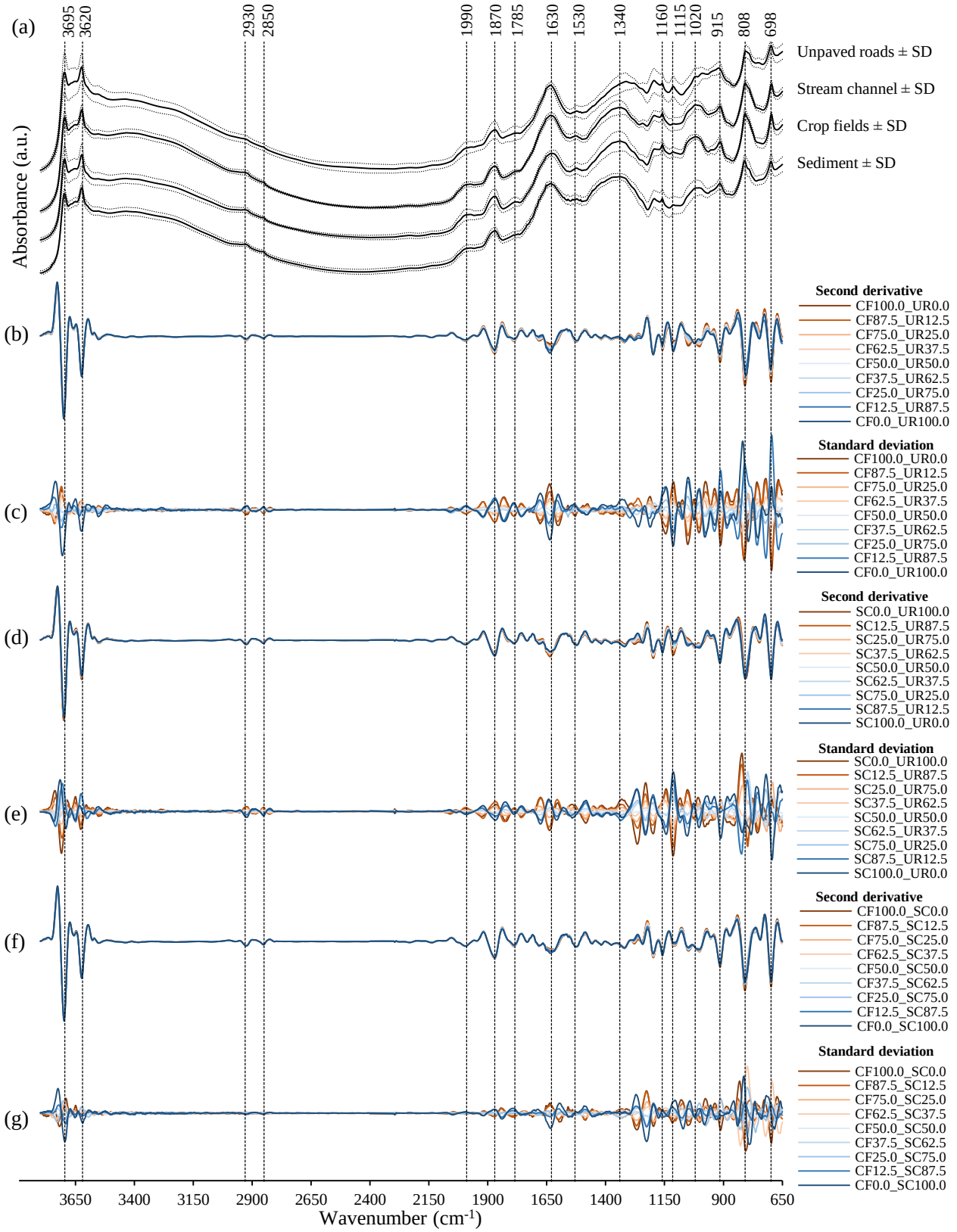

Figure 23 – Mean MIR spectra of the main sediment sources (unpaved road [UR], stream channel [SC], and crop field [CF]) and suspended sediment (a), and second-derivative of the simple mixtures used to calibrate MIR-PLSR models (b, d, f) and standard deviation of the simple mixtures (c, e, g). Values after the source abbreviation in the legend indicate the percentage of each source in the mixture. The standard deviation was calculated each 2 cm^{-1} by using the spectra of the 9 simple mixtures of each pair of sediment sources.

Table 15 – Characteristics of the absorption features detected by MIR spectroscopy. Kt, kaolinite; Sm, smectite; Mc, micas; HIV, hydroxy-interlayered vermiculite; Gb, gibbsite; Qz, quartz; OC, organic compounds.

Spectral feature	Wavenumber (cm^{-1})	Wavenumber from literature (cm^{-1})	Soil constituent	Functional group	MIR mode
1	3695	3695[a]	Kt	O–H	ν_{1a}
2	3620	3620[a]	Kt	O–H	ν_{1b}
		3620[a]	Sm	O–H	ν_1
		3620[a]	Mc	O–H	ν_1
3	2930	2930[a]	OC (aromatic)	C–H	ν_3
4	2850	2850[a]	OC (aliphatic)	C–H	ν_1
5	1990	1975[b]	Qz	Si–O	ν
6	1870	1867[b]	Qz	Si–O	ν
7	1785	1790[b]	Qz	Si–O	ν
8	1630	1628[b]	Kt, Sm, Mc, HIV	O–H	δ
		1628[b]	Qz	Si–O	ν
9	1530	1527[b]	Qz	Si–O	ν
		1525[c]	OC (aromatic)	C=C	ν
10	1340	1527[b]	Qz	Si–O	ν
		1350[c]	OC (aliphatic)	C–H	ν
11	1160	1157[b]	OC (polysaccharide)	C–O	ν
		1157[b]	OC (aliphatic)	C–OH	ν
		1157[b]	Kt, Sm, Mc, HIV	O–Al–OH	δ
12	1115	1111[b]	Kt, Sm, Mc, HIV	Si–O–Si	ν
		1111[b]	Gb	Al–O–OH	δ
13	1020	1018[b]	Kt, Sm, Mc, HIV	Si–O–Si	ν_5
14	915	915[a]	Kt	Al–OH	δ
		915[a]	Sm	Al–OH	δ_a
15	808	814[b]	Qz	Si–O	ν
		814[b]	Kt, HIV, Gb	Al–OH	δ
16	698	702[b]	Kt, Sm, Mc, HIV	Si–O	ν

[a] Viscarra Rossel; Behrens (2010)
[b] Terra (2011)
[c] Yang; Mouazen (2012)

The potential of MIR-spectroscopy to discriminate sediment sources was analyzed based on the scores obtained from the principal component analysis (PCA). The scores of 39 principal components (PC) obtained in the PCA were then entered in the DFA (PC-DFA model) where six PCs were selected (Table 12). These six PCs together explained 70.8% of the total variation obtained from the 39 PCs. In the DFA, the final Λ^* value was 0.0342 (Table 12). It means that 96.6% of variation in these six PCs was due to differences between sediment sources, i.e. only 3.4% of the variation was due to the intra-source variation. The PC-DFA

model enables to correctly classify 97.5% of the sediment source samples with an average uncertainty of 3.426% (Table 13). The square Mahalanobis distance between SC and CF was smaller (18.4) than the distance between these sources and UR (SC vs. UR = 38.7, CF vs. UR = 29.7) (Figure 21). Nonetheless, the distances between sediment sources were always significant (p<6.5E–09) (Table 13).

6.2.1.4 Alternative method based on UV-VIS spectroscopy

Two approaches to discriminate sediment sources using UV-VIS spectroscopy information were performed. The first one based on PC-DFA models using the whole UV-VIS spectra range. The second one used colour parameters derived from VIS region, and then sediment sources were discriminated by using VIS-based-colour parameters alone and coupled to the geochemical tracers.

6.2.1.4.1 Source discrimination using VIS-based-colour parameters in a two-step procedure

Figure 24 and Figure 25 display the colours of each source materials and suspended sediment samples. Linear relationships between VIS-based-colour parameters with SSA and TOC in source and sediment was evaluated by Pearson correlation coefficients (Table 16). For VIS-based-colour parameters in crop fields samples, only h* was negatively correlated to SSA (r = –0.50, p = 0.026), and λd (nm) was positively correlated to SSA (r = 0.51, p = 0.021). For stream channels samples, only h* was negatively correlated to TOC (r = –0.69, p = 0.028), and λd (nm) was negatively correlated to SSA (r = –0.64, p = 0.047). All the other possible pairs of SSA and TOC with VIS-based-colour parameters were not significant correlated. For this reason, we assumed that a positive linear relationship between SSA or TOC and colour parameters cannot be assumed to apply uniformly to all the tracer properties examined in the present study. Therefore, VIS-based-colour parameters were not corrected for SSA and TOC because we assumed that the errors incurred through inappropriate corrections could exceed those resulting from the use of uncorrected data.

Table 16 – Pearson's correlation coefficients (*r*) and associated *p* values for correlations between total organic carbon (TOC) and specific surface area (SSA) with VIS-based-colour parameters for source soil and suspended sediment samples. Bold values indicate significant correlation at $p<0.05$.

VIS-based-colour parameter property	Crop fields				Unpaved roads				Stream channels				Suspended sediments			
	SSA		TOC		SSA		TOC		SSA		TOC		SSA		TOC	
	r	*p*	*r*	*p*	*r*	*p*	*r*	*p*	*r*	*p*	*r*	*p*	*r*	*p*	*r*	*p*
R	0.11	0.645	–0.35	0.133	0.29	0.421	–0.25	0.481	–0.15	0.671	–0.53	0.118	0.27	0.150	–0.10	0.586
G	0.15	0.527	–0.41	0.076	0.28	0.434	–0.34	0.339	–0.23	0.528	–0.50	0.145	0.29	0.125	–0.10	0.613
B	0.23	0.335	–0.36	0.116	0.17	0.647	–0.31	0.382	–0.35	0.323	–0.38	0.278	0.32	0.089	–0.07	0.732
H_{RGB}	0.39	0.085	0.25	0.290	–0.49	0.151	0.37	0.290	–0.49	0.148	0.56	0.090	–0.12	0.537	–0.17	0.378
I_{RGB}	0.17	0.486	–0.38	0.097	0.24	0.504	–0.31	0.384	–0.24	0.496	–0.47	0.166	0.29	0.117	–0.09	0.631
S_{RGB}	–0.17	0.476	–0.05	0.850	0.06	0.880	0.30	0.407	0.49	0.154	–0.46	0.179	0.06	0.733	–0.13	0.509
x	–0.23	0.330	0.22	0.355	–0.12	0.732	0.40	0.258	0.55	0.102	0.10	0.784	–0.19	0.325	–0.07	0.713
y	–0.33	0.153	0.08	0.745	0.09	0.807	0.20	0.576	0.62	0.056	–0.12	0.732	–0.24	0.210	–0.10	0.612
Y	0.14	0.558	–0.40	0.082	0.28	0.437	–0.28	0.427	–0.20	0.588	–0.49	0.148	0.27	0.149	–0.09	0.634
X	0.13	0.573	–0.38	0.095	0.27	0.454	–0.26	0.465	–0.19	0.604	–0.49	0.146	0.27	0.152	–0.09	0.633
Z	0.22	0.350	–0.37	0.111	0.17	0.629	–0.26	0.472	–0.31	0.376	–0.39	0.265	0.30	0.104	–0.07	0.706
L	0.15	0.541	–0.39	0.091	0.28	0.441	–0.32	0.365	–0.22	0.549	–0.50	0.139	0.29	0.126	–0.10	0.605
u*	–0.10	0.683	0.03	0.888	–0.14	0.693	0.46	0.181	0.43	0.210	–0.31	0.387	0.07	0.701	–0.10	0.585
v*	–0.23	0.324	–0.12	0.610	0.21	0.558	0.11	0.764	0.49	0.147	–0.58	0.081	0.07	0.721	–0.14	0.458
a*	–0.01	0.958	0.17	0.475	–0.33	0.351	0.56	0.093	0.35	0.327	0.07	0.840	0.06	0.766	–0.05	0.786
b*	–0.24	0.312	–0.02	0.928	0.10	0.783	0.23	0.520	0.58	0.080	–0.40	0.247	0.00	0.990	–0.13	0.479
c*	–0.20	0.396	0.01	0.958	0.03	0.930	0.31	0.387	0.56	0.092	–0.34	0.331	0.01	0.974	–0.13	0.493
h*	–0.50	**0.026**	–0.33	0.152	0.41	0.237	–0.32	0.375	0.51	0.135	–0.69	**0.028**	–0.10	0.603	–0.07	0.712
H	–0.31	0.188	–0.28	0.233	0.47	0.172	–0.49	0.149	0.27	0.459	–0.62	0.055	–0.12	0.542	0.04	0.848
V	0.15	0.541	–0.39	0.091	0.28	0.441	–0.32	0.365	–0.22	0.549	–0.50	0.139	0.29	0.126	–0.10	0.605
C	–0.17	0.471	0.01	0.972	0.00	0.994	0.35	0.325	0.53	0.116	–0.36	0.310	0.03	0.872	–0.13	0.497
λ_d (nm)	0.51	**0.021**	0.10	0.665	–0.25	0.482	0.20	0.576	–0.64	**0.047**	0.40	0.256	0.31	0.100	0.05	0.794
Pe	–0.26	0.276	0.19	0.414	–0.05	0.894	0.34	0.343	0.57	0.088	0.05	0.892	–0.21	0.260	–0.06	0.743
RI	–0.15	0.525	0.36	0.120	–0.26	0.466	0.42	0.223	0.26	0.465	0.54	0.105	–0.32	0.081	0.13	0.486
Sign. correl.	2		0		0		0		1		1		0		0	
Pos. sign. correl.	1		0		0		0		0		0		0		0	

Figure 24 – Colour pictures of the 40 sediment source samples analyzed and the colour picture of the average of stream channel, unpaved road, and crop fields.

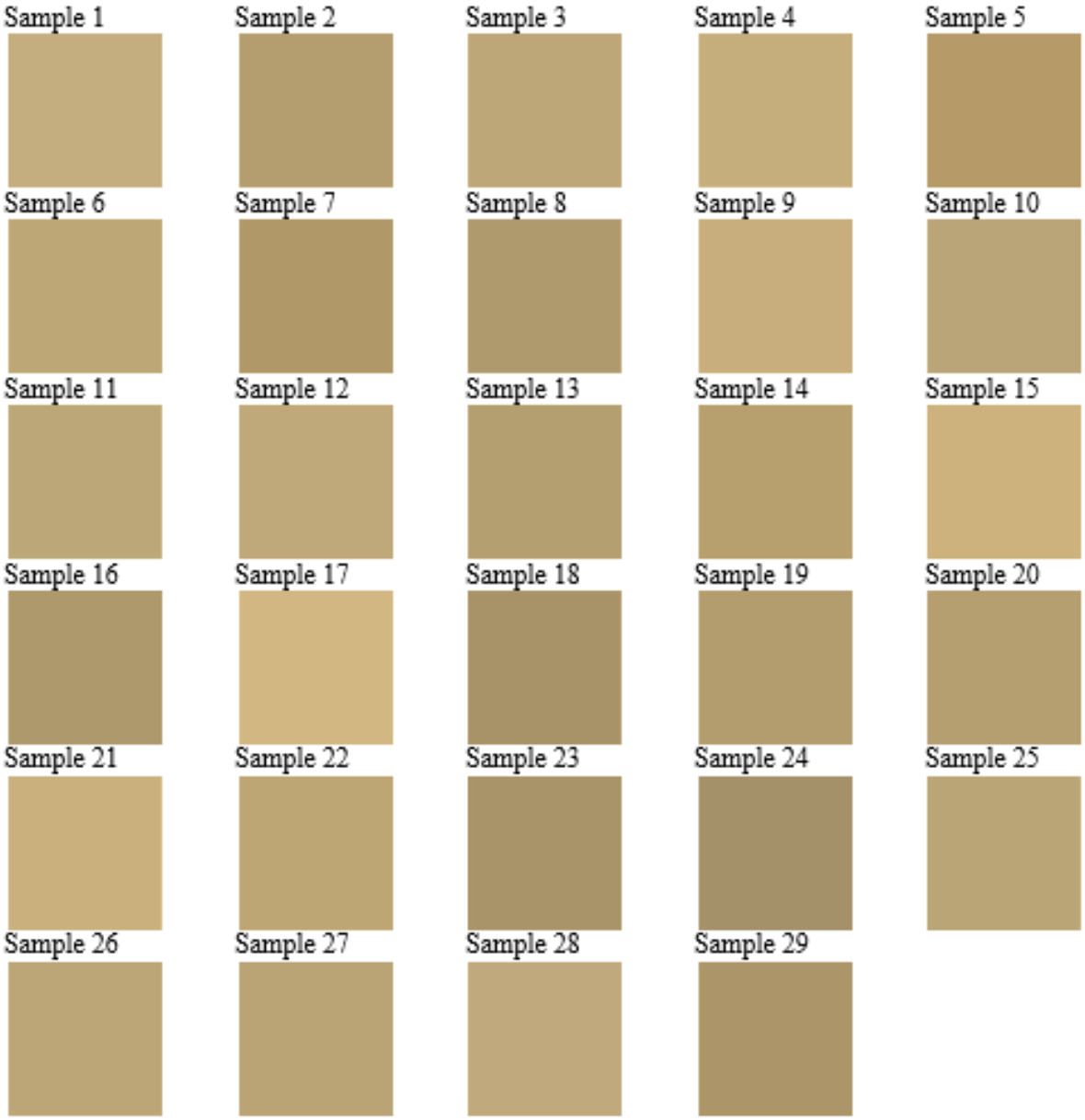

Figure 25 – Colour pictures of the 29 suspended sediment samples analyzed.

Outliers were not detected in all 24 colour parameters derived from VIS spectra range for all sediment sources (see Appendix 2). The values of H and h* in the 29 sediment samples were higher than the highest source value plus one standard deviation (Table 17). The values of a* and λ_d (nm) in all sediment samples were lower than the lowest source value (Table 17). Thereby, H, h*, a*, and λ_d (nm) parameters were considered as non-conservative (GELLIS; NOE, 2013) and were then excluded from the next steps. The remaining colour parameters in suspended sediments laid between the range values found in the source materials and were kept.

Table 17 – Test of sediment source range ("*range test*") of individual VIS-based-colour parameters for suspended sediments in Arvorezinha catchment. SD, standard deviation. Max+SD, maximum source concentration plus one standard deviation. Min+SD, minimum source concentration minus one standard deviation.

VIS-based-colour parameter	Crop fields (n = 20)		Unpaved roads (n = 10)		Stream channels (n = 10)		Suspended sediments (n = 29)	Source range		Sediment samples out of source range (%)	
property	Mean	SD	Mean	SD	Mean	SD	Mean	Max+SD	Min+SD	Higher	Lower
R	173.6	15.1	179.0	14.3	164.9	16.0	192.6	193.3	148.9	14	0
G	136.8	13.0	136.9	17.6	128.4	15.2	162.7	154.5	113.2	23	0
B	109.1	13.4	104.7	21.3	100.0	15.1	123.1	126.0	83.4	16	0
H_{RGB}	2.3	0.5	2.5	1.1	2.0	0.4	2.4	3.6	1.3	0	0
I_{RGB}	139.8	13.4	140.2	17.4	131.1	15.3	159.4	157.6	115.8	17	0
S_{RGB}	32.3	4.1	37.2	5.1	32.5	2.9	34.8	42.3	28.2	0	0
x	0.4	0.0	0.4	0.0	0.4	0.0	0.4	0.4	0.4	0	7
y	0.4	0.0	0.4	0.0	0.4	0.0	0.4	0.4	0.4	2	0
Y	28.2	5.6	29.0	7.0	24.8	6.3	39.0	36.0	18.5	20	0
X	29.4	5.7	30.5	6.8	26.0	6.4	38.7	37.3	19.6	17	0
Z	18.7	4.6	17.9	6.9	15.8	5.0	24.4	24.8	10.8	16	0
L	59.8	5.1	60.3	6.4	56.5	5.9	68.6	66.6	50.6	20	0
u*	26.0	3.4	30.3	4.2	25.9	2.2	21.7	34.5	22.5	0	20
v*	24.2	3.1	27.4	4.2	24.4	2.5	31.5	31.6	21.1	13	0
a*	10.1	1.3	11.9	2.0	10.1	0.8	5.3	13.9	8.9	0	**29**
b*	20.2	2.8	23.5	4.2	20.8	2.1	24.7	27.8	17.4	1	0
c*	22.6	3.0	26.4	4.4	23.1	2.2	25.2	30.8	19.6	0	0
h*	1.1	0.0	1.1	0.1	1.1	0.0	1.4	1.2	1.0	**29**	0
H	18.5	0.5	18.0	0.9	18.6	0.4	22.7	19.0	17.1	**29**	0
V	5.8	0.5	5.9	0.6	5.5	0.6	6.7	6.5	4.9	20	0
C	3.8	0.5	4.4	0.7	3.9	0.3	4.0	5.1	3.3	0	0
λ_d (nm)	588.4	1.0	588.5	1.7	587.9	0.8	583.6	590.2	586.8	0	**29**
Pe	29.3	4.9	34.9	9.2	31.9	4.7	29.9	44.1	24.4	0	0
RI	0.3	0.1	0.3	0.2	0.3	0.2	0.1	0.5	0.1	0	17

Table 18 presents the Kruskal–Wallis *H*-values, as well as the percentage of samples correctly classified by each VIS-based-colour parameters using discriminant function analysis (DFA). From the 20 remaining VIS-based-colour parameters, only 11 were selected as potential tracers by applying the Kruskal-Wallis *H*-test (H>4.576; p<0.1) (Table 18). Discriminatory power of individual variables for VIS-based-colour parameters ranged from 35.0 to 60.0%.

Table 18 – The ability of individual VIS-based-colour parameters to distinguish sediment source type, assessing the Kruskal−Wallis *H*-test and discriminant function analysis (DFA). Bold values indicate significant differences between the sediment sources at $p<0.1$. Means followed by the same letter in the row are not different by the Kruskal–Wallis H-test at $p<0.05$. ns, not significant, *$p<0.1$, **$p<0.05$, ***$p<0.01$, ****$p<0.001$, *****$p<0.0001$.

Fingerprint property	Kruskal-Wallis test			DFA - correctly classified	Crop fields	Unpaved roads	Stream channels
	p-value	*H*-value	Signif.	samples (%)	(*n* = 20)	(*n* = 10)	(*n* = 10)
R	0.1134	4.4	ns	-	173.6 ±15.1 a	179.0 ±14.3 a	164.9 ±16.0 a
G	0.2403	2.9	ns	-	136.8 ±13.0 a	136.9 ±17.6 a	128.4 ±15.2 a
B	0.2194	3.0	ns	-	109.1 ±13.4 a	104.7 ±21.3 a	100.0 ±15.1 a
H_{RGB}	0.1951	3.3	ns	-	2.26 ±0.49 a	2.48 ±1.14 a	2.03 ±0.42 a
I_{RGB}	0.2105	3.1	ns	-	139.8 ±13.4 a	140.2 ±17.4 a	131.1 ±15.3 a
S_{RGB}	**0.0354**	6.7	**	47.5	32.3 ±4.1 b	37.2 ±5.1 a	32.5 ±2.9 b
x	**0.0782**	5.1	*	57.5	0.39 ±0.01 b	0.40 ±0.02 a	0.39 ±0.01 b
y	**0.0789**	5.1	*	60.0	0.37 ±0.01 b	0.38 ±0.01 a	0.37 ±0.01 b
Y	0.2010	3.2	ns	-	28.2 ±5.6 a	29.0 ±7.0 a	24.8 ±6.3 a
X	0.1745	3.5	ns	-	29.4 ±5.7 a	30.5 ±6.8 a	26.0 ±6.4 a
Z	0.2258	3.0	ns	-	18.7 ±4.6 a	17.9 ±6.9 a	15.8 ±5.0 a
L	0.2010	3.2	ns	-	59.8 ±5.1 a	60.3 ±6.4 a	56.5 ±5.9 a
u*	**0.0270**	7.2	**	45.0	26.0 ±3.4 b	30.3 ±4.2 a	25.9 ±2.2 b
v*	**0.0787**	5.1	*	45.0	24.2 ±3.1 b	27.4 ±4.2 a	24.4 ±2.5 b
a*	**0.0271**	7.2	**	50.0	10.1 ±1.3 b	11.9 ±2.0 a	10.1 ±0.8 b
b*	**0.0803**	5.0	*	50.0	20.2 ±2.8 b	23.5 ±4.2 a	20.8 ±2.1 b
c*	**0.0609**	5.6	*	50.0	22.6 ±3.0 b	26.4 ±4.4 a	23.1 ±2.2 b
h*	0.4403	1.6	ns	-	1.11 ±0.03 a	1.10 ±0.06 a	1.12 ±0.03 a
H	**0.0801**	5.0	*	35.0	18.5 ±0.5 a	18.0 ±0.9 b	18.6 ±0.4 a
V	0.2010	3.2	ns	-	5.83 ±0.50 a	5.88 ±0.62 a	5.51 ±0.58 a
C	**0.0515**	5.9	*	50.0	3.81 ±0.48 b	4.42 ±0.66 a	3.87 ±0.33 b
λ_d (nm)	0.3401	2.2	ns	-	588.4 ±1.0 a	588.5 ±1.7 a	587.9 ±0.8 a
P_e	**0.0885**	4.8	ns	57.5	29.3 ±4.9 b	34.9 ±9.2 a	31.9 ±4.7 b
RI	0.2246	3.0	ns	-	0.26 ±0.12 a	0.26 ±0.16 a	0.35 ±0.15 a

VIS-based-colour parameters identified by the Kruskal-Wallis test as providing statistically significant discrimination between the source material samples were then entered into the stepwise multivariate DFA to select the optimum set for maximizing discrimination, whilst minimizing dimensionality. DFA analysis was performed separately for colour parameters and combining both data set (hereafter referred as geochemical + VIS-based-

colour). Table 12 shows the progressive change of the Wilks' Lambda value (Λ*) as the variables are introduced into the analysis. The set of variables selected by DFA analyses comprised four (x, v*, c*, and u*) and eleven (Mo, Cr, Ag, Fe, u*, c*, b*, P, As, La, and v*) variables, for VIS-based-colour parameters alone and for geochemical + VIS-based-colour, respectively (Table 12). When combining the data sets in the DFA, the variables selected were almost the same as the ones obtained when conducting DFA separately. The differences were the inclusion of La, and selection of b* instead of x. When performing DFA separately, there were variables explaining the same variation in both dataset. Thus, when combining both dataset in DFA, some variables were automatically removed or replaced by DFA to avoid redundancy and, consequently, over-parameterization of sediment mixing model.

The final value of the Λ* parameter was 0.4311 and 0.0043 for DFA using VIS-based-colour parameters and geochemical + VIS-based-colour, respectively (Table 12). As the value of Λ* is the proportion of the total variance due to the error of the source discrimination, the selected variables provided an error of 43.1 and 0.4% when using VIS-based-colour parameters and geochemical + VIS-based-colour, respectively. It means the set of selected variables explains approximately 56.9 and 99.6% of the differences between the sources, for DFA using VIS-based-colour parameters and geochemical + VIS-based-colour, respectively (Table 13).

When combining geochemical tracers and VIS-based-colour parameters, all the source samples (100%) were correctly classified in their respective groups (Table 13). The Mahalanobis distance values shows that the sediment sources were well separated from each other by a significant distance of 87.2±11.3 (Table 13 and Figure 21f). Furthermore, there was a great improvement in source discrimination when combining geochemical tracers and VIS-based-colour parameters, decreasing the uncertainty to values close to zero (1.3×10^{-10} %) (Figure 21f and Table 13). However, when using VIS-based-colour parameters alone, only 62.5% of the samples were correctly classified. At least 11 geochemical tracers (Ag, As, Cd, Cu, Fe, La, Mg, Mo, P, Sb, and Zn) alone were able to discriminate the sediment sources better than the set of VIS-based-colour parameter selected by DFA (Table 11). VIS-based-colour parameters were only able to discriminate UR from the other sources (CF and SC), and although significant, the distances were very short (Table 13 and Figure 21e). When analyzing the VIS-based-colour parameters separately by applying Kruskal–Wallis *H* test, it is also possible verify that no VIS-based-colour parameter was able to differentiate CF and SC (Table 18).

6.2.1.4.2 Source discrimination using UV-VIS spectra ratios and the PC-DFA model

Figure 26 displays the average UV-VIS spectra and its first derivative of the fraction <63 µm for suspended sediments and each sediment source material. Spectra were very similar between suspended sediments and sediment sources. In all sediment and source samples several absorption bands were found mainly related to iron oxides in the UV-VIS spectra.

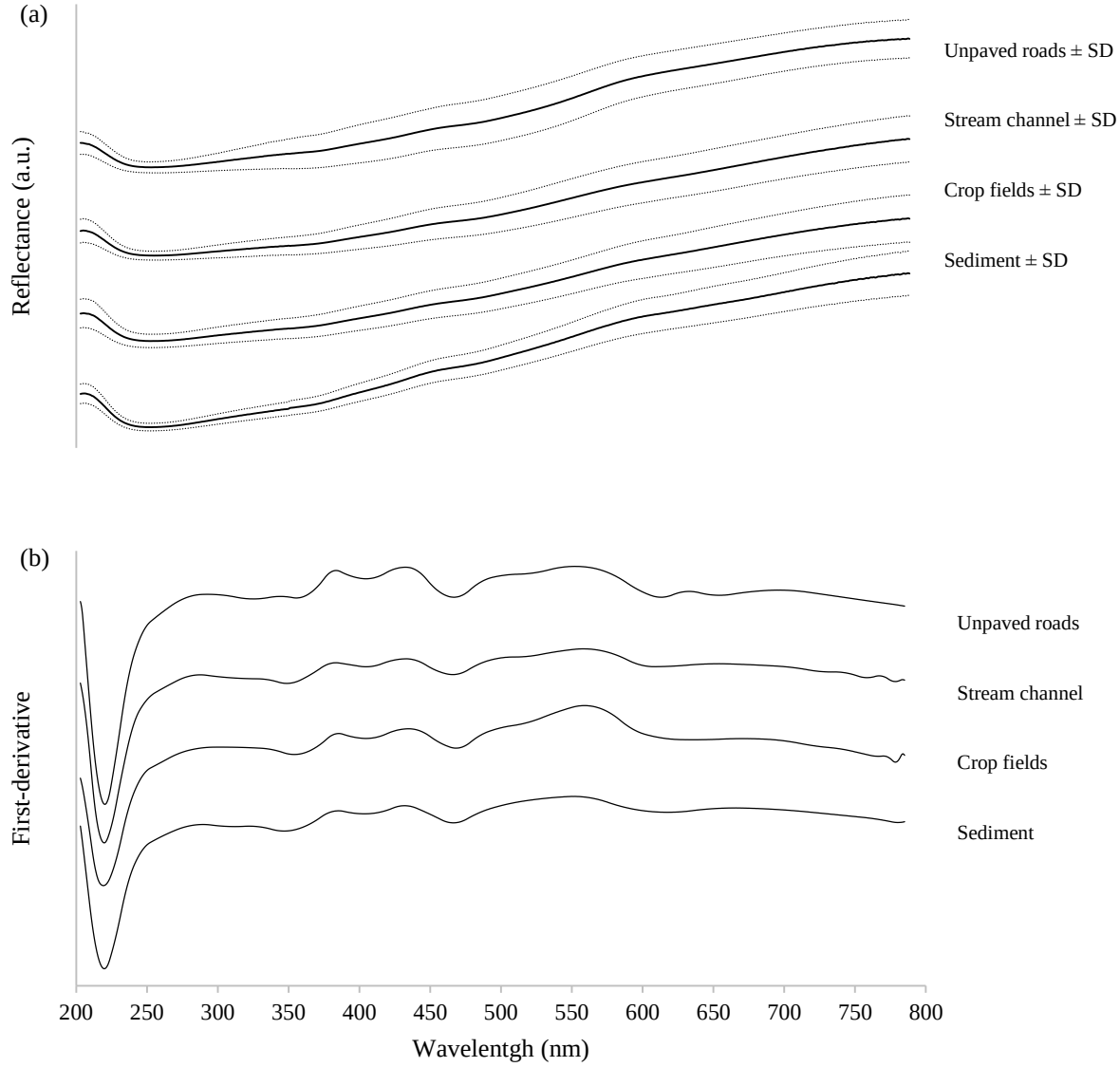

Figure 26 – Mean UV-VIS reflectance spectra (a) and their first-derivative (b) of the suspended sediment and the three sediment sources in Arvorezinha catchment.

To facilitate the interpretation of some of these differences, we elaborated Figure 27 and Table 19, which present several ratios between different absorption bands of the UV-VIS spectrum frequently used in the literature. The second-derivative curves of remission functions in the visible range of fine earth samples displayed three major absorption bands commonly assigned to Fe-oxides (Figure 27). The first band at low wavelength (A1 in Figure 27) correspond to a single electron transition of Fe in goethite (CANER et al., 2011; FRITSCH et al., 2005; KOSMAS et al., 1984; VISCARRA ROSSEL; BEHRENS, 2010). The two other bands (A2 and A3) correspond to an electron pair transition, which is observed at lower wavelength for Fe in goethite (A2, in Figure 27) than for Fe in hematite (A3). The band intensities were measured from the amplitude between each band minimum and its nearby maximum at a higher wavelength (Figure 27, A1, A2 and A3 in Table 19). This procedure enabled to estimate the proportion of hematite (Hr) in the pool of Fe-oxides (hematite+goethite) by applying the equation Hr (%) = A3/(A1+A3). Thereby, it is possible to verify the enrichment of hematite in the Fe-oxides pool in the order SC<CF<UR (Table 19). Munsell hue also shows this sequence order of redness for sediment sources (SC=5.79YR < CF=5.76YR < UR=5.63YR, data not shown).

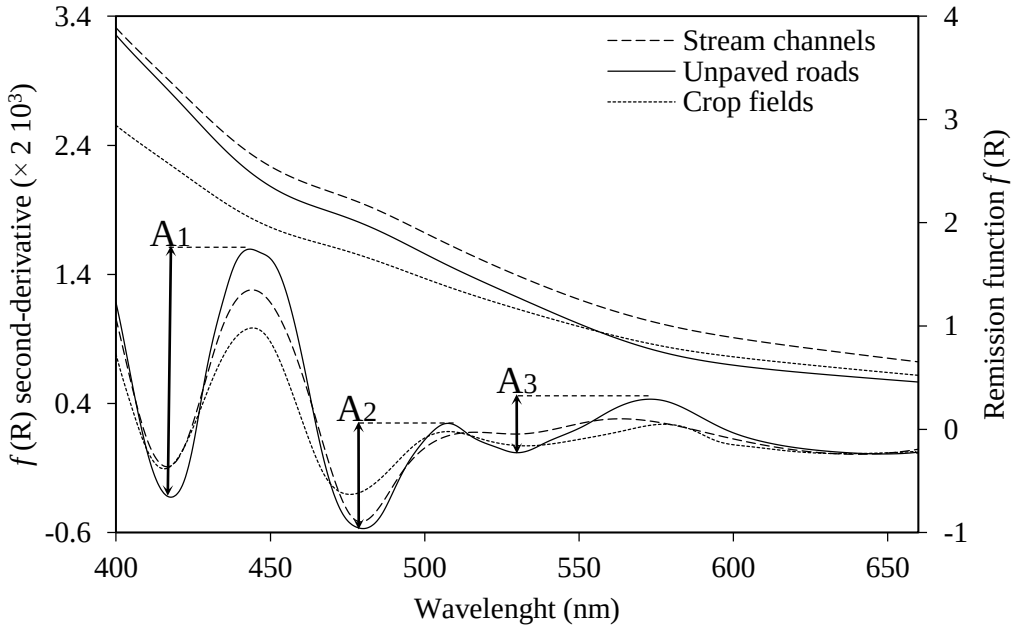

Figure 27 – Second-derivative spectra of the remission function *f* (R) from VIS-diffuse reflectance spectroscopy curves showing the absorption bands (minima) of Fe-oxides in the sediment sources. A_1 indicates the single electron transition of goethite, A_2 indicates the electron pair transition of goethite, A_3 indicates the electron pair transition of hematite.

Table 19 – UV-VIS spectra ratios for organic and mineral soil components. Bold values indicate significant differences between the sediment sources at $p<0.1$ by Kruskal−Wallis H-test. SET, single electron transition; EPT, electron pair transition; Gt, goethite; Hm, hematite; A, amplitudes of the SET and the EPT of the diffuse reflectance spectra illustrated in Figure 27; Hr, proportion of Hm in the Fe-oxides pool.

UV-VIS parameter	Wavelength ratio (nm)	Soil constituent	Stream channels	Unpaved roads	Crop fields	Kruskal−Wallis test	
						H-value	*p*-value
Organic compounds							
E2/E3	254/365	Organic matter	1.04 ±0.02	1.06 ±0.05	1.06 ±0.02	3.3	0.1882
E4/E6	465/665	Organic matter	1.30 ±0.08	1.39 ±0.07	1.34 ±0.09	5.6	**0.0597**
Iron oxides							
A1	420/450	SET Gt	1.80 ±0.83	2.41 ±1.58	1.44 ±0.76	3.1	0.2119
A2	480/510	EPT Gt	0.88 ±0.43	1.01 ±0.88	0.61 ±0.31	2.3	0.3198
A3	535/575	EPT Hm	0.21 ±0.11	0.49 ±0.42	0.24 ±0.12	4.3	0.1143
Hr (%)	A3/(A1 + A3)	-	10.66 ±2.96	18.39 ±8.15	15.20 ±5.29	9.7	**0.0078**

Absorption bands in the UV-VIS spectra related to organic compounds were also found in all soil and sediment samples. Compared to CF and SC, the organic matter of UR showed lower molecular weight and lower degree of condensation of the aromatic rings as indicated by higher E4/E6 ratio (Table 19).

Scores obtained from the principal component analysis (PCA) were used to evaluate the potential use of UV-VIS spectra for discriminating sediment sources. The first 20 principal components (PC) explained 79.4% of the total variation in the spectra. These 20 PCs were then entered into a DFA (PC-DFA model), resulting in a final Λ^* value of 0.0485 (Table 13). It means 95.2% of variation in these 20 first PCs were due to differences between the sediment sources, i.e. only 4.8% of the variation was due to the variation intra group. Despite the similarity between sediment and sources signatures, the PC-DFA model enable to correctly classify 97.5% of the sediment source samples with an average uncertainty of 4.35% (Table 13).

The square Mahalanobis distance between the sources was on average 22.5±6.5, almost 2 and 4 times shorter than obtained by the geochemical tracers and geochemical + VIS-based-colour (Table 13 and Figure 21d). Nonetheless, unlike colour parameters based on VIS spectra, the distances between sediment sources were always significant for the PC-DFA model based on UV-VIS spectra (Table 13). This is somehow explained by a loss of information and,

consequently, loss of discriminating power, when using colour parameters based on VIS-spectra instead of the whole UV-VIS spectrum.

6.2.2 Building partial least-squares models based on spectroscopy analyses

The performance of predictive models used for the spectroscopy approaches is given in Table 20. The correlations between actual and predicted proportions were excellent, with R^2 close to 1 for all the models (Table 20 and Figure 28), even using only 3 to 4 components for each independent PLSR model (Table 20). According to Chang et al. (2001), values of RPD lower than 2 (RPD = ratio RMSECV/standard deviation) indicate models of high quality. As all our independent models showed RPD values always higher than 5, we can conclude the models have good predictability. Moreover, the average difference between predicted and actual values on the set of calibration for the samples that were not used to build the model, measured by the RMSEP parameter, was always lower than 13.8%.

Table 20 – Predictive performance of the PLSR models based on spectroscopy analyses.

Sediment source	NC	R_{adj}	RMSEC (%)	RMSEP (%)	RMSECV (%)	RPD (%)
NIR-spectroscopy						
Crop fields	3	0.9970	1.1	5.4	2.4	11.9
Unpaved roads	4	0.9996	0.4	5.3	1.9	15.5
Stream channels	3	0.9946	0.5	6.4	3.1	9.2
MIR-spectroscopy						
Crop fields	4	0.9903	2.1	4.7	2.9	10.0
Unpaved roads	4	0.9978	1.2	2.1	1.5	19.8
Stream channels	4	0.9929	1.6	3.9	2.3	12.4
UV-VIS-spectroscopy						
Crop fields	3	0.9822	2.2	13.8	5.8	5.0
Unpaved roads	3	0.9903	1.9	8.3	3.9	7.4
Stream channels	3	0.9900	1.7	10.5	4.4	6.5

NC, number of components used in the UV-VIS-PLSR model; R_{adj}, coefficient of determination; RMSEC, root mean square error of calibration; RMSEP, root mean square error of prediction; RMSECV: root mean square error of cross-validation; RPD, ratio between the standard deviation and RMSECV.

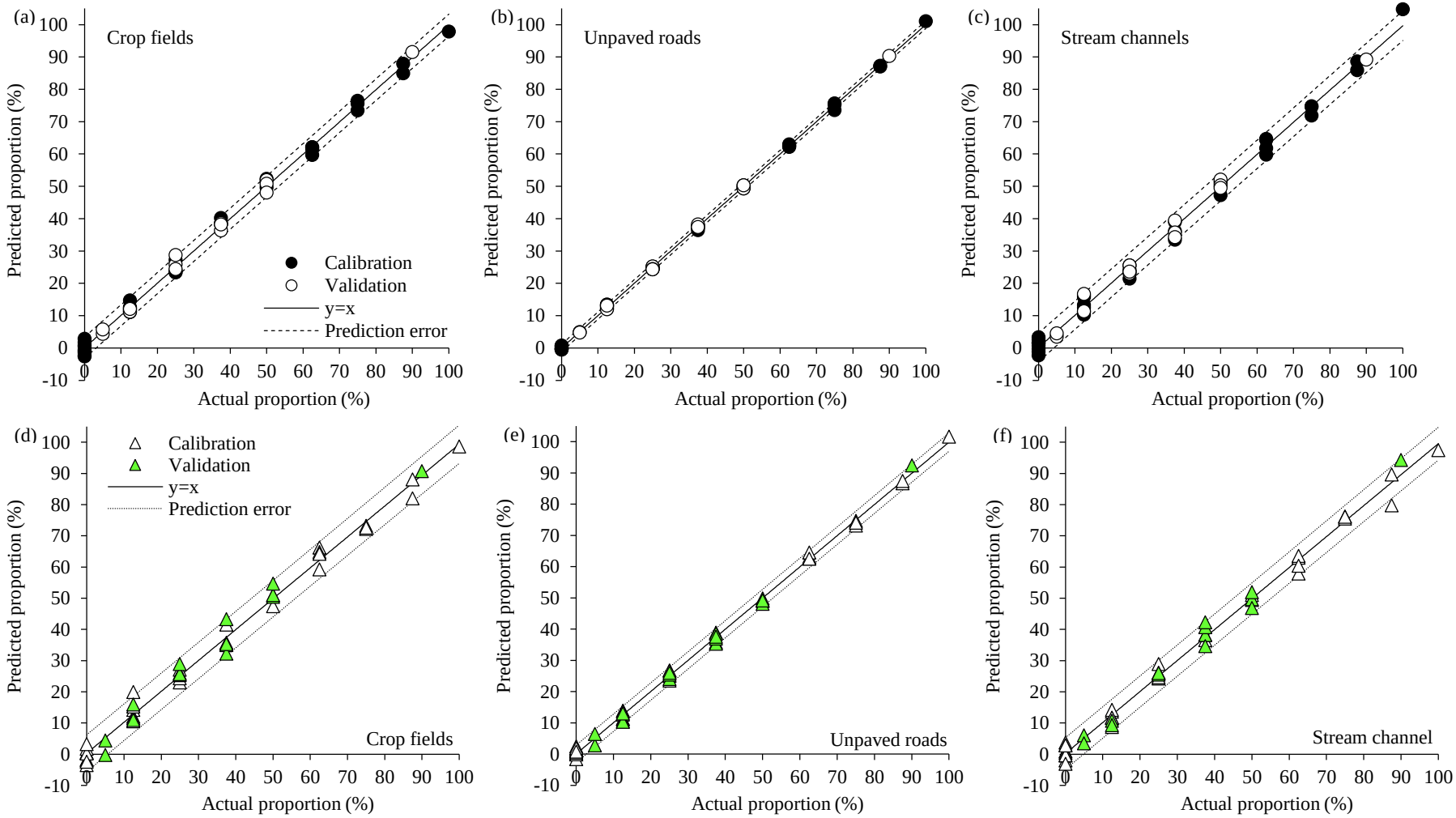

Figure 28 – Relationship between actual and PLSR models calculated percentage of sediment sources in experimental mixtures for NIR-spectroscopy [crop fields (a), unpaved roads (b), and stream channels (c)], MIR-spectroscopy [crop fields (d), unpaved roads (e), and stream channels (f)], and UV-VIS-spectroscopy [crop fields (g), unpaved roads (h), and stream channels (i)]. Dashed lines represent the confidence interval limit (95%).

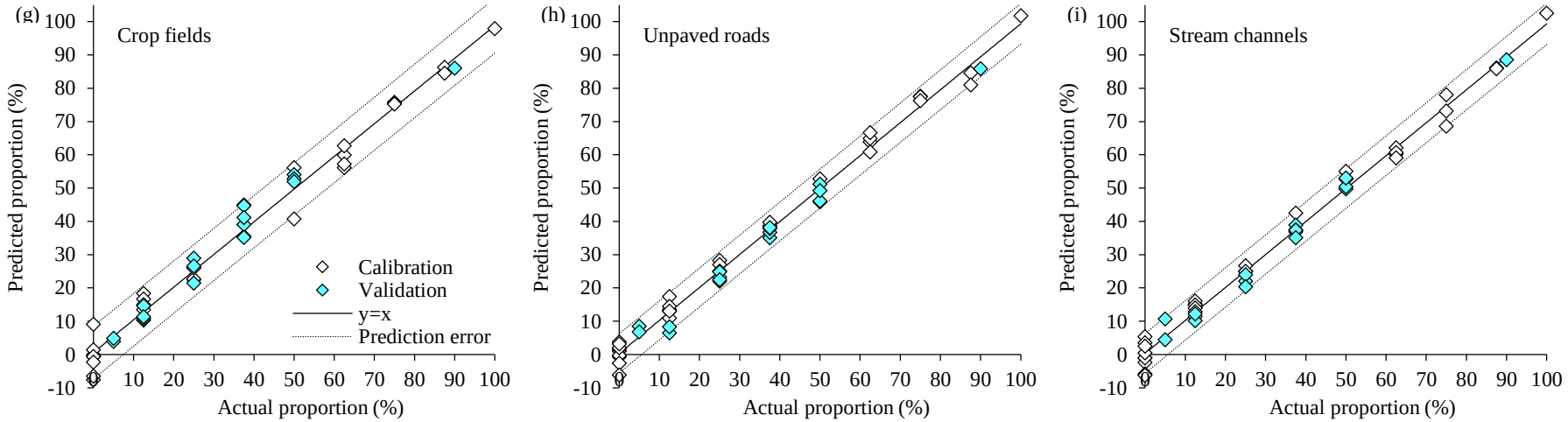

Figure 28 – Continued…

According to Legout et al. (2013), the sum of the predicted proportions for the independent PLSR models can provide a way to control the reliability of the predictions. Considering the whole data set used in the construction of the PLSR models (i.e. training and validation) led to an average sum of the three predicted source proportions of 100.0±1.2, 100.0±0.5, and 100.0±3.0% for NIR, MIR, and UV-VIS approaches, respectively (data not shown). The sum of the three predicted source proportions for each approach ranged from 97.4 to 102.8%, 99.0 to 101.1%, and 90.1 to 106.5%, for NIR, MIR, and UV-VIS, respectively (data not shown). These results highlight the good prediction performance of PLSR models based on spectroscopy methods.

Figure 22 displays the regions in NIR spectra which allows for the differentiation between the sediment sources. In the Figure 22b,d,f, the second-derivative of NIR spectra of all the simple mixtures (composed by only two sediment sources each) used to construct the NIR-PLSR models are presented. To facilitate the visualization of differences in the spectral features according to the variation in the proportion of each source, the standard deviation of these same spectra are shown in Figure 22c,e,g. The standard deviation was calculated each 2 cm^{-1} by using the spectra of the 9 simple mixtures of each pair of sediment sources. These figures clearly show a higher variation between the sources UR vs. CF and UR vs. SC than between the sources CF vs. SC. In the NIR region, spectral features at 4331 and 4192 cm^{-1} corresponding to stretching of C–H of methyl groups and stretching of C–O of carbohydrates, respectively, allowed for the better discrimination of UR. This is explained by the lower content of TOC in UR (12.0±5.5 g kg^{-1}) compared to the CF and SC (20.5±6.6 and 21.3±3.1 g kg^{-1}, respectively). Moreover, the higher abundance of 2:1 clay minerals in the UR compared to the CF and SC (Figure 29) contributed to the better discrimination of UR at the spectral features 2 and 5. Thus, the combined effect of differences in mineral composition and organic matter content resulted in the lowest prediction error (±1.1%) for the UR NIR-PLSR models (Figure 28).

As the abundance of Kt in all the three sources (Figure 29) and the carbon content (Table 11) of the CF and SC sources were very similar, their differentiation was possible mainly due to differences in SCM relative abundance. The X-ray diffraction patterns showed a higher abundance of 2:1 clay minerals in SC compared to CF (Figure 29). In the NIR region, these differences are also displayed by the bands at 7072 and 4530 cm^{-1}. The closest mineral composition and organic carbon content of these sources resulted in higher prediction errors (±3.3 and ±4.4% for CF and SC, respectively) than those obtained for the UR (±1.1%) (Figure 28a,b,c). However, the errors remained far below 15%, which is often considered as ‘acceptable’ for such studies (COLLINS; WALLING, 2002).

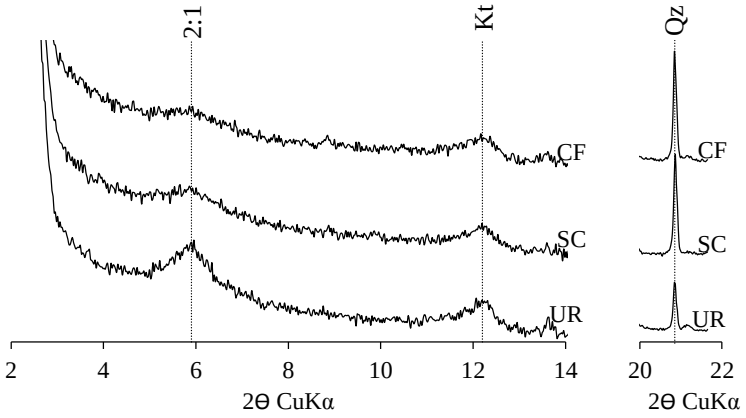

Mineral	Sediment source		
	CF	SC	UR
Peak height			
2:1 clay minerals (2:1)	479	422	783
Kaolinite (Kt)	384	332	390
Quartz (Qz)	2585	2042	1299
Peak area			
2:1 clay minerals (2:1)	127	205	472
Kaolinite (Kt)	269	233	305
Quartz (Qz)	20452	15145	9990
Abundance			
2:1 clay minerals (2:1)	+	++	+++
Kaolinite (Kt)	+	+	+
Quartz (Qz)	+++	++	+

Figure 29 – X-ray diffraction (XRD) patterns of the sediment sources in Arvorezinha catchment. CF, crop fields; SC, stream channels; UR, unpaved roads.

Regions in MIR spectra which allow for the differentiation between the sediment sources are presented in Figure 23. Figure 23b,d,f displays the second-derivative of MIR spectra of all the simple mixtures (composed by only two sediment sources each) used to construct the MIR-PLSR models. To facilitate the visualization of differences in the spectral features according to the variation in the proportion of each source, the standard deviations of these same spectra are shown in Figure 23c,e,g. The standard deviation was calculated each 2 cm^{-1} by using the spectra of the 9 simple mixtures of each pair of sediment sources. These figures clearly show a greater variation between the sources UR vs. CF and UR vs. SC than between the sources CF vs. SC.

Spectral features at 2930 and 2850 cm^{-1} corresponding to CH stretching of aromatic and aliphatic functional compounds, respectively, allowed for a better discrimination of UR, whilst such variation is almost inexistent between CF and SC. The same interpretation can be extended to a lesser extent for the spectral feature at 1160 cm^{-1} (OC + SCM) and at 1530 and 1340 cm^{-1} (OC + Qz). It primarily occurred due to the lower content of TOC in UR (12.0±5.5 g C kg^{-1}) compared to the CF and SC (20.5±6.6 and 21.3±3.1 g C kg^{-1}, respectively), and secondly due to the differences in the nature of the organic matter as demonstrated by Py-GC/MS analyses. Thus, CF and SC samples contain more polysaccharides-like, amino acids/sugars-like biomarkers than UR samples (Figure 30).

Moreover, the higher abundance of 2:1 clay minerals and the lower quantity of Qz in the UR compared to the CF and SC (Figure 29) contributed to the better discrimination of UR with the spectral features 1, 2, 12, 13, 14 and 16 (SCM), and at the spectral features 5, 6 and 7 (Qz). Thus, the combined effect of differences in the mineral composition and in quantity and

quality of organic matter resulted in the lowest predictor error (±2.8%) for the UR MIR-PLSR models (Figure 28e).

The CF and SC sources presented very similar abundance of Kt, organic carbon content, and composition of organic matter (Figure 29, Figure 30, Table 11). Thus, their differentiation was possible mainly due to differences in SCM contents. The X-ray diffraction patterns showed a slightly higher abundance of 2:1 clay minerals and lower abundance of Qz in SC compared to CF (Figure 29). As a result of the closest mineral and organic composition of CF and SC sources, the predictions errors were higher (±5.9 and ±5.1% for CF and SC, respectively) than those obtained for the UR (±2.8%) (Figure 28d,e,f). However, the errors for all MIR-PLSR models remained far below 15%, which is considered as 'acceptable' for such studies (COLLINS; WALLING; LEEKS, 1997).

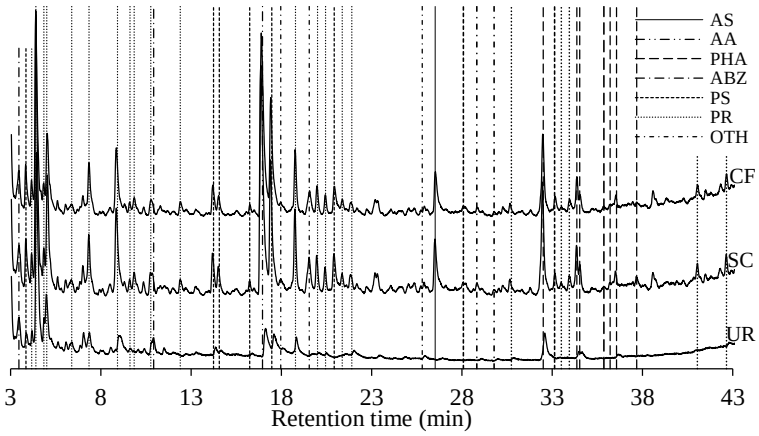

Carbon form	Sediment source		
	CF	SC	UR
	%	%	%
Protein (PR)	45.7	46.1	64.8
Polysaccharides (PS)	17.1	15.4	8.7
Amino acids (AA)	16.0	16.5	8.1
Amino sugar (AS)	3.9	3.3	0.0
Phenol (PHA)	10.8	11.7	10.2
Alkyl benzene (AB)	2.7	2.8	7.3
Other compounds (OTH)	3.8	4.2	0.8
Total	100	100	100

Figure 30 – Pyrolysis-gas chromatography/mass spectrometry (Py-GC/MS) of the sediment sources in Arvorezinha catchment. CF, crop fields; SC, stream channels; UR, unpaved roads.

6.2.3 Source apportionment

6.2.3.1 Classical fingerprinting based on geochemical composition

The contribution of sediment sources during different stages of the water flow during nine rainfall events evaluated by the conventional approach based on geochemical composition is shown in

Figure *31* to Figure 35. The prediction error was on average 6.4±3.6% (1.9–13.7% - Table 21), and all suspended sediment samples were associated with error values below 15%, which is considered acceptable for such studies. There was a great variation in sediment source contributions between the storm-events, as well as in different discharge stages during each rainfall-runoff event. On average for the 29 suspended sediment samples, the contribution of the sediment sources was 57±14, 23±14, and 20±12% for the CF, UR, and SC, respectively (Table 21).

During the storm-event that occurred on 29 July 2011 in Arvorezinha catchment (Figure 35), for which it was possible to obtain a high sampling frequency (7 sediment samples collected in the rising and recession limb), the CF and SC contribution increases during the rising stage of hydrograph, while there is a reduction in UR contribution (values close to 0%) at maximum flow. Subsequently, after the maximum flow, during the recession limb, the UR contribution increases its contribution gradually to values close to 30%, whereas the CF and SC contributions decreases. During the storm-event that occurred on 2 December 2010 (Figure 33a) only the recession stage of the flood could be sampled. However, it was possible to verify a similar trend, where CF and SC contribution decrease while UR contribution increases during falling stage. These two rainfall events occurred in different seasons where soil management and land use was also different. However, both events were characterized by similar total precipitation (35 and 46 mm) and maximum water flow (196 and 200 l s^{-1}).

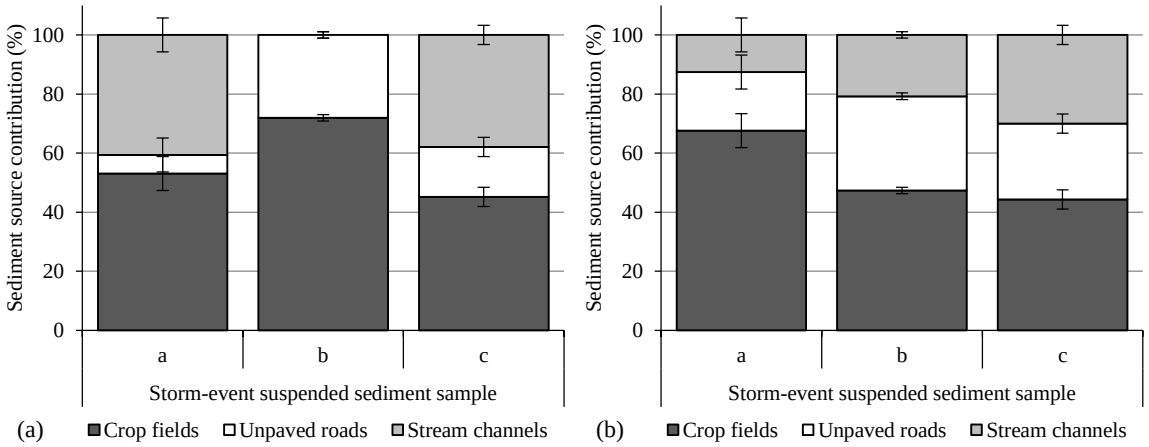

Figure 31 – Sediment source contribution during the storm events that occurred on 17 October 2009 (a) and on 18 October 2009 (b) in Arvorezinha catchment. Records of precipitation, discharge, and suspended sediment concentration are not available for these floods.

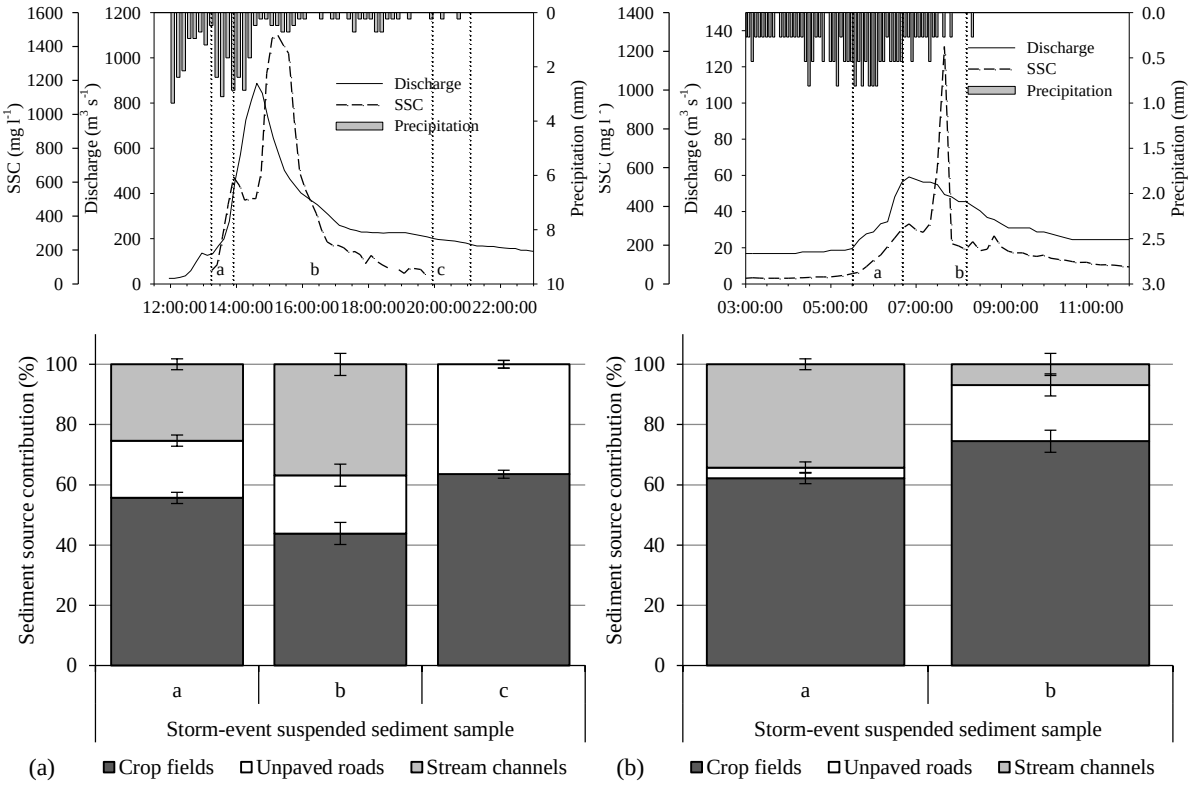

Figure 32 – Records of precipitation, discharge, suspended sediment concentration, and the sediment source contribution during the storm events that occurred on 7 November 2009 (a) and on 7 October 2010 (b) in Arvorezinha catchment.

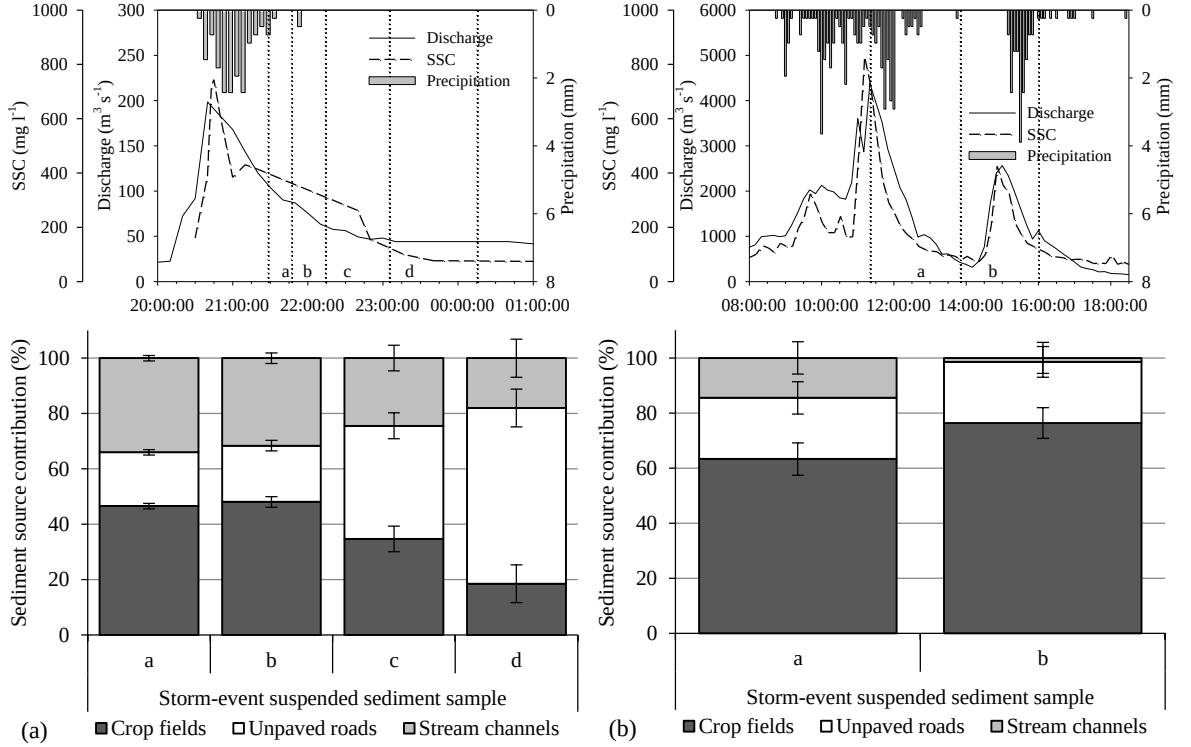

Figure 33 – Records of precipitation, discharge, suspended sediment concentration, and the sediment source contribution during the storm events that occurred on (a) 2 December 2010 and on (b) 26 March 2011 in Arvorezinha catchment.

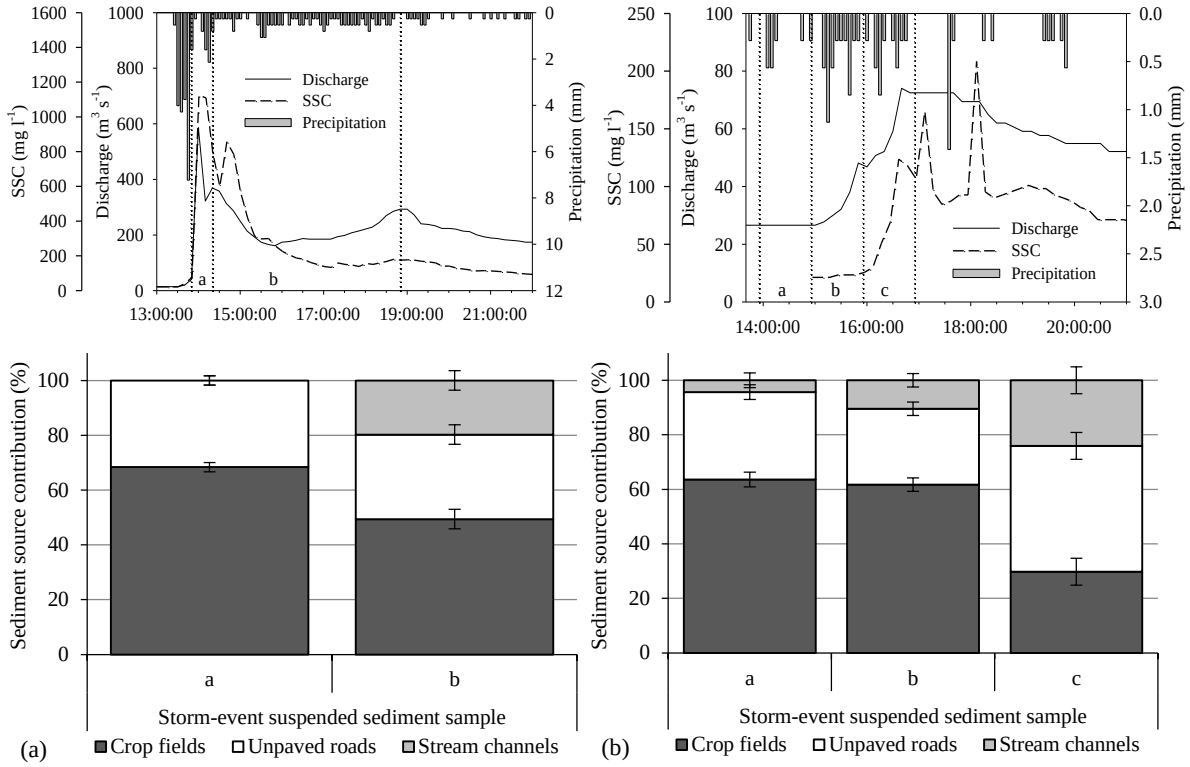

Figure 34 – Records of precipitation, discharge, suspended sediment concentration, and the sediment source contribution during the storm events that occurred on 14 April 2011 (a) and on 28 July 2011 (b) in Arvorezinha catchment.

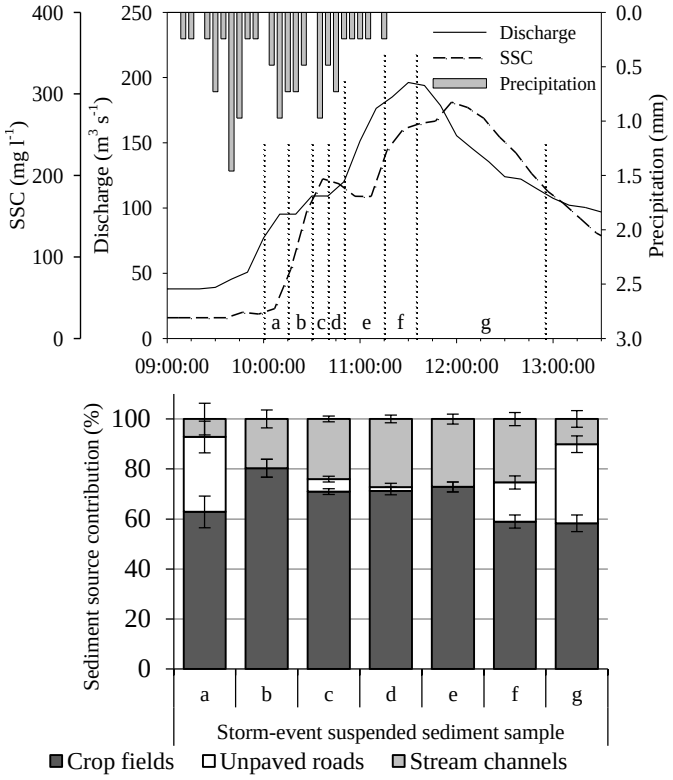

Figure 35 – Records of precipitation, discharge, suspended sediment concentration, and the sediment source contribution during the storm events that occurred on 29 July 2011 in Arvorezinha catchment.

6.2.3.2 Alternative method based on spectroscopy-PLSR models

Sediment source contributions predicted by alternative method based on spectroscopy analyses are shown in Table 21. PLSR models based on spectroscopy analyses show that sediment source contributions vary from one rainfall-runoff event to another as well as within a single rainfall event. During the calibration step of PLSR models, variations of the contributions predicted by the model with a 95% confidence interval (dashed lines on Figure 28) was on average ±2.9, ±4.6, and ±6.6% for the three sources using NIR, MIR, and UV-VIS spectroscopy parameters (Table 21).

There was no correlation between sediment source contributions provided by NIR-PLSR and geochemical approaches (Table 22). For UV-VIS-PLSR approach, only UR contribution was significantly correlated with geochemical UR predictions. Moreover, for MIR-PLSR approach, only the CF contribution presents a positive correlation with geochemical CF predictions (Figure 36). Furthermore, the UR contribution predicted by spectroscopic method was negatively correlated to the total organic carbon in suspended sediments (Figure 37).

For alternative methods based on NIR, MIR, and UV-VIS PLSR models, the sum of the contribution of sediment sources ranged from 99.2 to 106.5, 96.1 to 131.5, and 98.6 to 129.8%, respectively (Table 21). It should be noted that the PLSR models based on spectroscopy analyses used to estimate the contribution of each source were independent, i.e., each model estimates the proportion of one source, independently of the two others. However, the sum of the contributions that they provided was very close to 100% (100.7, 101.4, and 104.0% on average for NIR, MIR, and UV-VIS approaches). Following the interpretation of Poulenard et al. (2012), it is evident that (i) the main sediment sources in Arvorezinha catchment were sampled and (ii) the PLSR models were able to deal with possible difference in absolute particle size distributions between sources and suspended sediment.

Table 21 – Sediment source contribution predicted by the different approaches in Arvorezinha catchment. RME, relative mean error.

Storm event	ID	Crop fields contribution (%)					Unpaved roads contribution (%)					Stream channels contribution (%)					Total (%)			RME (%)	
		Geoch	NIR	MIR	UV-VIS	Geoch Colour	Geoch	NIR	MIR	UV-VIS	Geoch Colour	Geoch	NIR	MIR	UV-VIS	Geoch Colour	NIR	MIR	UV-VIS	Geoch	Geoch Colour
17-Oct-09	1	53.1	30.6	50.8	66.4	39.6	6.3	47.5	13.8	36.6	11.9	40.7	23.2	32.5	0.0	48.5	101.3	97.1	103.0	11.5	8.5
	2	72.0	61.0	10.7	39.4	68.0	28.0	13.2	19.4	42.0	32.0	0.0	26.4	68.8	18.8	0.0	100.6	98.9	100.1	2.2	2.9
	3	45.1	41.1	33.3	68.1	38.4	17.0	33.2	6.6	30.1	20.5	37.9	26.6	56.2	1.8	41.1	100.9	96.1	100.1	6.5	5.3
18-Oct-09	4	67.6	60.7	31.4	65.4	59.0	19.9	18.5	12.4	32.8	26.0	12.5	21.2	54.6	1.1	15.0	100.3	98.4	99.3	2.3	3.0
	5	47.3	74.7	16.3	19.8	37.8	31.9	26.2	30.8	69.3	36.4	20.8	0.0	52.0	12.3	25.8	100.9	99.1	101.4	2.8	3.2
	6	44.3	59.7	27.9	81.3	37.9	25.7	34.7	22.5	48.6	29.8	30.0	7.0	47.8	0.0	32.4	101.4	98.1	129.8	5.4	4.7
7-Nov-09	7	55.7	60.5	17.6	42.5	45.6	19.0	30.1	18.8	46.9	23.7	25.4	9.5	61.9	12.1	30.7	100.1	98.4	101.5	3.7	3.8
	8	43.9	56.4	16.5	55.3	37.2	19.3	8.2	12.1	29.1	22.2	36.8	35.9	71.2	16.0	40.6	100.6	99.8	100.4	7.4	5.9
	9	63.5	62.3	14.0	57.4	59.4	36.5	31.1	26.3	42.0	40.6	0.0	6.6	58.5	0.0	0.0	100.0	98.8	99.4	2.6	3.2
7-Oct-10	10	62.2	20.6	76.0	89.8	49.2	3.5	11.5	0.0	0.0	9.4	34.3	67.1	42.5	11.1	41.4	99.2	118.5	100.9	10.7	8.4
	11	74.5	36.2	50.1	74.8	57.3	18.7	33.1	2.0	31.0	22.5	6.9	30.7	45.4	0.0	20.2	100.0	97.5	105.8	7.4	6.6
2-Dec-10	12	46.6	15.7	30.6	59.1	39.8	19.4	53.8	35.1	39.7	23.7	34.0	31.0	33.5	1.7	36.5	100.5	99.2	100.5	1.9	2.9
	13	48.1	38.9	9.9	78.4	40.8	20.3	41.1	29.4	22.7	23.8	31.6	19.9	59.1	0.0	35.5	99.9	98.5	101.1	3.9	4.3
	14	34.7	69.5	13.3	29.8	30.0	40.8	32.7	36.6	62.5	43.6	24.4	0.0	49.6	7.5	26.4	102.1	99.5	99.8	9.3	6.5
	15	18.5	61.6	9.8	60.6	15.4	63.5	32.5	12.5	44.9	65.1	18.0	6.3	75.0	0.0	19.5	100.5	97.3	105.5	13.7	9.0
26-Mar-11	16	63.3	45.6	28.5	56.8	46.1	22.2	10.3	11.7	18.8	23.4	14.5	44.5	59.1	24.4	30.5	100.4	99.3	99.9	11.7	8.5
	17	76.4	70.2	42.9	74.0	62.3	22.2	15.7	10.8	39.8	29.1	1.4	14.0	46.1	0.0	8.6	99.9	99.9	113.8	11.2	8.3
14-Apr-11	18	68.4	69.2	51.5	48.9	60.6	31.6	7.4	8.0	31.0	31.7	0.0	23.9	40.3	21.1	7.7	100.5	99.7	100.9	3.4	3.9
	19	49.4	68.0	22.2	62.6	39.8	30.9	15.5	19.2	34.9	31.0	19.8	16.9	57.8	3.7	29.3	100.3	99.1	101.1	7.2	5.5
28-Jul-11	20	63.6	93.4	78.1	48.1	55.5	32.0	13.1	16.8	62.4	35.0	4.3	0.0	5.0	0.0	9.6	106.5	99.8	110.5	5.4	4.7
	21	61.8	79.2	48.9	80.2	54.8	27.8	10.7	20.8	33.0	32.3	10.4	9.8	30.1	0.0	13.0	99.7	99.7	113.2	4.9	4.4
	22	29.8	78.7	43.3	43.6	26.4	46.1	12.0	16.7	51.7	48.4	24.1	9.3	39.9	5.0	25.3	100.0	99.9	100.3	9.9	6.7
29-Jul-11	23	62.8	68.8	88.8	60.1	52.2	30.0	1.1	0.0	25.6	29.8	7.2	30.8	27.2	14.0	18.0	100.7	116.1	99.7	12.7	9.1
	24	80.3	62.9	108.0	74.7	71.6	0.0	6.2	0.0	18.7	5.0	19.7	31.2	23.5	7.5	23.4	100.4	131.5	100.8	7.1	6.5
	25	71.0	52.9	83.0	79.9	60.2	5.0	27.8	23.2	33.1	10.1	24.0	19.9	0.0	0.0	29.7	100.6	106.3	113.0	2.3	3.8
	26	71.3	59.2	67.7	74.9	59.2	1.5	32.1	17.9	32.8	8.1	27.3	9.3	12.0	0.0	32.7	100.5	97.6	107.6	3.1	4.0
	27	72.8	63.2	69.6	73.5	61.0	0.0	21.3	9.3	21.7	4.5	27.2	15.5	19.2	4.2	34.4	100.0	98.1	99.5	3.9	4.2
	28	59.0	48.1	47.5	95.8	49.0	15.7	25.0	15.0	12.6	17.6	25.4	27.6	35.4	0.0	33.3	100.8	97.9	108.4	5.2	4.4
	29	58.3	67.9	31.3	35.9	50.3	31.7	19.5	22.2	45.5	34.0	10.1	14.3	45.7	17.2	15.7	101.7	99.1	98.6	6.7	5.2
Mean		57.4	57.8	42.1	62.0	48.4	23.0	22.9	16.2	35.9	26.6	19.6	19.9	43.1	6.2	25.0	100.7	101.4	104.0	6.4	5.4
SD		14.8	17.5	26.8	18.2	13.0	14.4	13.1	9.9	15.1	13.4	12.4	14.6	19.1	7.6	12.6	1.3	7.7	6.8	3.6	2.0
Maximum		80.3	93.4	108.0	95.8	71.6	63.5	53.8	36.6	69.3	65.1	40.7	67.1	75.0	24.4	48.5	106.5	131.5	129.8	13.7	9.1
Minimum		18.5	15.7	9.8	19.8	15.4	0.0	1.1	0.0	0.0	4.5	0.0	0.0	0.0	0.0	0.0	99.2	96.1	98.6	1.9	2.9
Prediction PLSR error		-	3.3	5.9	7.9	-	-	1.1	2.8	5.9	-	-	4.4	5.1	6.0	-	2.9	4.6	6.6	-	-

Table 22 – Linear correlation between the sediment source contributions predicted by geochemical composition and the alternative approaches based on spectroscopy analyses. Bold values indicate significant correlation of source ascription between the methods at $p<0.05$.

Alternative approach	Crop fields		Unpaved roads		Stream channels	
	r	*p*	*r*	*p*	*r*	*p*
NIR-PLSR	0.01	0.962	–0.07	0.718	0.22	0.251
MIR-PLSR	0.57	**0.001**	0.30	0.108	–0.01	0.940
UV-VIS-PLSR	0.31	0.098	0.59	**0.001**	–0.22	0.253
Geochemical+VIS-based-colour	0.97	**0.000**	0.99	**0.000**	0.95	**0.000**

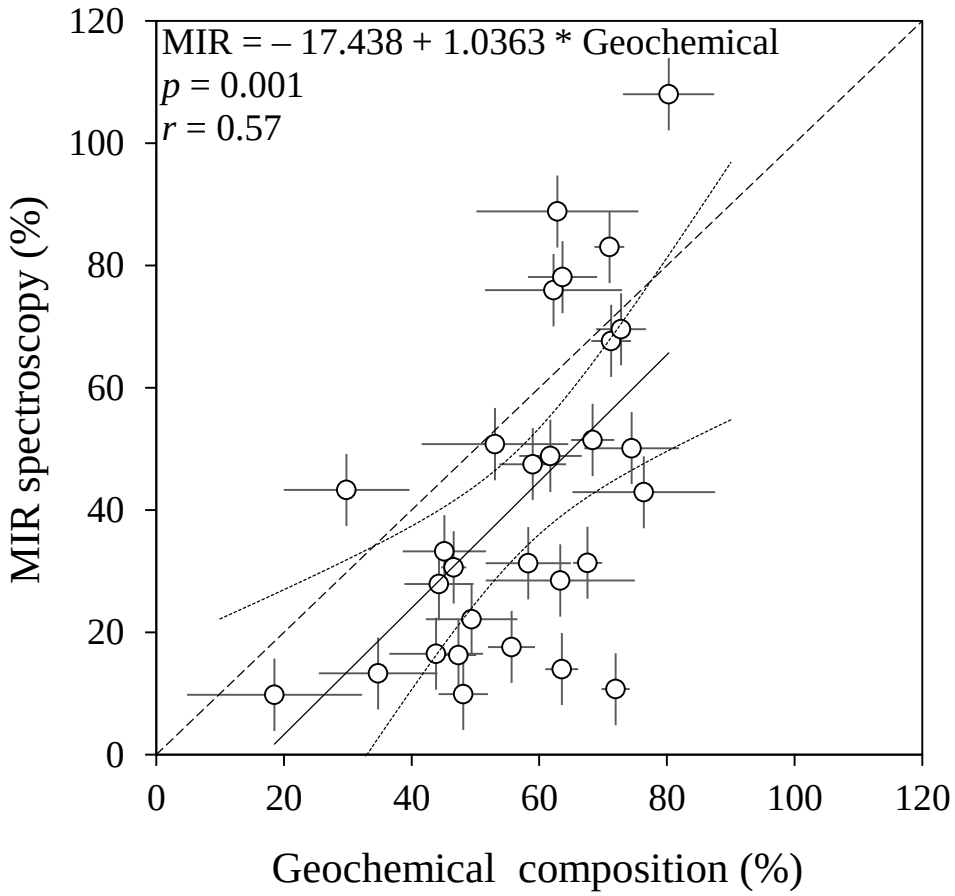

Figure 36 – Comparison of the cropland contribution predicted by conventional method based on geochemical composition and predicted by the partial least-squares regression model based on MIR spectroscopy. Error bars correspond to the estimated error of prediction of each method. The dashed line is the 1:1 line. Dotted line are the confidence interval limit (95%).

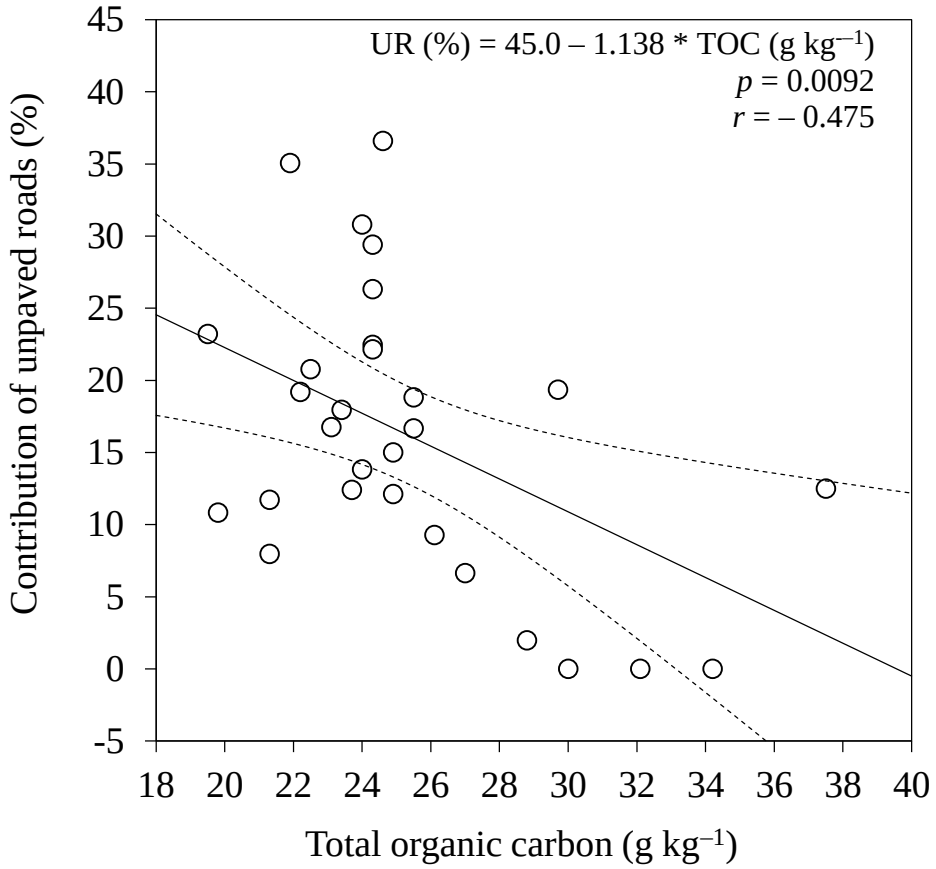

Figure 37 – Relationship between the unpaved roads proportions predicted by the partial least-squares regression model based on MIR spectroscopy and the total organic carbon content. The dashed lines are the confidence interval limits (95%).

The slight variation around 100% for the sum of the predictions may be due to the fact that samples used to draw up the model (CF, SC and UR samples) are not the same as the ones used to make the predictions (suspended sediment) (POULENARD et al., 2009), which are subject to selectivity and biogeochemical changes during transport and erosion process. Furthermore, contrary to the method based on geochemical composition, the alternative approach does not include boundary conditions as the ones introduced by Equations 5 and 6, which explains that the sum of results does not reach exactly 100%. In the classical fingerprinting approach, the sum of the sources contribution provided by the linear mixed model would be always 100% because of the constraint of the Equation 6, however, the relative mean error would be too high.

For UV-VIS-PLSR models, there was an overestimation of UR at the expense of SC contribution (Figure 38 and Figure 39). Despite the lack of correlation between contributions of sediment sources provided by NIR-PLSR and geochemical approaches (Table 22), the source

apportionment obtained with both approaches were very similar, with an average relative contribution of 57±14 and 58±17% for CF, 23±14 and 23±13% for UR, and 20±12 and 20±14% for SC, respectively for geochemical and spectroscopy methods (Figure 38 and Figure 39).

The CF contribution was underestimated by MIR-PLSR model compared to classical geochemical fingerprinting (Figure 36, Figure 38, and Figure 39). For SC contribution, although there was no significant correlation between the methods, the average prediction using MIR-PLSR models (43.1±19.1%) was clearly higher than the geochemical composition method (19.6±12.4%) (Figure 38 and Figure 39). For UR, however, contribution was very similar between methods (23.0±14.4 and 16.2±9.9% for geochemical and spectroscopic approaches, respectively - Table 21).

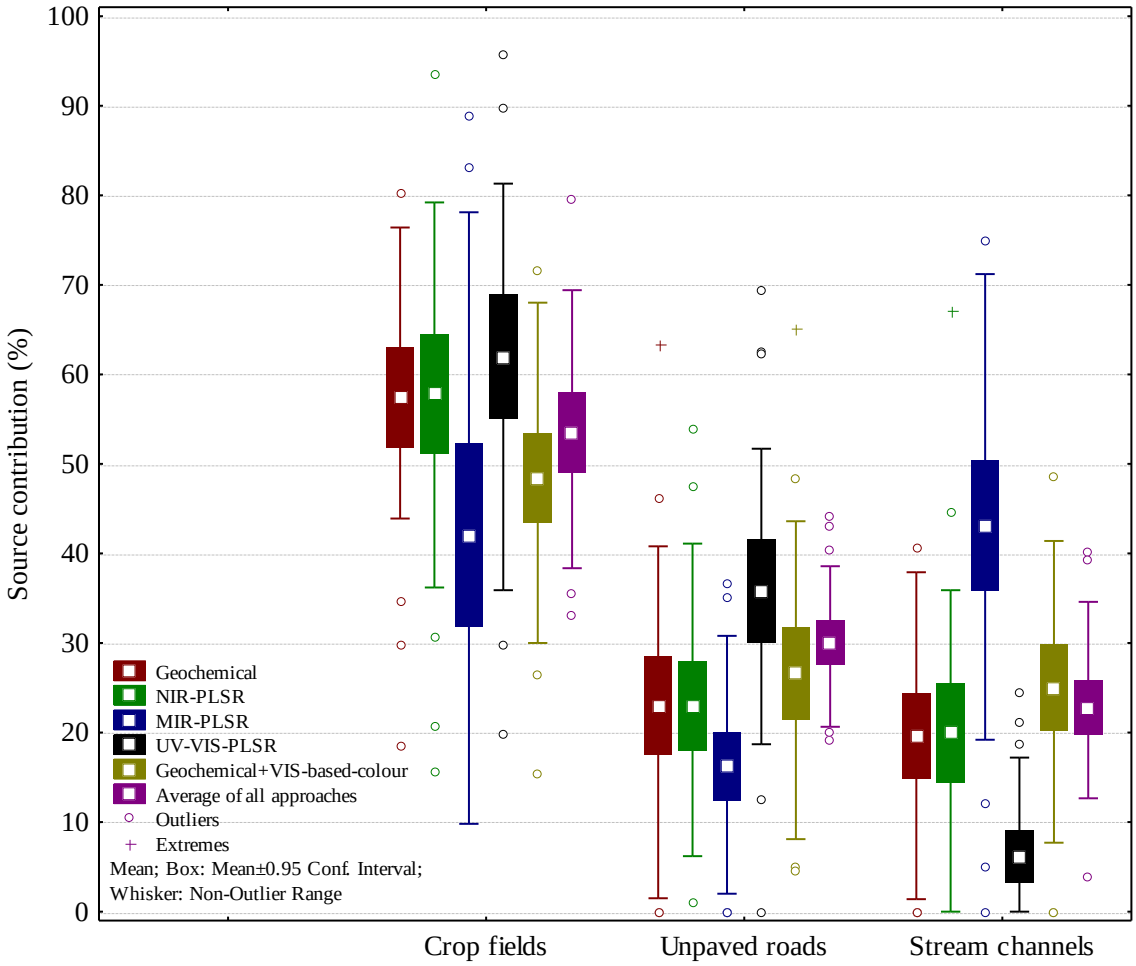

Figure 38 – Box plot of the sediment source contributions predicted by the different fingerprinting approaches in the 29 suspended sediment samples collected in Arvorezinha catchment.

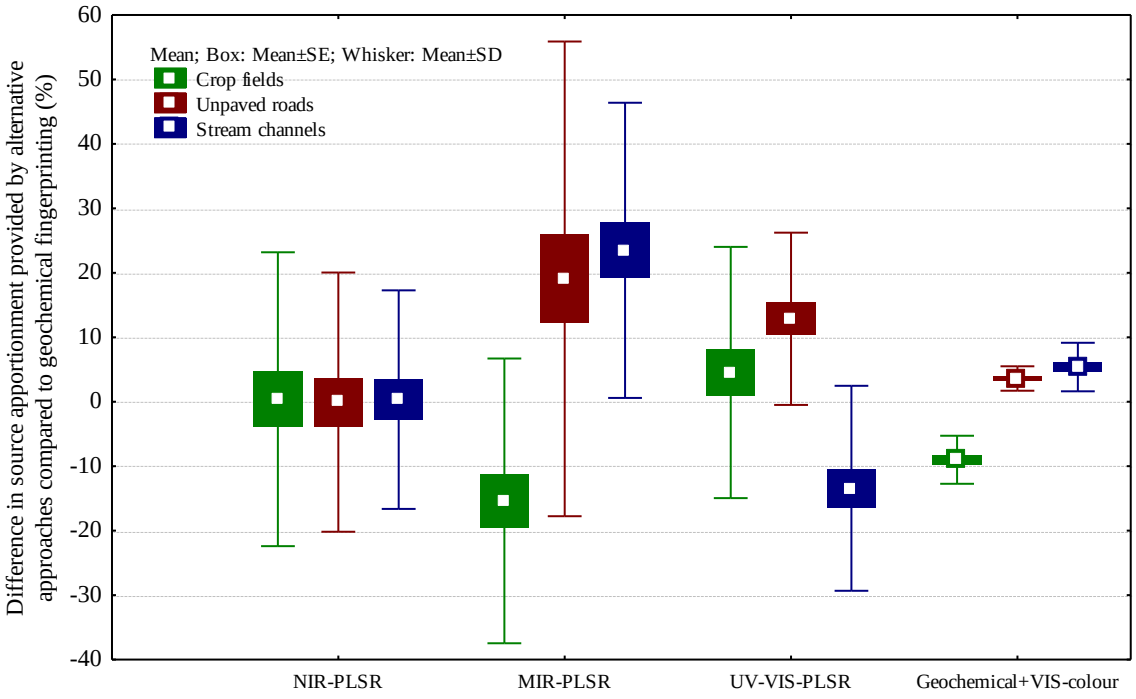

Figure 39 – Box plot of the differences in source apportionments provided by alternative approaches compared to geochemical fingerprinting for the 29 suspended sediment samples collected in Arvorezinha catchment.

6.2.3.3 Alternative method based on colour parameters derived from VIS reflectance

Sediment source apportionment was not evaluated for colour parameters because it was not possible to discriminate two of the three sediment sources using only the colour parameters obtained from the visible reflectance (Table 13). However, when coupled to geochemical tracers, VIS-based-colour parameters were able to discriminate all potential sediment sources (Table 13). Thereby, the second step was performed sediment source apportionment. The contributions of sediment sources predicted by geochemical tracers combined with VIS-based-colour parameters (geochemical + VIS-based-colour) are shown in Table 21. As for the others approaches, there was a great variation in sediment source contributions from one rainfall event to another as well as within a single rainfall event. Overall, there was a good agreement with geochemical source apportionment results (Figure 38 and Figure 39), and all sediment sources were significantly correlated with the results of the classical approach (Table 22). This was somehow expected, once that all geochemical tracers were kept by DFA using geochemical + VIS-based-colour (Table 12).

6.2 Júlio de Castilhos catchments

6.2.1 Source discrimination

In both catchments from Júlio de Castilhos, comparison of geochemical tracer concentrations between sediment sources and suspended sediment samples indicate sieving to 150 µm was not sufficient to overcome differences in grain size distribution (Table 23). Concentrations in suspended sediment was higher than the highest source concentration plus one standard deviation for almost all geochemical tracers.

Sand is mainly composed of silicates (Si and O) that are chemically inert and that, therefore, "dilute" geochemical tracer concentrations that are present in the fine fraction of soil and sediments. Therefore, to overcome problems due to differences in grain size, a correction factor based on fine sand concentration was calculated (Table 24). Suspended sediments contained no fine sand and therefore were not corrected for grain size distribution. Sediment sources sieved to 150 µm, however, presented sand concentration ranging from 43 to 65%, resulting in a correction factor ranging from 1.8 to 2.9 (Table 24).

If the tracer value for a given source sample exceeded three times the standard deviation of the average value, this sample was considered an outlier and the entire sample was removed for all tracers (WAINER, 1976). After grain size correction based on factors listed in Table 24 no outliers were detected for all tracers and for all sediment sources in both Júlio de Castilhos catchments (data not shown). However, concentration of Ba, Be, Ca, Mn, P, Sr, and TOC in JC80, and Be, P, and TOC in JC140 for most suspended sediments samples were higher than the highest source concentration plus one standard deviation (Table 25 and Table 26). Moreover, most of sediment samples in both catchments showed concentrations of Na and K lower than the lowest source concentration minus one standard deviation (Table 25 and Table 26). These elements were then considered as non-conservative and were then excluded from the next steps. The concentration in sediments for the remaining geochemical tracers laid between the concentration ranges of the sources and were then kept.

Table 25 and Table 26 displays the Kruskal–Wallis *H*-values and the percentage of samples correctly classified by each tracer using discriminant function analysis (DFA). At this step, from the 13 and 17 remaining geochemical variables from JC80 and JC140, 10 and 15, respectively, were selected as potential tracers by applying the Kruskal–Wallis *H*-test (H>6.145

and $p<0.1$,) (Table 25 and Table 26). No variable alone was able to correctly classify 100% of the source samples in their respective groups. The discriminatory power of these individual variables ranged from 30.0 to 66.7% and from 30.0 to 63.3%, for JC80 and JC140, respectively.

Table 23 – Geochemical tracer concentrations of sediment sources and suspended sediments sieved to 150 µm, and test of sediment source range for suspended sediments, in Júlio de Castilhos catchments. SD, standard deviation.

Fingerprint property	Sediment sources				Suspended sediment			% sediment samples	
	Stream channels	Unpaved roads	Crop fields	Grasslands	Mean	Max	Min	Higher Max+SD	Lower Min–SD
Júlio de Castilhos 80									
Al (g kg^{-1})	16.1	27.8	23.3	14.5	36.9	53.3	23.0	30.0	0.0
Ba (mg kg^{-1})	71.0	112.3	77.8	62.8	336.3	656.0	195.3	100.0	0.0
Be (mg kg^{-1})	0.3	0.5	0.2	0.1	6.3	9.6	4.7	100.0	0.0
Ca (g kg^{-1})	0.2	0.2	0.8	0.2	3.3	13.2	1.4	100.0	0.0
Co (mg kg^{-1})	8.8	12.0	4.7	3.9	25.7	112.2	12.2	73.3	0.0
Cr (mg kg^{-1})	9.8	16.5	16.3	8.7	30.1	49.1	20.3	100.0	0.0
Cu (mg kg^{-1})	10.1	32.6	15.4	8.7	31.6	62.0	18.9	23.3	0.0
Fe (g kg^{-1})	16.2	26.6	15.5	8.5	29.0	59.7	18.4	10.0	0.0
K (g kg^{-1})	0.2	0.9	0.8	0.4	2.3	25.1	0.0	23.3	26.7
La (mg kg^{-1})	17.8	20.0	17.1	13.3	39.8	48.1	26.7	96.7	0.0
Li (mg kg^{-1})	11.2	18.1	24.7	12.7	38.8	56.8	25.5	73.3	0.0
Mg (g kg^{-1})	1.2	1.5	1.2	0.9	3.1	9.5	2.2	93.3	0.0
Mn (g kg^{-1})	0.3	0.6	0.4	0.2	1.7	5.7	0.6	63.3	0.0
Na (mg kg^{-1})	59.5	71.0	64.3	72.9	539.1	5929.6	0.0	56.7	30.0
Ni (mg kg^{-1})	3.1	7.2	5.8	3.0	12.2	30.1	8.3	100.0	0.0
P (mg kg^{-1})	76.8	87.1	196.2	102.8	556.2	909.9	358.3	100.0	0.0
Pb (mg kg^{-1})	8.2	11.3	11.3	6.7	16.4	21.7	11.6	46.7	0.0
Sr (mg kg^{-1})	11.0	9.5	11.0	8.3	56.1	178.4	33.2	100.0	0.0
Ti (g kg^{-1})	2.7	3.2	2.5	2.1	5.8	6.9	3.7	96.7	0.0
V (mg kg^{-1})	46.5	102.3	60.0	34.4	103.5	151.6	78.4	13.3	0.0
Zn (mg kg^{-1})	3.1	3.9	4.5	2.2	9.8	40.7	5.7	93.3	0.0
TOC (g kg^{-1})	8.1	4.6	19.3	21.6	68.6	100.5	39.0	100.0	0.0
Júlio de Castilhos 140									
Al (g kg^{-1})	16.0	27.7	27.5	22.9	41.9	49.2	31.6	80.0	0.0
Ba (mg kg^{-1})	100.9	168.1	95.0	88.1	334.2	452.6	228.9	100.0	0.0
Be (mg kg^{-1})	0.7	0.4	0.0	1.3	5.7	6.9	4.5	100.0	0.0
Ca (g kg^{-1})	0.4	0.5	1.1	0.3	2.6	7.0	1.3	50.0	0.0
Co (mg kg^{-1})	7.5	13.9	5.8	7.2	23.4	31.1	16.5	96.7	0.0
Cr (mg kg^{-1})	7.1	12.4	16.3	8.2	21.9	29.1	16.4	73.3	0.0
Cu (mg kg^{-1})	16.0	33.9	17.9	26.7	42.7	56.5	32.7	13.3	0.0
Fe (g kg^{-1})	13.5	33.0	18.4	17.3	29.3	32.8	23.7	0.0	0.0
K (g kg^{-1})	0.4	0.5	0.7	0.8	0.6	4.2	0.0	10.0	53.3
La (mg kg^{-1})	17.6	24.2	19.7	20.0	48.2	54.6	40.2	100.0	0.0
Li (mg kg^{-1})	13.2	24.4	29.2	11.8	35.6	43.2	26.5	30.0	0.0
Mg (g kg^{-1})	1.3	1.5	1.6	1.0	2.5	3.5	2.1	56.7	0.0
Mn (g kg^{-1})	0.4	0.9	0.5	0.4	1.5	2.9	0.7	73.3	0.0
Na (mg kg^{-1})	73.1	105.3	68.4	8.0	109.2	1040.6	0.0	16.7	40.0
Ni (mg kg^{-1})	2.2	4.3	5.8	3.3	8.2	9.7	6.0	76.7	0.0
P (mg kg^{-1})	145.2	134.1	207.1	137.7	569.4	867.4	333.5	100.0	0.0
Pb (mg kg^{-1})	8.2	12.8	10.4	10.8	16.0	18.9	12.5	36.7	0.0
Sr (mg kg^{-1})	15.8	17.2	13.4	14.8	55.2	102.4	38.6	100.0	0.0
Ti (g kg^{-1})	2.7	3.7	2.7	2.5	8.0	9.1	7.0	100.0	0.0
V (mg kg^{-1})	43.0	83.3	63.0	57.3	115.8	134.7	98.6	86.7	0.0
Zn (mg kg^{-1})	2.4	7.1	3.3	3.8	9.5	12.2	7.3	73.3	0.0
TOC (g kg^{-1})	10.7	7.7	19.8	15.6	54.9	92.3	32.4	100.0	0.0

Table 24 – Concentration of fine sand and <63 µm fraction, and grain size correction factor for sediment sources and suspended sediments in Júlio de Castilhos catchments.

Catchment	Source	Fine sand (%)	<63µm fraction (%)	Correction factor
JC80	Stream channels	65	35	2.9
	Unpaved roads	43	57	1.8
	Crop fields	47	53	1.9
	Grasslands	60	40	2.5
	Sediment	0	100	1.0
JC140	Stream channels	58	42	2.4
	Unpaved roads	49	51	2.0
	Crop fields	47	53	1.9
	Grasslands	51	49	2.0
	Sediment	0	100	1.0

The 10 and 15 remaining geochemical tracers identified as potential tracers that laid in the sediment source ranges were then entered into the stepwise multivariate DFA to select the optimum set for maximizing discrimination, whilst minimizing dimensionality. The progressive change of the Wilks' Lambda value (Λ*) as the variables are introduced into the analysis are presented in the Table 27. The final set of elements selected by DFA analyses was Al, Co, Cr, Cu, Ni, Ti, and Zn for JC80 and Zn, Li, Ni, and Co for JC140, resulting in a final value of the Λ* parameter of 0.0056 and 0.0411, respectively. It means that the set of selected variables explains approximately 99.4 and 95.9% of the differences between the sources, respectively, and only 0.6 and 4.1% of the difference was due to the intra-source variation for JC80 and JC140 (Table 28). For JC80 and JC140, 96.7 and 93.3% of the sediment source samples were correctly classified into their respective groups (Table 28). Mahalanobis distance shows the sediment sources in JC80 and in JC140 were well separated by a significant distance of 65.7±48.0 and 16.1±8.3 from each other (Table 28 and Figure 40).

Table 25 – The ability of individual geochemical fingerprints corrected to <63 µm fraction to distinguish sediment source types, assessing the Kruskal−Wallis *H*-test and discriminant function analysis (DFA), and test of sediment source range for suspended sediments, in JC80 catchment. SD, standard deviation. ns, not significant, *p<0.1, **p<0.05, ***p<0.01, ****p<0.001, *****p<0.0001.

Fingerprint property	Stream channels (n = 6)		Unpaved roads (n = 8)		Crop fields (n = 8)		Grasslands (n = 8)		Kruskal-Wallis test			Correctly classified samples - DFA (%)	Source range		Suspended sediment (n = 27)		Sediment samples out of source range (%)		Fingerprint property removed
									H-value	*p*-value	Signif						Higher	Lower	
	Mean	SD	Mean	SD	Mean	SD	Mean	SD					Max+SD	Min–SD	Mean	SD	Max+SD	Min–SD	
Al (g kg^{-1})	42.4	15.9	47.7	8.9	43.4	8.0	33.8	11.8	6.3	0.0996	*	30.0	58.4	22.0	36.9	6.2	0.0	0.0	
Ba (mg kg^{-1})	192.0	69.9	191.9	44.3	145.9	22.6	148.7	57.5	7.5	0.0585	*	26.7	261.8	91.1	336.3	92.0	**83.3**	0.0	*
Be (mg kg^{-1})	0.6	0.7	0.8	0.5	0.4	0.2	0.2	0.4	10.5	0.0146	**	50.0	1.3	-0.3	6.3	1.3	**100.0**	0.0	*
Ca (g kg^{-1})	0.5	0.3	0.3	0.2	1.5	0.8	0.6	0.3	15.9	0.0012	***	53.3	2.2	0.2	3.3	2.3	**70.0**	0.0	*
Co (mg kg^{-1})	22.3	12.1	21.6	5.1	9.1	1.5	9.3	2.7	19.9	0.0002	****	53.3	34.4	6.7	25.7	18.1	16.7	0.0	
Cr (mg kg^{-1})	27.0	5.6	30.0	4.8	30.8	4.2	21.0	5.5	12.0	0.0073	***	46.7	35.1	15.5	30.1	6.4	20.0	0.0	
Cu (mg kg^{-1})	26.0	13.8	58.3	4.8	29.0	1.6	19.7	9.4	19.7	0.0002	****	66.7	63.1	10.2	31.6	11.3	0.0	0.0	
Fe (g kg^{-1})	38.5	30.4	45.7	7.0	29.1	3.5	19.1	10.4	16.2	0.0010	***	60.0	68.9	8.0	29.0	8.1	0.0	0.0	
K (g kg^{-1})	0.6	0.4	1.6	0.5	1.5	0.3	1.1	0.4	12.2	0.0068	***	40.0	2.0	0.2	2.3	5.8	16.7	**53.3**	*
La (mg kg^{-1})	46.2	20.0	36.0	4.0	32.0	5.7	31.3	12.2	5.7	0.1289	ns	-	66.2	19.0	39.8	4.5	0.0	0.0	
Li (mg kg^{-1})	31.6	3.4	31.3	12.0	45.9	13.9	30.0	12.2	8.3	0.0401	**	40.0	59.8	17.8	38.8	7.3	0.0	0.0	
Mg (g kg^{-1})	3.0	2.1	2.8	0.6	2.3	0.7	2.1	1.3	5.7	0.1292	ns	-	5.1	0.7	3.1	1.3	3.3	0.0	
Mn (g kg^{-1})	0.7	0.6	1.0	0.4	0.7	0.2	0.4	0.2	11.7	0.0085	***	40.0	1.3	0.1	1.7	1.2	**50.0**	0.0	*
Na (mg kg^{-1})	173.6	32.8	129.9	34.6	120.2	29.5	186.0	56.0	9.3	0.0254	**	50.0	242.0	90.8	539.1	1236.2	26.7	**43.3**	*
Ni (mg kg^{-1})	8.5	1.5	13.3	3.7	10.9	2.0	7.0	2.2	14.0	0.0029	***	56.7	17.0	4.9	12.2	3.9	3.3	0.0	
P (mg kg^{-1})	227.1	33.5	144.7	56.0	379.1	67.0	259.3	61.9	21.0	0.0001	****	63.3	446.1	88.7	556.2	128.9	**80.0**	0.0	*
Pb (mg kg^{-1})	21.8	6.9	19.3	3.9	21.1	4.4	16.2	4.2	6.0	0.1138	ns	-	28.7	12.0	16.4	2.6	0.0	3.3	
Sr (mg kg^{-1})	28.4	12.0	16.7	2.7	20.8	2.9	19.9	4.9	8.7	0.0329	**	53.3	40.3	14.0	56.1	27.1	**90.0**	0.0	*
Ti (g kg^{-1})	7.6	1.6	6.1	1.8	4.8	0.9	5.3	0.7	11.8	0.0083	***	53.3	9.2	3.9	5.8	0.6	0.0	3.3	
V (mg kg^{-1})	124.2	43.7	188.6	51.3	113.5	14.9	81.9	23.8	17.0	0.0007	****	56.7	239.9	58.0	103.5	14.4	0.0	0.0	
Zn (mg kg^{-1})	8.5	2.6	6.9	1.5	8.3	1.7	5.1	2.6	8.6	0.0345	**	50.0	11.1	2.6	9.8	6.6	16.7	0.0	
TOC (g kg^{-1})	26.2	12.8	8.0	2.7	36.7	4.1	50.1	17.7	19.8	0.0002	****	73.3	67.8	5.3	68.6	14.8	**46.7**	0.0	*

Table 26 – The ability of individual geochemical fingerprints corrected to <63 µm fraction to distinguish sediment source types, assessing the Kruskal−Wallis *H*-test and discriminant function analysis (DFA), and test of sediment source range for suspended sediments, in JC140 catchment. SD, standard deviation. ns, not significant, *p<0.1, **p<0.05, ***p<0.01, ****p<0.001, *****p<0.0001.

Fingerprint property	Stream channels (n = 7)		Unpaved roads (n = 8)		Crop fields (n = 8)		Grasslands (n = 7)		Kruskal-Wallis test			Correctly classified samples - DFA (%)	Source range		Suspended sediment (n = 27)		Sediment samples out of source range (%)		Fingerprint property removed
									H-value	*p*-value	Signif.						Higher	Lower	
	Mean	SD	Mean	SD	Mean	SD	Mean	SD					Max+SD	Min–SD	Mean	SD	Max+SD	Min–SD	
Al (g kg^{-1})	37.5	2.5	54.4	8.7	51.4	6.7	43.2	19.4	11.1	0.0113	**	50.0	63.1	23.8	41.9	4.7	0.0	0.0	
Ba (mg kg^{-1})	237.8	21.1	341.9	152.8	177.4	17.7	180.0	45.2	18.5	0.0003	****	50.0	494.7	134.8	334.2	50.1	0.0	0.0	
Be (mg kg^{-1})	1.6	0.6	0.9	0.4	0.1	0.1	2.8	0.7	25.6	0.0000	****	83.3	3.5	0.0	5.7	0.6	**100.0**	0.0	*
Ca (g kg^{-1})	1.0	1.1	0.9	0.4	2.0	2.1	0.8	0.4	4.2	0.2360	ns	-	4.1	-0.1	2.6	1.1	10.0	0.0	
Co (mg kg^{-1})	18.1	2.8	28.2	10.2	10.9	3.3	14.3	6.9	17.4	0.0006	****	63.3	38.4	7.4	23.4	3.5	0.0	0.0	
Cr (mg kg^{-1})	17.0	1.8	24.6	6.3	30.5	6.5	16.3	3.7	18.4	0.0004	****	56.7	37.0	12.6	21.9	2.5	0.0	0.0	
Cu (mg kg^{-1})	37.4	3.9	66.6	29.6	33.3	5.7	48.9	30.0	9.5	0.0232	**	43.3	96.3	18.9	42.7	5.6	0.0	0.0	
Fe (g kg^{-1})	32.1	3.0	66.7	17.5	34.4	4.2	31.8	19.3	15.9	0.0012	***	53.3	84.2	12.5	29.3	2.4	0.0	0.0	
K (g kg^{-1})	1.0	0.3	1.0	0.4	1.2	0.3	1.6	0.6	6.7	0.0808	*	56.7	2.3	0.6	0.6	1.1	10.0	**73.3**	*
La (mg kg^{-1})	41.4	3.8	48.2	10.3	36.7	3.8	39.0	10.5	7.2	0.0666	*	43.3	58.5	28.5	48.2	4.0	0.0	0.0	
Li (mg kg^{-1})	29.9	7.8	47.4	11.9	54.4	13.7	23.2	6.7	17.8	0.0005	****	53.3	68.1	16.5	35.6	4.3	0.0	0.0	
Mg (g kg^{-1})	2.9	1.5	3.0	0.5	2.9	1.3	1.9	0.6	7.0	0.0704	*	30.0	4.4	1.3	2.5	0.3	0.0	0.0	
Mn (g kg^{-1})	1.0	0.3	1.8	1.0	0.9	0.2	0.8	0.4	12.1	0.0070	***	53.3	2.8	0.4	1.5	0.5	3.3	0.0	
Na (mg kg^{-1})	180.1	48.7	207.3	38.3	130.0	42.9	17.9	17.0	20.8	0.0001	****	73.3	245.6	0.9	109.2	221.4	13.3	**40.0**	*
Ni (mg kg^{-1})	5.2	0.8	8.2	2.0	10.8	2.3	6.4	2.6	15.9	0.0012	***	60.0	13.1	3.8	8.2	1.0	0.0	0.0	
P (mg kg^{-1})	345.6	101.8	264.8	41.4	386.5	49.8	290.0	51.1	15.3	0.0016	***	46.7	447.4	223.4	569.4	104.0	**100.0**	0.0	*
Pb (mg kg^{-1})	19.3	1.6	26.4	11.5	19.4	2.3	21.9	2.5	5.5	0.1372	ns	-	37.9	14.9	16.0	1.6	0.0	23.3	
Sr (mg kg^{-1})	37.6	21.6	34.2	9.2	24.9	3.4	30.2	4.6	7.8	0.0497	**	43.3	59.1	16.0	55.2	11.7	23.3	0.0	
Ti (g kg^{-1})	6.5	1.0	7.4	1.2	5.2	1.2	5.1	1.4	12.7	0.0054	***	33.3	8.6	3.7	8.0	0.5	13.3	0.0	
V (mg kg^{-1})	103.1	11.5	165.7	43.9	118.4	17.8	110.3	45.5	10.1	0.0180	**	46.7	209.6	64.7	115.8	9.0	0.0	0.0	
Zn (mg kg^{-1})	5.6	1.1	14.3	3.5	6.1	0.9	7.3	2.8	17.3	0.0006	****	60.0	17.7	4.5	9.5	1.5	0.0	0.0	
TOC (g kg^{-1})	25.3	4.4	14.9	3.9	37.1	4.2	33.6	10.8	21.6	0.0001	****	63.3	44.5	11.0	54.9	12.9	**93.3**	0.0	*

Table 27 – Results of the stepwise discriminant function analysis as indicated by the Wilks' Lambda values for the different fingerprinting approaches in Júlio de Castilhos catchments.

Step	Fingerprint property selected	Wilks' Lambda	*p* to remove	Cumulative % of source type samples correctly classified
Júlio de Castilhos 80				
1	Cu	0.2007	4.2E-09	66.7
2	Al	0.1406	3.6E-04	66.7
3	Ti	0.0390	6.4E-04	90.0
4	Cr	0.0193	1.0E-03	90.0
5	Zn	0.0117	1.4E-02	93.3
6	Ni	0.0086	2.9E-02	96.7
7	Co	0.0056	3.3E-02	96.7
Júlio de Castilhos 140				
1	Zn	0.2731	1.6E-04	60.0
2	Li	0.1081	5.8E-04	80.0
3	Ni	0.0619	9.6E-03	83.3
4	Co	0.0411	2.2E-02	93.3

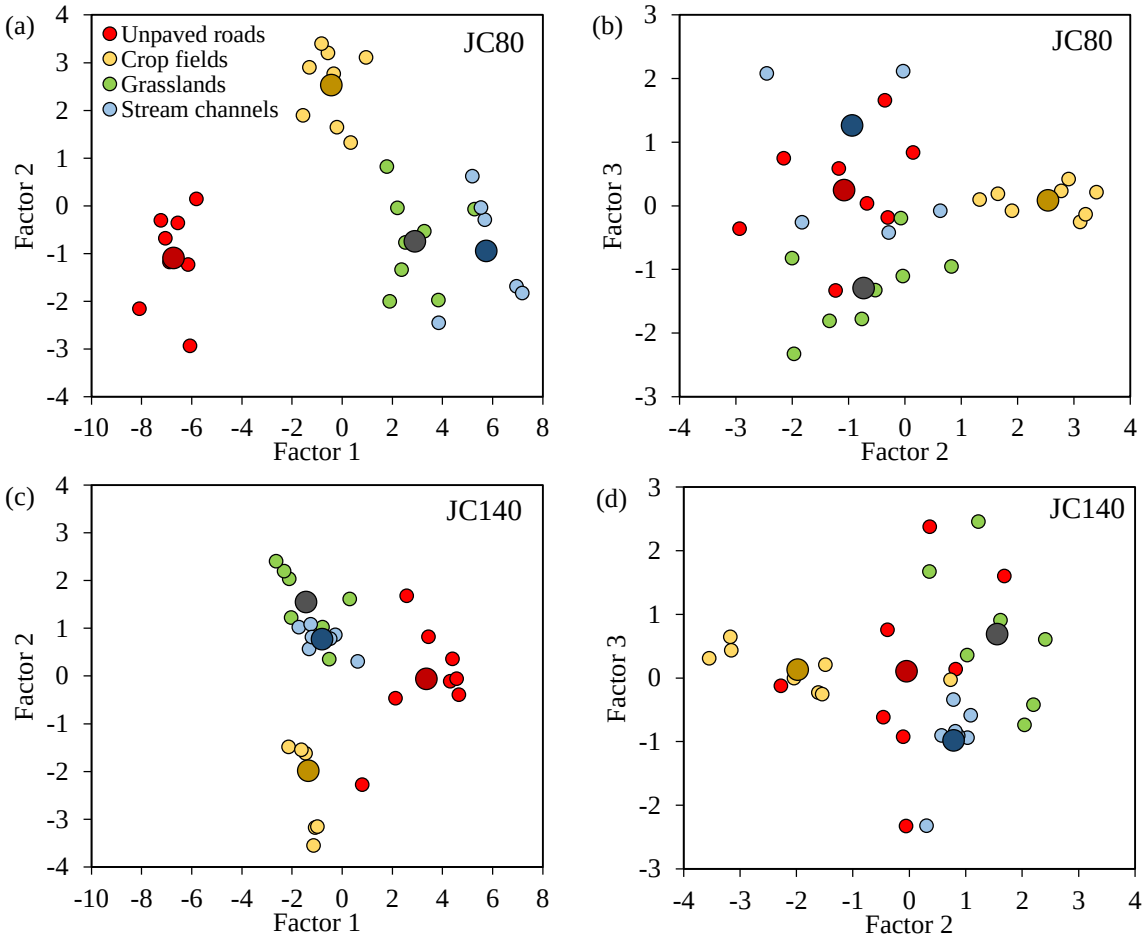

Figure 40 – Two-dimensional scatter plots of the first and second (a, c), and the second and third (b, d), discriminant functions from stepwise discriminant function analysis (DFA) for JC80 and JC140. Larger symbols represent the centroids of each source.

Table 28 – Discriminant function analysis (DFA) output for Júlio de Castilhos catchments.

DFA parameters	JC80	JC140
DFA output		
Wilks' Lambda	0.0056	0.0411
Variance explained by the variables (%)	99.4	95.9
Degrees of freedom	21;57	12;61
$F_{calculated}$	14.0	11.9
$F_{critical}$	1.74	1.91
p-value	<0.0001	<0.0001
F-values		
Degrees of freedom	7;20	4;23
$F_{critical}$	2.51	2.80
Unpaved roads vs. Crop fields	23.1	23.0
Unpaved roads vs. Grasslands	41.8	21.4
Unpaved roads vs. Stream channels	58.9	15.9
Crop fields vs. Grasslands	10.4	10.6
Crop fields vs. Stream channels	19.4	7.6
Grasslands vs. Stream channels	5.5	2.9
p-levels		
Unpaved roads vs. Crop fields	2.8E-08	9.5E-08
Unpaved roads vs. Grasslands	1.4E-10	1.8E-07
Unpaved roads vs. Stream channels	5.7E-12	2.3E-06
Crop fields vs. Grasslands	1.8E-05	5.2E-05
Crop fields vs. Stream channels	1.2E-07	4.9E-04
Grasslands vs. Stream channels	1.2E-03	4.3E-02
Squared Mahalanobis distances		
Unpaved roads vs. Crop fields	52.6	25.9
Unpaved roads vs. Grasslands	95.1	26.0
Unpaved roads vs. Stream channels	156.3	19.2
Crop fields vs. Grasslands	23.7	12.8
Crop fields vs. Stream channels	51.6	9.2
Grasslands vs. Stream channels	14.6	3.8
Average	65.7	16.1
Source type samples classified correctly (%)		
Unpaved roads	100.0	87.5
Crop fields	100.0	87.5
Grasslands	87.5	100.0
Stream channels	100.0	100.0
Total	96.7	93.3

6.2.2 Source apportionment

Figure 41 to Figure 49 display records of precipitation, discharge, suspended sediment concentration, hysteresis pattern, and contribution of sediment sources during different stages of the flood during the nine rainfall events sampled in Júlio de Castilhos catchments. For both catchments, there was a great variation in sediment source contributions between the storm-events, as well as in different discharge stages during each rainfall-runoff event. The JC80 showed a higher hysteresis index compared to the JC140 (1.33 and 0.72 respectively).

The relative mean error (RME) for JC80 was on average 3.4±2.9% (ranging from 0.3 to 10.5%), while for JC140 the RME was on average 1.0±0.6% (ranging from 0.1 to 2.2%) (Figure 50), far below the 15% which are considered acceptable for such studies (COLLINS; WALLING; LEEKS, 1997). The main sediment source in JC80 was stream channels, with a contribution of 48.6±22.7% (ranging from 0 to 87.7%), whereas in JC140 the main sediment source was unpaved roads, accounting to 41.3±19.2% (ranging from 14.6 to 77.8%) (Figure 50).

The results of source apportionment for sediment samples collected at varying intervals along the rising and recession limb of the hydrograph during floods reveal some trends for Júlio de Castilhos catchments. From eighteen storm-events sampled in Júlio de Castilhos catchments (nine storm-events in each catchment), GR contribution of seven storm-events decrease continuously throughout the flood (rising>peak>recession) (Figure 45 e, f, Figure 46 e, f, Figure 48 e, f, Figure 49 e), and seven increased during the rising limb stage and decreased in the recession limb stage (Figure 41e, f, Figure 42 e, f , Figure 43 e, Figure 44 e, f). All the storm-events in JC140 catchment and five storm-events in JC80 (Figure 42 e, Figure 45 e, Figure 46 e, Figure 48 e, Figure 49 e) showed increase in CF contribution during recession limb. In JC80 catchment, six showed SC contribution decrease from rising to recession limb (rising>peak>recession) (Figure 43 e, Figure 45 e, Figure 46 e, Figure 47 e, Figure 48 e, Figure 49 e).

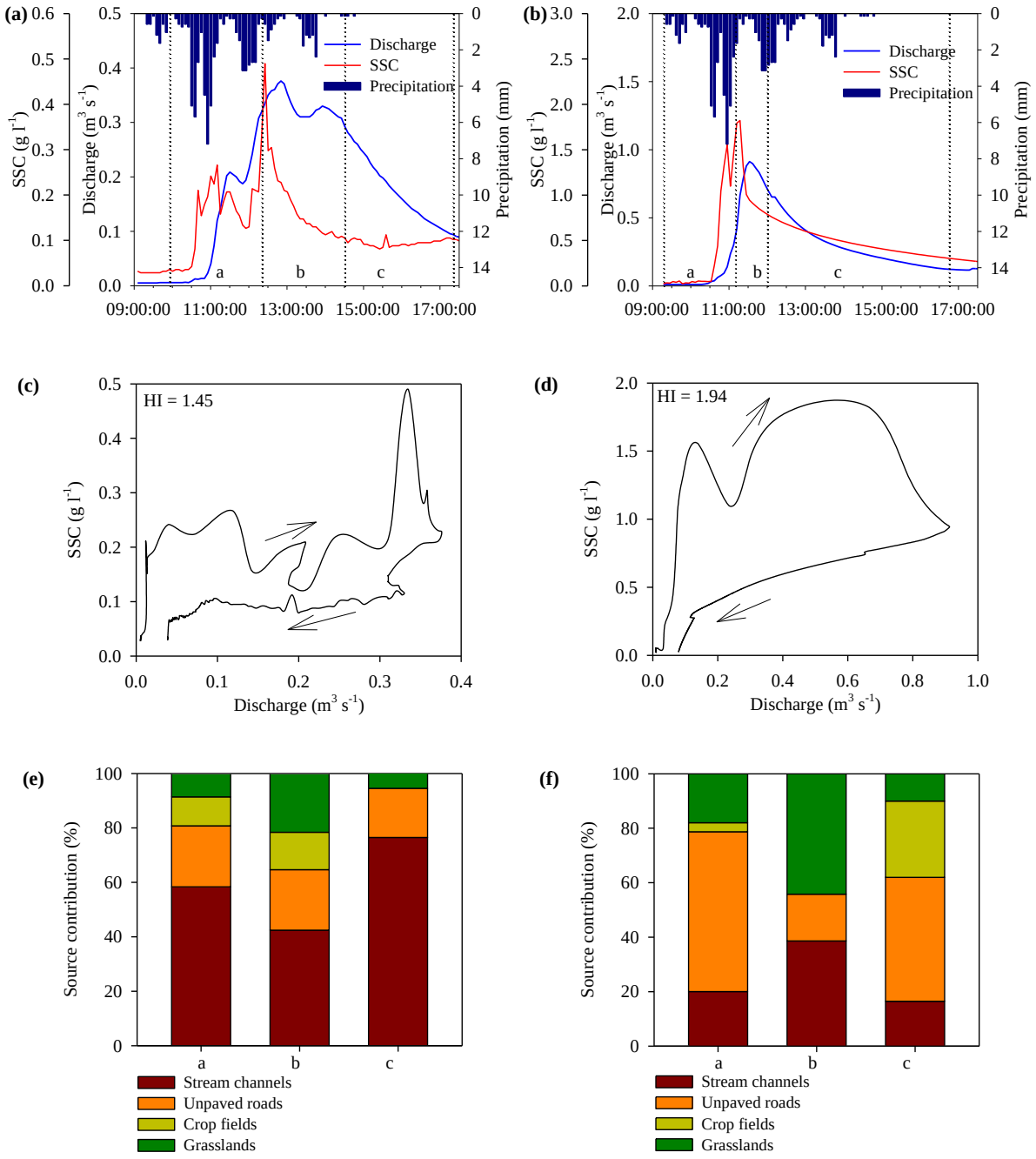

Figure 41 – Records of precipitation, discharge, suspended sediment concentration (a = JC80, b = JC140), suspended sediment concentration (SCC) – discharge hysteresis (c = JC80, d = JC140), and the sediment source contribution (e = JC80, f = JC140) during the storm event that occurred on 14 April 2011 in Júlio de Castilhos.

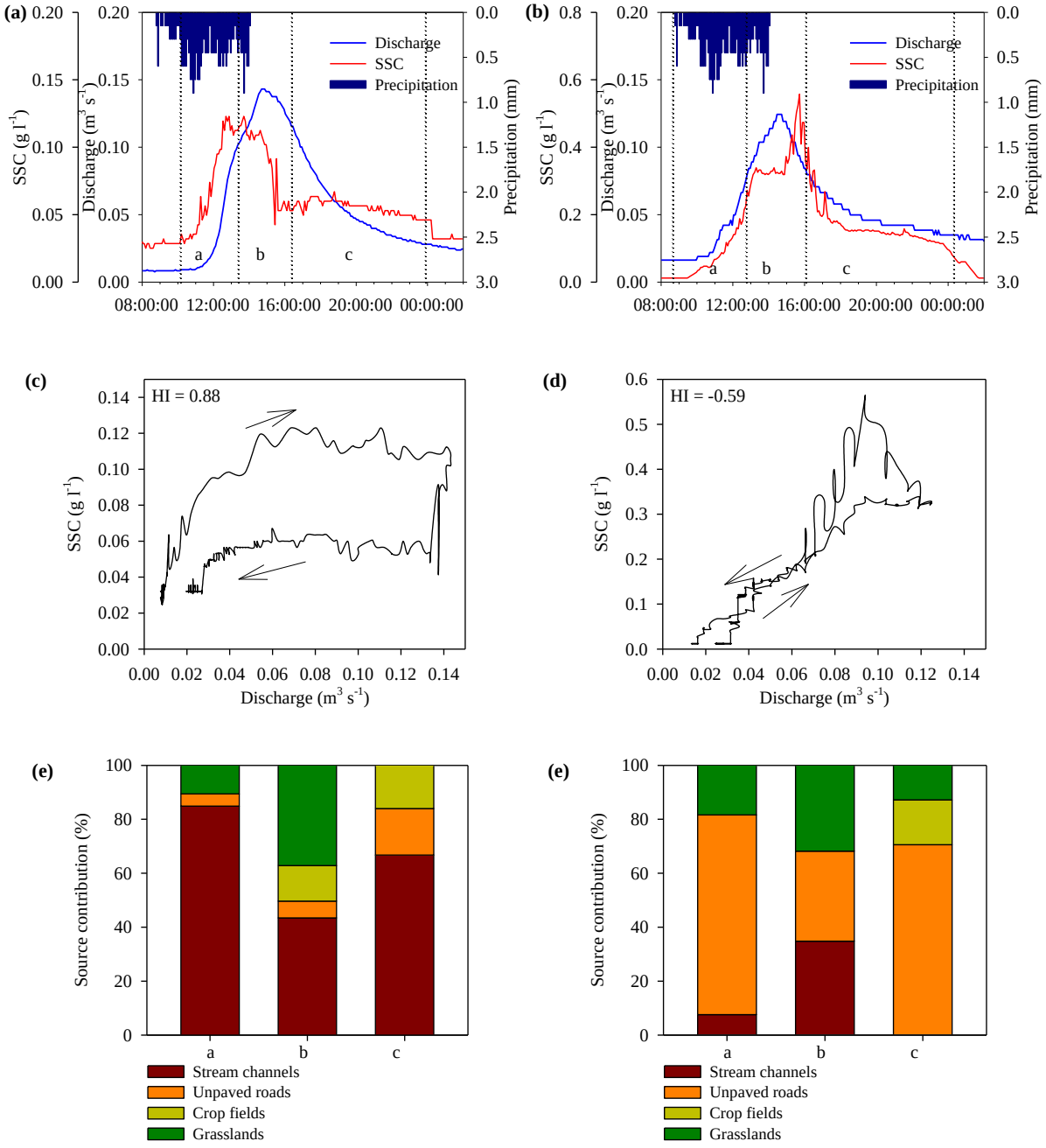

Figure 42 – Records of precipitation, discharge, suspended sediment concentration (a = JC80, b = JC140), suspended sediment concentration (SCC) – discharge hysteresis (c = JC80, d = JC140), and the sediment source contribution (e = JC80, f = JC140) during the storm event that occurred on 17 June 2011 in Júlio de Castilhos.

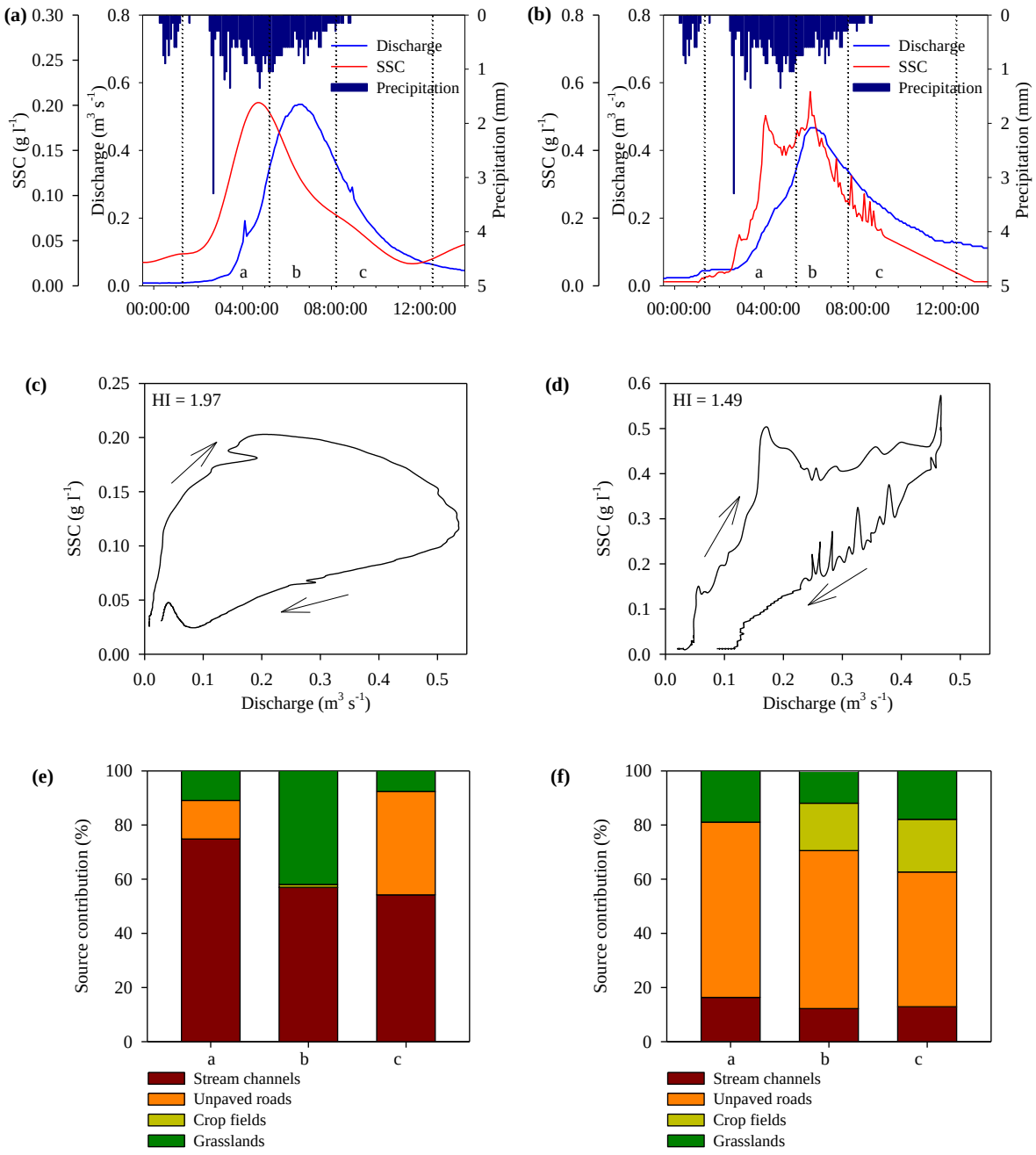

Figure 43 – Records of precipitation, discharge, suspended sediment concentration (a = JC80, b = JC140), suspended sediment concentration (SCC) – discharge hysteresis (c = JC80, d = JC140), and the sediment source contribution (e = JC80, f = JC140) during the storm event that occurred on 1st October 2011 in Júlio de Castilhos.

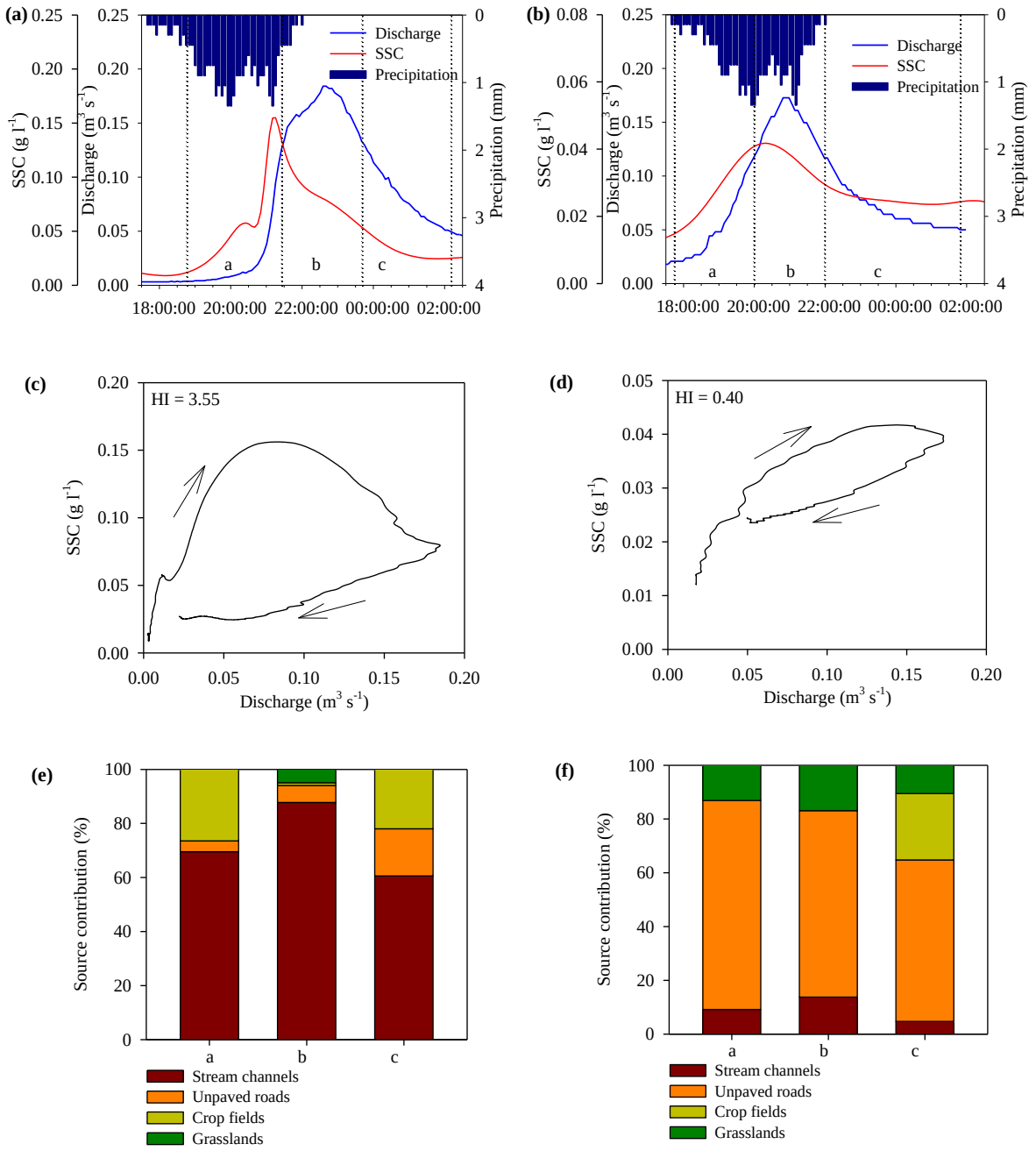

Figure 44 – Records of precipitation, discharge, suspended sediment concentration (a = JC80, b = JC140), suspended sediment concentration (SCC) – discharge hysteresis (c = JC80, d = JC140), and the sediment source contribution (e = JC80, f = JC140) during the storm event that occurred on 24 October 2011 in Júlio de Castilhos.

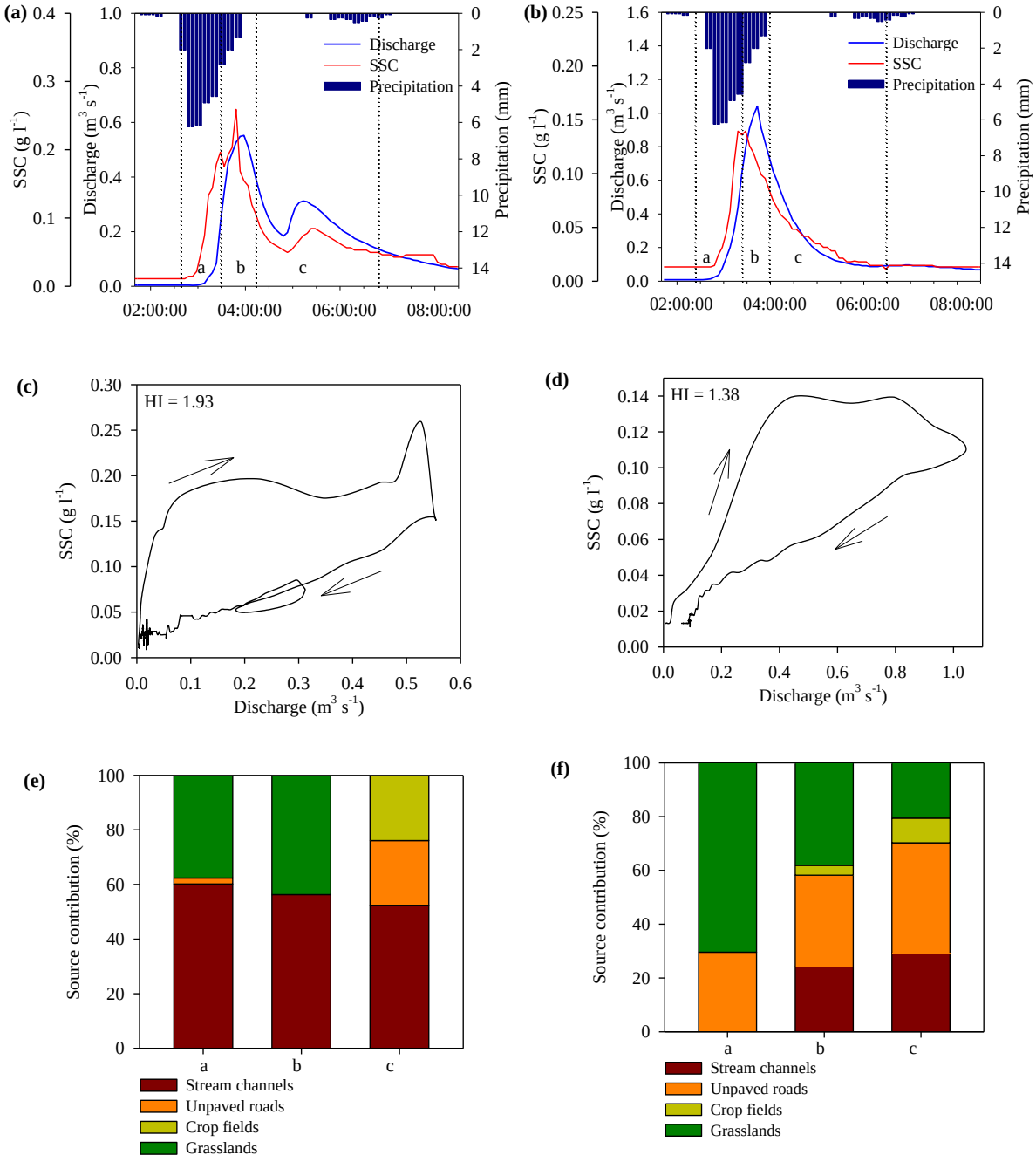

Figure 45 – Records of precipitation, discharge, suspended sediment concentration (a = JC80, b = JC140), suspended sediment concentration (SCC) – discharge hysteresis (c = JC80, d = JC140), and the sediment source contribution (e = JC80, f = JC140) during the storm event that occurred on 30 May 2012 in Júlio de Castillhos.

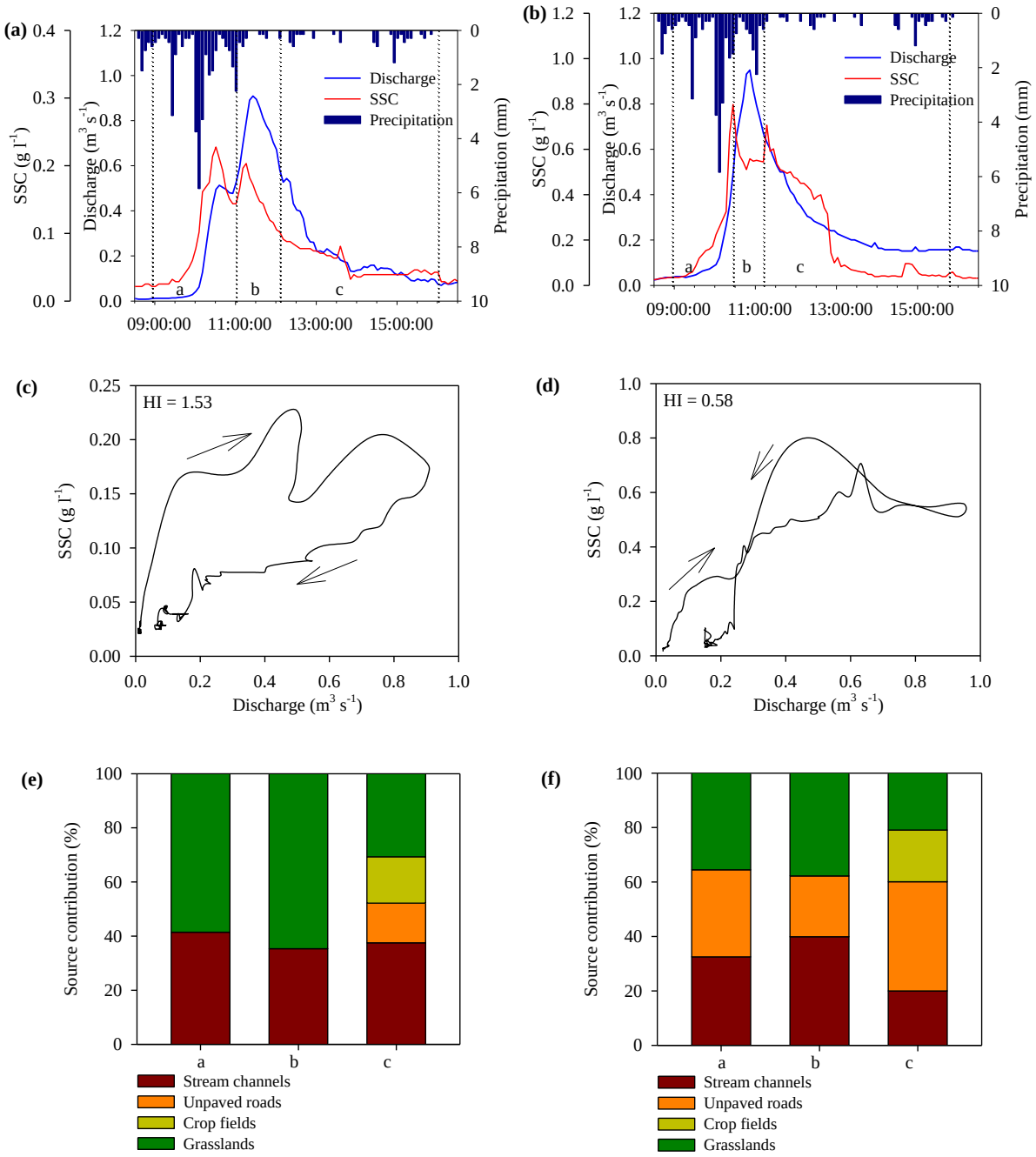

Figure 46 – Records of precipitation, discharge, suspended sediment concentration (a = JC80, b = JC140), suspended sediment concentration (SCC) – discharge hysteresis (c = JC80, d = JC140), and the sediment source contribution (e = JC80, f = JC140) during the storm event that occurred on 18 September 2012 in Júlio de Castillhos.

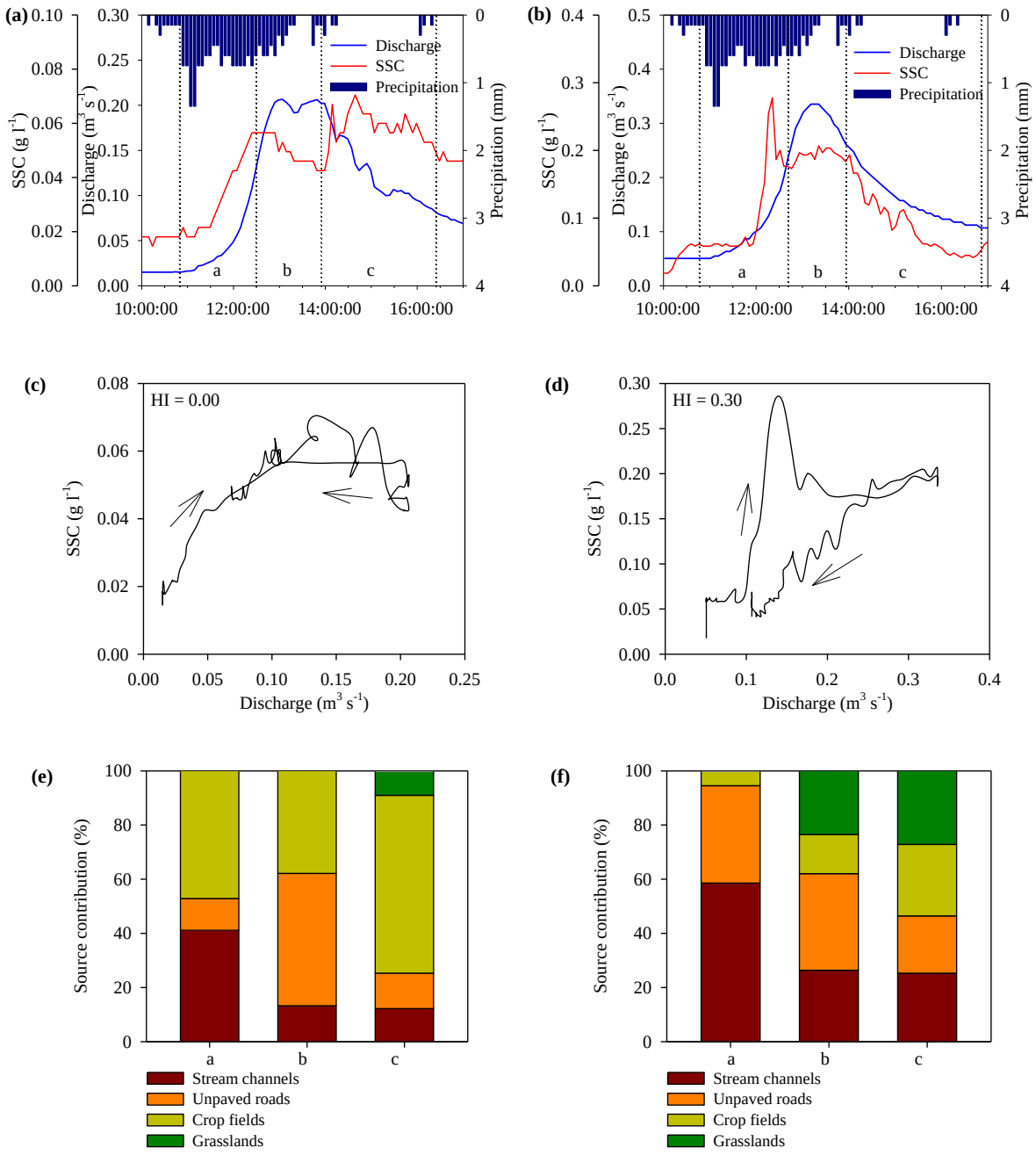

Figure 47 – Records of precipitation, discharge, suspended sediment concentration (a = JC80, b = JC140), suspended sediment concentration (SCC) – discharge hysteresis (c = JC80, d = JC140), and the sediment source contribution (e = JC80, f = JC140) during the storm event that occurred on 10 February 2013 in Júlio de Castillhos.

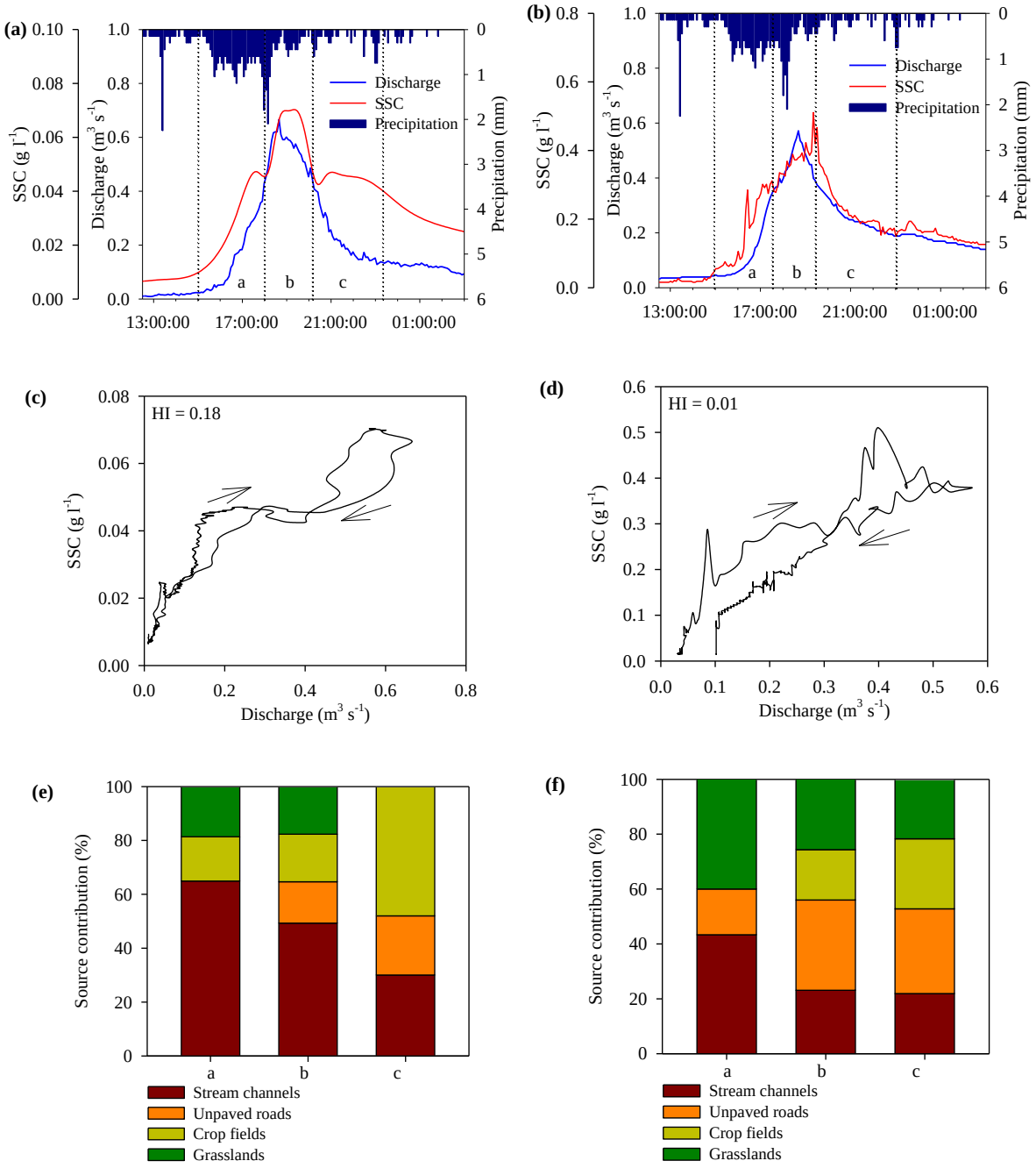

Figure 48 – Records of precipitation, discharge, suspended sediment concentration (a = JC80, b = JC140), suspended sediment concentration (SCC) – discharge hysteresis (c = JC80, d = JC140), and the sediment source contribution (e = JC80, f = JC140) during the storm event that occurred on 10 September 2013 in Júlio de Castillhos.

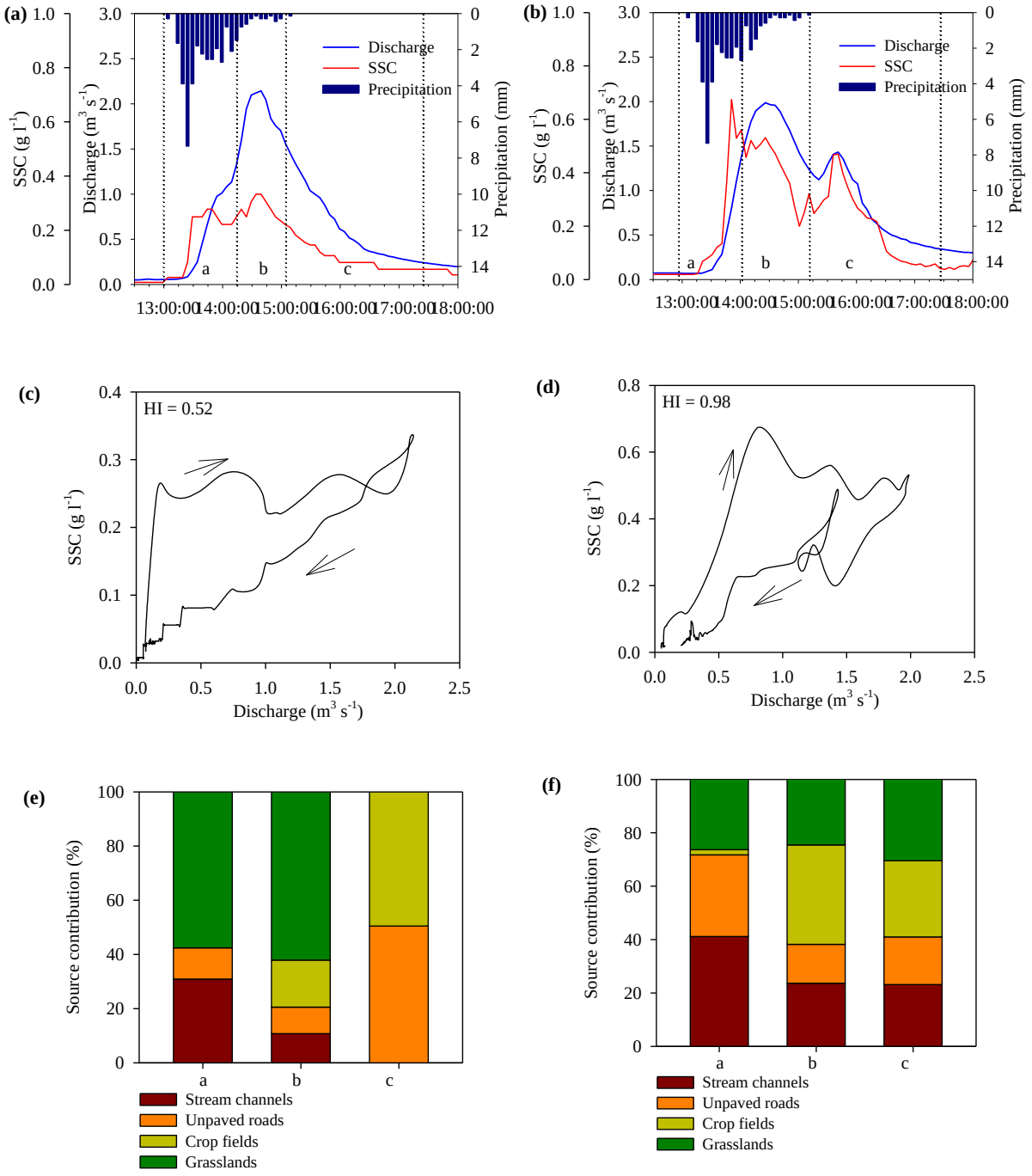

Figure 49 – Records of precipitation, discharge, suspended sediment concentration (a = JC80, b = JC140), suspended sediment concentration (SCC) – discharge hysteresis (c = JC80, d = JC140), and the sediment source contribution (e = JC80, f = JC140) during the storm event that occurred on 22 October 2013 in Júlio de Castillhos.

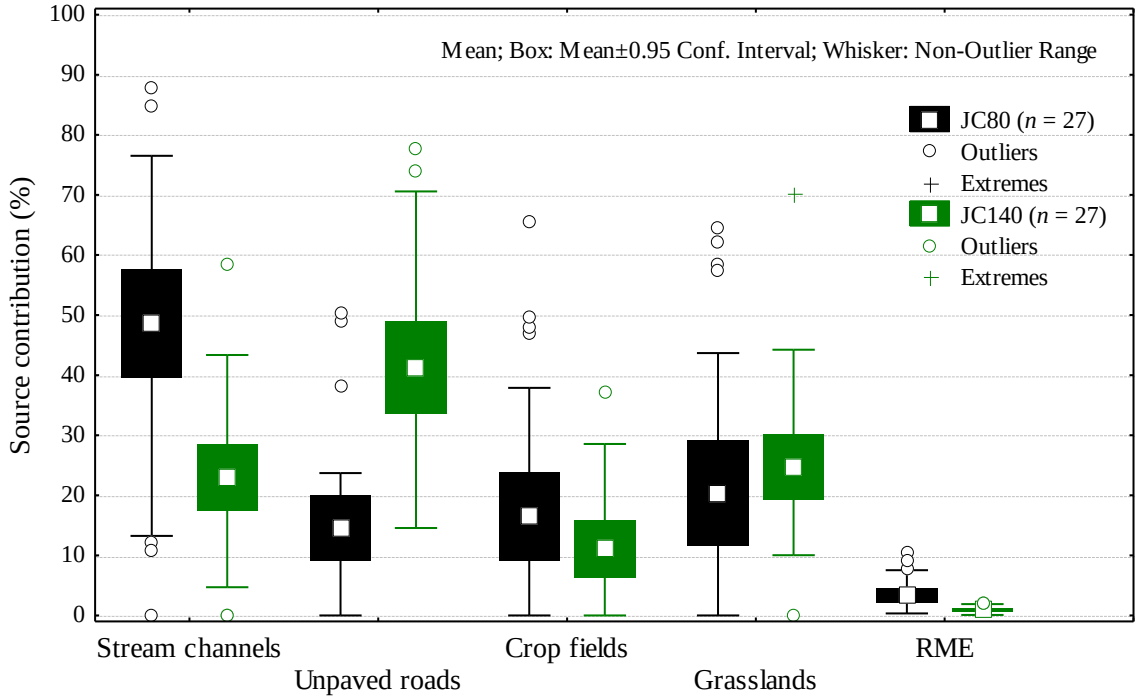

Figure 50 – Box plot of the sediment source contributions for 27 suspended sediment samples collected in Júlio de Castilhos catchments.

Table 29 display the sediment exported from each source for the nine floods evaluated in Júlio de Castilhos catchments. Sediment yield by kilometer of stream channels during the nine floods evaluated was 1,428 and 1,087 kg km^{-1} for JC80 and JC140, respectively. For crop fields and grasslands, JC140 exports approximately 2 times more sediments per hectare than the JC80 catchment. Furthermore, unpaved roads from JC140 supply about 4 times more sediment per unit of area than the JC80 catchment.

Unpaved roads yields about 8 and 17 times more sediment per unit of area than grasslands for JC80 and JC140, respectively, and approximately 44 and 86 times more sediments than crop fields, respectively (Table 29). Moreover, for both catchments grasslands supply approximately 5 times more sediment to rivers than the crop fields per unit of area.

Table 29 – Rainfall characteristics, hysteresis patterns, and sediment delivery from of each source in the nine floods investigated in Júlio de Castilhos catchments. C, clockwise hysteresis, 8, eight-shaped form hysteresis.

Variable	Storm-events evaluated in Júlio de Castilhos catchments									Total	
Day	14-Apr	17-Jun	1-Oct	24-Oct	30-May	18-Sep	10-Feb	10-Sep	22-Oct		
Year	2011	2011	2011	2011	2012	2012	2013	2013	2013	(kg)	(%)
Total precipitation (mm)	77.4	26.7	52.8	34.4	66.4	44.6	22.5	54.3	48.3	-	-
Rain intensity (mm h^{-1})	14.1	5.0	6.1	6.6	30.6	5.6	5.4	4.1	7.2	-	-
Maximum rain intensity (mm h^{-1})	36.0	4.5	16.5	6.8	31.2	29.3	6.8	11.3	36.8	-	-
JC80 catchment											
Hysteresis index	1.45	0.88	1.97	3.55	1.93	1.53	0.00	0.18	0.52	-	-
Sense of hysteresis	C	C	C	C	C	C	8	8	C	-	-
Stream channels (kg)	440	143	587	422	211	331	19	208	351	2713	37.7
Unpaved roads (kg)	178	24	81	40	34	26	34	65	536	1019	14.2
Crop fields (kg)	85	29	7	44	34	31	67	110	583	990	13.8
Grasslands (kg)	126	50	294	18	104	495	6	60	1323	2475	34.4
Total (kg)	830	246	969	524	384	883	126	443	2793	7197	100.0
Stream channels (kg km^{-1})	231.7	75.2	309.1	222.0	111.3	174.4	10.1	109.3	184.6	1428	-
Unpaved roads (kg ha^{-1})	147.0	19.6	67.2	33.3	28.2	21.8	28.1	54.0	443.2	842	-
Crop fields (kg ha^{-1})	1.7	0.6	0.1	0.9	0.7	0.6	1.3	2.1	11.4	19	-
Grasslands (kg ha^{-1})	5.3	2.1	12.2	0.7	4.3	20.6	0.2	2.5	55.1	103	-
JC140 catchment											
Hysteresis index	1.94	–0.59	1.49	0.40	1.38	0.58	0.30	0.01	0.98	-	-
Sense of hysteresis	C	8	C	C	C	8	C	8	C	-	-
Stream channels (kg)	1521	159	344	8	77	812	166	551	1360	4999	24.9
Unpaved roads (kg)	1849	358	1497	53	126	855	163	667	929	6497	32.3
Crop fields (kg)	744	41	347	6	16	238	86	415	1601	3494	17.4
Grasslands (kg)	1495	183	383	11	141	807	107	570	1408	5104	25.4
Total (kg)	5608	741	2572	78	359	2712	522	2204	5298	20095	100.0
Stream channels (kg km^{-1})	330.6	34.6	74.9	1.7	16.6	176.6	36.1	119.9	295.6	1087	-
Unpaved roads (kg ha^{-1})	973.3	188.4	788.1	28.0	66.1	449.8	85.8	351.3	488.9	3420	-
Crop fields (kg ha^{-1})	8.4	0.5	3.9	0.1	0.2	2.7	1.0	4.7	18.2	40	-
Grasslands (kg ha^{-1})	58.4	7.1	15.0	0.4	5.5	31.5	4.2	22.3	55.0	199	-

6.3 Conceição catchment

6.3.1 Source discrimination

A total of 18 source sediment samples with one or more outliers were detected and then excluded from the further steps of source discrimination analysis (crop fields = 6, grasslands = 3, unpaved roads = 6, stream channels = 3). Concentration of Ca, K, Mg, Na, Sr, and Ti of most sediment samples (especially storm-event suspended sediments – SESS), were higher than the highest source concentration (Table 30). In the same way, concentration of Al, Li, Pb, and TOC of most sediment samples (especially fine-bed sediments – FBS) were lower than the lowest source concentration. These elements were considered as non-conservative for Conceição catchment and were then excluded from the next steps. The concentration in sediments for the remaining 13 geochemical tracers (Ba, Be, Co, Cr, Cu, Fe, La, Mn, Ni, P, Sr, V, and Zn) laid between the concentration ranges of the sources and were then kept.

Table 31 presents the Kruskal–Wallis *H*-values, as well as the percentage of samples correctly classified by each tracer using discriminant function analysis (DFA). When using four sediment sources, 11 from the 13 remaining geochemical variables were selected as potential tracers by applying the Kruskal-Wallis *H*-test ($p<0.1$). It means that these 11 geochemical tracers present difference at least between two sources. The discriminatory power of these 11 tracers ranged from 24.8 to 51.5%, and no variable alone was able to correctly classify 100% of the source samples in their respectively groups. The 11 tracer properties identified by the Kruskal-Wallis test as providing statistically significant discrimination between the source material samples were then entered into the stepwise multivariate DFA, in order to select the optimum set for maximizing discrimination, whilst minimizing dimensionality. Table 32 shows the progressive change of the Wilks' Lambda value (Λ^*) as the variables are introduced into the analysis. The set of elements selected by DFA analyses comprised seven elements, namely P, V, La, Be, Fe, Co, and, Mn. The final value of the Λ^* parameter was 0.2669. As the value of Λ^* is the proportion of the total variance due to the error of the sources discrimination, the selected variables provided an error of ~ 26.7%. It means the set of selected variables explains approximately 73.3% of the differences between the sources (Table 33). Although all the four sediment sources were separated by significant Mahalanobis distances ($p<0.001$), the distances between CF and GR, and between GR and SC were very short (Table 33 and Figure 51a). It

resulted in only 72.1% of the samples correctly classified in their respective groups (Table 33), mainly due to low classification of CF and GR (68.5 and 62.5%).

Because grasslands is much less important in both area and erosion intensity for Conceição catchment, and because it created a confounding effect in source samples classification, especially when contrasting with SC and CF (Table 33 and Figure 51a), we removed this sediment source for subsequent steps. Besides, modeling four sediment sources provided unrealistic source contributions. On average for all sediment samples, source contribution using four sediment sources was 56, 29, 12, and 3% for GR, SC, CF, and UR, respectively, with and RME higher than 20%. Moreover, the results for more than 20% of sediment samples results was 100% of GR contribution. These results were considered unsatisfactory because the magnitude of the contribution of each source is inconsistent with field observations of the erosion processes in Conceição catchment. These results demonstrate that the model used to estimate the contribution of sediment sources have limitation to find a viable solution when using four sediment of in large catchments.

When using three sediment sources (SC, UR, CF), the same 11 (Ba, Be, Co, Cr, Fe, La, Mn, P, Sr, V, and Zn) were selected as potential tracers by applying the Kruskal-Wallis *H*-test (p <0.1) (Table 31). The discriminatory power of these tracers ranged from 31.2 to 62.4%, and again no variable alone was able to correctly classify 100% of the source samples in their respectively groups. The optimum set of tracers selected by DFA for maximizing discrimination, whilst minimizing dimensionality, was almost the same from the DFA with four sources, comprising six tracers (P, La, V, Mn, Be, and Ba - Table 32). The final value of the Λ^* parameter was also almost the same ($\Lambda^* = 0.2702$), meaning that the set of selected variables explains approximately 73.0% of the differences between the sources (Table 33). However, compared to the approach with four sediment sources, the three remaining sediment sources (SC, UR, CF) were well separated by a Mahalanobis distance of 6.0±1.1 (p<2.50E−14) (Table 33 and Figure 51b), resulting in 84.4% of samples correctly classified in their respective groups (Table 33).

Table 30 – Geochemical tracer concentrations in sediment sources and suspended sediments sieved to 63 µm, and test of sediment source range for suspended sediments, in Conceição catchment. SD, standard deviation; TISS, time-integrated suspended sediment; SESS, storm-event suspended sediment; FBS, fine-bed sediment.

Fingerprint property	Stream channels		Unpaved roads		Crop fields		Grasslands		Source range		TISS		SESS		FBS		TISS		SESS		FBS		Fingerprint property removed
	(*n* = 33)		(*n* = 35)		(*n* = 73)		(*n* = 24)		A	B	(*n* = 33)		(*n* = 20)		(*n* = 34)		% of sediment samples out of source range						
	Mean	SD	Mean	SD	Mean	SD	Mean	SD	Max*2.0	Min*0.75	Mean	SD	Mean	SD	Mean	SD	>A	<B	>A	<B	>A	<B	
Al (g kg^{-1})	59.9	12.5	91.6	13.2	71.5	13.8	57.6	9.3	183.3	43.2	51.3	8.5	53.7	8.6	41.1	8.0	0	12	0	19	0	**58**	*
Ba (mg kg^{-1})	210.9	55.3	123.2	79.0	191.7	79.4	207.6	72.8	421.7	92.4	350.6	84.4	337.7	38.5	404.4	211.4	24	0	0	0	36	0	
Be (mg kg^{-1})	3.9	0.6	3.4	0.5	3.7	0.6	3.7	0.6	7.8	2.6	6.1	3.3	4.6	1.3	5.8	3.2	24	0	5	0	36	11	
Ca (g kg^{-1})	1.8	0.9	0.6	1.0	2.1	1.1	2.1	1.3	4.2	0.4	4.1	2.5	13.0	6.5	3.2	0.6	24	0	**100**	0	3	0	*
Co (mg kg^{-1})	58.9	19.5	25.6	17.4	45.5	20.6	54.2	18.2	117.8	19.2	76.6	14.6	53.1	8.5	126.1	48.8	0	3	0	0	37	0	
Cr (mg kg^{-1})	79.2	14.0	67.0	12.5	75.3	18.9	74.3	14.8	158.5	50.3	97.6	23.8	70.8	7.7	141.0	54.0	0	3	0	0	33	0	
Cu (mg kg^{-1})	323.8	71.7	315.7	73.5	321.7	60.4	314.3	52.9	647.7	235.7	293.0	58.1	240.5	40.0	441.3	130.5	0	3	0	29	11	0	
Fe (g kg^{-1})	92.1	20.7	88.1	10.2	92.5	11.9	87.8	14.1	185.1	65.8	70.5	13.7	64.2	11.9	98.6	19.7	0	34	0	38	0	3	
K (g kg^{-1})	0.4	0.4	0.7	0.6	0.9	0.6	0.8	0.7	1.9	0.3	0.9	0.5	3.1	2.5	0.6	0.4	6	12	**67**	5	0	25	*
La (mg kg^{-1})	36.8	7.3	32.3	8.4	35.1	10.1	31.7	7.4	73.6	23.8	40.7	6.3	29.8	5.3	30.1	5.3	0	0	0	14	0	8	
Li (mg kg^{-1})	50.4	13.4	75.1	24.5	57.6	19.2	45.1	15.0	150.3	33.8	37.8	9.3	43.7	6.0	30.3	5.0	0	18	0	0	0	**78**	*
Mg (g kg^{-1})	2.9	0.9	2.1	0.9	3.0	1.4	3.3	1.4	6.6	1.6	4.2	1.4	10.2	3.8	3.8	0.7	9	0	**86**	0	3	0	*
Mn (g kg^{-1})	2.3	0.9	1.0	0.4	1.9	0.6	2.1	0.7	4.5	0.8	2.9	0.6	2.3	0.4	3.8	1.6	3	0	0	0	25	0	
Na (mg kg^{-1})	82.5	35.1	79.2	101.6	74.2	69.9	82.1	74.2	165.1	55.6	896.4	1277.2	1847.2	1811.4	412.7	447.3	**76**	6	**90**	5	**50**	28	*
Ni (mg kg^{-1})	46.8	13.6	49.4	14.7	49.1	15.0	47.6	11.2	98.7	35.1	60.1	16.3	44.5	6.5	74.0	22.1	0	3	0	10	17	0	
P (mg kg^{-1})	327.6	104.5	291.2	76.6	476.2	105.8	392.0	64.9	952.5	218.4	549.2	130.3	512.0	62.3	368.8	110.1	0	0	0	0	0	3	
Pb (mg kg^{-1})	16.3	3.6	11.9	5.5	13.9	4.7	12.7	4.7	32.5	8.9	9.9	12.4	4.1	4.3	14.3	16.1	6	**56**	0	**90**	17	**56**	*
Sr (mg kg^{-1})	25.2	8.8	14.2	9.7	22.4	9.1	26.3	11.9	52.6	10.7	48.5	24.5	108.9	44.0	38.7	7.8	18	0	**100**	0	3	0	
Ti (g kg^{-1})	3.5	1.0	2.4	0.8	3.0	0.8	4.0	1.2	8.0	1.8	11.5	5.6	12.5	1.8	14.7	9.6	**62**	0	**100**	0	**61**	3	*
V (mg kg^{-1})	377.1	62.1	301.0	59.9	362.4	56.8	398.9	68.9	797.8	225.7	473.6	99.5	359.9	57.8	726.6	142.7	0	3	0	5	31	0	
Zn (mg kg^{-1})	14.8	3.1	12.1	2.4	13.4	2.6	14.7	3.3	29.6	9.1	18.1	4.7	15.8	10.5	24.5	8.3	0	3	5	0	25	0	
TOC (g kg^{-1})	15.6	4.9	7.3	4.6	22.2	4.2	25.1	5.8	50.3	5.5	30.8	6.0	44.3	12.3	15.0	6.6	0	**47**	24	0	0	**64**	*

Table 31 − The ability of individual fingerprint properties to distinguish sediment source type, assessing the Kruskal−Wallis *H*-test and discriminant function analysis (DFA) in Conceição catchment. ns = not significant, *p<0.1, ** p <0.05, *** p <0.01, **** p <0.001.

Fingerprint property	Kruskal-Wallis test – 4 sediment sources			DFA – 4 sources	Kruskal-Wallis test – 3 sediment sources			DFA – 3 sources
	H-value	*p*-value	Signif.	Correctly classified samples (%)	*H*-value	*p*-value	Signif.	Correctly classified samples (%)
Al	72.0	<0.001	****	43.6	57.1	<0.001	****	53.2
Ba	33.7	<0.001	****	38.8	31.5	<0.001	****	45.4
Be	13.2	0.004	***	30.3	12.6	0.002	***	34.8
Ca	56.8	<0.001	****	32.1	54.9	<0.001	****	50.4
Co	42.1	<0.001	****	38.8	37.0	<0.001	****	45.4
Cr	13.5	0.004	***	30.3	12.7	0.002	***	36.2
Cu	2.6	0.455	ns	-	1.7	0.421	ns	-
Fe	6.9	0.090	*	32.7	4.6	0.099	*	41.8
K	19.1	<0.001	****	40.0	19.1	<0.001	****	46.8
La	7.4	0.060	*	24.8	4.7	0.090	*	31.2
Li	33.1	<0.001	****	37.6	22.0	<0.001	****	42.6
Mg	29.6	<0.001	****	29.1	24.4	<0.001	****	41.8
Mn	51.7	<0.001	****	48.5	47.4	<0.001	****	58.2
Na	6.4	0.093	*	37.6	6.7	0.036	*	45.4
Ni	0.5	0.917	ns	-	0.5	0.775	ns	-
P	75.8	<0.001	****	51.5	67.5	<0.001	****	62.4
Pb	15.7	0.001	***	32.7	14.1	<0.001	****	35.5
Sr	48.9	<0.001	****	42.4	45.7	<0.001	****	51.1
Ti	34.8	<0.001	****	35.8	20.2	<0.001	****	41.1
V	37.1	<0.001	****	39.4	30.0	<0.001	****	48.2
Zn	17.0	<0.001	****	27.3	13.6	0.001	***	32.6
TOC	100.6	<0.001	****	53.3	87.8	<0.001	****	73.0

Table 32 − Results of the stepwise discriminant function analysis (DFA) as indicated by the Wilks' Lambda values using three and four sediment sources in Conceição catchment.

Step	Fingerprint property selected	Wilks' Lambda	*p* to remove	Cumulative % of source type samples correctly classified
DFA – 4 sediment sources				
1	P	0.5900	0.0E+00	51.5
2	V	0.4577	6.5E-06	60.6
3	La	0.4212	1.9E-04	64.8
4	Be	0.3831	1.7E-02	62.4
5	Fe	0.3670	3.3E-02	62.4
6	Co	0.2797	5.4E-02	69.7
7	Mn	0.2669	6.3E-02	72.1
DFA – 3 sediment sources				
1	P	0.5733	0.0E+00	62.4
2	La	0.5284	1.9E-05	66.7
3	V	0.4126	8.1E-05	76.6
4	Mn	0.3092	1.0E-04	81.6
5	Be	0.2871	5.3E-03	83.0
6	Ba	0.2702	1.8E-02	84.4

Table 33 − Discriminant function analysis (DFA) output in Conceição catchment.

DFA parameters	4 sediment sources	3 sediment sources
Wilks' Lambda	0.2669	0.2702
Variance explained by the variables (%)	73.3	73.0
Degrees of freedom	21;445	12;226
$F_{calculated}$	12.40	20.47
$F_{critical}$	1.58	1.80
p-value	<0.00001	<0.00001
F-values		
Degrees of freedom	7;155	6;133
$F_{critical}$	2.07	2.17
Unpaved roads vs. Stream channels	14.9	16.75
Crop fields vs. Stream channels	16.0	17.84
Grasslands vs. Stream channels	5.2	-
Unpaved roads vs. Crop fields	22.4	26.53
Unpaved roads vs. Grasslands	13.7	-
Crop fields vs. Grasslands	4.2	-
p-levels		
Unpaved roads vs. Stream channels	8.5E-15	2.5E-14
Crop fields vs. Stream channels	1.0E-15	4.2E-15
Grasslands vs. Stream channels	2.2E-05	-
Unpaved roads vs. Crop fields	9.7E-21	1.3E-20
Unpaved roads vs. Grasslands	9.7E-14	-
Crop fields vs. Grasslands	3.2E-04	-
Squared Mahalanobis distances		
Unpaved roads vs. Stream channels	6.4	6.1
Crop fields vs. Stream channels	5.1	4.9
Grasslands vs. Stream channels	2.7	-
Unpaved roads vs. Crop fields	6.9	7.0
Unpaved roads vs. Grasslands	7.0	-
Crop fields vs. Grasslands	1.7	-
Source type samples classified correctly (%)		
Unpaved roads	75.8	84.8
Crop fields	82.9	82.9
Stream channels	68.5	84.9
Grasslands	62.5	-
Total	72.1	84.4

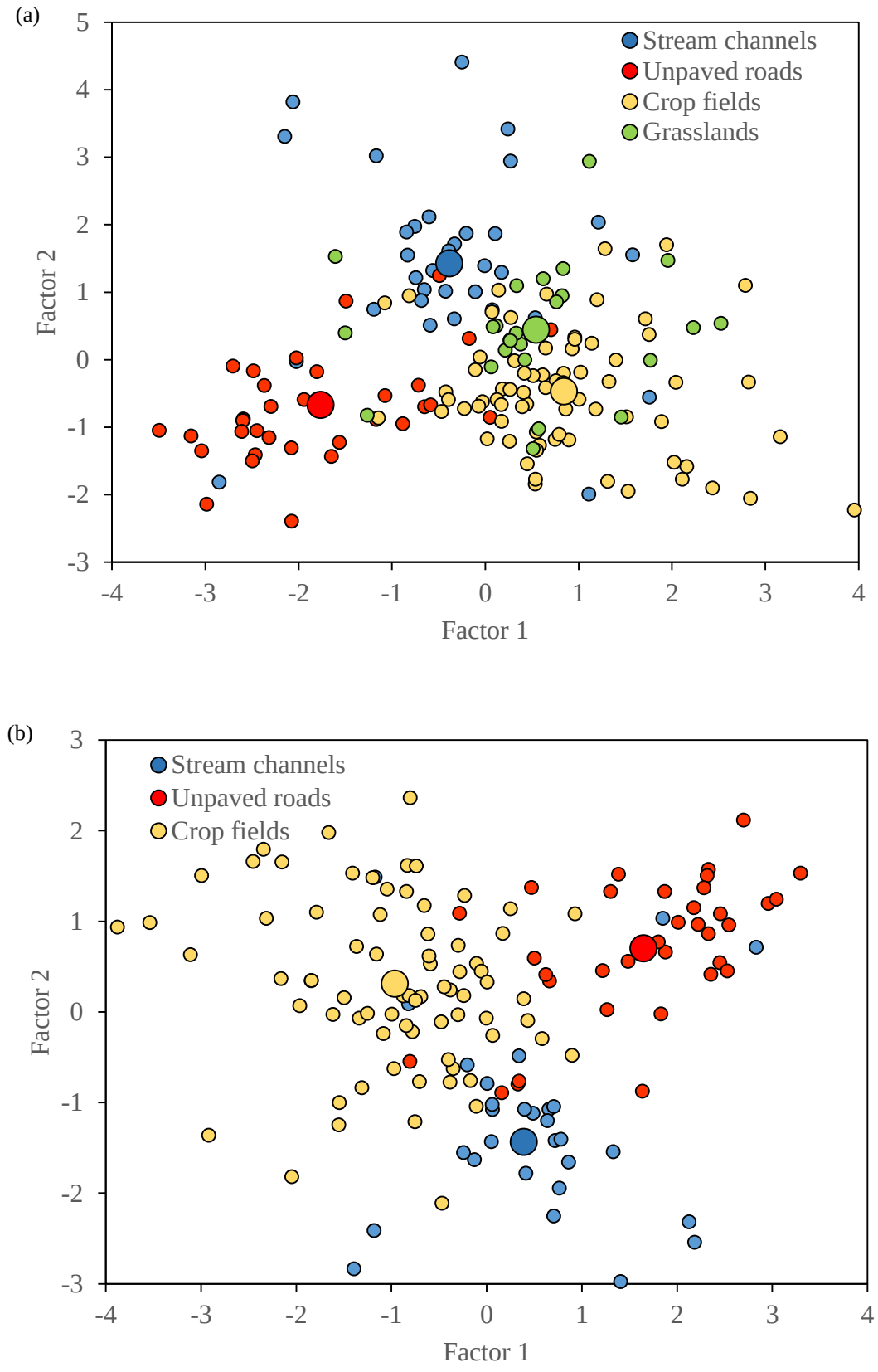

Figure 51 − Two-dimensional scatter plots of the first and second discriminant functions from stepwise discriminant function analysis (DFA) using four (a) and three (b) sediment sources from Conceição catchment. Larger symbols represents the centroids of each source.

6.3.2 Source apportionment

6.3.2.1 Spatial and temporal variability of suspended sediment source contributions

Suspended sediment exports at the watershed outlet varied throughout the study period (Figure 52f). The monthly suspended sediment yield was correlated to the total amount of rainfall ($r = 0.69$, $p<0.0001$). The contribution of sources delivering suspended sediment to the river also varied among different sites. Sediment source apportionment using suspended sediment collected with time-integrate traps (TISS) indicate no contribution of UR, and highlights CF and SC as the main sediment sources at Conceição catchment (Figure 52a,b,c,d,e).

Sites 1 and 2, both along the main river, showed very similar source apportionments (Figure 52a,b). Average contribution of CF for sites 1 and 2 were about 56.0±19.6 and 54.9±11.9%. For site 3, however, placed at Leal river (a major tributary of Conceição river), CF contribution was lower than at sites 1 and 2 (overall average of 28.9%), mainly between January 2013 and March 2014 (summer), when SC contribution was predominant (94.4±5.1%). For the same period, the higher SC contribution from site 3 increased SC contribution in site 4, diluting the CF contribution from sites 1 and 2. At the catchment outlet (site 5), contribution of CF and SC was very similar and stable over time (Figure 52e). On average CF contribution was about 44.5±12.4% and SC contribution was 55.5±12.4.

6.3.2.2 Intra-storm variability of suspended sediment source contribution

Suspended sediment samples collected at varying intervals along the rising and recession limb of the hydrograph during floods were taken only at site 5, at the catchment outlet. All four floods were characterized by clockwise hystereses. The hysteresis index (HI) varied according to the amount of rainfall. The HI for the events 1, 2, 3 and 4 (6 July 2012, 19 September 2012, 2 October 2012, 22 October 2012) was 5.6, 19.7, 24.2, and 5.4 (Figure 53 and Figure 54), and total rainfall was 84.7, 125.4, 121.5, and 47.9 mm, respectively.

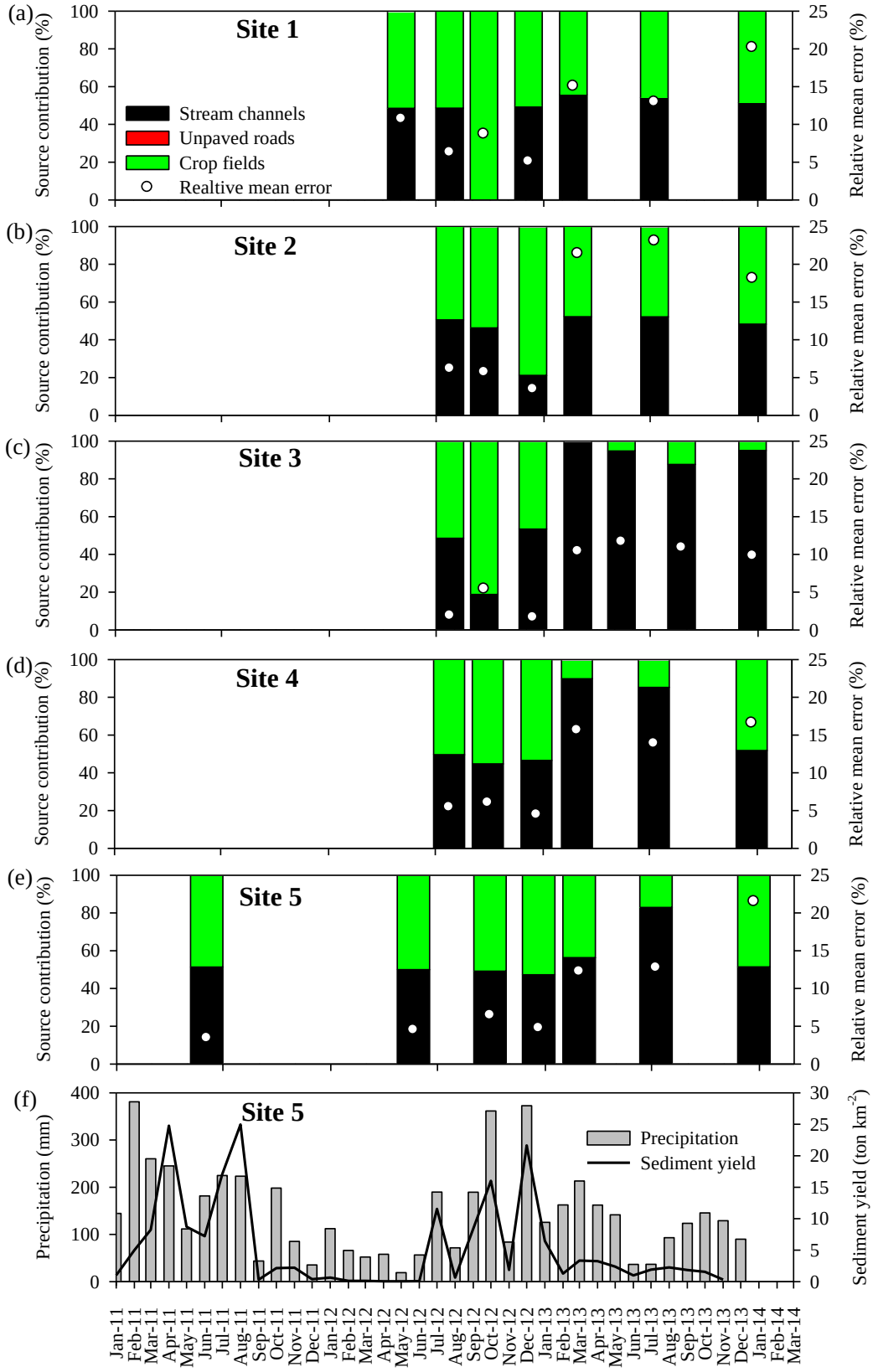

Figure 52 − Spatial and temporal variation in source contributions for suspended sediments collected with time-integrate samplers in Conceição catchment (a, b, c, d, e), and records of monthly precipitation and sediment yield at the catchment outlet (f).

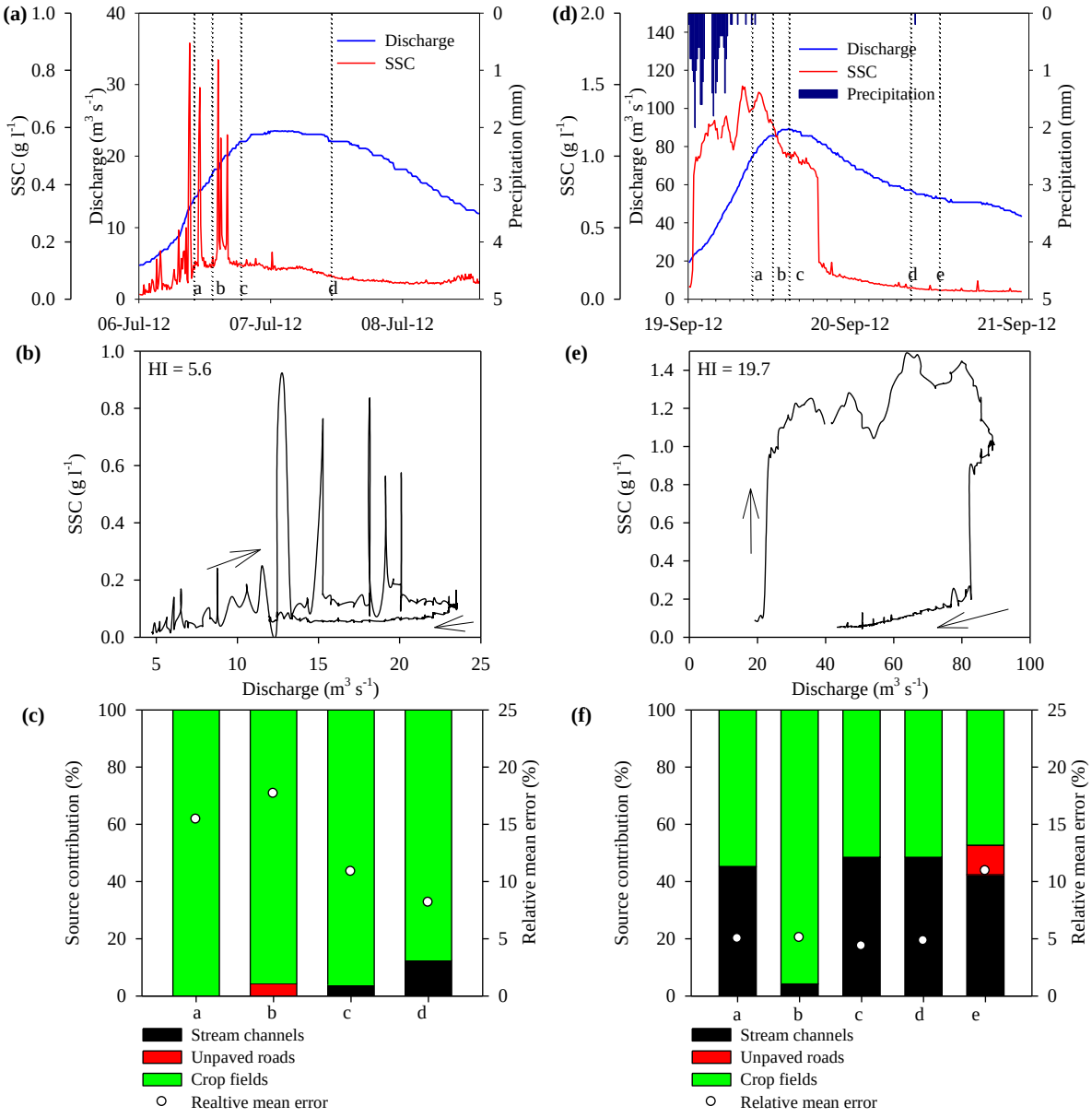

Figure 53 – Records of precipitation, discharge, suspended sediment concentration (SSC), hysteresis pattern, and the sediment source contributions during the floods that occurred on 6 July 2012 (a, b, c) and 19 September 2012 (d, e, f) in Conceição catchment.

For suspended sediment samples collected during floods, the main sediment source was CF (70±21%), and SC accounted to 30±21% on average. However, when considering the sediment yield of for each event, contribution of CF decreased to 59% (Table 34). Unlike samples collected with time-integrate sampler, storm suspended sediment samples contained very low UR contributions for the two firsts storm-events (Figure 53). CF contribution

increased with discharge for three floods, while SC decreased during the rising limb and increased during recession limb Figure 53f and Figure 54c,f).

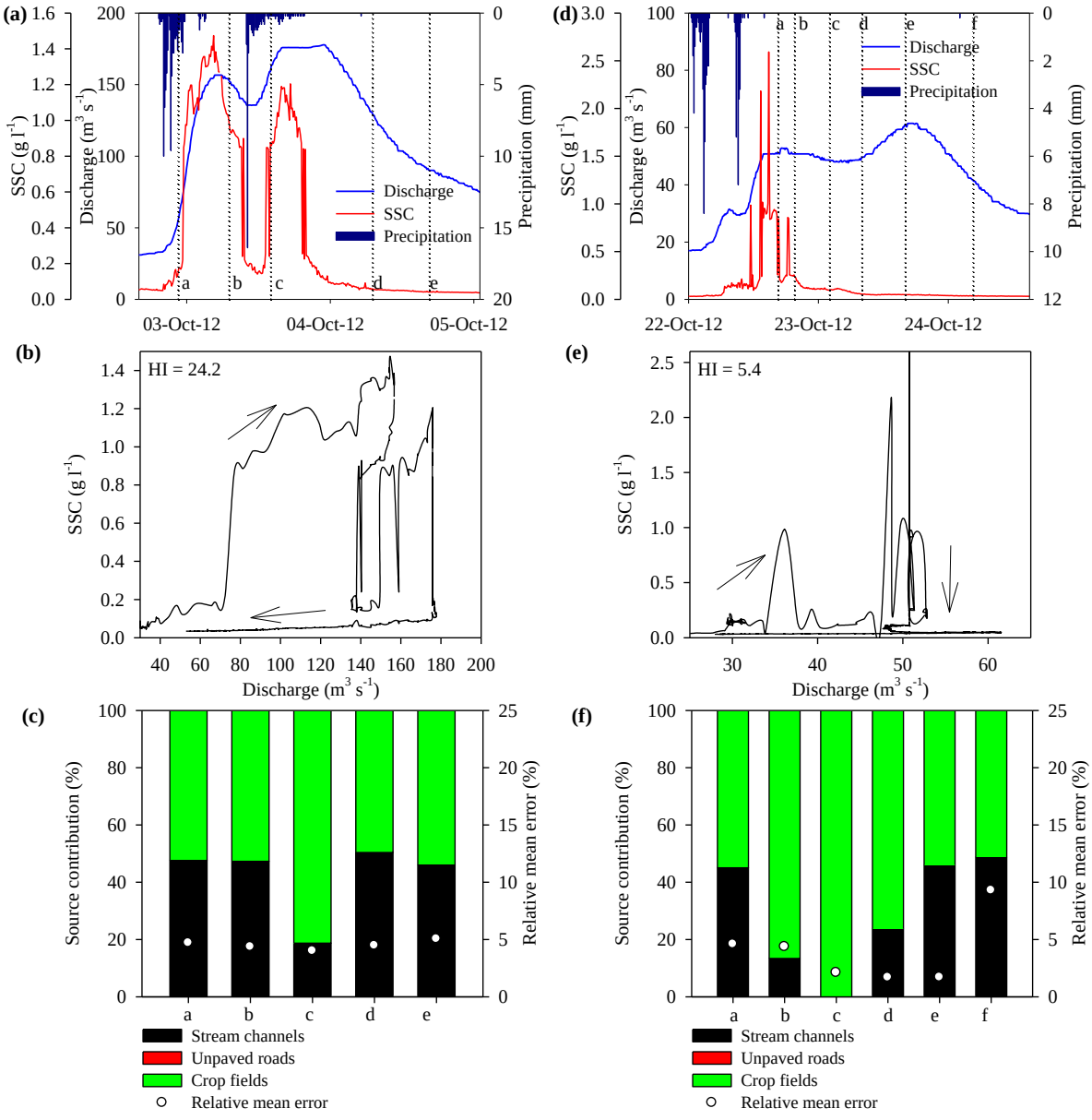

Figure 54 – Records of precipitation, discharge, suspended sediment concentration (SCC), hysteresis pattern, and the sediment source contributions during the floods that occurred on 2 October 2012 (a, b, c) and 23 October 2012 (d, e, f) in Conceição catchment.

Table 34 – Sediment yield supplied by each source during the four floods investigated in Conceição catchment. SSC, suspended sediment concentration.

Date	Hour	Discharge ($m^3 s^{-1}$)		SSC ($g l^{-1}$)		Sediment yield (tons)			
		Max	Mean	Max	Mean	Total	Stream channels	Unpaved roads	Crop fields
6-Jul-12	10:00	15.27	13.63	0.89	0.25	39.3	0.0	0.0	39.3
6-Jul-12	13:15	20.10	17.71	0.84	0.19	52.1	0.0	2.3	49.9
6-Jul-12	18:30	23.54	22.45	0.57	0.13	103.3	4.0	0.0	99.3
7-Jul-12	11:00	23.54	21.75	0.12	0.08	136.6	16.9	0.0	119.7
8-Jul-12	12:00	18.15	13.14	0.13	0.07	81.1	0.0	67.6	13.5
Sum	-	-	-	-	-	412.4	20.9	69.9	321.6
19-Sep-12	9:08	80.16	72.29	1.49	1.39	1027.3	465.0	0.0	562.4
19-Sep-12	12:08	87.81	84.58	1.43	1.26	1023.4	42.8	0.0	980.6
19-Sep-12	14:28	89.48	82.96	1.09	0.64	1886.0	914.3	0.0	971.6
20-Sep-12	7:58	72.31	62.06	0.15	0.10	255.6	123.9	0.0	131.7
20-Sep-12	12:08	55.04	52.87	0.10	0.07	53.8	22.8	5.5	25.4
Sum	-	-	-	-	-	4246.1	1568.8	5.5	2671.8
2-Oct-12	22:30	166.11	145.61	1.08	0.57	2477.7	1179.9	0.0	1297.8
3-Oct-12	7:00	176.86	175.21	1.20	0.76	3574.0	1690.9	0.0	1883.1
3-Oct-12	14:00	177.76	147.12	0.15	0.08	496.9	93.1	0.0	403.7
4-Oct-12	7:00	110.38	91.94	0.05	0.04	178.9	90.2	0.0	88.7
4-Oct-12	16:30	78.99	69.22	0.04	0.04	87.7	40.3	0.0	47.4
Sum	-	-	-	-	-	6815.2	3094.4	0.0	3720.8
22-Oct-12	21:30	52.83	51.45	0.94	0.59	292.8	131.9	0.0	160.8
23-Oct-12	0:30	52.83	51.03	0.86	0.23	202.3	27.0	0.0	175.3
23-Oct-12	7:00	50.77	48.88	0.12	0.11	121.0	0.0	0.0	121.0
23-Oct-12	13:00	55.04	50.56	0.09	0.06	74.1	17.6	0.0	56.6
23-Oct-12	21:00	61.49	58.85	0.05	0.05	102.7	47.2	0.0	55.5
24-Oct-12	9:30	54.97	42.75	0.04	0.04	67.3	32.8	0.0	34.5
Sum	-	-	-	-	-	860.3	256.5	0.0	603.7
Total (ton)	-	-	-	-	-	12333.9	4940.6	75.4	7317.9
Total (%)	-	-	-	-	-	100.0	40.1	0.6	59.3

6.3.2.3 Comparison between fine-bed sediment and suspended sediment sources

Fine-bed sediment has been used as a surrogate for suspended sediment in fingerprinting studies (WILKINSON et al., 2013). Results indicate that the relative contributions from different sources to fine-sediment deposited on the stream bed and suspended sediment collected with time-integrate samplers and manually collected during storm-events might not be always similar. Considering the overall mean, SC was the main source for fine-bed sediments

(76±30%), and CF was the main source for storm-event suspended sediment (70±21%), whilst time-integrated suspended sediments showed similar contribution for SC and CF (56±22 and 44±22, respectively - Figure 55).

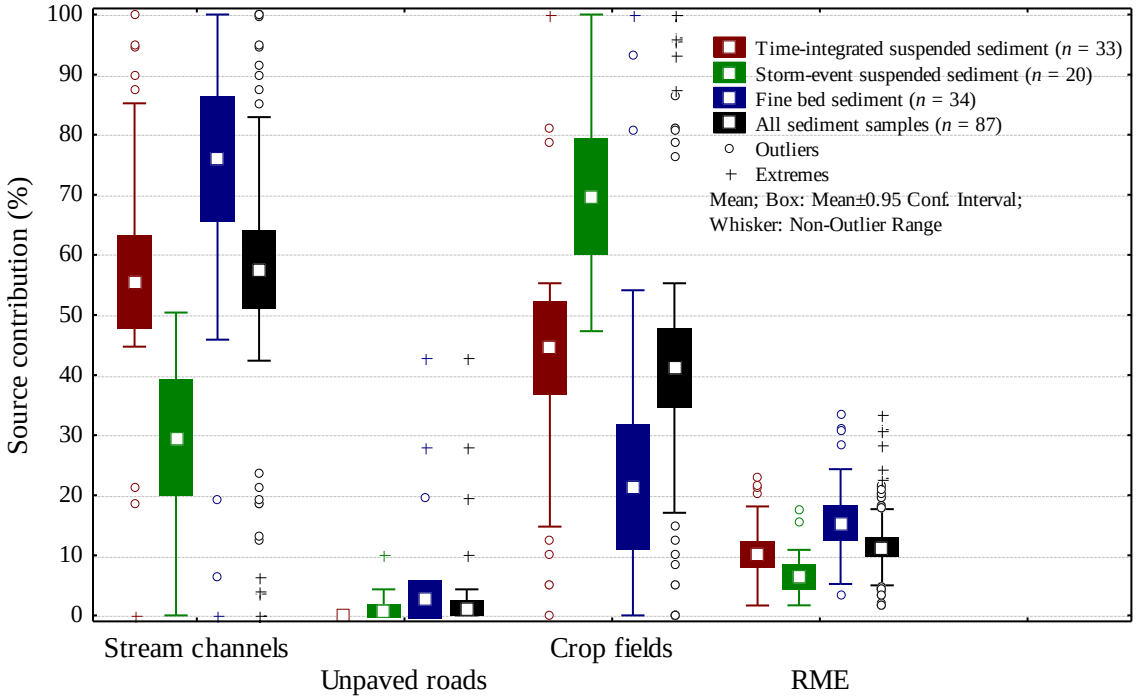

Figure 55 – Box plot of the sediment source contribution for time-integrated suspended sediments, storm-events suspended sediments, and fine-bed sediments collected in Conceição catchment.

Analyzing in more detail for fine bed-sediment, the main sediment source at the sites 1, 2, 3, and 4 was the SC, with an average contribution of 89±17%, ranging from 54 to 100% (Figure 56a,b,c,d). At catchment outlet, however, CF was the main sediment source from April to August 2011, whereas SC was the main sediment source from November 2012 to October 2013 (Figure 56e).

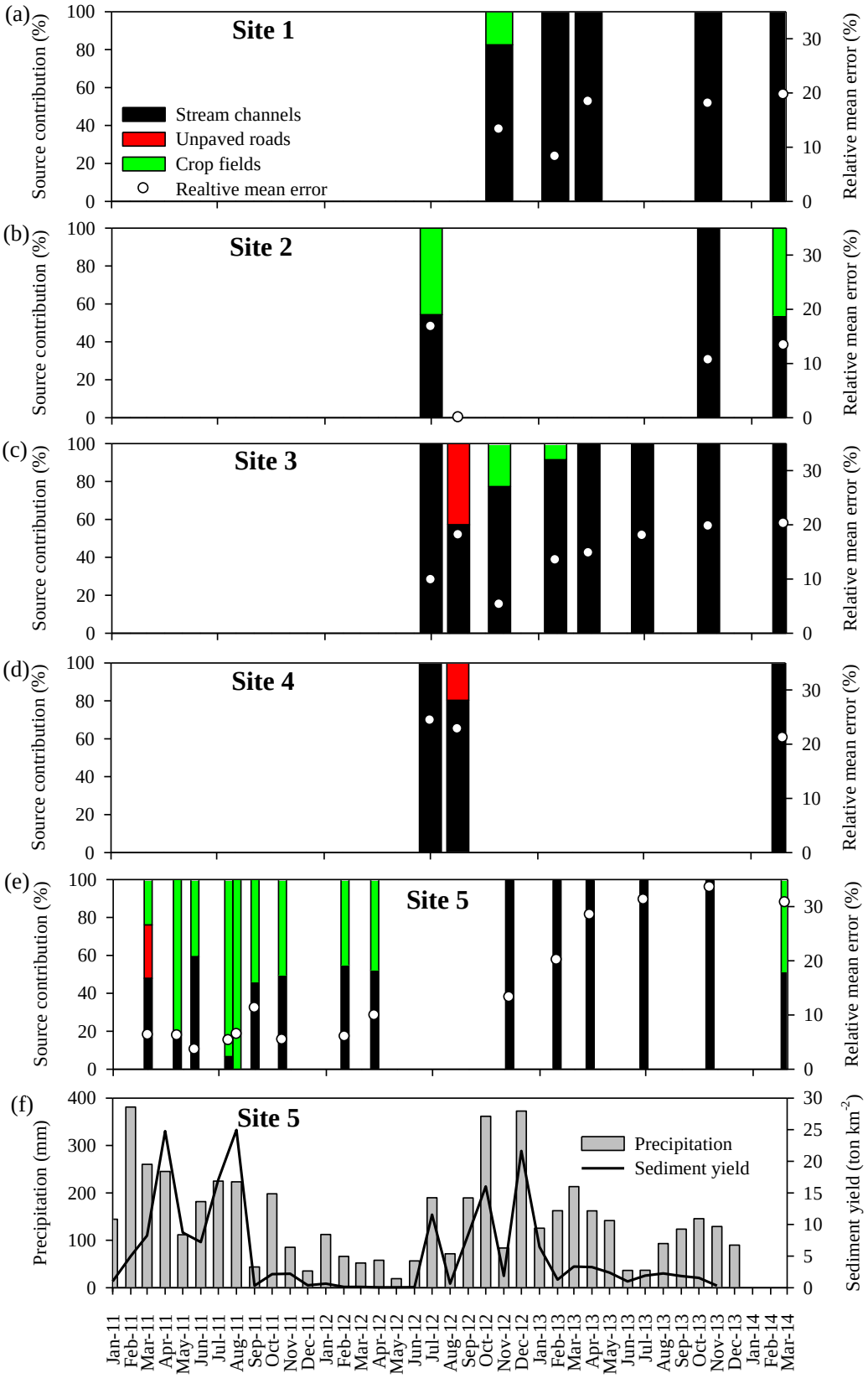

Figure 56 − Spatial and temporal variation in source contributions for fine-bed sediments collected in Conceição catchment (a, b, c, d, e), and records of monthly precipitation and sediment yield at the catchment outlet (f).

6.4 Guaporé catchment

6.4.1 Source discrimination

A total of 37 source sediment samples with one or more outliers were detected and then excluded from the next steps of source discrimination analysis (18 crop fields samples, 6 grasslands samples, 7 unpaved roads samples, and 6 stream channels samples). Concentration of Ba, Be, Ca, K, Mg, Na, Sr, Ti, TOC, and Zn of most sediment samples (especially storm-event suspended sediments – SESS), were higher than the highest source concentration (Table 35). In contrast, concentration of Fe and Pb in most sediment samples were lower than the lowest source concentration. These elements were considered as non-conservative for Guaporé catchment and were then excluded from the next steps of fingerprinting approach. The concentration in sediments for the remaining 10 geochemical tracers (Al, Co, Cr, Cu, La, Li, Mn, Ni, P, and V) laid between the concentration ranges of the source materials and were then kept.

Table 36 presents the Kruskal–Wallis H-values, as well as the percentage of samples correctly classified by each tracer using discriminant function analysis (DFA). When using four sediment sources, all the 10 remaining geochemical variables were selected as potential tracers by applying the Kruskal-Wallis H-test ($p<0.1$). The discriminatory power of these 10 tracers ranged from 18.4 to 45.6%, and no variable alone was able to correctly classify 100% of the source samples in their respectively groups. The 10 geochemical tracers identified by the Kruskal-Wallis test as providing statistically significant discrimination between the source material samples were then entered into the stepwise multivariate DFA, in order to select the optimum set for maximizing discrimination, whilst minimizing dimensionality.

Table 37 shows the progressive change of the Wilks' Lambda value (Λ^*) as the variables are introduced into the analysis. The set of elements selected by DFA analyses comprised seven elements, namely P, Al, Ni, Cr, V, Co, and, Mn. The final value of the Λ^* parameter was 0.3616. As the value of Λ^* is the proportion of the total variance due to the error of the sources discrimination, the selected variables provided an error of ~ 36.2%. It means the set of selected variables explains approximately only 63.8% of the differences between the sources (Table 38).

Table 35 – Geochemical tracer concentrations of sediment sources and suspended sediments sieved to 63 µm, and test of sediment source range for suspended sediments, in Guaporé catchment. SD, standard deviation; TISS, time-integrated suspended sediment; SESS, storm-event suspended sediment; SESS-U59, storm-event suspended sediment collected with US-U59 sampler; FBS, fine-bed sediment. Bold values indicate geochemical tracers excluded from the next steps.

Fingerprint property	Sediment sources								Sediment samples								Sediment samples out of source range (%)							
	Stream channels (*n* = 40)		Unpaved roads (*n* = 51)		Crop fields (*n* = 141)		Grasslands (*n* = 40)		TISS (*n* = 50)		SESS (*n* = 12)		SESS-U59 (*n* = 26)		FBS (*n* = 62)		TISS		SESS		SESS-U59		FBS	
	Mean	SD	Mean	SD	Mean	SD	Mean	SD	Mean	SD	Mean	SD	Mean	SD	Mean	SD	Higher	Lower	Higher	Lower	Higher	Lower	Higher	Lower
Al (g kg^{-1})	46.0	8.4	66.3	20.5	48.8	11.8	44.3	7.5	37.5	11.0	42.9	3.3	36.4	5.0	36.0	6.5	0	32	0	0	0	23	0	33
Ba (mg kg^{-1})	212.7	45.3	169.5	67.4	199.7	60.5	231.1	74.3	289.9	89.4	418.8	43.7	313.5	106.3	330.8	101.8	25	3	**92**	0	31	0	**47**	4
Be (mg kg^{-1})	3.5	1.0	3.0	1.1	3.2	1.5	3.7	1.1	4.1	3.2	8.3	0.5	1.9	1.9	4.3	2.9	24	**54**	**100**	0	9	**77**	33	**41**
Ca (g kg^{-1})	1.7	0.9	1.6	1.5	2.0	1.1	2.6	1.2	3.1	1.5	10.1	4.9	3.8	1.4	3.3	0.9	19	0	**100**	0	**46**	0	25	0
Co (mg kg^{-1})	44.0	26.5	33.3	21.5	42.3	27.6	50.4	21.5	40.9	17.1	49.9	5.9	44.0	19.2	52.5	20.7	3	19	0	0	9	11	13	11
Cr (mg kg^{-1})	24.6	9.8	28.4	13.1	24.9	13.5	27.3	13.6	31.6	16.9	31.9	4.7	31.1	11.0	36.7	19.3	16	19	0	0	23	9	29	13
Cu (mg kg^{-1})	156.4	99.5	201.9	120.1	186.5	138.9	227.3	106.4	135.4	49.7	138.1	19.1	164.7	45.0	176.4	62.6	0	34	0	17	0	14	0	15
Fe (g kg^{-1})	69.8	26.8	78.2	24.2	74.7	35.7	84.0	26.5	48.7	14.6	50.3	5.8	51.5	9.1	59.7	16.2	0	**57**	0	**67**	0	**54**	0	30
K (g kg^{-1})	1.3	0.6	1.5	0.8	1.4	0.7	1.9	0.9	1.7	1.0	6.4	3.5	2.4	1.0	1.5	0.5	7	19	**92**	0	14	3	0	13
La (mg kg^{-1})	38.0	14.0	33.5	14.3	31.7	12.4	26.0	11.3	34.2	9.9	36.8	5.7	32.8	8.7	32.1	8.8	3	7	0	0	0	6	0	8
Li (mg kg^{-1})	40.5	9.0	53.0	21.3	40.9	13.1	35.7	7.4	33.6	7.7	38.1	4.3	34.4	6.5	33.4	3.4	0	4	0	0	0	0	0	2
Mg (g kg^{-1})	3.7	1.3	4.1	1.9	3.4	1.4	4.2	1.5	4.1	1.1	7.2	1.5	4.8	1.1	4.2	1.1	7	9	**75**	0	14	3	7	5
Mn (g kg^{-1})	2.0	1.0	1.4	0.7	2.0	0.9	2.3	0.8	1.8	0.6	1.8	0.3	1.9	0.4	2.0	0.7	2	7	0	0	0	3	1	5
Na (mg kg^{-1})	78.2	52.8	136.9	176.8	64.4	98.7	79.0	67.9	442.8	835.7	2095.6	1317.2	517.8	569.8	280.2	232.7	35	**46**	**100**	0	**51**	20	**40**	28
Ni (mg kg^{-1})	17.0	9.8	25.4	15.8	19.7	15.4	25.3	14.0	19.1	7.8	23.0	2.0	22.2	9.5	23.2	8.6	0	24	0	0	6	17	2	11
P (mg kg^{-1})	267.3	77.7	253.4	98.3	437.2	123.1	382.2	144.2	452.5	251.2	502.4	42.7	431.9	102.0	427.8	128.7	7	3	0	0	0	0	4	4
Pb (mg kg^{-1})	27.1	8.4	19.6	8.6	24.0	6.9	21.3	8.6	19.1	6.4	15.7	3.2	20.5	5.6	19.3	7.4	0	25	0	**50**	0	17	0	33
Sr (mg kg^{-1})	30.9	8.4	26.1	16.3	26.2	10.8	33.7	15.6	41.9	16.4	104.9	39.6	47.7	16.3	44.0	12.9	25	7	**100**	0	37	3	28	4
Ti (g kg^{-1})	4.0	0.9	3.4	1.2	3.6	1.0	3.9	1.2	7.1	5.1	10.8	1.1	4.5	2.1	7.3	5.5	**43**	19	**100**	0	11	20	**40**	18
V (mg kg^{-1})	256.5	147.2	252.1	133.9	281.7	196.0	366.6	168.1	245.8	118.2	289.0	42.5	268.6	107.5	343.7	139.0	2	35	0	0	0	26	8	13
Zn (mg kg^{-1})	12.6	3.7	12.8	3.7	14.3	5.1	15.9	4.6	32.9	28.7	14.2	1.5	38.2	15.8	33.5	20.1	**49**	3	0	0	**69**	0	**49**	0
TOC (g kg^{-1})	13.3	2.7	8.9	3.9	21.5	6.2	24.2	7.3	39.2	15.4	41.1	8.8	38.3	15.7	30.8	13.2	**48**	0	**75**	0	**57**	0	25	0

Although all the four sediment sources were separated by significant Mahalanobis distances (p<0.001), the distances between CF and GR, and between GR and SC were very short (Table 38 and Figure 57a). Thus, only 66.9% of the samples were correctly classified in their respective groups (Table 38), mainly due to low classification of GR samples (52.5%). Because grasslands is much less important in both area and erosion intensity for Guaporé catchment, and because it created a confounding effect in source samples classification, especially when contrasting with SC and CF (Figure 57a, Table 38), we removed this sediment source from further analysis. Moreover, as in Conceição catchment, modeling four sediment sources provided unrealistic source ascriptions, mainly for fine-bed sediments, were the average contribution was 67±43, 17±30, 3±1, 16±32% for GR, CF, UR, and SC, respectively, wherein more than 50% of the samples showed contribution of 100% for GR. These results were considered unsatisfactory because the magnitude of the contribution of each source is inconsistent with field observations of the erosion processes in Guaporé catchment. These results demonstrate that the model used to estimate the contribution of sediment sources have limitation to find a viable solution when using four sediment of in large catchments.

When using three sediment sources (SC, UR, CF), 8 from the same 10 remaining elements (Al, Co, Cr, La, Li, Mn, Ni, and P) were selected as potential tracers by applying the Kruskal-Wallis H-test (p <0.1) (Table 36). The discriminatory power of these tracers ranged from 22.4 to 62.9%, and again no variable alone was able to correctly classify 100% of the source samples in their respectively groups. The optimum set of tracers selected by DFA for maximizing discrimination, whilst minimizing dimensionality, was almost the same from the DFA with four sources (V was replaced by La), comprising seven tracers (P, Al, Cr, Ni, Co, La, and Mn – Table 37). The final value of the Λ^* parameter was also almost the same (Λ^* = 0.3537), meaning that the set of selected variables explains approximately 64.6% of the differences between the sources. However, compared to the approach with four sediment sources, the three remaining sediment sources (SC, UR, CF) were well separated by a Mahalanobis distance of 4.9±1.7 (p<2.1E−16) (Table 38 and Figure 57b), resulting in 80.2% of samples correctly classified in their respective groups.

Table 36 − The ability of individual fingerprint properties to distinguish sediment source type, assessing the Kruskal−Wallis *H*-test and discriminant function analysis (DFA) in Guaporé catchment. ns = not significant, *p<0.1, **p<0.05, ***p<0.01, ****p<0.001.

Fingerprint property	Kruskal-Wallis test – 4 sediment sources			DFA – 4 sources	Kruskal-Wallis test – 3 sediment sources			DFA – 3 sources
	H-value	*p*-value	Signif.	Correctly classified samples (%)	*H*-value	*p*-value	Signif.	Correctly classified samples (%)
Al	43.1	0.0000	****	39.3	35.2	0.0000	****	43.1
Ba	20.3	0.0001	****	30.5	13.2	0.0013	***	33.2
Be	7.2	0.0663	*	20.2	2.9	0.2308	ns	-
Ca	20.8	0.0001	****	30.1	9.4	0.0090	***	45.7
Co	10.5	0.0148	**	21.7	5.5	0.0647	*	22.8
Cr	6.8	0.0784	*	19.5	5.9	0.0525	*	22.4
Cu	8.0	0.0450	**	18.4	3.4	0.1833	ns	-
Fe	4.3	0.2296	ns	-	1.5	0.4719	ns	-
K	9.0	0.0290	**	22.8	1.2	0.5525	ns	-
La	15.5	0.0015	***	23.9	6.0	0.0495	**	44.8
Li	25.4	0.0000	****	26.8	16.4	0.0003	****	28.0
Mg	13.0	0.0045	***	44.1	5.7	0.0565	*	53.9
Mn	24.1	0.0000	****	26.1	15.5	0.0004	****	27.2
Na	24.3	0.0000	****	52.2	21.4	0.0000	****	60.8
Ni	11.7	0.0083	***	21.7	7.4	0.0250	**	28.0
P	103.2	0.0000	****	45.6	101.8	0.0000	****	62.9
Pb	26.3	0.0000	****	27.9	21.8	0.0000	****	39.7
Sr	17.6	0.0005	****	21.7	11.4	0.0034	***	26.3
Ti	10.8	0.0129	**	26.5	9.9	0.0071	***	31.5
V	11.0	0.0115	**	21.0	0.9	0.6395	ns	-
Zn	14.1	0.0027	***	23.5	4.8	0.0905	*	40.1
TOC	145.3	0.0000	****	47.8	127.5	0.0000	****	74.1

Table 37 − Results of the stepwise discriminant function analysis (DFA) as indicated by the Wilks' Lambda values using three and four sediment sources in Guaporé catchment.

Step	Fingerprint property selected	Wilks' Lambda	*p* to remove	Cumulative % of source type samples correctly classified
DFA – 4 sediment sources				
1	P	0.6748	0.0E+00	45.6
2	Al	0.4942	6.9E-11	54.4
3	Ni	0.4610	8.1E-05	57.7
4	Cr	0.4300	9.8E-05	58.5
5	V	0.4052	5.3E-04	61.8
6	Co	0.3743	1.1E-02	65.8
7	Mn	0.3616	2.8E-02	66.9
DFA – 3 sediment sources				
1	P	0.6184	0.0E+00	62.9
2	Al	0.4587	4.6E-09	68.1
3	Cr	0.4489	2.8E-04	68.1
4	Ni	0.4048	1.2E-02	73.3
5	Co	0.3722	3.4E-02	78.4
6	La	0.3628	5.7E-02	78.9
7	Mn	0.3537	6.0E-02	80.2

Table 38 − Discriminant function analysis (DFA) output in Guaporé catchment.

DFA parameters	4 sediment sources	3 sediment sources
Wilks' Lambda	0.3616	0.3537
Variance explained by the variables (%)	63.8	64.6
Degrees of freedom	21;752	14;446
$F_{calculated}$	15.24	21.71
$F_{critical}$	1.57	1.71
p-value	<0.00001	<0.00001
F-values		
Degrees of freedom	7;262	7;223
$F_{critical}$	2.0	2.1
Unpaved roads vs. Stream channels	14.2	13.9
Crop fields vs. Stream channels	13.3	15.4
Grasslands vs. Stream channels	6.6	-
Unpaved roads vs. Crop fields	34.3	35.2
Unpaved roads vs. Grasslands	17.7	-
Crop fields vs. Grasslands	6.3	-
p-levels		
Unpaved roads vs. Stream channels	1.1E-15	6.4E-15
Crop fields vs. Stream channels	1.2E-14	2.1E-16
Grasslands vs. Stream channels	3.2E-07	-
Unpaved roads vs. Crop fields	0.0E+00	0.0E+00
Unpaved roads vs. Grasslands	3.7E-19	-
Crop fields vs. Grasslands	7.6E-07	-
Squared Mahalanobis distances		
Unpaved roads vs. Stream channels	4.6	4.5
Crop fields vs. Stream channels	3.1	3.6
Grasslands vs. Stream channels	2.4	-
Unpaved roads vs. Crop fields	6.6	6.8
Unpaved roads vs. Grasslands	5.6	-
Crop fields vs. Grasslands	1.4	-
Source type samples classified correctly (%)		
Unpaved roads	75.0	90.0
Crop fields	70.6	74.5
Stream channels	67.4	79.4
Grasslands	52.5	-
Total	66.9	80.2

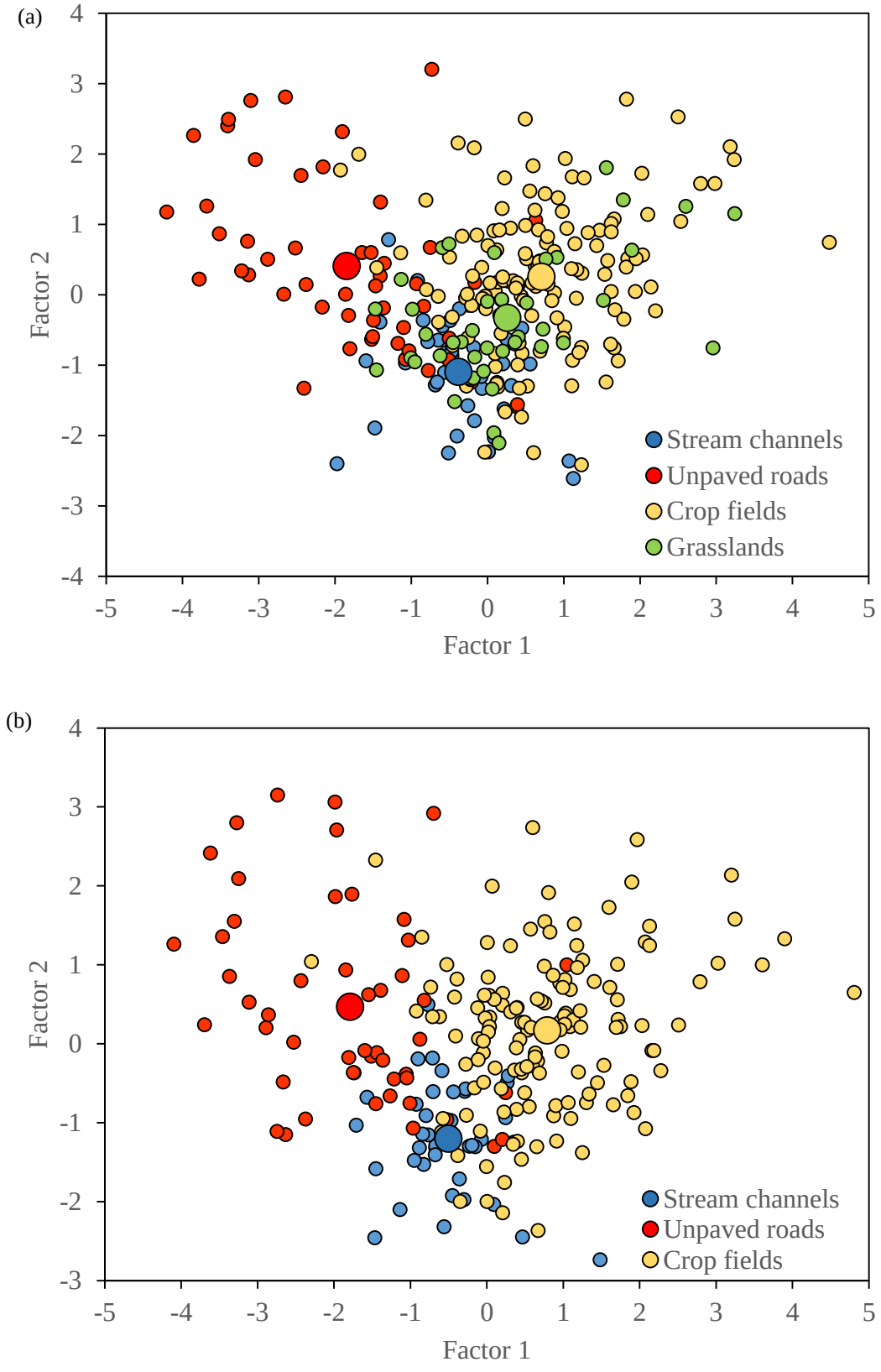

Figure 57 − Two-dimensional scatter plot of the first and second discriminant functions from stepwise discriminant function analysis (DFA) using four (a) and three (b) sediment sources from Guaporé catchment. Larger symbols represents the centroids of each source.

6.4.2 Source apportionment

Suspended sediment yield at the watershed outlet varied throughout the study period (Figure 58k). The monthly suspended sediment yield was correlated to the total amount of rainfall (r = 0.567, p=0.001). Contrary to Conceição catchment, results indicate that the relative source contributions was not influenced by the sediment sampling strategy. Furthermore, no clear trend of seasonal variation in source apportionment was observed at the sampling sites. Nevertheless, the contribution of sediment sources varied between sediment sampling sites in Guaporé catchment (Figure 58, Figure 59, and Figure 60), as well as during the storm-events (Figure 61).

Suspended sediment samples collected at varying intervals along the rising and recession limb of the hydrograph of the floods investigated were taken only at site 10, in the catchment outlet. For both floods investigated, CF contribution was predominant in the rising limb of the hydrograph (Figure 61). In the recession limb, however, CF contribution decreased, while SC Figure 61a,b) and UR (Figure 62b) increased.

The sampling sites 1 and 7 showed sediment source ascriptions different from the other sites of the Guaporé catchment (Figure 58, Figure 59, and Figure 60). As shown in Figure 62, the importance of SC contribution increased following as the order: site 1 > site 7 > rest of Guaporé catchment (sites 2, 3, 4, 5, 6, 8, 9, and 10), delivering 78±20, 42±31, and 10±18% of suspended sediment to the river, respectively. In contrary, CF contribution increased in the reverse order (21±21, 52±33, and 88±19% for site 1, site 7, and the rest of Guaporé catchment, respectively). The UR, however, provided a very low contribution of sediment to the river in the entire catchment (2±6).

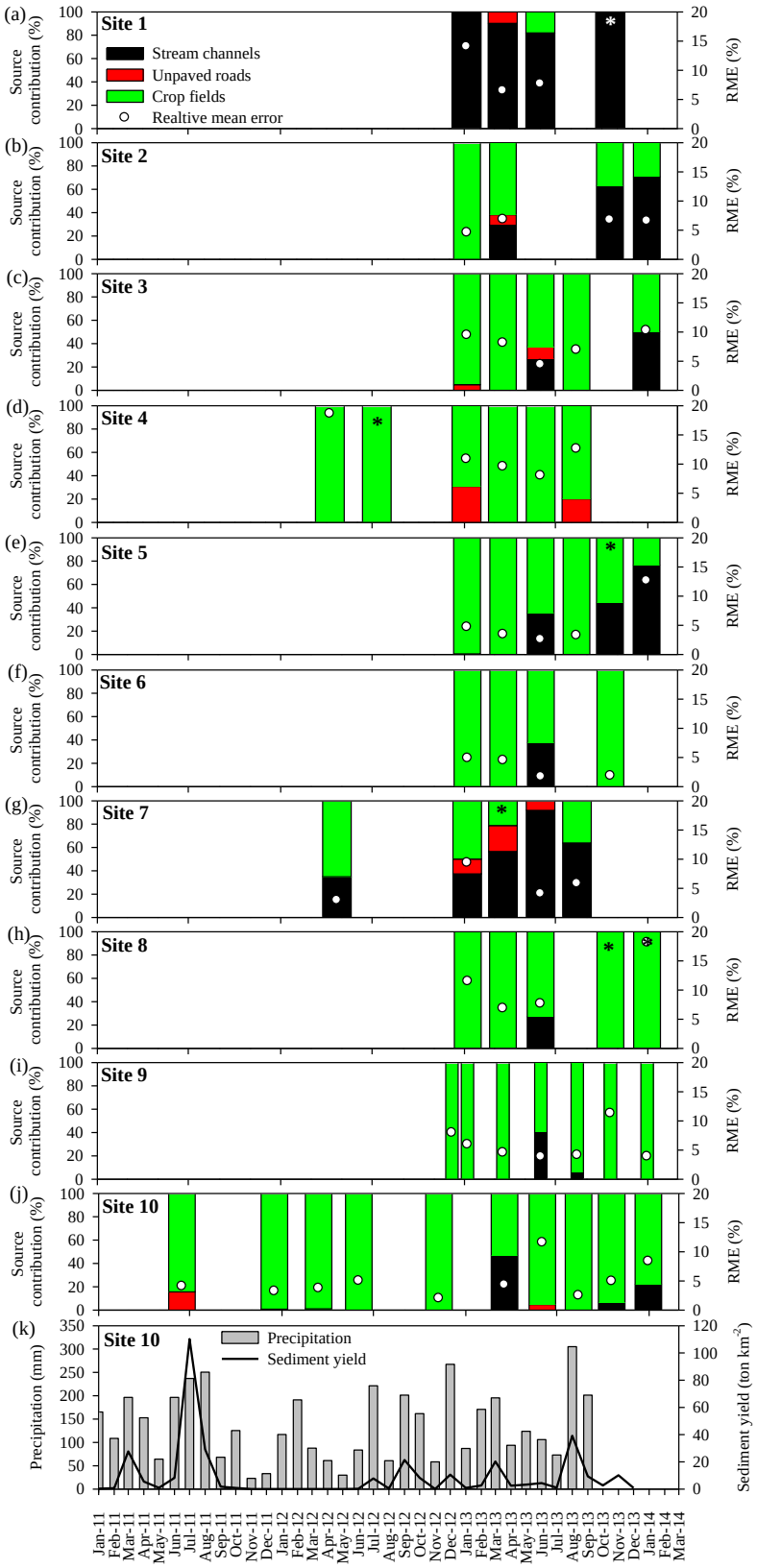

Figure 58 − Spatial and temporal variation in source contributions for suspended sediment samples collected with time-integrate samplers in Guaporé catchment (a, b, c, d, e, f, g, h, I, j), and records of monthly precipitation and sediment yield at the catchment outlet (k). Asterisk indicate relative mean error for prediction higher than 20%.

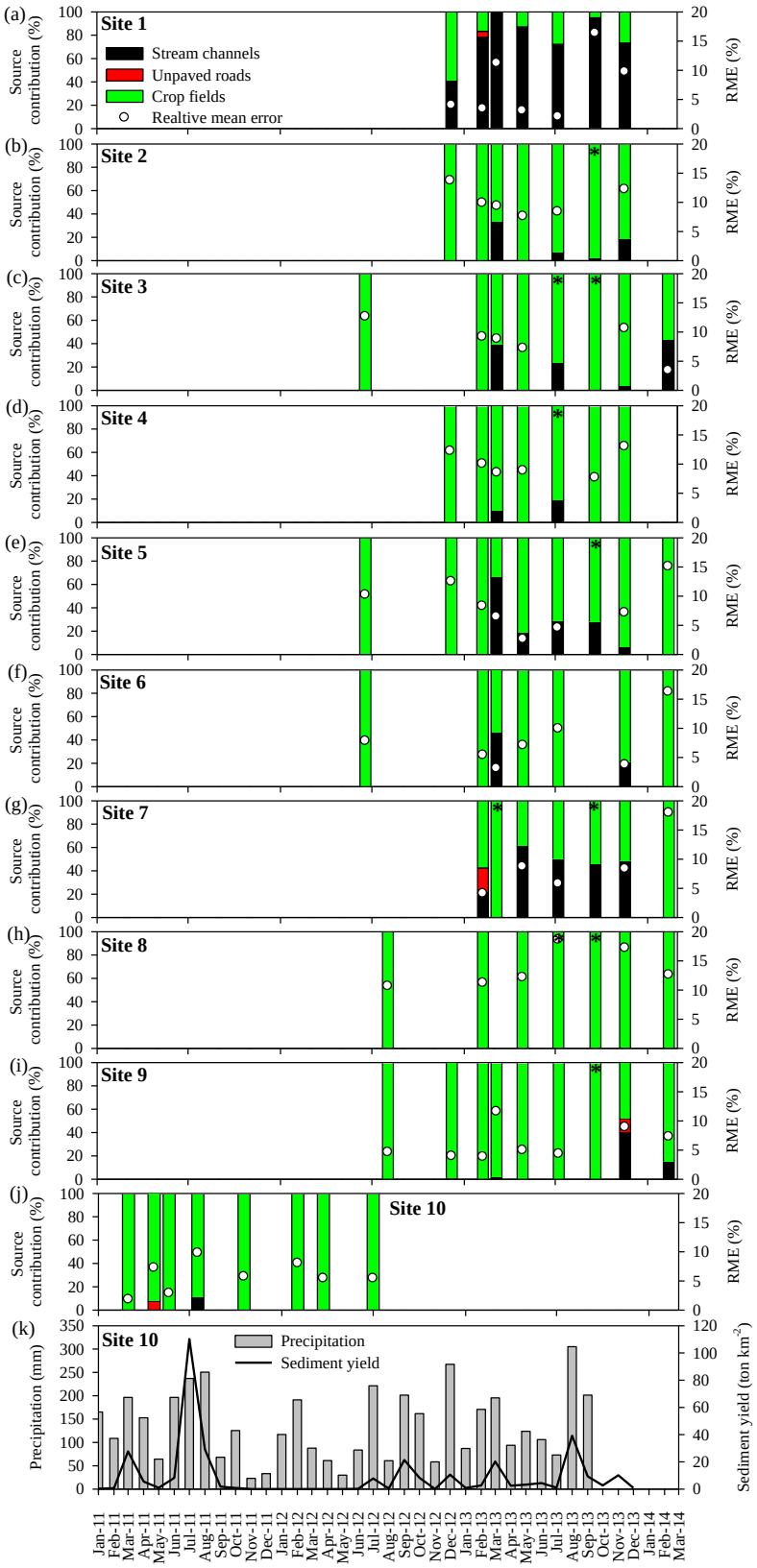

Figure 59 − Spatial and temporal variation in source contributions for fine-bed sediment samples collected in Guaporé catchment (a, b, c, d, e, f, g, h, I, j), and records of monthly precipitation and sediment yield at the catchment outlet (k). Asterisk indicate relative mean error for prediction higher than 20%.

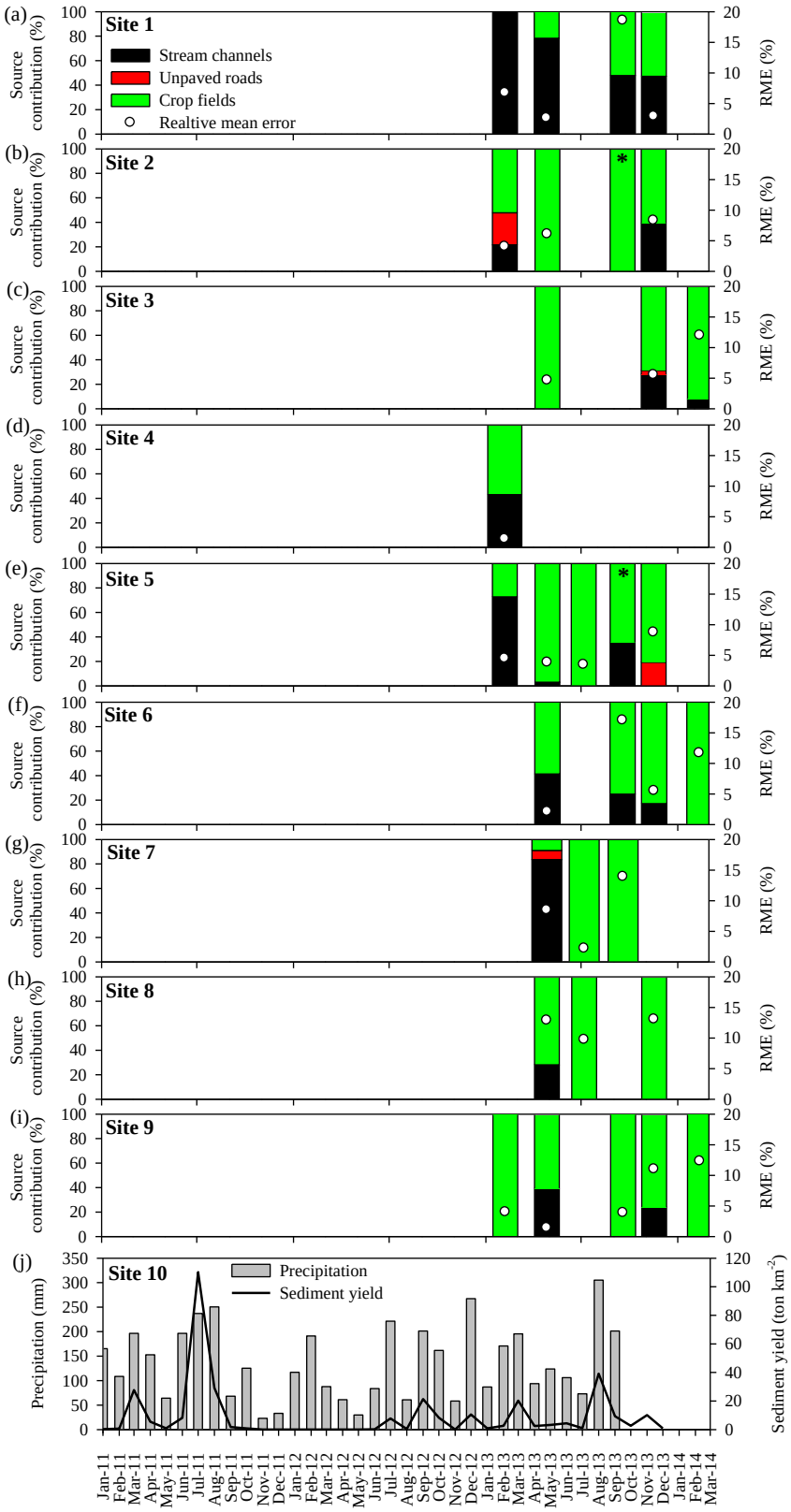

Figure 60 − Spatial and temporal variation in source contributions for storm-event suspended sediment samples collected with US-U59 in Guaporé catchment (a, b, c, d, e, f, g, h, I), and records of monthly precipitation and sediment yield at the catchment outlet (j). Asterisk indicate relative mean error for prediction higher than 20%.

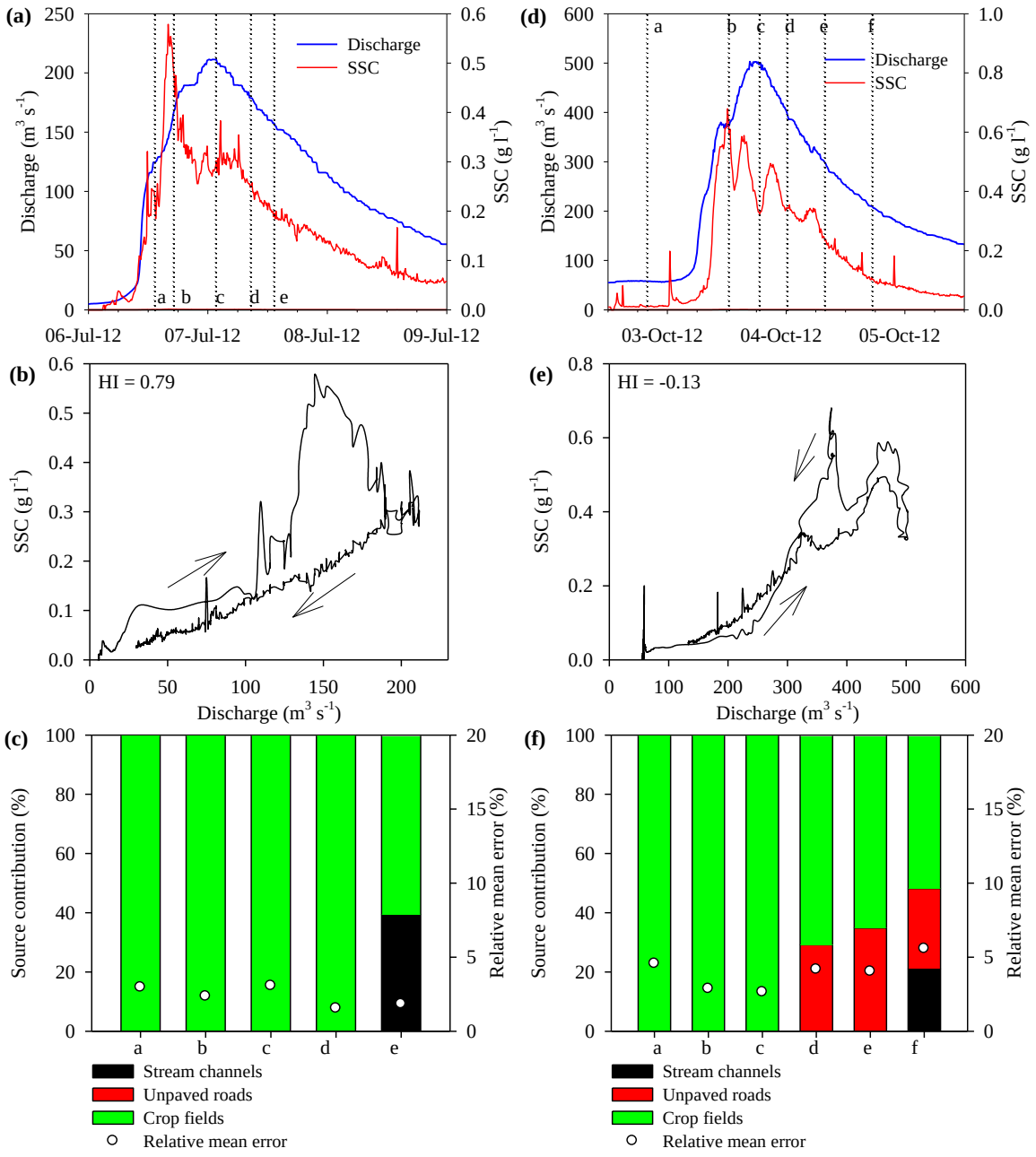

Figure 61 – Records of precipitation, discharge, suspended sediment concentration (SSC), hysteresis pattern, and the sediment source contribution during the floods that occurred on 6 July 2012 (a, b, c) and 2 October 2012 (d, e, f) in Guaporé catchment.

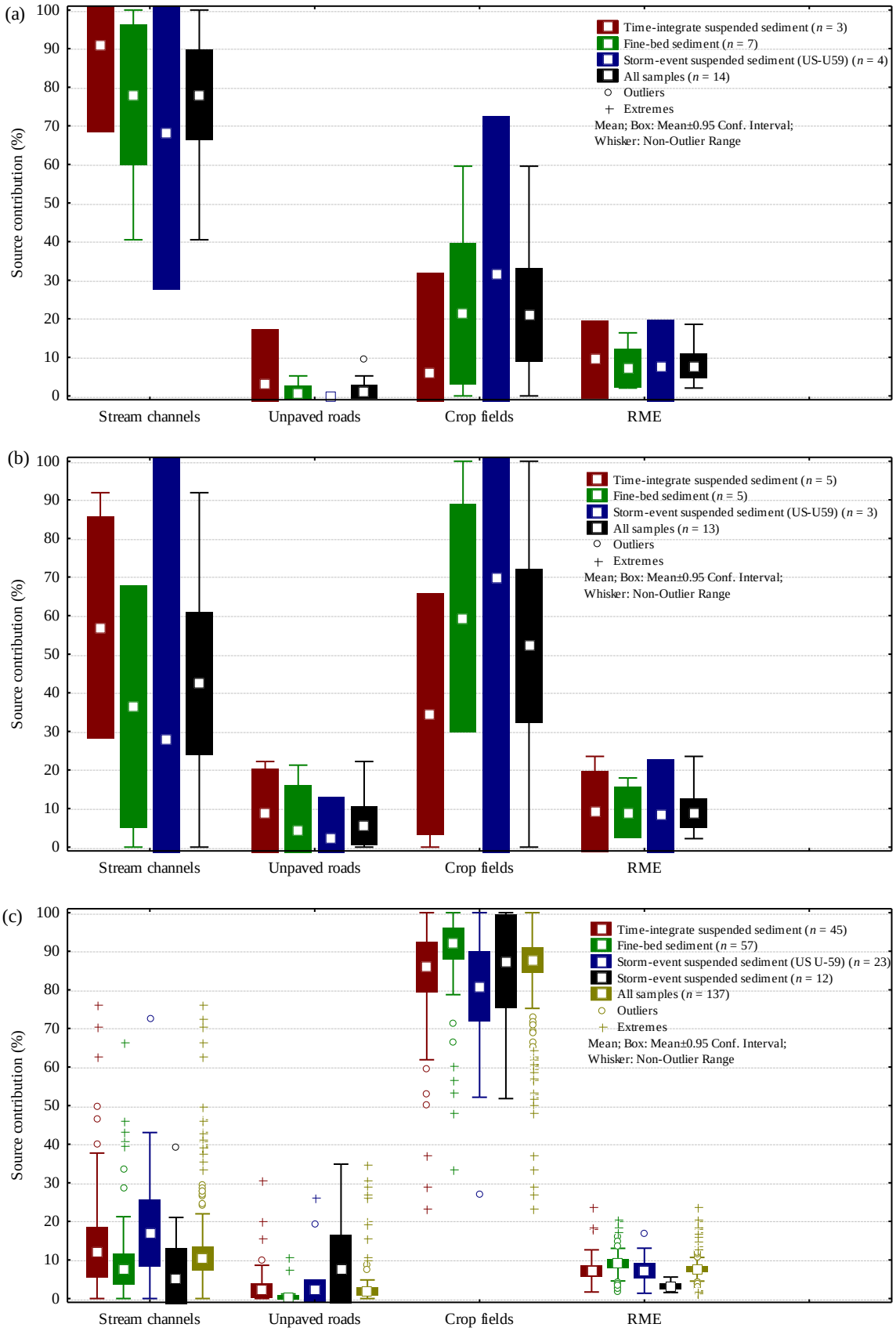

Figure 62 – Box plot of the sediment source contribution for different sediment sampling strategy for (a) site 1, (b) site 7, and (c) the others monitored points in Guaporé catchment (sites 2, 3, 4, 5, 6, 8, 9, and 10).

6.5 Specific sediment yield of cropland in agricultural catchments from Southern Brazil

Specific sediment yield (SSY) of croplands in the study catchments was estimated based on sediment yields estimated in previous studies (DIDONÉ et al., 2014; MINELLA; WALLING; MERTEN, 2014; PELLEGRINI A., 2013). In order to compare the results observed in the five catchments, the calculation was performed using only the results of sources apportionment of suspended sediment sampled during storm-events at catchment outlet, as it was the only common sampling technique applied in all five catchments (Figure 63). Figure 63 shows that crop fields were the main sediment source in the large catchments and in Arvorezinha catchment, and a significant contribution of unpaved roads, especially in the small catchments. Table 39 display the parameters used to calculate SSY of cropland. SSY of cropland in the catchments from Júlio de Castilhos was much lower than in the others (Table 39). The highest SSY of cropland was estimated for crop fields from Guaporé catchment, which were about 1.8 and 3.0 times higher than the SSY of crop fields in Arvorezinha and Conceição catchments, respectively.

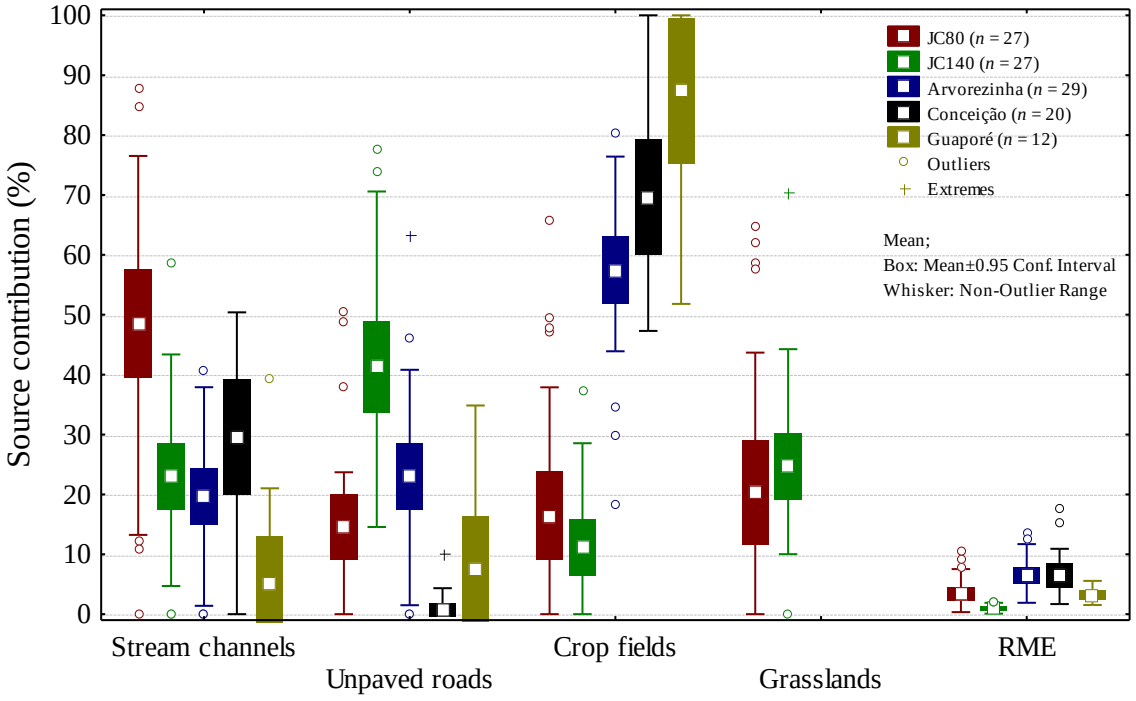

Figure 63 – Comparison of source contributions in suspended sediment samples collected during floods in the five study catchments.

Table 39 – Parameters for calculation of sediment supply from cropland yield (t km^{-2} of cropland yr^{-1}) in agricultural catchments from Southern Brazil. SD, standard deviation. RME, relative mean error.

Catchment	Year	Total sediment yield	Total area	Crop fields area		Crop fields contribution (%)				Specific sediment yield of crop fields
		t km^{-2} yr^{-1}	km^2	%	km^2	Mean	SD	RME	*n*	t km^{-2} yr^{-1}
JC80	2011-2012[a]	24.6	0.802	64.0	0.51	16.5	18.7	3.4	27	6.3
	2011	32.4								8.3
	2012	16.8								4.3
JC140	2011-2012[a]	66.7	1.426	64.7	0.92	11.1	11.8	1.0	27	11.4
	2011	89.1								15.3
	2012	44.3								7.6
Arvorezinha	2002-2011[b]	156.0	1.190	40.0	0.48	57.4	15.0	6.4	29	223.8
	2010	293.0								420.4
	2011	128.0								183.7
Conceição	2003-2012[c]	139.7	804.30	73.1	587.94	68.1	19.9	6.0	20	130.1
	2011	242.0								225.4
	2012	41.1								38.3
Guaporé	2003-2012[c]	139.8	2031.91	30.9	628.87	87.4	19.1	3.2	12	394.6
	2011	390.2								1101.5
	2012	158.7								447.9

[a] Average of 2 years records from 2011 to 2012 (PELLEGRINI A., 2013)
[b] Average of 10 years records from 2002 to 2011 (MINELLA; WALLING; MERTEN, 2014)
[c] Estimative of 2 years records from 2011 to 2012 extended to 10 years series by the use of a discharge rating curve (DIDONÉ et al., 2014)

7 DISCUSSION

Contrary to the results section, the discussion was not organized separated by catchment. It was constructed around broader topics encompassing all the study catchments that are representative of the main geographical regions of the state of Rio Grande do Sul where environmental problems, especially those related to water erosion, are widespread in agricultural catchments. To this end, I first present some insights related to the selection of geochemical tracers and sediment source discrimination. Then, I discuss the applicability of spectrometry techniques for fingerprinting sediment sources based on the preliminary study conducted in Arvorezinha catchment. I also discussed the inter- and intra-storm variation in source contributions for the five study catchments. Finally, while in the last part of the discussion section, I provide an overview of sediment source contributions in agricultural catchments from Southern Brazil.

7.1 Insights on source discrimination and selection of geochemical tracers

Table 40 and Table 41 were built in order to facilitate the discussion regarding the selection of geochemical tracers. These tables summarize results from Table 11, Table 12, Table 23, Table 25, Table 26, Table 27, Table 30, Table 31, Table 32, Table 35, Table 36, and Table 37, which indicate the ability of individual geochemical fingerprints to distinguish between sediment sources based on sediment source range test, the Kruskal−Wallis *H*-test, and discriminant function analysis (DFA) in the five study catchments.

Table 40 – Number of catchments where each tracer passed the KW-test before and after source range test, number of catchments where concentration of each tracer was higher or lower than source range, number of catchments where each tracer was selected by DFA, and estimative of tracer conservativeness.

Geochemical tracer	Numer of catchment where each tracer passed in KW-test before source range test	Number of catchments where concentration of each tracer was higher than source range	Number of catchments where concentration of each tracer was lower than source range	Conservativeness (% of catchments where tracers fits into source range)	Numer of catchment where each tracer passed in KW-test after source range test	Number of catchments where each tracer was selected by DFA
K	3	3	2	0	0	0
Na	5	3	2	0	0	0
TOC	5	4	1	0	0	0
Ca	3	4	0	20	1	0
Be	4	4	0	20	1	1
Pb	2	0	2	60	0	0
Ba	5	2	0	60	1	1
Mg	4	2	0	60	2	0
Sr	5	2	0	60	3	0
Li	5	1	1	60	3	1
Ti	5	2	0	60	3	1
P	5	2	0	60	3	3
Al	4	0	1	80	3	2
Mn	4	1	0	80	3	2
Ni	3	1	0	80	3	3
Fe	4	0	1	80	4	1
Zn	5	1	0	80	4	2
Cu	3	0	0	100	3	1
V	3	0	0	100	3	1
La	4	0	0	100	4	2
Co	4	0	0	100	4	3
Cr	5	0	0	100	5	3

Table 41 – Summary of the ability of individual geochemical fingerprints to distinguish between sediment sources based on sediment source range-test, the Kruskal−Wallis H-test, and discriminant function analysis (DFA) in the five catchments studied. In the colour scale, the greener, the greater the potential for discrimination, while the redder, the lower the potential for discrimination.

Number of tracers	Catchment									
	Arvorezinha		JC80		JC140		Conceição		Guaporé	
Area	1.19 km^2		0.802 km^2		1.426 km^2		804.3 km^2		2,031.9 km^2	
Number of sources	Three		Four		Four		Three		Three	
Higher than source range - values indicate % of source samples correctly classified by each tracer										
1	Ca	52.5	Ba	26.7	Be	83.3	Ca	50.4	Ba	33.2
2	Be	62.5	Be	50.0	P	46.7	K	46.8	Be	22.4
3	Li	57.5	Ca	53.3	TOC	63.3	Mg	41.8	Ca	45.7
4	Ni	55.0	Mn	40.0			Na	45.4	K	25.9
5	TOC	60.0	P	63.3			Sr	51.1	Mg	53.9
6			Sr	53.3			Ti	41.1	Na	60.8
7			TOC	73.3					Sr	26.3
8									Ti	31.5
9									TOC	74.1
10									Zn	40.1
Lower than source range - values indicate % of source samples correctly classified by each tracer										
1			Na	50.0	Na	73.3	Al	53.2	Fe	22.4
2			K	40.0	K	56.7	Li	42.6	Pb	39.7
3							Pb	35.5		
4							TOC	73.0		
Failed in Kruskal-Wallis H-test - values indicate % of source samples correctly classified by each tracer										
1	B	52.5	La	43.3	Ca	26.7	Cu	29.8	Cu	21.6
2	Co	50.0	Mg	36.7	Pb	50.0	Ni	24.1	V	42.7
3	K	55.0	Pb	30.0						
4	Mn	50.0								
5	Pb	47.5								
6	V	55.0								
Passed in Kruskal-Wallis H-test - values indicate % of source samples correctly classified by each tracer										
1	Ag	77.5	Al	30.0	Al	50.0	Ba	45.4	Al	43.1
2	As	72.5	Co	53.3	Ba	50.0	Be	34.8	Co	22.8
3	Ba	57.5	Cr	46.7	Co	63.3	Co	45.4	Cr	22.4
4	Cd	85.0	Cu	66.7	Cr	56.7	Cr	36.2	La	44.8
5	Cr	55.0	Fe	60.0	Cu	43.3	Fe	41.8	Li	28.0
6	Cu	65.0	Li	40.0	Fe	53.3	La	31.2	Mn	27.2
7	Fe	77.5	Ni	56.7	La	43.3	Mn	58.2	Ni	28.0
8	La	75.0	Ti	53.3	Li	53.3	P	62.4	P	62.9
9	Mg	65.0	V	56.7	Mg	30.0	V	48.2		
10	Mo	80.0	Zn	50.0	Mn	53.3	Zn	32.6		
11	Na	52.5			Ni	60.0				
12	P	72.5			Sr	43.3				
13	Sb	67.5			Ti	33.3				
14	Se	55.0			V	46.7				
15	Sr	55.0			Zn	60.0				
16	Ti	55.0								
17	Tl	60.0								
18	Zn	65.0								
	Max	85.0	Max	66.7	Max	63.3	Max	62.4	Max	62.9
	Min	52.5	Min	30.0	Min	30.0	Min	31.2	Min	22.4
Selected by DFA - values indicate cumulative % of source samples correctly classified										
1	Mo	72.5	Cu	66.7	Zn	60.0	P	62.4	P	62.9
2	Ag	97.5	Al	66.7	Li	80.0	La	66.7	Al	68.1
3	P	100.0	Ti	90.0	Ni	83.3	V	76.6	Cr	68.1
4	Fe	100.0	Cr	90.0	Co	93.3	Mn	81.6	Ni	73.3
5	As	100.0	Zn	93.3			Be	83.0	Co	78.4
6	Cr	100.0	Ni	96.7			Ba	84.4	La	78.9
7			Co	96.7					Mn	80.2

7.1.1 Understanding origin of geochemical tracers

In this section, an effort was made to try to identify the origin of elements statistically selected as relevant geochemical tracers. Many elements did not show the same trend for all catchments. Still, for some elements it is possible to establish the physicochemical basis for discrimination of sediment sources.

Phosphorus was a good tracer for crop field source in the five study catchments (Table 11, Table 25, Table 26, Table 31, and Table 36). P is one of the most limiting nutrients in highly weathered sub-tropical soils. Therefore, to achieve high crop yields phosphate fertilizers are frequently applied to these soils, which leads to an increase in total P concentration in cropland topsoil (CALEGARI et al., 2013; TIECHER; RHEINHEIMER; CALEGARI, 2012; TIECHER et al., 2012). Subsequently, intensive agriculture results in high P content in fluvial suspended sediment (BALLANTINE et al., 2008, 2009; PELLEGRINI J. et al., 2010; POULENARD; DORIOZ; ELSASS, 2008). Thereby, P can be considered as a tracer of human activities such as agriculture. Potassium is another element that is widely used as fertilizer in crop fields from Southern Brazil. However, because soils have considerable total K content, especially younger soils (MEDEIROS et al., 2014) that contain large amounts of less weathered minerals such as feldspars ($KAlSi_3O_8$), which have high K content, this element has a lower discrimination power than P as a tracer of cropland.

As expected, TOC content was higher in grasslands and crop fields than in unpaved roads and stream channels in all study catchments (Table 11, Table 25, Table 26, Table 31, and Table 36) (DE BROGNIEZ et al., 2014). These results highlights the potential use of TOC as a tracer to discriminate topsoil sources, i.e. grasslands and crop fields, and subsuperficial sources, i.e. unpaved roads and stream channels.

Cu was a conservative tracer, but only effective for discriminating sediment sources in the small catchments (Table 40 and Table 41). In the larger catchments the use of Cu as a tracer property was probably hampered by the higher variability in this metal content in parent material and soil types found in these catchments. For Arvorezinha and Júlio de Castilhos catchments, however, Cu content was a good tracer for UR. In these catchments, UR are composed by subsurface horizons of the soil due to rectification of roads and erosion over the years. The higher Cu content in UR sources is in agreement with the study of Udo; Ogunwale; Fagbami (2008) who found a higher content of total Cu in the subsoils than in the surface

horizons in 11 Nigerian soil profiles formed from various parent materials including coastal plain sands, shales, basalt, granite and banded gneiss.

In Arvorezinha catchment, some extra tracers were evaluated and among them, Ag, As, and Mo were kept until the final DFA selection. The Ag content in crop fields and stream channel in Arvorezinha catchment was higher than in the unpaved roads. Published data concerning Ag in soils are rare. Nonetheless, Ag is highly immobile in the soil environment and is strongly adsorbed to organic matter (SETTIMIO et al., 2014). Thus, the higher content of Ag in these sediment sources seems to be related to their higher organic carbon content. Mo and As enrichment in crop fields from Arvorezinha catchment may be due to the repeated micronutrient and phosphate fertilizers applications (CHARTER; TABATABAI; SCHAFER, 1995). Estimations show that almost 60% of the As present in the environment has an anthropogenic origin (NRIAGU, 1989), as phosphate and micronutrient fertilizers (CHEN et al., 2008) and pesticides (WALSH; SUMNER; KEENEY, 1977).

Except for TOC, P, and Cu, there is no obvious consistency in the absolute performance for the other geochemical tracers. Generally, they did not show the same trend for all study catchments. For example, Cr was conservative and selected by Kruskal-Wallis H-test in all five study catchments, and was selected by DFA in three of them (Table 40). According to Pils; Karathanasis; Mueller (2004), total Cr content tend to increase with soil depth. Higher Cr content would therefore be expected in subsuperficial sources (i.e. unpaved roads and stream channels) compared to topsoil sources (i.e. grasslands and crop fields). This was observed in Arvorezinha and Guaporé catchments. In Conceição catchment, however, the lowest Cr content was found in unpaved roads, whereas for Júlio de Castilhos catchments the highest Cr content was found in crop fields. In the same way, the content of Co, Fe, Mn, V, and Ti in unpaved roads was the lowest in sediment sources of the larger catchments (Guaporé and Conceição), whereas in the smaller catchments (Arvorezinha, JC80, and JC140) the UR was the sediment source with the highest concentration of these transition metals. No plausible explanation could be found for these findings. According to Davis; Fox (2009), while organic tracers tend to discriminate sediment sources through differences in soil organic matter cycling and radionuclide tracers tend to discriminate sediment sources through differences with depth, inorganic tracers have been less attributed to a specific soil-environmental process. In this regard, Haddadchi et al. (2013) warn that achieving discrimination among land use sources based on chemical elements such as rare earth elements or metals is poorly studied, and should be urgently addressed in future fingerprinting studies.

The wider adaptation of the fingerprinting technique as a management tool is hampered due to several reasons (MUKUNDAN et al., 2012). The main constrain relies in the choice of successful fingerprint properties, which is highly site-specific (COLLINS; WALLING, 2002). This is in agreement with our findings. The lack of general guidelines for the pre-selection of tracer properties able to discriminate sediment sources make the approach very time-consuming and costly. This is the main reason why recent studies have focused on robust, time-efficient, and cost-effective measurements methods to fingerprinting sediment samples, such as spectroscopy (BROSINSKY et al., 2014a, 2014b; EVRARD et al., 2013; LEGOUT et al., 2013; MARTÍNEZ-CARRERAS et al., 2010a, 2010b, 2010c; POULENARD et al., 2009, 2012; VERHEYEN et al., 2014).

7.1.2 Selecting geochemical tracers: conservativeness and individual potential for discrimination

The results of the statistical analysis remain in agreement with findings of Collins; Walling (2002). Results clearly demonstrate that no single geochemical tracer was capable of classifying 100% of the source material samples into the correct source categories for any of the study catchments. According to Walling (2013), although a single sediment property was used as the source fingerprint in some early investigations, subsequent work rapidly recognized that several fingerprint properties incorporated into a composite fingerprint are required in order to discriminate between several potential sources in order to provide reliable estimates of the relative contribution of those sources.

In order to estimate the conservativeness of each geochemical tracer, it was take into account the number of catchments where each geochemical tracer concentration in sediment samples laid between the geochemical concentrations ranges of the sources materials. Total organic carbon (TOC) was one of the best tracers in all the five catchments. TOC alone correctly classified more than 60% of source samples, ranging from 60.0% in Arvorezinha catchment to 74.1% in Conceição catchment. Indeed, some studies demonstrated that TOC might be used as a reliable and cost-effective alternative to ^{137}Cs for sediment fingerprinting. This assumption is based on TOC conservativeness in nature and because strong positive correlations between ^{137}C and TOC have been used in studies involving soil and soil organic carbon redistribution at the landscape scale (MUKUNDAN et al., 2012; RITCHIE; MCCARTY, 2003; RITCHIE et al.,

2007). For the five studied catchments, however, TOC content laid out of sediment source range for most sediment samples, highlighting its low conservativeness during the erosion processes. As stated by D'Haen; Verstraeten; Degryse (2012), organic material is subject to enrichment or depletion, leading to a severe impact on the conservativeness of TOC. Phosphorus also presented high potential to discriminate sediment sources in all catchments. However, P concentration in sediment samples from Júlio de Castilhos catchments were higher than the highest sediment source concentration. Nonetheless, for the other catchments, P was kept until the final DFA selection. P proved to be an excellent tracer for crop fields in agricultural catchments from Southern Brazil, but care should be taken to evaluate its conservativeness in the target catchment. Some fingerprinting studies have excluded organic carbon and phosphorus because these nutrients are generated within the stream environment via phytoplankton and macrophyte production (autochthonous), thereby rendering these tracers non-conservative (COOPER et al., 2015). Despite their potentially unconservative behavior during transport, the use of N, C, P, $\delta^{15}N$, and $\delta^{13}C$ to discriminate between sources among land uses was successful for most of the studies reviewed by Haddadchi et al. (2013) and Laceby et al. (2015).

As shown in Table 40, transition metals were the more conservative tracers in the studied catchments. Co, Cr, Cu, La, and V concentrations laid between the source range in all the five catchments, while, Al, Fe, Mn, Ni, and Zn concentrations in sediment samples laid between source range in four of these. In general, these transition metals were good tracers, especially Co, Cr, and Ni, which were kept until the final DFA selection in three catchments. Ti and Pb were the less conservative transition metals. Ti discriminated between sediment sources in all five catchments, whereas Pb was only effective in distinguishing sediment source in the larger ones (Conceição and Guaporé). However, in Conceição and Guaporé catchments, the sediment samples were enriched in Ti and depleted in Pb. In this context, only Ti was kept until the final DFA selection in PB80 catchment. Other transition metals such as Ag and Mo, and As (semi-metal) were only analyzed for Arvorezinha catchment. They showed conservativeness and good discriminate potential, and, thereupon, were selected by DFA. Altogether, 18 different geochemical tracers (Ag, Al, As, Ba, Be, Co, Cr, Cu, Fe, La, Li, Mn, Mo, Ni, P, Ti, V, and Zn) were selected at least for one catchment by DFA to estimate sediment sources in the linear mixed model, and in 80% of cases the tracer chosen was a transition metal. These results, therefore, point out the transition metals as the more suitable geochemical tracers to be used in agricultural catchments from Southern Brazil due to their conservativeness and their discrimination potential.

Alkaline metals, however, were the less conservative tracers. Despite they discriminated sediment sources in three and five catchments, as indicated by Kruskal−Wallis *H*-test before the source range-test, K and Na concentration in sediment samples, respectively, were always out of the source concentration range (Table 40). There was a depletion of K and Na in sediment samples from Júlio de Castilhos catchments (Table 25, Table 26), which have more sandy and coarser soil and sediments, whereas there was an enrichment of K and Na in the material collected in the other catchments (Table 30, Table 35), where soil and sediments are clay-sized. Alkaline earth metals also did not show good conservativeness. Be and Ca were able to discriminate sources in four and three catchments before applying the source range-test, but they were conservative for only one catchment each. Ba, Mg, and Sr were also good tracers in almost all the cases (except by Mg in JC80 catchment), but all of them were enriched in at least two catchments. Because of their low conservativeness despite a good discrimination potential, from all alkaline earth metals, only Ba and Be were kept until the final DFA selection, both in Conceição catchment (Table 40). Thus, despite the potential for discriminating sediment sources of alkaline metals and alkaline earth metals in some cases, these elements tend to be less conservative during the erosion process and should be avoided for fingerprinting sediment sources in agricultural catchments from Southern Brazil.

These findings highlight that sediment fingerprinting based on geochemical composition can be an extremely labor intensive exercise, which is often observed in other studies as well. For example, recently, Stone et al. (2014) evaluated the use of composite fingerprints to quantify sediment sources in a wildfire impacted landscape in Alberta, Canada. In total, they evaluated 60 potential tracers, including major elements (Al_2O_3,Fe_2O_3, MnO, MgO, CaO, Na_2O, K_2O, TiO_2, P_2O_5, Cr_2O_3, SiO_2) and loss on ignition (LOI) determined by X-rayfluorescence, organic C determined with Leco carbon analyzer, and concentrations of several elements (Al, As, Ba, Bi, Cd, Ce, Co, Cr, Cs, Cu, Dy, Er, Eu, Fe, Ga, Gd, Gd, Hf, Ho, In, K, La, Li, Mg, Mn, Mo, Na, Nd, Ni, Pb, Pd, Pr, Rb, Sb, Sc, Sm, Sn, Sr, Tb, Ti, Tl, U, V, Y, Yb, Zn, and Zr) determined using ICP-MS after aqua regia digestion. From these 60 tracers, 45 failed the mass conservation test and were therefore not included in either further statistical analysis or the numerical modeling. Only Ag, As, B, C-organic, Er, Eu, Ga, Hg, Li, Na_2O, Nb, Pr, Sc, Th, and Y were taken forward for statistical analysis for source discrimination, and from this set of properties, four failed in the KW-*H* test (As, B, Nb, and Th).

Given these difficulties, a key line of research for the future is the development of tracers requiring inexpensive and rapid analysis approaches that are able to process quickly a large number of samples (GUZMÁN et al., 2013). According to Mukundan et al. (2012), another

possible alternative to conducting sediment source studies in each and every watershed could be to develop tracer signature libraries of potential sediment source types (e.g., pastures, forests, stream-banks, etc.) for each ecologically and geographically defined region (ecoregion) to be investigated. In that case, sediment samples could be evaluated by comparing it with the library of reference values for tracers from potential sediment sources analysed in the same ecoregion. The authors indicate that tracers such as ^{137}Cs and $\delta^{15}N$ could be good candidates for such libraries. However, these tracers are still inaccessible to most research groups in Southern Brazil.

7.1.3 Discriminating sediment sources: relationship with catchment size and number of sources studied

For Arvorezinha catchment, where only three sources were studied in a total area of 1,19 km^2, the range of samples correctly classified by each geochemical tracers passed the Kruskal−Wallis *H*-test (52.5−85.0%) were far higher than for the other catchments (22.4−66.7%). Moreover, considering the final set of tracers selected by DFA, for catchments with the same number of sediment sources, there is a decrease of cumulative source samples correctly classified with increasing catchment size (three source catchments: Arvorezinha = 100% < Conceição = 84.4% < Guaporé = 80.2%; four source catchments: JC80 = 96.7% < JC140 = 93.3%). In addition, for catchments of approximately similar size, there is a decrease of cumulative source samples correctly classified with increasing number of sediment sources (Arvorezinha = 100% > JC80 = 96.7% and JC140 = 93.3%). These trends demonstrate that in general, the smaller the catchment and the lower the number of sources taken into account, the more effective the tracers were to discriminate sediment sources (Table 40 and Table 41).

Discrimination of grasslands was only possible in the small catchments from Júlio de Castilhos. In the large catchments (Conceição and Guaporé), the Mahalanobis distances were significant but very short among GR, CF, and SC. The substantial overlapping of these sources (Figure 51a, Figure 57a) hampered their discrimination, resulting in a low proportion of GR samples correctly classified. A possible explanation for this may be the lower sampling density in Guaporé and Conceição catchments (0.15 and 0.23 samples per km^{-2}, respectively) compared to the Júlio de Castilhos catchments (ranging from 21 to 37 samples km^{-2}) (Table 6).

Furthermore, generally, plant uptake and fertilization leads to a formation of vertical gradient of nutrients, but soil plowing in conventional soil management systems homogenizes nutrient distribution up to 30 cm depth approximately, which could facilitate discrimination of CF and GR. However, a few years of cultivation under no-tillage system are enough to allow the formation of nutrient gradient in depth, especially for TOC and elements related to fertilization as P, K, Ca and Mg (CALEGARI et al., 2013). Such vertical distribution is also common for grasslands and forest due to uplift of soil nutrients by plants (JOBBÁGY; JACKSON, 2004). Thereby, for Southern Brazil conditions, GR and CF tend to present very similar geochemical composition, especially when CF are cultivated under no-tillage system, which represents more than 80% of the total cultivated area in the Northern part of Rio Grande do Sul State (DIDONÉ et al., 2014). Therefore, discrimination of GR and CF in Guaporé and Conceição catchments was not possible due to their similar geochemical composition, the high variability in soil types and lithology, and the low source sampling density (Figure 8, Figure 13, and Table 6), hampering tracer selection. In Júlio de Castilhos catchments, however, the lower variability of lithological material and soil types combined to the higher source sampling density, allowed to find a geochemical signature able to differentiate satisfactorily the CF and GR sources.

These results indicate that further studies are needed in Guaporé and Conceição catchments in order to find tracers able to discriminate topsoil sources, i.e. GR and CF. Recently, compound specific stable isotope (CSSI) analyses have been successfully used to trace crop-specific sediment sources in agricultural catchments (BLAKE et al., 2012). The $\delta^{13}C$ signatures of particle-associated fatty acids extracted from soil enabled sediment in streams to be linked back to fields under specific crop cover. The CSSI signature of plant-derived material is primarily determined by the plant carbon fixation pathway wherein C3 plants have been shown to exhibit a $\delta^{13}C$ range of −21 to −35‰ and C4 plants −9 to −20‰. However, it can be probably difficult to discriminate GR and CF in Guaporé and Conceição catchments because crop fields are alternately cultivated with corn (C4) and soybeans (C3). Furthermore, natural grasslands from Southern Brazil also present a similar problem. Such pastures include approximately 3000–4000 species of plants of which almost all the grass species are perennials, most C4 and few are C3 (warm and cool-season growth, respectively) (OVERBECK et al., 2007). Fallout radionuclide activities (^{137}Cs, ^{210}Pb, ^{7}Be) are commonly high in topsoil and very low in subsurface, and they frequently distinguish cultivated from uncultivated soils because radionuclides are generally mixed throughout the ploughed layer (HADDADCHI et al., 2013).

In soils under no-tillage, however, it is possible that these tracers are not effective in discriminating the topsoil sources as GR and CF.

7.2 The suitability of spectrometry analyses for fingerprinting sediment sources

7.2.1 Alternative fingerprinting methods based on spectroscopy-PLSR models

Despite the lack of correlation in some cases, the alternative methods based on spectroscopy-PLSR models remained in agreement with contributions derived from classical fingerprinting based on geochemical composition, especially the NIR-PLSR approach (Figure 38 and Figure 39). As shown in Figure 38, CF was the main source of sediments in Arvorezinha catchment for all spectroscopy-PLSR models. Moreover, the low prediction errors of spectroscopy-PLSR models (±2.9, ±4.6, and ±6.6% on average for NIR, MIR, and UV-VIS PLSR models – Table 21) demonstrates that despite the do not provide identical source apportionment, the use of spectral-based fingerprinting can be as precise as the geochemical tracers for this catchment. The lack of correlation between conventional and alternative approaches demonstrated that the methods explain different sediment properties, and that they are, therefore, complementary approaches.

Considering the low prediction errors derived from spectroscopy-PLSR models, the slight sub- and over-estimation of the three sediment source contributions in some cases (102±6% on average - Table 21) can be considered irrelevant, especially because the PLSR models were independent, i.e., each model estimates the proportion of one source, independently of the two others. Therefore, the spectroscopy-PLSR models can be considered more robust than the mixed linear model, which uses two boundary conditions (see Equations 5 and 6). Furthermore, it is important to take into account the advantages of the procedure (i.e. low cost and rapidity) and the facilitate the achievement of numerous measurements and hence high-resolution predictions essential for better understanding the behavior of catchments which exhibit highly variable hydro-sedimentary dynamics (LEGOUT et al., 2013).

The differences in the results obtained by conventional and alternative methods are due to the nature of the variables used in each case, which are not mandatorily correlated. The differences found between the approaches seems to create a perspective issue (Figure 64).

However, the relevant information is that the magnitude of predictions was very similar. Spectroscopic methods are based on organic and mineral bounds that cannot be accessed by analyzing the geochemical composition, and vice versa. Furthermore, according to Legout et al. (2013), the differences between these fingerprinting techniques may be also due to two additional reasons. First, due to the ability of each method to consider the variability of the fingerprinting properties in the source materials. Second, due to the potential alteration of the selected fingerprinting properties during the transit of particles in the watershed, recognizing that different techniques are more or less sensitive to these alterations depending on the properties selected. As the average contribution of the sediment sources was very similar between conventional and alternative approaches, the best method to be used will depend on the infrastructure available in each laboratory.

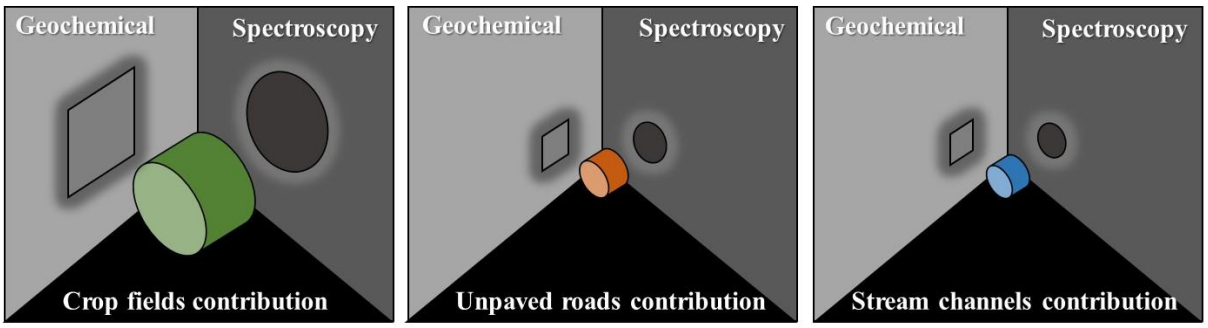

Figure 64 – Perspective issue of source apportionment obtained by geochemical composition approach and alternative method spectroscopy-PLSR models in Arvorezinha catchment.

It has been demonstrated that the signatures of different organic compounds in the mid-infrared region can be very useful by facilitating discrimination between the top soils (relatively rich in organic matter) and the deep horizons and gullies depleted in organic matter (EVRARD et al., 2013; POULENARD et al., 2009). However, depending on the situation, the high sensitivity of mid-infrared spectra to organic carbon content can also become a problem. In one of the catchments from Mexico studied by Evrard et al. (2013), the predictions of spectroscopic method greatly differed from the ones obtained with classical fingerprinting. The authors stated that probably a source of soluble organic matter delivered by anthropogenic activities (excess of cow dung) caused an enrichment of carbon in sediments, leading to an overestimation of the contribution of surface soil (the richest source in organic carbon).

The discrimination of sediment sources using NIR, MIR, and UV-VIS spectroscopy was possible due to differences in content (*Table 11*) and nature (Figure 30) of organic carbon, as well as differences in mineral composition, i.e., proportion of the different clay minerals (Figure 29) and the proportion of Fe-oxides contents (proportion of goethite and hematite - Figure 27 and Table 19).

In Arvorezinha catchment, UR are basically composed by subsurface horizons of the soil due to rectification of roads and erosion over the years. Therefore, UR has lower organic carbon content compared to CF and SC, leading to a better discrimination of this source from CF and SC (see Mahalanobis distances in Figure 21). Regarding to UV-VIS spectroscopy, the lower molecular weight and lower degree of condensation of the aromatic rings indicated by higher E4/E6 ratio for UR compared to CF and SC (Table 19) are in agreement with the results obtained by Py-GC/MS analyses (Figure 30). Py-GC/MS analyses demonstrate a higher proportion of proteins and alkyl benzenes, and a lower proportion of polysaccharides, amino sugars, and amino acids in UR compared to SC and CF.

The higher abundance of clay minerals 2:1 in the UR samples is due to the fact that most of the soils in Arvorezinha catchment are Acrisols (~57% of the total area). These soils are characterized by the migration of clay and the formation of a clay-enriched textural B subsurface horizon. It resulted in the higher abundance of 2:1 clay minerals in UR due to the selective eluviation of smectite compared to other sources, which also contributed to the better discrimination of UR samples. The correlation of UR contribution estimated by MIR-PLSR models demonstrate that the mid-infrared signature was clearly influenced by the low organic carbon content originating from the deep horizons, as the UR materials, and it led to UR predictions very similar between MIR-PLSR and geochemical composition (Figure 37).

Discrimination of CF and SC, however, was hampered due to their similar content and composition of organic carbon, generating a confusion effect on their predictions in the spectroscopic method. Even the molecular distribution of biopolymers is not efficient to discriminate them (Figure 30). Their discrimination was possible exclusively due to their differences in proportion of mineral components, such as the higher proportion of Qz and the lower content of 2:1 clay minerals in CF compared to SC. This result is in agreement with previous statements about the distribution of the mineral groups in the soil profile of Acrisols, which present higher contents of sand and gravels and lower content of clay in the topsoil compared to the subsoil. As CF represent a superficial source of sediments, and the SC are composed by a mixture of the soil profile (sampling was made taking soil from the whole stream wall because generally erosion occurs through bank collapse), their differentiation was possible

due to the differences in mineral component proportions. Lowland soils next to the water courses are in a biogeochemical environment were reactions of oxide reduction modify mineral composition. In this sense, the second-derivative curves of remission functions in the visible range (Table 19 and Figure 27) demonstrate an enrichment of hematite in the Fe-oxides pool in the order SC<CF<UR, which may have contributed to the discrimination between CF and SC using UV-VIS spectroscopy.

In studies carried out in catchment with very distinct mineralogies, a simple qualitative comparison of mid-infrared spectra proved to be a fast way to identify the predominant sediment sources. In Mexico, Evrard et al. (2013) have shown that the mid-infrared spectrum of Acrisols was characterized by the dominance of kaolinite in the clay fraction (bands at 3600–3700 cm^{-1}), whereas Andisol spectrum was characterized by gibbsite bands. In the French Alps, Poulenard et al. (2012) have shown that soils developed on gypsum substrates were characterized by absorption bands at 3500 cm^{-1} and between 2370 and 2060 cm^{-1}, corresponding to the presence of $CaSO_4$; whilst soils developed on molasses were characterized by absorption bands at 2430–2640 cm^{-1} corresponding to calcite ($CaCO_3$) and absorption bands at 3500–3700 cm^{-1} corresponding to aluminosilicates. However, for catchments characterized by more complex sources of sediment (variations in soil types and land uses), Poulenard et al. (2012) warned that the application of MIR-PLSR models could be more uncertain. In Arvorezinha catchment, we did not find any specific mineral related to the sediment sources. It was somehow expected as we did not evaluate the contribution of geological areas or sub-catchments that are more likely to present site-specific minerals. Nonetheless, even covering the entire range of different soil types found in the catchment (Acrisols – 57%, Cambisols – 33%, and Leptosols – 10%), it was possible to distinguish the signature of the different source types by spectroscopy analysis.

As spectroscopy (especially MIR) is very sensitive to the presence of organic matter, the discrimination of sediment sources with similar organic carbon contents (e.g. topsoil from pasturelands and crop fields, especially when cultivated under no-tillage system) can be difficult to achieve if there are no differences in mineral composition. Thereby, further studies should be conducted on larger number of sources, in order to provide more information about the nature of the eroded topsoils, i.e., cultivated vs. pasture, as in Haddadchi; Nosrati; Ahmadi (2014), or rangelands vs. orchard, as in Nosrati et al. (2014). The discrimination of sediment sources in larger catchments should also be tested using spectroscopy. In order to evaluate the accuracy of the spectroscopy approach, a comparison with results obtained with radioactive tracers as ^{137}Cs, ^{7}Be and ^{210}Pb should be conducted in the future.

7.2.2 Improving discrimination and predictions of sediment source by using VIS-based-colour parameters

The use of geochemical tracers and VIS-based-colour parameter in a single estimative of sediment source contribution provided source apportionments that are in agreement with the results of classical fingerprinting based on geochemical composition only (Figure 38). The higher Mahalanobis distance between source groups when using geochemical + VIS-based-colour parameters combined highlights that the use of different tracer variable sets makes the discrimination model more robust (Figure 21 and Table 13). In addition, combining VIS-based-colour parameters with geochemical tracers also decreased the prediction errors of source contributions (Table 21). Indeed, composite fingerprints combining several groups of tracer properties are commonly used to better discriminate sediment sources. It reduces the potential of spurious source–sediment linkages by being more representative of source material mixtures containing sediment samples. In this sense, Collins; Walling (2002) have shown that measurements of a combination of acid and pyrophosphate-dithionite extractable metals, base cations and organic constituents should provide an effective basis for establishing composite fingerprints for discriminating individual source types. Furthermore, for Collins; Walling (2002), whilst it is not possible to identify a universally applicable optimum composite fingerprint, they suggested that, if resources permit, laboratory analysis should include a range of different fingerprinting properties drawn from different groups of properties. However, it can make the fingerprinting exercise highly labor-intensive and costly, constraining the adoption of the procedure as a standard methodology to estimate sediment sources.

Because conventional fingerprinting methods based on geochemical composition still require a time-consuming and critical preliminary sample preparation, several studies have been carried out in the last years suggesting the use of visible reflectance and colour parameters as a rapid and cheap method for investigating sediment sources (LEGOUT et al., 2013; MARTÍNEZ-CARRERAS et al., 2010a, 2010b, 2010c). UV-VIS spectrometry are very affordable equipment used in a wide range of science fields (e.g. chemistry, pharmacology, plant physiology, food science, soil science, etc.), and there are even portable devices that allow *in situ* analysis (BROSINSKY et al., 2014a, 2014b). Nevertheless, so far, none of these studies have used this information in combination with classical fingerprinting properties such as geochemical tracers. To our knowledge, this study has been provided the first attempt to combine both properties groups (i.e. VIS-based-colour parameters and geochemical tracers) to

estimate sediment source contributions. Our findings prove that the use of VIS-based-colour parameters combined with classical geochemical tracers can be a rapid and inexpensive way to enhance discrimination between source types and to improve precision of sediment sources apportionment. In this sense, efforts should be also taken to try to combine the information of NIR and MIR spectra with geochemical composition in a single approach in order to generate estimations of sediment source contributions with an even higher precision.

7.3 The inter and intra-storm variation in source contributions

The results of source apportionment for sediment samples collected at varying intervals along the rising and recession limb of the hydrograph during floods reveal that there is a high variability in the source contributions not only between storms, which is highly dependent on rainfall intensity as previously demonstrated by Minella; Walling; Merten (2008), but also during single storms. Due to the relatively low number of storm-events investigated in the larger catchments, we could not find any clear seasonal trend in these catchments. According to Carter et al. (2003), such variations reflect antecedent conditions, such as soil moisture, and changes in landuse and land-cover between events, exhaustion of sources as an event proceeds, and the timing of sampling in relation to the hydrograph peak.

Intra-storm variations suggest that changing in sediment source contribution during storm-events tends to be gradual. In the smaller catchments, source contributions were highly variable. Nonetheless, this may be due to the small number of samples collected during each flood (usually equal or less than three). However, when taking into account a higher sampling frequency, the intra-storm variation becomes smoother and more gradual, as during the floods that occurred on 2 December 2010 and 29 July 2011 in Arvorezinha catchment (Figure 33, Figure 35).

Overall, the interpretation of intra-storm variation in source contributions was complicated for several reasons, as (*i*) the low number of storm-events sampled in some catchments, (*ii*) the sometimes low sediment sampling frequency, and (*iii*) the irregular time interval between samples due to difficulties inherent to the manual collection of sediment samples. Even so, some interesting trends on intra-storm variation emerged.

At Guaporé and Conceição catchments, there is a slight increase in the proportion of SC material supplied during the latter stages of the event (Figure 53, Figure 54, Figure 61). The

delayed SC input may reflect streambanks failure as the water levels recede (CARTER et al., 2003). This phenomenon was often observed, mainly in Conceição catchment, as shown in Figure 65 a, b. According to Wynn (2006), mass failures often occur following floods. In these cases, precipitation and the rising stream flow increase the moisture content and weight of stream bank. It reduces apparent soil cohesion due to the decrease of matric suction. During prolonged rainfall, positive pore pressures may develop and result in a reduction of frictional soil strength. In addition, the bank height or angle might be amplified as floodwaters corrode streambanks. Later, the combined effect of these changes and the fast loss of confining pressure as the stream flow retreats, can generate streambank mass failures. The effect of cattle trampling in Guaporé catchment may also have contributed to the input of stream channels material, but on a much lower extent (Figure 65 c, d).

The results from Arvorezinha catchment are consistent with the findings of Walling; Owens; Leeks (1999). They suggested that SC material is entrained at high discharges and that higher amounts of bank material can thus be expected at the discharge peak or shortly afterwards (see storm-events on 7 November 2009 and 29 July 2011 - Figure 33a, Figure 35), depending on the distance from the source of the material to the sampling site.

At Júlio de Castilhos, however, especially in JC80 catchment, most storm-events indicated that sediments delivery from SC are mainly resuspended at the beginning of the flood because the flow has lower sediment concentration and thus has energy to erode riverbank (see Figure 43, Figure 45a, Figure 47, Figure 48, Figure 49). Moreover, a higher proportion of SC sediment in the beginning of the flood may be due to remobilization of SC sediment eroded and deposited in the riverbed in previous floods. Over time, the concentration of suspended sediment increases and the flow loses erosion power, decreasing SC contribution. These findings are in agreement with the higher hysteresis index for JC80 catchment compared to the JC140 (1.33 and 0.72 respectively). It indicates sediments arrives earlier in JC80, indicating a contribution of sediment sources next to the channel network, i.e. in this case, the stream channel itself.

For intra-storm contribution of unpaved roads, no clear pattern was found in all study catchments. The unpaved roads are constantly subject to periodic rectifications (Figure 66 a, b, c, d). Furthermore, the heavy agricultural machinery traffic often damages unpaved roads structure, mainly under high humidity conditions (Figure 66 e, f). In many points of the study catchments, unpaved roads display direct connection with stream network (Figure 67). However, the arrival time of sediment from UR at the catchment outlet depends on the distance from the source to the sampling site.

(a)

(b)

(c)

(d)

(e)

Figure 65 – Effect of riverbank failure in Conceição (a, b) and Guaporé (e) catchments, and effect of cattle trampling on channel scour in Guaporé catchment (c, d).

Figure 66 – Rectification of unpaved roads at Guaporé (a, b) and Conceição (c, d) catchments, and damages on unpaved roads structure induced by heavy agricultural machinery traffic under high humidity conditions (e, f).

At Conceição and Arvorezinha catchments, crop fields inputs increase in higher flow conditions. In Arvorezinha it occurred because the eroding crop areas are directly linked to the drainage system at several locations (MINELLA et al., 2007). At Júlio de Castilhos, however, for both catchments, there is a delay in CF inputs verified during most of floods investigated. The higher CF contribution in the recession limb is a combined effect of the lower slope, the high distance of CF from the drainage system, and the high proportion of wetlands and artificial ponds present in Júlio de Castilhos catchments, which promotes sediment trapping and reduce connectivity of crops fields with channel network (Figure 68).

Figure 67 – Connections of unpaved roads with the tributaries (a, b) and the main river (c, d) in Guaporé catchment.

(a)

(b)

(c)

(d)

(e)

(f)

Figure 68 – Effect of vegetation in wetlands (a, b, c, d) and artificial pounds (e, f) trapping sediments from crop fields in Júlio de Castilhos. Source: Pellegrini A. and Rasche J.W.A.

The higher proportion of GR contribution during the rising stage and at peak flow compared to the recession limb is also a function of the short distance between grasslands and the stream in Júlio de Castilhos catchment (Figure 6). These findings are in agreement with Collins; Walling; Leeks (1997) and Martínez-Carreras et al. (2010b) who also found that maximum pasture contributions generally coincide with the hydrograph peak, followed by a decrease in GR contribution after the maximum flow. Mckinley; Radcliffe; Mukundan (2013) also found a higher proportion of sediment from pasture in the rising limb of the hydrograph in a Southern Piedmont watershed, in USA. The authors inferred that it may be due to runoff which reaches the stream during the rising limb before conceding predominance to interflow and ground-water during later stages. In Júlio de Castilhos catchments, the higher contribution of GR in the firsts stages are in agreement with their close position to the stream network in both catchments, which may facilitate the transfer of sediments by runoff (Figure 6).

The source apportionment results from the five-catchments monitored provide quantitative confirmation that precipitation events are associated with an increase in sediment transfer from topsoil, as found by Cooper et al. (2015). Furthermore, the intra-storm variations in source contributions in agricultural catchments of Southern Brazil demonstrate the specificity of each particular flood event in different hydrosedimentological environments. These results emphasize the need of a high sampling frequency to understand erosion processes during floods, especially in small headwater catchments where the hydrological responses are faster.

7.4 Overviews of sediment source apportionment in agricultural catchments from Southern Brazil

7.4.1 A feedback on Arvorezinha catchment fingerprinting studies

The dominance of CF contribution in Arvorezinha catchment is in agreement with the higher proportion of this source in the entire catchment area and its higher erosion rates due to location on steep slopes and sometimes their sparse vegetation cover due to plowing where tobacco is cultivated. These results are in agreement with previous findings obtained by Minella; Merten; Clarke (2009) (from April 2002 to October 2002); and Minella; Walling; Merten (2008) (from May 2002 to March 2006), who studied the same sediment sources in this

catchment before and after the adoption of improved soil management practices. After the adoption of these practices by most farmers, they founded an average absolute (load-weighted mean) contribution of 54, 24 and 22% for CF, UR and SC, respectively, for 23 rainfall events during the period from May 2004 to March 2006. In our study (from October 2009 to July 2011), the contribution of the sediment sources was 57±14, 23±14 and 20±12% for the CF, UR and SC, respectively (average of 29 suspended sediment samples). It could be expected such similar source apportionment once the area under improved soil management practices was almost the same in our study (Table 4). However, as the sediment source samples and the tracers used were different in both studies, it proves the fingerprinting approach is a robust methodology to estimate sediment sources contribution in small headwater catchments. Minella et al (2009) stated that the catchment was still in a state of transition and that the incising channel system may further stabilize, with a progressive decrease in channel contribution to the sediment yield. However, the results obtained in the present study confirm the source contribution remained stable during the post-treatment period.

7.4.2 Progresses in source apportionment in Júlio de Castilhos catchments: the lesson for choosing potential sediment sources

In a previous fingerprinting approach conducted in JC80 catchment, Tiecher et al. (2014) evaluated the contribution of two sediment sources for a monitoring period of 22 months (May 2009 to April 2011) using time-integrating sediment samplers. Results indicate a of crop field contribution ranging from 31 to 57%, and unpaved roads contribution ranging from 43 to 69%, with means of 44±11 and 56±11% for CF and UR, respectively. However, results and field observations made by Pellegrini A. (2013) and Alvarez (2014) indicated that other sources than CF and UR could be contributing significantly to the sediment yield in the same study area. Therefore, grasslands and stream channels were then included in the present study. The findings from the present work indicate a relative contribution of 16±19% and 15±14 for CF and UR, respectively (Figure 50). Although these values are about three times lower than in the previous work, the ratio of contribution for CF and UR remains close to a proportion equal to 1:1, indicating that contribution of these sources were diluted when other potential sources of sediment (i.e. stream channels and grasslands) were taken into account. These findings highlight that success for fingerprinting sediment sources is highly dependent on the correct

choice of potential sources of sediment to be studied. This cornerstone of fingerprint approaches relies strongly on prior knowledge of erosion processes prevailing in the target catchment, which depends deeply on field observations and practical experiences.

7.4.3 The surrogate for suspended sediment samples in fingerprinting studies

The use of time-integrating samplers still requires considerable resources, and the requirement to collect samples that are fully representative of sediment export from a catchment (e.g. different seasons and different event magnitudes) could necessitate deploying samplers for a year or more (WALLING, 2013b). Furthermore, the manual sampling of suspended sediments during storm-events is expensive and time-consuming. Therefore, different sediment sampling strategies were employed in this work to obtain as much information as possible. Fine-bed sediment has been used as a surrogate for suspended sediment to represent the suspended sediment load transported by a river over a longer period of time (WILKINSON et al., 2013). Such strategy can provide representative results more quickly when sampling of both sources and the target are made in a single campaign (WALLING, 2013b). Fine-bed sediments are representative samples of the entire watershed, and allow to collect enough quantity of sample in a short sampling time (HADDADCHI et al., 2013). Besides, according to Horowitz et al. (2012), the <63 µm fraction of near-surface (upper 1 cm) bed sediments can be an useful surrogate for the estimation of suspended sediment-associated chemical concentrations.

In general, there was a good agreement between the different sampling strategies for Guaporé catchment. These results are in agreement with Pulley; Foster; Antunes (2015), who found similar results for overbank, suspended, and channel bed sediment, indicating that sediment sampling location has little effect on the consistency of provenance predictions in the Nene river basin, UK. The similar ascriptions found in Guaporé catchment indicate that tracer conservatism is not primarily affected by selective deposition of specific particle size fractions onto channel beds. Moreover, it suggests that during the period of sediment storage on channel beds, few post-depositional alterations to the sediment are occurring, due to short residence times of the sediment and the well-oxygenated appearance as observed by Pulley; Foster; Antunes (2015).

The findings obtained in Conceição catchment indicate, however, that the relative contributions from different sources to fine sediment deposited on the stream bed and

suspended sediment (i.e. time-integrated samples and manually collected storm-event samples) might not be always similar. These findings are in agreement with Koiter et al. (2013), Haddadchi; Nosrati; Ahmadi (2014), and Lamba; Karthikeyan; Thompson (2015) who also reported that relative source contributions to bed and suspended sediments might not necessarily be the same. Suspended sediments are primarily composed of finer sediment (<63μm), while sediment from eroded banks can be present as individual particles or aggregates due to stream bank mass failure, which is an important erosion process in Conceição catchment as stated before (Figure 65 d, e). The aggregates are more likely to deposit on the stream bed than individual fine particles (i.e. suspended sediments). Furthermore, sediments eroded during the recession stage after the flood peak, which contains higher proportion of SC material (Figure 53, Figure 54), are more likely to deposit on the stream bed.

7.4.4 Stream channel contribution: the role of soil texture and riparian vegetation

Streams are dynamic and constantly changing systems. Stream bank erosion is, therefore, natural and common along rivers. However, anthropogenic pressures due to conversion of forests into agriculture or urban development have often accelerated this process by altering the stream system. Bernhardt et al. (2005) estimated that over one billion dollars have been spent annually since 1990 for stream restoration in the United States.

According to Osman; Thorne (1988), increase in soil clay content enhances their resistance to erosion from the streambank due to the hydraulic forces occurring during flood events. Therefore, as expected, stream channel contribution was more important in Júlio de Castilhos catchment, where soils are sandy and coarser (Figure 69a, b) (sand content >60% - Tiecher et al. (2014)). In the same way, it could then be expected then that stream channel contribution in Conceição catchment should be low, since soils are clayey and Fe-oxides rich. However, as demonstrated by Couper (2003), soils with high clay contents are more sensitive to the effects of subaerial processes, as soil desiccation, which reduces soil strength, making soils less resistant to erosion by hydraulic forces (Figure 69c, d). Subaerial processes are mainly controlled by climatic conditions and largely independent of flow (WYNN, 2006). They are also described as preparatory processes because they render the streambank more susceptible to erosion when upon occurrence of flood events (LAWLER, 1993).

In the study catchments, riparian forest seems to be a key factor controlling stream channel erosion. Stream channel contribution seems to be higher for JC80 ($p < 0.0001$), compared to JC140. The higher contribution of SC at JC80 is relevant with field observations. The higher hysteresis index for JC80 catchment compared to the JC140 site (1.33 and 0.72 respectively) also indicates that sediment supply in JC80 catchment came from sediment sources located close to the channel network (i.e. the stream channel itself). The lower contribution of stream channel in JC140 seems to be related to the higher proportion of riparian forest in this catchment (10.2 and 1.5% for JC140 and JC80 respectively – Figure 6, Table 5). Indeed, as shown in Figure 69e, riparian vegetation has a significant impact on stream stability and morphology (ABERNETHY; RUTHERFURD, 2001). The presence of mature trees on the banks increases their stability against mass failure by reinforcing the bank sediment with roots, preventing banks from failing due to oversteepening from lateral toe scour (ABERNETHY; RUTHERFURD, 2000). In contrast, the Guaporé catchment, which possesses a large variety of soils, having clay contents as those from Conceição catchment, is characterized by a six times higher stream channel contribution (Figure 63). The proportion of forest in Conceição catchment is, however, about 7 times lower (7.8 and 56.6% for Conceição and Guaporé catchments, respectively). As shown in Figure 69c, d, riparian forests are scarce in Conceição catchment, and in many riverside areas are fully cultivated.

7.4.5 The unpaved roads contribution in agricultural catchments: a scale-related source?

Unpaved road surfaces have extremely low infiltration rates compared with other land surfaces and are, therefore, significant sediment source areas (MIGUEL et al., 2014a; TIECHER et al., 2014; ZIEGLER; GIAMBELLUCA, 1997). Furthermore, roads play an important role on hydrosedimentological dynamics by increasing surface erosion above natural rates, and by increasing the hydrologic connectivity and efficiency of sediment delivery from hillslopes to fluvial networks (FU; NEWHAM; FIELD, 2009; FU; NEWHAM; RAMOS-SCHARRÓN, 2010; RIJSDIJK; SAMPURNO BRUIJNZEEL; SUTOTO, 2007; THOMAZ; VESTENA; RAMOS SCHARRÓN, 2014). However, most studies over unpaved roads have been conducted in forested landscapes (FRANSEN; PHILLIPS; FAHEY, 2001), but little is known about their significance in agricultural areas (THOMAZ; VESTENA; RAMOS SCHARRÓN, 2014).

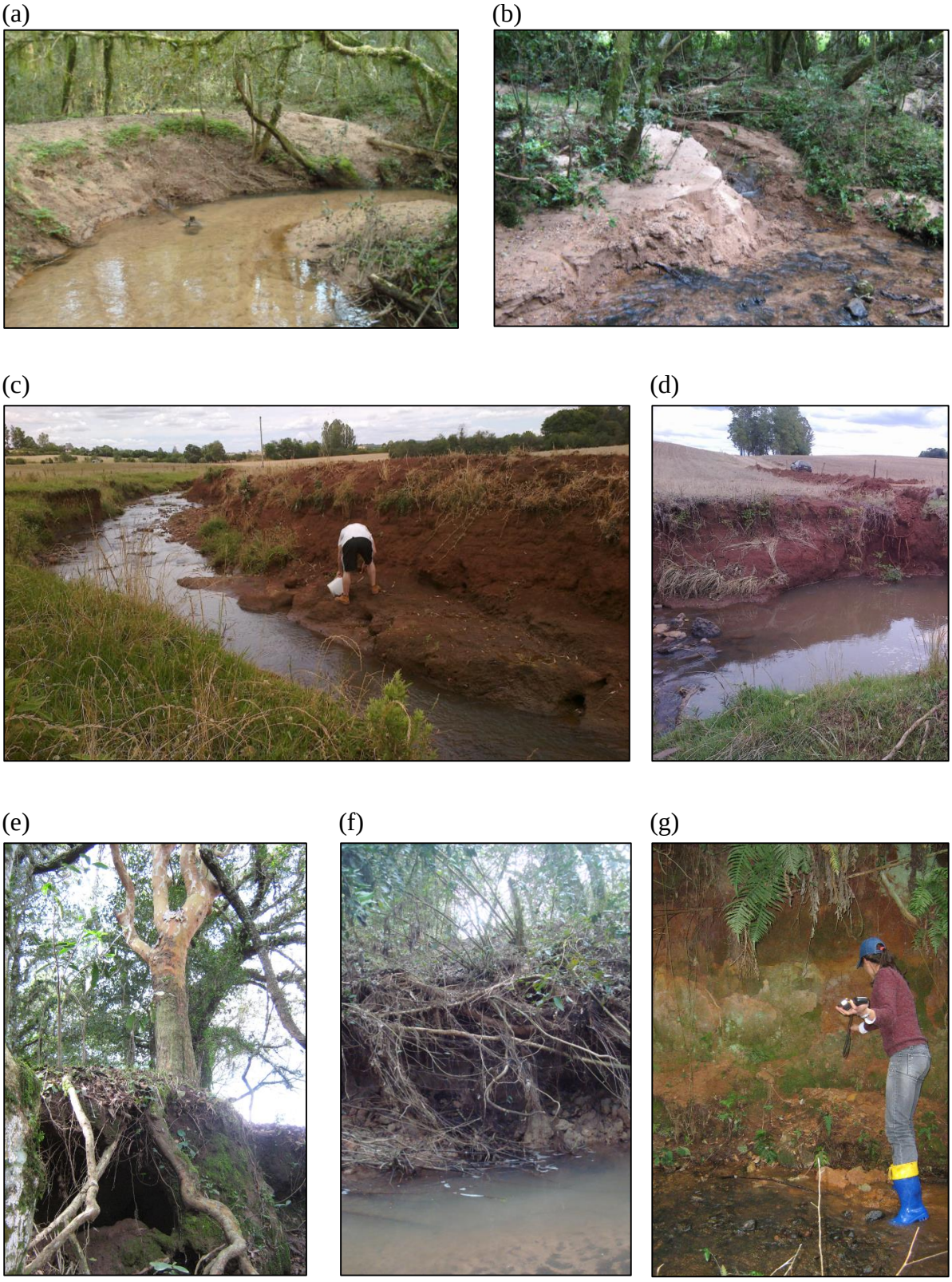

Figure 69 – Stream channel erosion (a, b) in Júlio de Castilhos catchments, presence of mature trees on the banks increasing stability against mass failure by reinforcing the bank sediment with roots (c, d) and soil desiccation reducing soil strength in Júlio de Castilhos (e) and Conceição (f, g) catchments. Source of images a, b, e, f, and g: Capoane V.

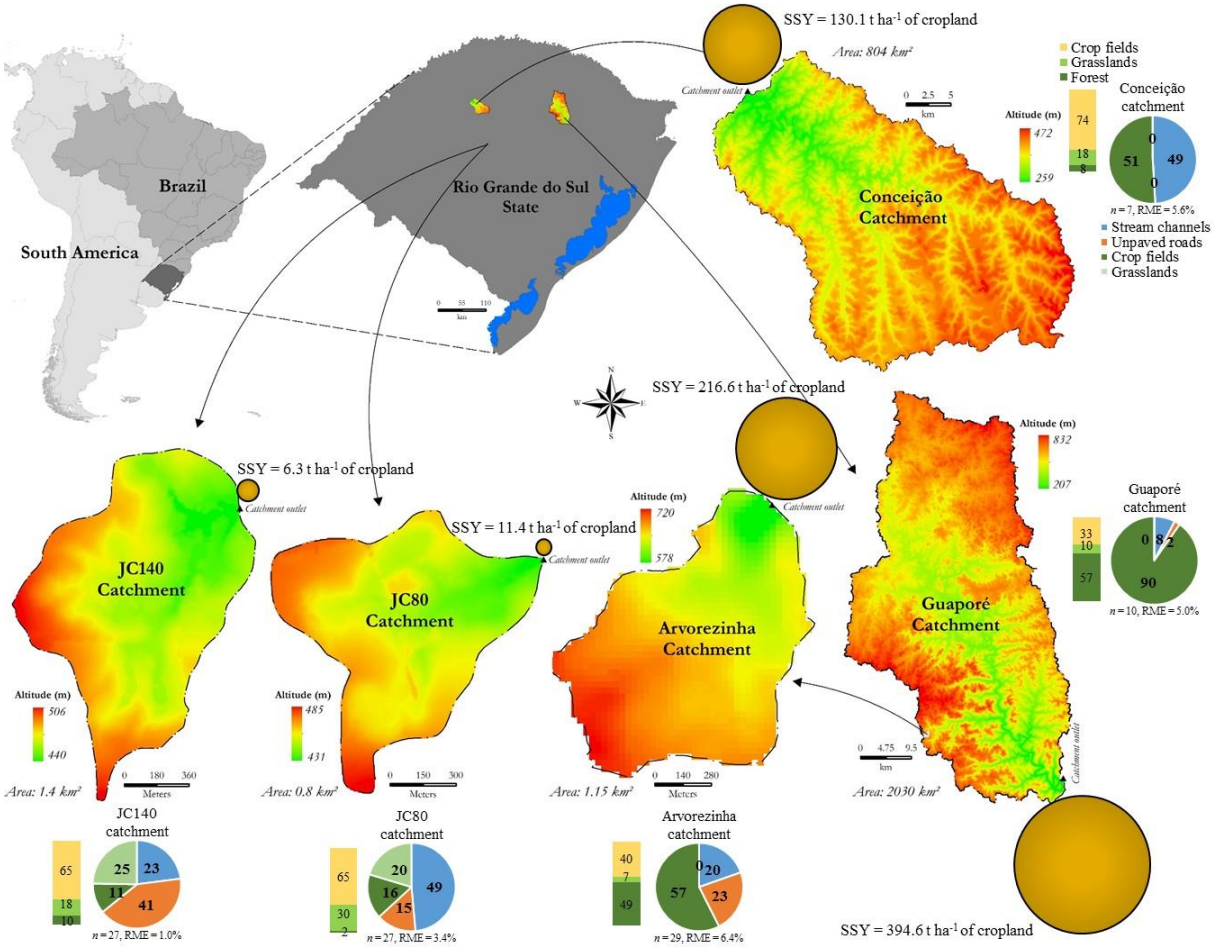

Figure 70 – Summary of sediment source contributions in suspended sediment samples in the outlet of the five catchments studied. Bars indicate percentage of crop fields, grasslands, and forest surface cover in each catchment. Pie charts indicate the average sediment source contributions for each catchment. Yellow circles indicate the specific sediment yield (SSY) of cropland in each catchment.

Rural road networks are a complex system that operate as a sediment source continuously during a year, especially in wet tropical regions (THOMAZ; VESTENA; RAMOS SCHARRÓN, 2014). Using the sediment source fingerprinting approach, Minella; Walling; Merten (2008) and Tiecher et al. (2014) estimated the contribution of unpaved roads in the production of sediments in two small catchments in the same study area. Both studies indicate that unpaved roads provide a significant contribution to the total sediment yield. However, according to Didoné et al. (2014), the values obtained for the smaller catchments might not necessarily be extrapolated to larger catchments. The comparison between the study catchments in the present study reveals that contribution of unpaved roads is significant in the sediment

yield in all catchments, but particularly in the small ones (Figure 70). Although severe erosive processes can be observed along the roads in Conceição catchment (DIDONÉ et al., 2014), the contribution of unpaved roads was the lowest among the studied catchments. This finding is particularly surprising because, in Conceição catchment, it is possible to verify that roads level are significantly lower when compared to the original level of surrounding cropfields (Figure 71). It can be hypothesized, therefore, that this is a cumulative effect of long periods, but that they are less important over the short- and medium-terms when compared with other potential sediment sources as crop fields and riverbanks.

According to García-Ruiz et al. (2015), different erosion processes are active at different spatial scales, e.g. sheet wash erosion and in some cases rill erosion are the prevailing erosion processes studied in erosion plots, whereas gullies and landslides can yield very large quantities of sediment in the case of small- and medium-size catchments. On the other hand, large basins are more related to long-term erosion and storage processes.

Figure 71 – Comparison of current roads level and the initial level of surrounding cropfields in Conceição catchment.

Further investigation is needed to better estimate unpaved roads contribution in Conceição catchment. Only few storm-event sediment samples show some relative contribution of unpaved road in this catchment. Time-integrated sediment samples showed no presence of unpaved road sediment. The use of a stochastic approach instead of the deterministic method used in the present study could provide a range of possible correct answers instead of one single answer to the problem, using the entire confidence intervals of source characteristics (HADDADCHI; OLLEY; LACEBY, 2014). A comparison of the use of stochastic and

deterministic approaches was conducted in Mill Stream Branch watershed, a tributary to the Chesapeake Bay, Maryland in USA. First, Banks; Gellis; Noe (2010) showed that for each of the five storm events sampled, the channel banks were 100% of the source of sediment using a deterministic unmixing model. Later, Massoudieh et al. (2012) used the Banks; Gellis; Noe (2010) dataset to analyze the significant sources of sediment using a Bayesian statistical approach. The findings of Massoudieh et al. (2012) still indicate river bank erosion as the major source of sediments, with a contribution of 83–99% with a 95% confidence interval. Nevertheless, a non-negligible contribution of cropland and forest was demonstrated this time, contributing to about 0.06–8% for cropland and 0.1–14% for forest, also with a 95% confidence interval. In this case, the geometrical means of the posterior frequency distributions of source contributions were 2.3, 1.25, and 93.55% for cropland, forestland, and stream bank, respectively.

The scale-related behavior of unpaved roads can also be observed in the embedded sub-catchments of Guaporé catchment. To better examine these findings we summarize the main results from Guaporé catchment in Figure 72. Taking into account the scale effect from Arvorezinha catchment (1.19 km^2), site 7 (88.3 km^2), and site 10 (outlet - 2,031.9 km^2), it is possible to observe a decrease in unpaved road contribution. These results are in agreement with Thomaz; Vestena; Ramos Scharrón (2014). The authors evaluated the localized impacts on stream suspended sediment concentration (SSC) of six unpaved road–stream crossings in the rural Guabiroba River catchment, in Southern Brazil. The findings from this work demonstrate that localized road effects on stream SSCs are strongly scale-dependent. According to Thomaz; Vestena; Ramos Scharrón (2014), unpaved road contribution is important for low-order headwater streams of third- to fourth-order streams draining less than 3 km^2, like the small catchments from Arvorezinha and Júlio de Castilhos, but it is undetectable in larger catchments.

When comparing both Júlio de Castilhos catchments, unpaved road contributions is higher for JC140 (p <0.00001). Although both catchments present similar proportion areas of unpaved roads (1.5 and 1.3% of the total area for JC80 and JC140, respectively), the higher contribution of UR in JC140 catchment might be due to the greater number of junctions between roads and stream network (Figure 6) due to a lack of planning for roads. These results are in agreement with Thomaz; Vestena; Ramos Scharrón (2014), who found a positive correlation between suspended sediment concentrations and the number of upstream road crossings, demonstrating the cumulative effect of individual road crossings in degrading water quality in rural headwater catchments.

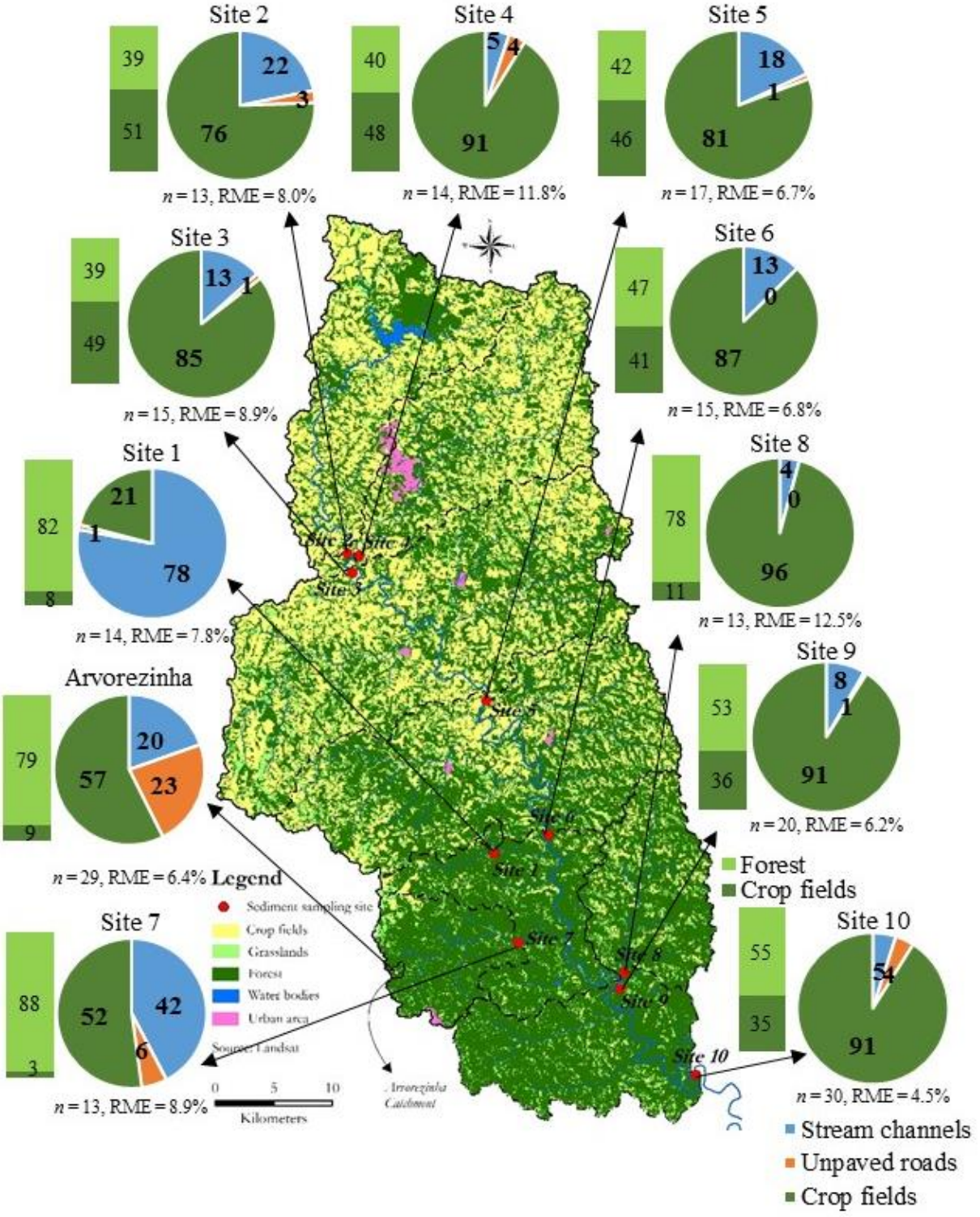

Figure 72 – Summary of spatial variability of sediment source contributions in Guaporé and Arvorezinha catchment. Bars indicate percentage of forest and crop fields surface cover in each sub-catchment. Pie charts indicate the average sediment source contributions for each sub-catchment.

In Southern Brazil, most of rural roads are built without planning and many principal roads and secondary access paths are often damaged by rills and gullies which disturb agricultural activities and increase maintenance costs (THOMAZ; VESTENA; RAMOS SCHARRÓN, 2014). Therefore, despite the low contribution of unpaved roads compared to crop fields in the larger catchments, they represent a static component of the landscape in a watershed, which makes their allocation planning primordial in programs aiming to mitigate sediment transfer (COLLINS et al., 2010).

7.4.6 Scale and spatial distribution of land use in landscape affecting crop fields contribution

For most fingerprinting studies, sediment is sampled only at the catchment outlet and source ascriptions are often attributed to the entire catchment. However, Figure 72 shows that from Arvorezinha catchment (1.19 km^2) to site 7 (88.3 km^2), crop field contribution remains very similar, whereas it increased drastically at the outlet of Guaporé catchment (2,031.9 km^2). This shows that although the crop areas are highly sensitive to erosion due to cultivation with plowing, the relative contribution of Arvorezinha and site 7 to the total sediment load in the Guaporé catchment is minor, since the source ascription of the sites 9 and 10 (outlet) remained virtually unchanged after site 7 input.

Except for sites 1 and 7, and the Arvorezinha catchment, the source ascription results for the entire Guaporé catchment remained similar among the sampling sites located on the main river (Figure 72). However, differences arise when analyzing the results for the tributaries. For example, site 1 and Arvorezinha catchment, the smallest subcatchments studied within the Guaporé catchment, present similar proportions of cropland (8.2 and 9.5% - Figure 72). However, source ascriptions indicate that crop fields and unpaved roads supply much more sediment in Arvorezinha catchment. The same comparison can be made for larger subcatchments, as for sites 7 and 8. Both present low proportions of cropland, but sediment ascriptions are rather different (Figure 72). These findings highlight that other factors than land use play an important role in sediment production, such as distribution of croplands and forests in the landscape. At site 1, most of cultivated areas are located in the uppermost part of the subcatchment and crop fields are separated from the fluvial network by a wide band of native forest. When studying a very steep rural catchment cultivated with tobacco in Southern Brazil, Pellegrini J. et al. (2010) reported that preserved riparian vegetation could play as a barrier to

decrease the amount of sediments transferred to the water bodies, and consequently to mitigate of off-site erosion problems. In the same way, in Chesapeake Bay watershed in USA, Massoudieh et al. (2012) found that the high percentage of forest cover around streams may be reducing the contribution of sediment from agriculture sources. The authors suggest that sediment resulting from overland flow on the agricultural fields may be deposited in the forested areas before it reaches the stream network.

Recently, Santos; Sparovek (2011) demonstrated the occurrence of sediment deposition in the forest-covered riparian area by using ^{137}Cs technique to quantify the effectiveness of this formation in retaining sediments from cropland. Indeed, runoff and erosion processes are often non-linear and scale dependent. Scale dependency is mainly due to the influence of sinks that decrease the hydrological connectivity and the sediment yield (LESSCHEN; SCHOORL; CAMMERAAT, 2009). Findings of the present work remain in agreement with Koiter et al. (2013) who assessed the role of connectivity and scale in assessing the sources of sediment in an agricultural watershed in the Canadian prairies using sediment source fingerprinting. The authors demonstrated that there was a switch in sediment sources between the headwaters and the outlet of the watershed.

Comparing the sediment sampling sites along the main river in Conceição catchment, there was an increase in the SC contribution from the sites 1 and 2 (~ 32%) compared to the sites 4 and 5 (~48%) (Figure 73). This increase in SC contribution was due to the high SC contribution in the sub-catchment 3 (64%), which possesses low proportion of riparian forest, as can be seen Figure 73 and Figure 69 c and d.

7.4.7 Soil management affecting sediment delivery from crop fields in Southern Brazil: implications for catchment management

In Brazil, quantitative data on sediment fluxes at the catchment scale are still scarce particularly in grain crop regions, which tend to adopt a conservationist no-tillage system for soil protection (DIDONÉ et al., 2014). So far, quantitative information on the impact of conservation agriculture on water resources is lacking. Still this information is essential to assess the current effectiveness of conservation systems and to propose conservation measures to reduce erosion processes in agricultural catchments. Our findings indicate that the cropland specific sediment supply was very different depending on the catchment (Figure 74). We

therefore present in this section a discussion to address the impact of soil management on the transfer of sediments from cropland to river network in Southern Brazil.

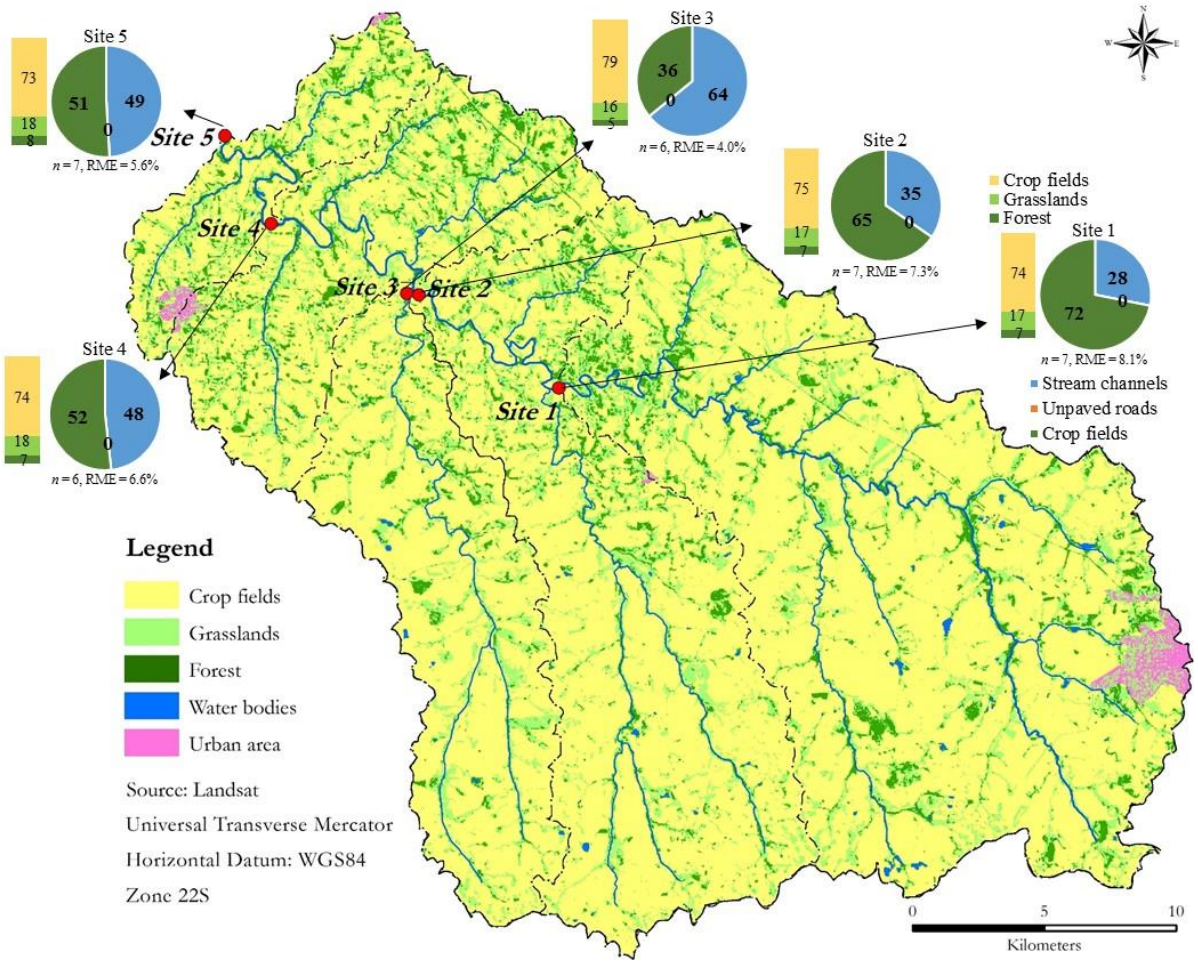

Figure 73 – Summary of spatial variability of sediment source contributions in suspended sediment samples collected with time-integrated sampler in Conceição catchment. Bars indicate percentage of crop fields, grasslands, and forest surface cover in each sub-catchment. Pie charts indicate the average sediment source contributions for each sub-catchment.

7.4.7.1 An overview on extremely different realities of small catchments in Southern Brazil

In Júlio de Castilhos catchments, soil management is based on crop-livestock integration under no-tillage system. Cultivation in based on soybean (*Glycine max*) in summer and oats (*A.*

strigosa) and ryegrass (*L. multiflorum*) in winter for cattle feeding. Crop fields are cultivated without the use of mechanical runoff control measures and without the application of crop rotation. The lack of physical barriers and the sparse vegetation cover of the soil enhance soil losses from crop fields. Moreover, integrated crop-livestock system under NT with inadequate management cause topsoil compaction (BELL et al., 2011; COLLARES et al., 2011; SHARROW, 2007) and/or reduce the soil vegetation cover for summer crops, facilitating water runoff and sheet erosion. According to Kurz; O'Reilly; Tunney (2006), the presence of cattle had a longer lasting effect on the soil hydrological parameters than on the nutrient concentrations measured in overland flow. However, sediment yield from crop fields in both Júlio de Castilhos catchments was much lower than in the other catchments. This is due to the smoother relief and due to the presence of wetlands and artificial ponds, which enhance sediment trapping and reduce connectivity between crops fields and the channel network (Figure 68). The effect of sediment trapping by wetlands was more pronounced at JC80 catchment where wetlands cover an area of approximately 18%, compared to only 5% at JC140. As a result, although relative contributions of crop fields was higher for JC80 than JC140 (16±19 and 11±12%, respectively - Table 39), the specific sediment yield from cropland in JC80 catchment was half of that observed in JC140 catchment (Figure 74). Therefore, it seems that in Júlio de Castilhos catchments, soil erosion in crop fields is generating more on-site than off-site problems. There is an evident decrease of soil fertility and water holding capacity in crop fields from both Júlio de Castilhos catchments, which are directly affecting the crop yields. This increases poverty in these rural areas and directly affects the local economy and society. However, the apparent low contribution of crop fields to the total sediment export from Júlio de Castilhos should be nuanced seen. Wetlands may indeed play an important role on sediment trapping, but they could be less effective in reducing the transfer of pollutants and nutrients from crop fields, like dissolved reactive P, by water runoff (HART; CORNISH, 2012).

Compared to Júlio de Castilhos, the soil use and management and the physiographic conditions in Arvorezinha catchment are completely different. Forest covers about half of total area and the main crops (40% of total area) are tobacco (*Nicotiana tabacum*) in summer, maize (*Z. mays*) in spring, and oats (*A. strigosa*) and ryegrass (*L. multiflorum*) in winter. The soil management is based on minimum tillage and conventional plow farming. The steep slopes and the implementation of soil plowing in crop fields from Arvorezinha catchment resulted in a sediment delivery approximately 35 and 20 times higher than in JC80 and JC140 catchments. In the same way, considering the European ecozones, Bosco et al. (2015) also find that the mountain system shows a mean soil erosion rate 2–3 times higher than the average (ranging

from 4.06 t km^{-2} yr^{-1} in the subtropical mountain system to 7.8 t km^{-2} yr^{-1} in the boreal mountain system). The findings obtained in Arvorezinha catchment raise concerns as in this catchment family farmers strictly follow the instructions established by the international industry to cultivate tobacco. It involves application of high doses of both phosphate fertilizers and pesticides, which leads to their accumulation in the cropland soils. Subsequently, the soil particles exported from the crop fields by runoff contribute to a significant transfer of contaminants such as pesticides (MAGNUSSON et al., 2013; YAHIA; ELSHARKAWY, 2014), and P (PELLEGRINI J. et al., 2010), and increase the environmental risk of eutrophication of the water bodies (DODD; MCDOWELL; CONDRON, 2014; GUO et al., 2014).

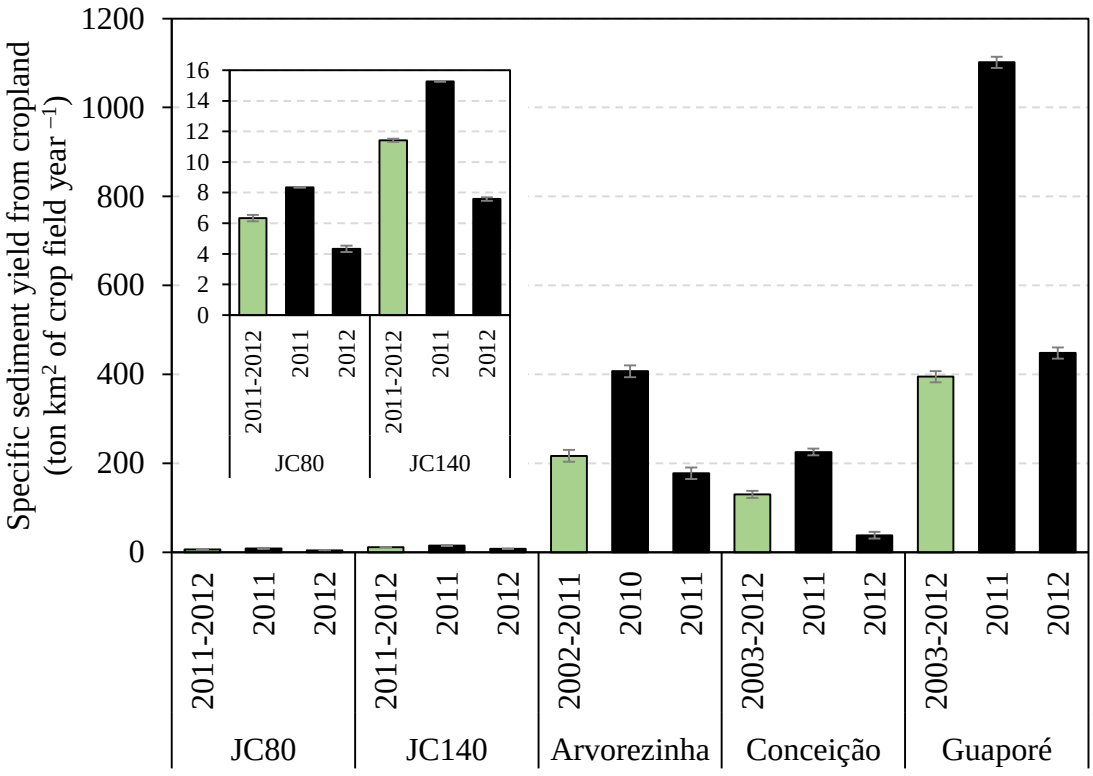

Figure 74 – Specific sediment yield from cropland in agricultural catchments from Southern Brazil. Whiskers indicate the average of the relative mean error (RME) obtained during minimization of process of unmixing linear model. Figure summarizes the results reported in Table 39.

In some regions of Rio Grande do Sul State (RS), the scarcity of land, both qualitatively and quantitatively, has led smallholder farmers to cultivate environmentally fragile areas with

intensive agricultural practices. Pellegrini J. (2011) analyzed the agro-environmental conflicts related to tobacco production arising from inappropriate use of soils, especially in areas of permanent preservation of riparian forest, in a small catchment from Agudo, RS, with similar physiographic and socioeconomic conditions to those found in Arvorezinha catchment. The author suggest that a replanning of the family production units is crucial to allow for a sustainable cultivation in these environments, while minimizing impacts on water resources. The preservation of natural resources is incompatible with the current tobacco production system based on cultivation guidelines established by the international tobacco industry. The transition to a sustainable agriculture could provide a way to overcome the agro-environmental conflicts in these regions that partly arise from low potential of land for agriculture. Pelegrini et al. (2012) adds that agroecology needs to be institutionalized as a public policy, in education, marketing, as well as farming organizations and their production practices providing a basis to develop a new scientific paradigm.

7.4.7.2 Looking at larger scales: the case of Guaporé and Conceição catchments

Although Guaporé and Conceição catchments show very similar sediment yields (~ 140 ton km^{-2} yr^{-1}), the specific yield from cropland is almost three times lower in Conceição than in Guaporé catchment. This latter catchment has natural characteristics that favor erosion and the transfer of sediment to water bodies, especially in the middle and lower sections, where the relief is hilly and the soils are shallow. The physiographic characteristics and land use in the upper part of the Guaporé catchment are very similar to those observed in the Conceição catchment. The soils are deeper and richer in Fe-oxides, the relief is smooth and no-tillage system is applied to most of cropland where grain is cultivated. In contrast, in the middle- and lower-parts of the Guaporé catchment, physiographic features, land use and soil management are similar to the conditions observed in Arvorezinha catchment. The main crops are tobacco, corn, soybeans, grasslands, eucalyptus plantations, and native forests. There is a wide variety of land uses and soil types, and almost no conservation measure is applied. Soil degradation by water erosion is widely observed. In many areas, crop selection and soil management do not take into account the fragile nature of the soils. Intensive cultivation with soil plowing on steep slopes accelerates the erosion process. Furthermore, soil plowing before growing tobacco is mainly performed during the most erosive months (September to November - Didoné et al.

(2014)). All these factors have caused soil degradation and low economic returns, leading to rural poverty.

The lower sediment yield from cropland in Conceição catchment compared to Guaporé catchment reflect these differences in soil management, soil types, and natural landscape characteristics. According to Didoné et al. (2014), the characteristics of the catchment leading to a low erosion potential are as follows: (*i*) soils are deep, clayey, and rich in iron oxides, which limits the detachment of particles by raindrop impact and runoff; (*ii*) average topography is characterized by gentle slopes and shear-flow energy controlled by steepness is small; and (*iii*) the no-tillage system (NTS) is used on most cultivated area (>80%). However, even in these favorable conditions, the amount of sediment supplied by cropland to fluvial network remains too high (specific sediment yield (SSY) = 1.3 ton ha^{-2} of cropland yr^{-1}). This indicates that additional efforts are necessary to further reduce soil erosion. Erosion monitoring on plots (3.5 × 22.1 m) installed in Southern Brazil indicates gross soil erosion of about 1.0 ton ha^{-2} of cropland yr^{-1} (overall mean for a ten years experiment - Bertol et al. (2007)). Taking into account that even on steep areas such as in Arvorezinha catchment, the in-field deposition of eroded material from cropland is higher than 50%, and that only ~ 7% of gross erosion reaches the catchment outlet due to deposition between hillslopes and the outlet (MINELLA; WALLING; MERTEN, 2014), it can be estimated that gross erosion for crop fields in Conceição catchment are rather higher. Indeed, estimation performed with the RUSLE model indicate a mean gross erosion of 8 ton ha^{-2} yr^{-1}, with values ranging from 2 to 16 ton ha^{-2} yr^{-1} (DIDONÉ, 2013).

Erosion by water is also a major problem in many parts of Europe. According to Bosco et al. (2015), the average rate of soil erosion by water across the EU-25 (excluding Cyprus, Greece, and Malta) is about 2.76 t ha^{-2} yr^{-1}. The same authors shows that for the same area, over 7 % of cultivated land (arable and permanent cropland) is estimated to suffer from moderate to severe erosion (erosion rates higher than 11 t ha^{-2} yr^{-1}), corresponding approximately to the entire area of Bulgaria. In comparison, only 2 % of permanent grasslands and pasture in the EU-25 is estimated to suffer from moderate to severe erosion, demonstration the importance of maintaining permanent vegetation cover as a mechanism to combat soil erosion.

In Conceição catchment, several characteristics of the agricultural production system that are reducing infiltration and increasing runoff and erosion may explain the high sediment delivery from crop fields despite a relatively low erosion potential. According to Didoné et al. (2014), these characteristics are: (*i*) the absence of crop rotation due to the high economic value

of soybean production; (*ii*) feeding of cattle with the biomass grown during winter (oat and ryegrass) instead of using it for soil covering and mulching; (*iii*) crop sowing parallel to the main slope lines, promoting increase of runoff speed and erosion potential; (*iv*) degradation of soil structure and soil compaction due to the traffic of heavy machinery often under inadequate moisture conditions; and (*v*) the absence of additional soil conservation practices as crop leveling, strip cropping, implementation of vegetated ridges, wide based terraces, and grassed channel sinks.

As a result of the sparse soil cover by crop residues, soil compaction, and the absence of terraces, sheet erosion is often observed on crop fields in Conceição catchment, even in areas with gentle slopes (Figure 75a). This is also frequently seen in Julio de Castilhos cropfields (Figure 75b, c). The erosion problem is worsened when crop sowing crops is performed following the main slope line. The soil mobilized during the sowing operation is more easily detached and transported. Subsequently, the sowing line acts as a preferential channel for water runoff (Figure 75d, e – in Júlio de Castilhos catchment, and Figure 75f in Conceição catchment). The sowing line then provide a preferential pathway for runoff and sediment transport, causing both on-site and off-site effects. The surface layer of the soil is the most fertile, it has the higher content of available nutrients and organic matter. Furthermore, the row sowing soil is the one that received the last fertilization (when the fertilization is made in the sowing row). Therefore, the erosion of this soil will cause a higher loss of fertility and a greater impact on aquatic environments.

Despite of the above-mentioned on-site erosion problems (loss of fertility, cultivable area, and soil water storage), the soils from Conceição catchment remain rich in clay and Fe-iron oxides that can act as a substrate for the adsorption of nutrients, especially P (BORTOLUZZI et al., 2013, 2015), and many contaminants such as heavy metals, pesticides and other persistent organic pollutants. Erosion of this soil can then generate off-site problems such as eutrophication and fish kills. Furthermore, it increases the cost of water treatment and the exposure of the human population to potentially hazardous substances.

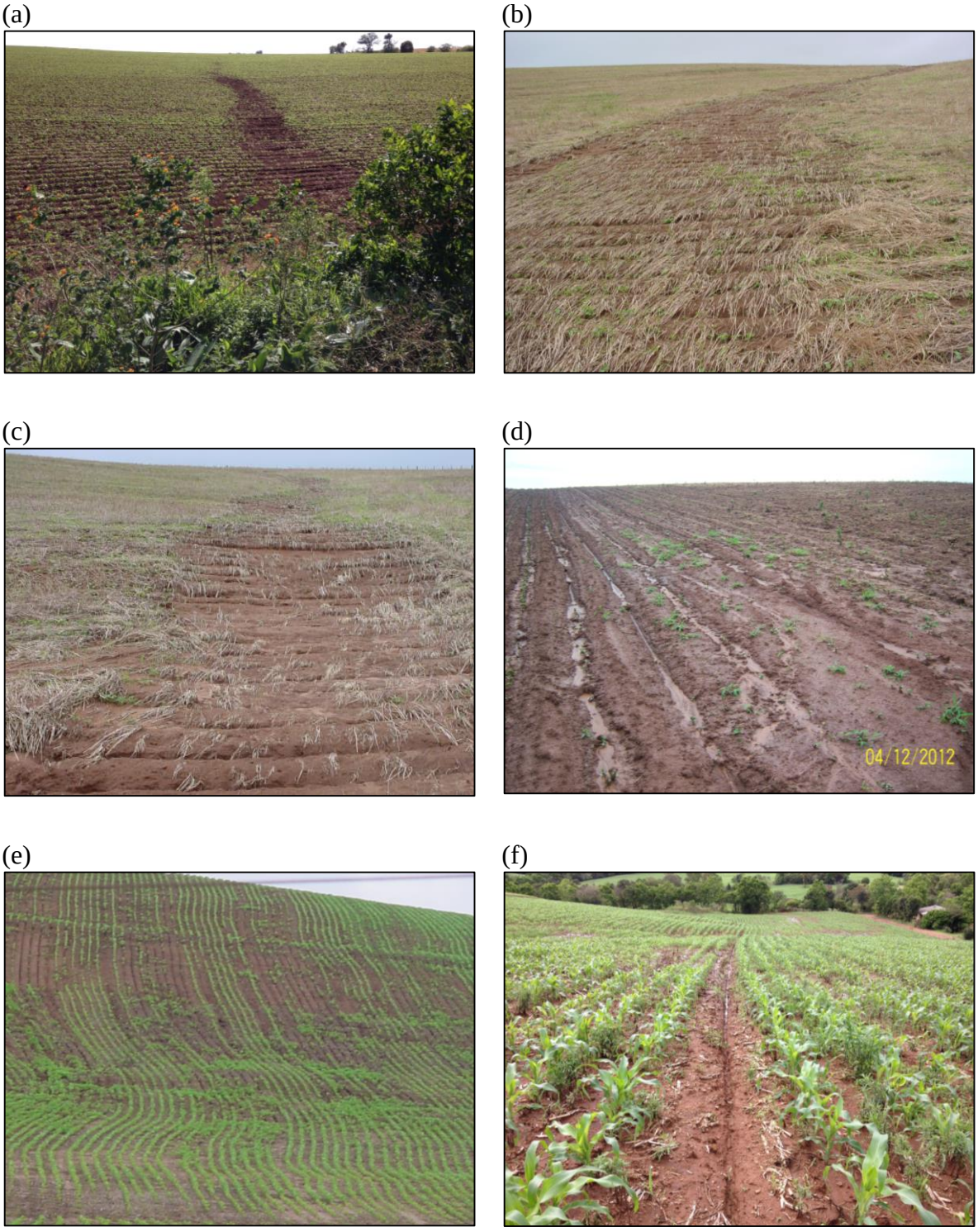

Figure 75 – Sheet erosion in Júlio de Castilhos (a, b) and Conceição catchments (c), and erosion generated in the planting furrow in areas cultivated parallel to the slope line without mechanical measures for controlling runoff in Júlio de Castilhos (d, e) and Conceição catchment. Source of images b, c, d, and e: Pellegrini A. and Rasche J.W.A.

Therefore, there is an urgent need to better plan land use and cover in Southern Brazil. Mitigation of soil loss from croplands in the study catchments can be achieved by implementing several measures, such as the use of crop rotation, the inclusion of mechanical runoff control strategies, and the planning and relocation of unpaved roads. These measures are not innovative, nor unknown to farmers, technicians, or the academic community, but in practice they are often neglected. This is partly due to the fact that decisions on land use planning and soil management have historically been taken independently by the farmers, who use their property as a basic unit for management and action. It makes difficult to raise awareness among farmers, technical staff members and public managers that efficient measures to alleviate sediment transfer at a catchment scale, such as planning and relocation of roads and the application of mechanical runoff control measures, must to be take jointly, beyond the rural property boundaries.

As stated by Lambin; Geist; Lepers (2003), the coupled human-environment systems should be considered as a whole when we assess sustainability and vulnerability. To this end, socio-economic issues must to be taken into account because they are closely related to soil erosion problems. Indeed, recently, Bhandari; Aryal; Darnsawasdi (2015) identified variables such as household size, farm labor availability, level of education, conservation cost, training, membership of organization committees, distance, farm size, migration, and farm income as predictor variables of soil erosion. Moreover, as warned by Speratti et al (2015), conservation agriculture education, information dissemination through extension agents and farmers, and greater policy support and social capital, can help change attitudes and conventional farming practices.

8 CONCLUSIONS

The conclusion section focus on provide an answer to the four main research questions involving: (*i*) provision of guidelines for tracer pre-selection, (*ii*) the relevance using of alternative spectroscopic methods for fingerprinting sediment provenance, (*iii*) the results of source apportionment at high-spatial and -temporal resolutions, and (*iv*) the influence of conservation practices on sediment delivery from cropland. Finally, some recommendations and perspectives for further investigations are given.

8.1 Guidelines for tracer pre-selection

It was found that 18 different geochemical tracers were selected as potential tracing parameters in at least one catchment by DFA to estimate sediment source contributions using a linear mixed model (Ag, Al, As, Ba, Be, Co, Cr, Cu, Fe, La, Li, Mn, Mo, Ni, P, Ti, V, and Zn). The findings suggest that the transition metals are the most suitable geochemical tracers in agricultural catchments from Southern Brazil due to their conservativeness and their discriminant potential. In contrast, alkaline metals and alkaline earth metals tend to be less conservative during the erosion process and should be avoided. Except for total organic carbon and phosphorus, there was no obvious consistency in the physicochemical basis supporting this selection. Phosphorus content was consistently higher in crop fields while total organic carbon was equally higher in topsoil sources, i.e. grasslands and crop fields. This result highlights that tracer selection is highly site-specific. Notwithstanding, care should be taken to evaluate conservativeness of P and TOC in each target catchment before their use as tracers.

Results clearly demonstrate that no single geochemical tracer was capable of classifying 100% of the source material samples into the correct source categories for any of the study catchments. It highlights that several fingerprint properties incorporated into a composite fingerprint are required in order to discriminate between several diffuse sources in order to provide reliable estimates of the relative contribution of these sources to river sediment in agricultural catchments. Different geochemical tracers can explain different erosion processes. Thus, using composite geochemical tracers can reduce uncertainty and enhances the model's

robustness, as well as the reliability of results. In general, the smaller the catchment and the lower the number of sources investigated, the more effective the tracers were to discriminate sediment sources.

Discrimination of grasslands was only possible in the small catchments of Júlio de Castilhos. In Guaporé and Conceição catchments, estimation of their contribution was not possible due to the similar geochemical composition of grasslands and crop fields as well as to the high variability in soil types and lithologies found in these catchments. A possible explanation for this may be the lower sampling density in Guaporé and Conceição catchments (0.15 and 0.23 samples per km^{-2}, respectively) compared to the Júlio de Castilhos catchments (ranging from 21 to 37 samples km^{-2}).

8.2 The potential use of alternative spectroscopic methods

The use of alternative spectroscopic methods in the range of UV-VIS, NIR, and MIR, was validated to fingerprint sediment sources in the small catchment from Arvorezinha by comparing their results with the ones obtained with a more classical fingerprinting approach based on geochemical composition. Source ascriptions obtained by alternative methods based on spectroscopy-PLSR models remained in agreement with ascriptions from classical fingerprinting, especially for the NIR-PLSR approach. Moreover, spectral-based fingerprinting can be as precise as the geochemical tracers for this catchment, even using independent PLSR models for each source, i.e., when each model estimates the proportion of one source, independently of the two others.

The spectroscopy-PLSR models is a promising approach because of its low cost and rapidity, facilitating the achievement of numerous measurements and hence high-resolution predictions that are essential for better understanding the erosive behavior of catchments which exhibit highly variable hydro-sedimentary dynamics. Moreover, combining VIS-based-colour to geochemical tracers proved to be a rapid and inexpensive way to enhance discrimination between source types and to improve precision of sediment sources apportionment.

8.3 Source apportionment at high-spatial and -temporal resolutions

The results of source apportionment for sediment samples collected at varying intervals along the rising and recession stages of the hydrograph of floods reveal a high variability in the source ascriptions at both inter- and intra-storm scales. The source apportionment results from the five catchments monitored provide quantitative confirmation that precipitation events are associated with an increase in topsoil-to-river sediment transfer (i.e. grasslands and crop fields). The delayed stream channel inputs in the larger catchments may reflect the occurrence of streambanks failures as the water levels recede. For intra-storm contribution of unpaved roads, however, no clear common pattern was found in all study catchments. The intra-storm variations in source contributions for agricultural catchments from Southern Brazil demonstrate the specificity of each particular flood event in different hydrosedimentological environments. These results emphasize the need of high sampling frequency to understand erosion processes during floods, especially in small headwater catchments where the hydrological responses are faster.

Results of sediment source apportionment in the different catchments and sub-catchments demonstrate that other factors than land use proportions play an important role in sediment production in Southern Brazil, such as distribution of croplands, forests, and unpaved roads across the landscape and its connectivity. Preserved riparian vegetation, wetlands, and artificial pounds promote sediment trapping and reduce connectivity between cropland and rivers, decreasing the amount of sediments transferred to the water bodies. The presence of riparian forest seems to be a key factor for controlling stream channel erosion. The presence of mature trees on the banks increases their stability. The findings from this work also demonstrate that unpaved road contributions are strongly scale-related and that this depends on the number of junctions between roads and the stream network. Sediment contribution of unpaved roads is significant in all catchments, but particularly in the smaller ones. Most of unpaved roads in the study catchments are unplanned, built parallel to the main slope line, and are often damaged by rills and gullies.

In Conceição catchment, the contribution of unpaved roads was the lowest among the studied catchments, which was particularly surprising because, in this catchment, it is possible to verify that roads level are significantly lower when compared to the original level of surrounding cropfields and severe erosive processes can be observed along the roads. Despite the low contribution of unpaved roads compared to cropland in the larger catchments, they

represent a static component of the landscape in a watershed, which makes their allocation planning primordial in programs aiming to mitigate sediment supply to rivers.

8.4 Effect of conservation practices on sediment delivery from crop fields

The hypothesis of this study was confirmed. The crop fields, even when no-tillage is implemented, are still the main source of sediment to rivers in agricultural catchments of Southern Brazil. The current application of conservation systems, as well as the impact of agriculture pressures on water resources when soil conservation practices are either partially or incorrectly used, was assessed using the fingerprinting approach.

Our results indicate that the cropland specific sediment yield was very different in the study catchments because of the natural conditions of relief and slope, but also land use and soil management. In the catchments of Júlio de Castilhos, the cropland specific sediment yield was very low (6–12 ton km^2 yr^{-1}) due to the smoother relief and to the presence of wetlands and artificial ponds, which promotes sediment trapping and reduces connectivity between crops fields and the river. In contrast, the steep slopes and shallow soils which are often plowed in cropland of Arvorezinha catchment resulted in a sediment delivery approximately 20–35 times higher than in Júlio de Castilhos, which raises concerns. Indeed, as the production system involves high doses of both phosphate fertilizers and pesticides that are bound to sediment, sediment supply to rivers increases the environmental risk of eutrophication and contamination of the water bodies.

Although Guaporé and Conceição catchments show very similar sediment yields, the cropland specific sediment yield is about three times lower in Conceição than in Guaporé. The Guaporé catchment has natural characteristics that favor erosion and the transfer of sediment to water bodies, especially in the middle and lower sections, where the relief is hilly and the soils are shallow. However, in many areas, the crop and soil management does not take into account the fragile nature of the soils, leading to very high erosion rates on crop fields. The lower cropland specific sediment yield estimated in Conceição catchment compared to Guaporé, reflect soil management (>80% of crop land area under no-till) and natural landscape characteristics that indicate a lower sensitivity of these catchment parts to erosion. However, the amount of sediment supplied from cropland that reach the fluvial network remain too high, indicating that additional efforts are necessary to further reduce soil erosion. The main causes

of this situation are the abandonment of mechanical practices for runoff control, the soybean monoculture neglecting crop rotation, the low biomass input limiting soil cover by vegetation and crop residues, and the excessive and uncontrolled traffic of heavy agricultural machinery, often under unfavorable moisture conditions. Therefore, there is an urgent need to better plan land use and occupation in these catchments, inasmuch as the soil management systems used by farmers are inefficient to reduce runoff and erosion in cropland areas in Southern Brazil.

8.5 Recommendations and perspectives for further investigations

Although the fingerprint approach proved to be a useful tool to achieve the objectives of the present study, there remain possibilities for further refinement of the method to adapt it to the Southern Brazilian conditions. Some recommendations and perspectives for further investigations are given below.

i) Although geochemical tracers tend to be highly site-specific, it is strongly suggested that sediment fingerprinting studies in agricultural catchments of Southern Brazil use the transition metals as potential tracers because of their conservativeness and discriminant potential. Phosphorus is a consistent tracer for crop fields and total organic carbon is a good indicator of sediments provenance from topsoil sources, i.e. grasslands and crop fields. However, care should be taken to evaluate conservativeness of P and TOC in each target catchment before using them as tracers.

ii) Efforts should be taken to evaluate the use of different fractions of geochemical tracers, mainly P and TOC, which were very sensitive to the land use but tend to be non-conservative. In this regard, sequential chemical fractionation aiming to estimate the more stable fraction of these elements and use them to fingerprint sediment origin could be very helpful. Another possibility is to use the approach suggested by Dabrin et al. (2014), who use the residual metal fraction content (non-reactive), obtained by the difference

between total concentration and HCl-available fraction, to determine sediment origin in the Marennes Oleron Bay, France.

iii) Regarding alternative methods based on spectroscopic measurements a wide range of further studies are needed. As spectroscopy (especially MIR) is very sensitive to organic matter, the discrimination of sediment sources with similar organic carbon content (e.g. topsoil from pasturelands and cropland, especially when they are cultivated under no-tillage system) can be difficult to achieve if there are no additional differences in mineral composition. In this context, further studies should include a larger number of sources, in order to provide more information about the mineralogical nature of the eroded topsoil, i.e., crop fields vs. grasslands. Furthermore, the discrimination of sediment sources in larger catchments should also be tested using spectroscopy. Moreover, efforts should also be made to combine the information of NIR and MIR spectra with geochemical composition in a common approach in order to generate estimates of sediment source contributions with a higher precision.

iv) Overall, the interpretation of intra-storm variation in source apportionment was complicated in the study catchments for several reasons. In this regard it is recommended to sample with a high frequency and in a larger number of floods. To this end, automated water samplers could be deployed because they allow the collection of instantaneous samples, and therefore to achieve a better temporal resolution for characterizing suspended sediment flux and source variations.

v) In the farms boundaries of Conceição catchment and in the uppermost part of Guaporé catchment, there is the formation of deep erosion channels and, in several cases, gullies, devoid of vegetation cover, is widely observed. Similar observations have been made in the converging part of crop fields. As a result, large sediment deposits can be observed on floodplains. In this context, two

research questions may be put forward. First, the inclusion of a subsuperficial sediment source different than the stream channels and the unpaved roads should be considered in these catchments. The measurement of ^{137}Cs could be used to this end. Second, the sediment fingerprinting technique could be applied to floodplain overbank sediment cores to estimate sediment source contribution changes over the medium to long term.

vi) Further studies are required in Guaporé and Conceição catchments in order to find additional tracers able to discriminate between topsoil sources, i.e. grasslands and crop fields. Their similar geochemical composition, the high variability in soil types and lithology and the cultivation of crop fields under no-tillage system may complicate tracer selection for this purpose.

vii) Further investigation is needed to better estimate source ascriptions in the studied catchments. A stochastic approach, e.g. the Bayesian statistical approach, could be used in order to provide a range of possible solutions instead of one single answer to the problem to avoid the equifinality problem, using the entire confidence intervals of the sediment source characteristics. Application of these methods would provide a better estimate for some sources that were assigned very low contributions when using deterministic unmixing linear models.

viii) Although the findings from Conceição catchment indicate that the relative contributions from different sources to fine sediment deposited on the stream bed and suspended sediment (i.e. time-integrated samples and manually collected storm-event samples) might not be always similar, further investigation should be performed to evaluate the suitability of fine-bed sediment as a surrogate for suspended sediment in small catchments.

REFERENCES

ABERNETHY, B.; RUTHERFURD, I. D. The effect of riparian tree roots on the mass-stability of riverbanks. **Earth Surface Processes and Landforms**, v. 25, n. 9, p. 921–937, ago. 2000.

ABERNETHY, B.; RUTHERFURD, I. D. The distribution and strength of riparian tree roots in relation to riverbank reinforcement. **Hydrological Processes**, v. 15, n. 1, p. 63–79, jan. 2001.

ALVAREZ, J. W. R. **Transferência de fósforo em pequenas bacias hidrográficas com predomínio de sistema plantio direto precário (Phosphorus transfers in small watersheds with predominance of the precarius no-till system)**. [s.l.] 2014. 202 f. Thesis (PhD in Soil Science) – Universidade Federal de Santa Maria, Santa Maria, 2014.

ANH, P. T. Q. et al. Linkages among land use, macronutrient levels, and soil erosion in northern Vietnam: A plot-scale study. **Geoderma**, v. 232-234, p. 352–362, nov. 2014.

ARAÚJO, J. C. DE. Assoreamento em Reservatórios do Semi-árido : Modelagem e Validação. v. 8, p. 39–56, 2003.

ARGENTA, D. P. B.; PANTE, A. R.; MERTEN, G. H. Evaluation erosivity index of production north-northeast of the state of Rio Grande do Sul. In: **Hall of Undergraduate Research: 13. Book of abstracts**. Porto Alegre: UFRGS, 2001. p. 37.

AVERILL, B.; ELDREDGE, P. **General chemistry: principles, patterns, and applications**. Disponível em: <http://catalog.flatworldknowledge.com/bookhub/4309?e=averill_1.0-ch06_s03>. Acesso em: 13 fev. 2015.

BALLANTINE, D. J. et al. The phosphorus content of fluvial suspended sediment in three lowland groundwater-dominated catchments. **Journal of Hydrology**, v. 357, n. 1-2, p. 140–151, jul. 2008.

BALLANTINE, D. J. et al. The content and storage of phosphorus in fine-grained channel bed sediment in contrasting lowland agricultural catchments in the UK. **Geoderma**, v. 151, n. 3-4, p. 141–149, jul. 2009.

BANKS, W.; GELLIS, A.; NOE, G. **Sources of fine-grained suspended sediment in Mill Stream Branch watershed, Corsica River Basin, a tributary to the Chesapeake Bay, Maryland.**2nd Joint Federal Interagency. **Anais**...Las Vegas, NV: 2010

BARRON, V.; TORRENT, J. Use of the Kubelka-Munk theory to study the influence of iron oxides on soil colour. **Journal of Soil Science**, v. 37, n. 4, p. 499–510, 28 dez. 1986.

BARROS, C. A. P. DE. **Comportamento hidrossedimentológico de uma bacia hidrográfica rural utilizando técnicas de monitoramento e modelagem (Hydrosedimentological behavior of a rural watershed using technical monitoring and modeling)**. [s.l.] 2012. 179 f. Master Dissertation (Master in Soil Science) - Universidade Federal de Santa Maria, Santa Maria, 2012.

BARROS, C. A. P. DE et al. Estimativa da infiltração de água no solo na escala de bacia hidrográfica. **Revista Brasileira de Ciência do Solo**, v. 38, n. 2, p. 557–564, abr. 2014a.

BARROS, C. A. P. DE et al. Description of hydrological and erosion processes determined by applying the LISEM model in a rural catchment in southern Brazil. **Journal of Soils and Sediments**, v. 14, n. 7, p. 1298–1310, 9 maio 2014b.

BELL, L. W. et al. Impacts of soil damage by grazing livestock on crop productivity. **Soil and Tillage Research**, v. 113, n. 1, p. 19–29, maio 2011.

BELMONT, P. et al. Toward generalizable sediment fingerprinting with tracers that are conservative and nonconservative over sediment routing timescales. **Journal of Soils and Sediments**, v. 14, n. 8, p. 1479–1492, 3 jun. 2014.

BELYAEV, V. R. et al. Using Chernobyl-derived 137 Cs to document recent sediment deposition rates on the River Plava floodplain (Central European Russia). **Hydrological Processes**, v. 27, n. 6, p. 807–821, 15 mar. 2013.

BEN SLIMANE, A. et al. Fingerprinting sediment sources in the outlet reservoir of a hilly cultivated catchment in Tunisia. **Journal of Soils and Sediments**, v. 13, n. 4, p. 801–815, 10 jan. 2013.

BERNHARDT, E. S. et al. Ecology. Synthesizing U.S. river restoration efforts. **Science (New York, N.Y.)**, v. 308, n. 5722, p. 636–7, 29 abr. 2005.

BERTOL, I. et al. Aspectos financeiros relacionados às perdas de nutrientes por erosão hídrica em diferentes sistemas de manejo do solo. **Revista Brasileira de Ciência do Solo**, v. 31, n. 1, p. 133–142, fev. 2007.

BHANDARI, K. P.; ARYAL, J.; DARNSAWASDI, R. A geospatial approach to assessing soil erosion in a watershed by integrating socio-economic determinants and the RUSLE model. **Natural Hazards**, v. 75, n. 1, p. 321–342, 18 jul. 2015.

BIRD, G. et al. Quantifying sediment-associated metal dispersal using Pb isotopes: application of binary and multivariate mixing models at the catchment-scale. **Environmental pollution (Barking, Essex : 1987)**, v. 158, n. 6, p. 2158–69, jun. 2010.

BLAKE, W. H. et al. Magnetic enhancement in wildfire-affected soil and its potential for sediment-source ascription. **Earth Surface Processes and Landforms**, v. 31, n. 2, p. 249–264, fev. 2006.

BLAKE, W. H. et al. Tracing crop-specific sediment sources in agricultural catchments. **Geomorphology**, v. 139-140, p. 322–329, fev. 2012.

BORTOLUZZI, E. C. et al. Mineralogy and nutrient desorption of suspended sediments during a storm event. **Journal of Soils and Sediments**, v. 13, n. 6, p. 1093–1105, 24 abr. 2013.

BORTOLUZZI, E. C. et al. Occurrence of iron and aluminum sesquioxides and their implications for the P sorption in subtropical soils. **Applied Clay Science**, v. 104, p. 196–204, fev. 2015.

BOSCO, C. et al. Modelling soil erosion at European scale: towards harmonization and reproducibility. **Natural Hazards and Earth System Science**, v. 15, n. 2, p. 225–245, 4 fev. 2015.

BRONSTERT, A. et al. Process-based modelling of erosion, sediment transport and reservoir siltation in mesoscale semi-arid catchments. **Journal of Soils and Sediments**, v. 14, n. 12, p. 2001–2018, 29 out. 2014.

BROSINSKY, A. et al. Spectral fingerprinting: sediment source discrimination and contribution modelling of artificial mixtures based on VNIR-SWIR spectral properties. **Journal of Soils and Sediments**, v. 14, n. 12, p. 1949–1964, 15 jun. 2014a.

BROSINSKY, A. et al. Spectral fingerprinting: characterizing suspended sediment sources by the use of VNIR-SWIR spectral information. **Journal of Soils and Sediments**, v. 14, n. 12, p. 1965–1981, 17 jun. 2014b.

BRUCHET, A.; ROUSSEAU, C.; MALLEVIALLE, J. Pyrolysis-GC-MS for investigating high-molecular-weight THM precursors and other refractory organics. **Journal of American Water Works Association**, v. 82, p. 66–74, 22 nov. 1990.

CAITCHEON, G. . The significance of various sediment magnetic mineral fractions for tracing sediment sources in Killimicat Creek. **Catena**, v. 32, n. 2, p. 131–142, maio 1998.

CAITCHEON, G. G. Sediment source tracing using environmental magnetism: A new approach with examples from Australia. **Hydrological Processes**, v. 7, n. 4, p. 349–358, out. 1993.

CALEGARI, A. et al. Long-term effect of different soil management systems and winter crops on soil acidity and vertical distribution of nutrients in a Brazilian Oxisol. **Soil and Tillage Research**, v. 133, p. 32–39, out. 2013.

CAÑASVERAS SÁNCHEZ, J. C. et al. Reflectance spectroscopy: a tool for predicting soil properties related to the incidence of Fe chlorosis. **Spanish Journal of Agricultural Research**, v. 10, n. 4, p. 1133, 28 nov. 2012.

CANER, L. et al. Accumulation of organo-metallic complexes in laterites and the formation of Aluandic Andosols in the Nilgiri Hills (southern India): similarities and differences with Umbric Podzols. **European Journal of Soil Science**, v. 62, n. 5, p. 754–764, 14 out. 2011.

CAPOANE, V. **Relações entre qualidade da água, uso da terra e zona ripária em duas pequenas bacias hidrográficas (Relations between water quality, land use and riparian zone two small watershed)**. [s.l.] 2011. 106 f. Master Dissertation (Master in Soil Science) – Universidade Federal de Santa Maria, Santa Maria, 2011.

CAPOANE, V. et al. Água para consumo humano em propriedades rurais de um assentamento de reforma agrária. **Hygeia : Revista Brasileira de Geografia Médica e da Saúde (Uberlândia)**, v. 7, p. 55–66, 2011.

CAPOANE, V.; RHEINHEIMER, D. DOS S. Análise qualitativa do uso e ocupação da terra no assentamento Alvorada , Júlio de Castilhos – Rio Grande do Sul (Qualitative analysis of the

use and occupation of land in the Alvorada settlement, Júlio de Castilhos – Rio Grande do Su). **Revista NERA**, v. 20, p. 193–205, 2012.

CAPOANE, V.; RHEINHEIMER, D. DOS S. Usos antrópicos em áreas de preservação permanente: estudo de caso em um assentamento de reforma agrária. **Extensão Rural (Santa Maria)**, v. 20, p. 7–23, 2013.

CARTER, J. et al. Fingerprinting suspended sediment sources in a large urban river system. **The Science of The Total Environment**, v. 314-316, n. 03, p. 513–534, 1 out. 2003.

CASÃO JUNIOR, R.; ARAÚJO, A. G.; LLANILLO, R. . **No-till agriculture in southern Brazil: Factors that facilitated the evoluti on of the system and the development of the mechanizati on of conservati on farming**. [s.l.] The Food and Agriculture Organization of the United Nations and Instituto Agronômico do Paraná, 2012. p. 83

CEW-EH-Y. **Engineering and design: sedimentation investigations of rivers and reservoirs. Manual no. 1110-2-4000**. US Army Co ed. Washington: Department of the Army, 1995. p. 177

CHANG, C. et al. Near-infrared reflectance spectroscopy-principal components regression analyses of soil properties. **Soil Science Society of America Journal**, v. 65, n. 2, p. 480–490, 2001.

CHARTER, R. A.; TABATABAI, M. A.; SCHAFER, J. W. Arsenic, molybdenum, selenium, and tungsten contents of fertilizers and phosphate rocks 1. **Communications in Soil Science and Plant Analysis**, v. 26, n. 17-18, p. 3051–3062, out. 1995.

CHEN, W. et al. Arsenic, Cadmium, and Lead in California Cropland Soils: Role of Phosphate and Micronutrient Fertilizers. **Journal of Environment Quality**, v. 37, n. 2, p. 689, 2008.

CLARK, R. L. Pollen as a chronometer and sediment tracer, Burrinjuck Reservoir, Australia. **Hydrobiologia**, v. 143, n. 1, p. 63–69, dez. 1986.

CLARKE, R. T. A bootstrap calculation of confidence regions for proportions of sediment contributed by different source areas in a “fingerprinting” model. **Hydrological Processes**, p. n/a–n/a, 12 dez. 2014.

COLLARES, G. L. et al. Compactação superficial de Latossolos sob integração lavoura: pecuária de leite no noroeste do Rio Grande do Sul. **Ciência Rural**, v. 41, n. 2, p. 246–250, fev. 2011.

COLLINS, A. L. et al. Assessing damaged road verges as a suspended sediment source in the Hampshire Avon catchment, southern United Kingdom. **Hydrological Processes**, v. 24, n. 9, p. 1106–1122, 30 abr. 2010.

COLLINS, A. L.; WALLING, D. E. Documenting catchment suspended sediment sources: problems, approaches and prospects. **Progress in Physical Geography**, v. 28, n. 2, p. 159–196, 1 jun. 2004.

COLLINS, A. L.; WALLING, D. E.; LEEKS, G. J. L. Source type ascription for fluvial suspended sediment based on a quantitative composite fingerprinting technique. **Catena**, v. 29, n. 1, p. 1–27, mar. 1997.

COLLINS, A. .; WALLING, D. . Selecting fingerprint properties for discriminating potential suspended sediment sources in river basins. **Journal of Hydrology**, v. 261, n. 1-4, p. 218–244, abr. 2002.

COMMISSION INTERNATIONALE DE L'ECLAIRAGE. **CIE Proceedings**. Cambridge, UK: Cambridge University Press, 1931.

COOPER, R. J. et al. Combining two filter paper-based analytical methods to monitor temporal variations in the geochemical properties of fluvial suspended particulate matter. **Hydrological Processes**, v. 28, n. 13, p. 4042–4056, 30 jun. 2014.

COOPER, R. J. et al. High-temporal resolution fluvial sediment source fingerprinting with uncertainty: a Bayesian approach. **Earth Surface Processes and Landforms**, v. 40, n. 1, p. 78–92, 22 jan. 2015.

COUPER, P. Effects of silt–clay content on the susceptibility of river banks to subaerial erosion. **Geomorphology**, v. 56, n. 1-2, p. 95–108, nov. 2003.

D'HAEN, K.; VERSTRAETEN, G.; DEGRYSE, P. Fingerprinting historical fluvial sediment fluxes. **Progress in Physical Geography**, v. 36, n. 2, p. 154–186, 3 fev. 2012.

DABRIN, A. et al. Origin of suspended matter and sediment inferred from the residual metal fraction: Application to the Marennes Oleron Bay, France. **Continental Shelf Research**, v. 72, p. 119–130, jan. 2014.

DALBIANCO, L. **Variabilidade espacial e estimativa da condutividade hidráulica e caracterização físico-hídrica de uma microbacia hidrográfica rural (Spacial variability and estimative of the hydraulic conductivity and physical-hidrics characterization of a rural watersh**. [s.l.] 2009. 116 f. Master Dissertation (Master in Soil Science) – Universidade Federal de Santa Maria, Santa Maria, 2009.

DALBIANCO, L. **Simulação hidrossedimentológica com o modelo lisem em uma pequena bacia hidrográfica rural (Hidrossedimentological simulation with lisem model in a small rural catchment)**. [s.l.] 2013. 92 f. Thesis (PhD in Soil Science) – Universidade Federal de Santa Maria, Santa Maria, 2013.

DASZYKOWSKI, M.; WALCZAK, B.; MASSART, D. L. Representative subset selection. **Analytica Chimica Acta**, v. 468, n. 1, p. 91–103, set. 2002.

DAVIS, C. M.; FOX, J. F. Sediment Fingerprinting: Review of the Method and Future Improvements for Allocating Nonpoint Source Pollution. **Journal of Environmental Engineering**, v. 135, n. 7, p. 490–504, jul. 2009.

DAY, S. S. et al. Measuring bluff erosion part 2: pairing aerial photographs and terrestrial laser scanning to create a watershed scale sediment budget. **Earth Surface Processes and Landforms**, v. 38, n. 10, p. 1068–1082, 25 ago. 2013.

DE ARAÚJO, J. C.; GÜNTNER, A.; BRONSTERT, A. Loss of reservoir volume by sediment deposition and its impact on water availability in semiarid Brazil. **Hydrological Sciences Journal**, v. 51, n. 1, p. 157–170, fev. 2006.

DE BOER, D. H.; CROSBY, G. Evaluating the potential of SEM/EDS analysis for fingerprinting suspended sediment derived from two contrasting topsoils. **Catena**, v. 24, n. 4, p. 243–258, out. 1995.

DE BROGNIEZ, D. et al. A map of the topsoil organic carbon content of Europe generated by a generalized additive model. **European Journal of Soil Science**, p. n/a–n/a, 16 out. 2014.

DEASY, C.; QUINTON, J. N. Use of rare earth oxides as tracers to identify sediment source areas for agricultural hillslopes. **Solid Earth**, v. 1, n. 1, p. 111–118, 26 nov. 2010.

DENGIZ, O.; YAKUPOGLU, T.; BASKAN, O. Soil erosion assessment using geographical information system (GIS) and remote sensing (RS) study from Ankara-Guvenc Basin, Turkey. **Journal of environmental biology / Academy of Environmental Biology, India**, v. 30, n. 3, p. 339–44, maio 2009.

DIDONÉ, E. J. **Erosão bruta e produção de sedimentos em bacia hidrográfica sob plantio direto no planalto do rio grande do sul (Gross erosion and sediment yield in a no-tillage catchment on the Rio Grande do Sul plateau)**. [s.l.] 2013. 228 f. Master Dissertation (Master in Soil Science) - Universidade Federal de Santa Maria, Santa Maria, 2013.

DIDONÉ, E. J. et al. Impact of no-tillage agricultural systems on sediment yield in two large catchments in Southern Brazil. **Journal of Soils and Sediments**, v. 14, n. 7, p. 1287–1297, 23 jan. 2014.

DODD, R. J.; MCDOWELL, R. W.; CONDRON, L. M. Is tillage an effective method to decrease phosphorus loss from phosphorus enriched pastoral soils? **Soil and Tillage Research**, v. 135, p. 1–8, jan. 2014.

EMBRAPA. **Sistema brasileiro de classificação de solos**. Brasília: Embrapa Produção de Informação, 1999. p. 412

ERSKINE, W. D. Soil colour as a tracer of sediment dispersion from erosion of forest roads in Chichester State Forest, NSW, Australia. **Hydrological Processes**, v. 27, n. 6, p. 933–942, 15 mar. 2013.

EVANS, R. Reducing soil erosion and the loss of soil fertility for environmentally-sustainable. **Annals of Applied Biology**, v. 146, n. 2, p. 137–146, 2005.

EVRARD, O. et al. Tracing sediment sources in a tropical highland catchment of central Mexico by using conventional and alternative fingerprinting methods. **Hydrological Processes**, v. 27, n. 6, p. 911–922, 15 mar. 2013.

FERNANDES, R. B. A. et al. Quantificação de óxidos de ferro de Latossolos brasileiros por espectroscopia de refletância difusa. **Revista Brasileira de Ciência do Solo**, v. 28, n. 2, p. 245–257, abr. 2004.

FOOLADMAND, H. R. Estimating soil specific surface area using the summation of the number of spherical particles and geometric mean particle-size diameter. **African Journal of Agricultural Research**, v. 6, n. 7, p. 1758–1762, 2011.

FRANSEN, P. J. B.; PHILLIPS, C. J.; FAHEY, B. D. Forest road erosion in New Zealand: overview. **Earth Surface Processes and Landforms**, v. 26, n. 2, p. 165–174, fev. 2001.

FRANZ, C. et al. Sediments in urban river basins: identification of sediment sources within the Lago Paranoá catchment, Brasilia DF, Brazil - using the fingerprint approach. **The Science of the total environment**, v. 466-467, p. 513–23, 1 jan. 2014.

FRITSCH, E. et al. Transformation of haematite and Al-poor goethite to Al-rich goethite and associated yellowing in a ferralitic clay soil profile of the middle Amazon Basin (Manaus, Brazil). **European Journal of Soil Science**, v. 56, n. 5, p. 575–588, out. 2005.

FRYIRS, K.; GORE, D. Sediment tracing in the upper Hunter catchment using elemental and mineralogical compositions: Implications for catchment-scale suspended sediment (dis)connectivity and management. **Geomorphology**, v. 193, p. 112–121, jul. 2013.

FU, B.; NEWHAM, L. T. H.; FIELD, J. B. Modelling erosion and sediment delivery from unsealed roads in southeast Australia. **Mathematics and Computers in Simulation**, v. 79, n. 9, p. 2679–2688, maio 2009.

FU, B.; NEWHAM, L. T. H.; RAMOS-SCHARRÓN, C. E. A review of surface erosion and sediment delivery models for unsealed roads. **Environmental Modelling & Software**, v. 25, n. 1, p. 1–14, jan. 2010.

GARCÍA-RUIZ, J. M. et al. A Meta-Analysis of soil erosion rates across the world. **Geomorphology**, v. 239, p. 160–173, mar. 2015.

GEBHARDT, M. R. et al. Conservation tillage. **Science (New York, N.Y.)**, v. 230, n. November, p. 625–630, 1985.

GELLIS, A. C.; NOE, G. B. Sediment source analysis in the Linganore Creek watershed, Maryland, USA, using the sediment fingerprinting approach: 2008 to 2010. **Journal of Soils and Sediments**, v. 13, n. 10, p. 1735–1753, 24 set. 2013.

GODFRAY, H. C. J. et al. Food security: the challenge of feeding 9 billion people. **Science (New York, N.Y.)**, v. 327, n. 5967, p. 812–8, 12 fev. 2010.

GOLOSOV, V. N.; BELYAEV, V. R.; MARKELOV, M. V. Application of Chernobyl-derived 137 Cs fallout for sediment redistribution studies: lessons from European Russia. **Hydrological Processes**, v. 27, n. 6, p. 781–794, 15 mar. 2013.

GUERRA, A. J. T. et al. Erosão e Conservação de Solos no Brasil. **Anuário do Instituto de Geociências - UFRJ**, v. 37_1, n. 1, p. 81–91, 9 abr. 2014.

GUO, W. et al. Agricultural non-point source pollution in the Yongding River Basin. **Ecological Indicators**, v. 36, p. 254–261, jan. 2014.

GUZMÁN, G. et al. Sediment tracers in water erosion studies: current approaches and challenges. **Journal of Soils and Sediments**, v. 13, n. 4, p. 816–833, 27 fev. 2013.

HADDADCHI, A. et al. Sediment fingerprinting in fluvial systems: review of tracers, sediment sources and mixing models. **International Journal of Sediment Research**, v. 28, n. 4, p. 560–578, dez. 2013.

HADDADCHI, A.; NOSRATI, K.; AHMADI, F. Differences between the source contribution of bed material and suspended sediments in a mountainous agricultural catchment of western Iran. **Catena**, v. 116, p. 105–113, maio 2014.

HADDADCHI, A.; OLLEY, J.; LACEBY, P. Accuracy of mixing models in predicting sediment source contributions. **The Science of the total environment**, v. 497-498, p. 139–52, 1 nov. 2014.

HANCOCK, G. J.; REVILL, A. T. Erosion source discrimination in a rural Australian catchment using compound-specific isotope analysis (CSIA). **Hydrological Processes**, v. 27, n. 6, p. 923–932, 15 mar. 2013.

HART, M. R.; CORNISH, P. S. Available soil phosphorus, phosphorus buffering and soil cover determine most variation in phosphorus concentration in runoff from pastoral sites. **Nutrient Cycling in Agroecosystems**, v. 93, n. 2, p. 227–244, 28 jun. 2012.

HOROWITZ, A. J. et al. Concentrations and annual fluxes of sediment-associated chemical constituents from conterminous US coastal rivers using bed sediment data. **Hydrological Processes**, v. 26, n. 7, p. 1090–1114, 30 mar. 2012.

HUGHES, A. O. et al. Sediment source changes over the last 250 years in a dry-tropical catchment, central Queensland, Australia. **Geomorphology**, v. 104, n. 3-4, p. 262–275, mar. 2009.

IUSS WORKING GROUP WRB. **World Reference Base for Soil Resources 2006, first update 2007**. Rome, Italy: Food and Agriculture Organization of the United Nations – FAO, 2007. p. World Soil Resources Reports No. 103.

JANSEEN, E. **Soil organic carbon stocks on subtropical agricultural land as affected by land use, soil management and erosion: a case study from Arvorezinha, RS-Brazil**. [s.l.] Master Dissertation (Master in Geography) – Catholic University of Leuven, 2011.

JOBBÁGY, E. G.; JACKSON, R. B. The uplift of soil nutrients by plants: biogeochemical consequences across scales. **Ecology**, v. 85, n. 9, p. 2380–2389, set. 2004.

JULIEN, C. et al. Investigation on the iron-uptake by natural biofilms. **Water research**, v. 50, p. 212–20, 1 mar. 2014.

KOCHEM, M. L. **Características granulométricas, carbono, nitrogênio e frações de fósforo em sedimentos durante eventos chuva-vazão em bacias hidrográficas no Rio Grande do Sul, Brasil (Physical and chemical caracteristics of suspended sediment during fluviometric events**. [s.l.] 2014. 120 f. Master Dissertation (Master in Soil Science) – Universidade Federal de Santa Maria, Santa Maria, 2014.

KOITER, A. J. et al. The behavioural characteristics of sediment properties and their implications for sediment fingerprinting as an approach for identifying sediment sources in river basins. **Earth-Science Reviews**, v. 125, p. 24–42, out. 2013a.

KOITER, A. J. et al. Investigating the role of connectivity and scale in assessing the sources of sediment in an agricultural watershed in the Canadian prairies using sediment source fingerprinting. **Journal of Soils and Sediments**, v. 13, n. 10, p. 1676–1691, 21 ago. 2013b.

KONDOLF, G. M. et al. Sustainable sediment management in reservoirs and regulated rivers: Experiences from five continents. **Earth's Future**, v. 2, n. 5, p. 256–280, 23 maio 2014.

KOSMAS, C. S. et al. Characterization of Iron Oxide Minerals by Second-Derivative Visible Spectroscopy1. **Soil Science Society of America Journal**, v. 48, n. 2, p. 401, 1984.

KOUHPEIMA, A. et al. An assessment of specific sediment yield of geological formations using investigated sedimentary deposits in reservoirs and fingerprinting. **Journal of Agricultural Science and Technology**, v. 14, n. 2, p. 435–447, 2012.

KREIN, A.; PETTICREW, E.; UDELHOVEN, T. The use of fine sediment fractal dimensions and colour to determine sediment sources in a small watershed. **Catena**, v. 53, n. 2, p. 165–179, set. 2003.

KURZ, I.; O'REILLY, C. D.; TUNNEY, H. Impact of cattle on soil physical properties and nutrient concentrations in overland flow from pasture in Ireland. **Agriculture, Ecosystems & Environment**, v. 113, n. 1-4, p. 378–390, abr. 2006.

LACEBY, J. P. et al. A comparison of geological and statistical approaches to element selection for sediment fingerprinting. **Journal of Soils and Sediments**, v. 8212, 24 mar. 2015.

LAL, R. Soil carbon sequestration impacts on global climate change and food security. **Science (New York, N.Y.)**, v. 304, n. 5677, p. 1623–7, 11 jun. 2004.

LAMBA, J.; KARTHIKEYAN, K. G.; THOMPSON, A. M. Apportionment of suspended sediment sources in an agricultural watershed using sediment fingerprinting. **Geoderma**, v. 239-240, p. 25–33, fev. 2015.

LAMBIN, E. F.; GEIST, H. J.; LEPERS, E. Dynamics of land use and land cover change in tropical regions. **Annual Review of Environment and Resources**, v. 28, n. 1, p. 205–241, nov. 2003.

LANSON, B. Decomposition of Experimental X-ray Diffraction Patterns (Profile Fitting): A Convenient Way to Study Clay Minerals. **Clays and Clay Minerals**, v. 45, n. 2, p. 132–146, 1997.

LARSEN, D. **ChemWiki: The dynamic chemistry E-textbook**. Disponível em: <http://chemwiki.ucdavis.edu/Organic_Chemistry/Organic_Chemistry_With_a_Biological_Emphasis/Chapter_04%3A_Structure_Determination_I/Section_4.2%3A__Infrared_spectroscopy>. Acesso em: 13 fev. 2015.

LAWLER, D. M. Needle ice processes and sediment mobilization on river banks: the River Ilston, West Glamorgan, UK. **Journal of Hydrology**, v. 150, n. 1, p. 81–114, set. 1993.

LEGOUT, C. et al. Quantifying suspended sediment sources during runoff events in headwater catchments using spectrocolorimetry. **Journal of Soils and Sediments**, v. 13, n. 8, p. 1478–1492, 12 jun. 2013.

LESSCHEN, J. P.; SCHOORL, J. M.; CAMMERAAT, L. H. Modelling runoff and erosion for a semi-arid catchment using a multi-scale approach based on hydrological connectivity. **Geomorphology**, v. 109, n. 3-4, p. 174–183, ago. 2009.

LI, J. et al. Quantitative effects of vegetation cover on wind erosion and soil nutrient loss in a desert grassland of southern New Mexico, USA. **Biogeochemistry**, v. 85, n. 3, p. 317–332, 12 jul. 2007.

LI, Y. Y.; SHAO, M. A. Change of soil physical properties under long-term natural vegetation restoration in the Loess Plateau of China. v. 64, p. 77–96, 2006.

LIM, Y. S. et al. Evaluation of suspended-sediment sources in the Yeongsan River using Cs-137 after major human impacts. **Quaternary International**, v. 344, p. 64–74, set. 2014.

LIU, S. et al. Magnetic properties of East China Sea shelf sediments off the Yangtze Estuary: Influence of provenance and particle size. **Geomorphology**, v. 119, n. 3-4, p. 212–220, jul. 2010.

LOPES, F. **Utilização do modelo Century para avaliar a dinâmica do carbono do solo em uma pequena bacia hidrográfica rural (Using of Century model to evaluate the carbon soil dynamic in a small rural catchment)**. [s.l.] 2006. 146 f. Master Dissertation (Master in Soil Science) - Universidade Federal do Rio Grande do Sul, Porto Alegre, 2006.

MADEJOVÁ, J.; BALAN, E.; PETIT, S. Application of vibrational spectroscopy to the characterization of phyllosilicates and other industrial minerals. In: CHRISTIDIS, G. E. (Ed.). . **Advances in the characterization of industrial minerals**. London, UK: European Mineralogical Union and the Mineralogical Society of Great Britain and Ireland, 2011. v. 9p. 171–226.

MAGNUSSON, M. et al. Pesticide contamination and phytotoxicity of sediment interstitial water to tropical benthic microalgae. **Water research**, v. 47, n. 14, p. 5211–21, 15 set. 2013.

MAIER, C. **Variabilidade intra-evento da origem das fontes de sedimentos em uma bacia hidrográfica rural (Intra-event variability of sources from sediment basin in a rural)**. [s.l.] 2013. 124 f. Thesis (PhD in Water Resources and Sanitation) – Universidade Federal do Rio Grande do Sul, Porto Alegre, 2013.

MANZATTO, C. V.; JUNIOR, E. D. F.; PERES, J. R. R. **Uso Agrícola dos Solos Brasileiros Uso Agrícola dos Solos Brasileiros**. Rio de Janeiro: Embrapa Solos, 2002. p. 174

MARTÍNEZ-CARRERAS, N. et al. A rapid spectral-reflectance-based fingerprinting approach for documenting suspended sediment sources during storm runoff events. **Journal of Soils and Sediments**, v. 10, n. 3, p. 400–413, 12 jan. 2010a.

MARTÍNEZ-CARRERAS, N. et al. The use of sediment colour measured by diffuse reflectance spectrometry to determine sediment sources: Application to the Attert River catchment (Luxembourg). **Journal of Hydrology**, v. 382, n. 1-4, p. 49–63, mar. 2010b.

MARTÍNEZ-CARRERAS, N. et al. Assessment of different colour parameters for discriminating potential suspended sediment sources and provenance: A multi-scale study in Luxembourg. **Geomorphology**, v. 118, n. 1-2, p. 118–129, maio 2010c.

MARTÍNEZ-CARRERAS, N. et al. The Influence of Sediment Sources and Hydrologic Events on the Nutrient and Metal Content of Fine-Grained Sediments (Attert River Basin, Luxembourg). **Water, Air, & Soil Pollution**, v. 223, n. 9, p. 5685–5705, 20 out. 2012.

MASSOUDIEH, A. et al. Suspended sediment source apportionment in Chesapeake Bay watershed using Bayesian chemical mass balance receptor modeling. v. 303, 2012.

MATISOFF, G. (210)Pb as a tracer of soil erosion, sediment source area identification and particle transport in the terrestrial environment. **Journal of environmental radioactivity**, v. 138, p. 343–54, dez. 2014.

MCKINLEY, R.; RADCLIFFE, D.; MUKUNDAN, R. A streamlined approach for sediment source fingerprinting in a Southern Piedmont watershed, USA. **Journal of Soils and Sediments**, v. 13, n. 10, p. 1754–1769, 29 maio 2013.

MEDEIROS, J. DOS S. DE et al. Formas de potássio em solos representativos do Estado da Paraíba. **Revista Ciência Agronômica**, v. 45, n. 2, p. 417–426, jun. 2014.

MELLO, N. A. DE. **Efeito do sistema de manejo nos atributos do solo, movimentação de sedimentos e exportação de carbono orgânico numa bacia rural sob cultura de fumo (Effect of management systems on soil attributes, sediments movement and organic carbon exportation in a ru**. [s.l.] 2006. 273 f. Thesis (PhD in Soil Science) – Universidade Federal do Rio Grande do Sul, Porto Alegre, 2006.

MERTEN, G. H. et al. Expansion of Brazilian agricultural territory: changes in land use. **Catena**, n. 41, p. 13–21, 2010.

MERTEN, G. H. et al. No-till surface runoff and soil losses in southern Brazil. **Soil and Tillage Research**, v. 152, p. 85–93, set. 2015.

MERTEN, G. H.; MINELLA, J. P. G. **Impact on sediment yield caused by intensification of tobacco production in a catchment in southern Brazil. In: Walling, D.E., Horowitz, A.J. (Eds.) Sediment Budgets**. Wallingford, UK: IAHS Press, 2005. v. 2p. 239–244

MERTEN, G. H.; MINELLA, J. P. G. Impact on sediment yield due to the intensification of tobacco production in a catchment in Southern Brazil. **Ciência Rural**, v. 36, n. 2, p. 669–672, abr. 2006.

MERTEN, G. H.; MINELLA, J. P. G. The expansion of Brazilian agriculture: Soil erosion scenarios. **International Soil and Water Conservation Research**, v. 1, n. 3, p. 37–48, dez. 2013.

MICHELAKI, K.; HANCOCK, R. G. V. Reassessment of elemental concentration data of sediments from the western delta of the Nile River. **Open Journal of Archaeometry**, v. 1, n. 1, p. 2, 27 jun. 2013.

MIGUEL, P. et al. Identificação de fontes de produção de sedimentos em uma bacia hidrográfica de encosta. **Revista Brasileira de Ciência do Solo**, v. 38, n. 2, p. 585–598, abr. 2014a.

MIGUEL, P. et al. Variáveis mineralógicas preditoras de fontes de produção de sedimentos, em uma bacia hidrográfica do Rio Grande do Sul. **Revista Brasileira de Ciência do Solo**, v. 38, n. 3, p. 783–796, jun. 2014b.

MINELLA, J. P. G. **Identificação de fontes de produção de sedimentos em uma pequena bacia rural (Identification of sediment sources in a small rural watershed)**. [s.l.] 2003. 90

f. Master Dissertation (Master in Water Resources and Sanitation) – Universidade Federal do Rio Grande do Sul, Porto Alegre, 2003.

MINELLA, J. P. G. **Utilização de técnicas hidrossedimentométricas combinadas com a identificação de fontes de sedimentos para avaliar o efeito do uso e do manejo do solo nos recursos hídricos de uma bacia hidrográfica (Combined use of hydrosedimentometric techniques and sed**. [s.l.] 2007. 172 f. Thesis (PhD in Water Resources and Sanitation) – Universidade Federal do Rio Grande do Sul, Porto Alegre, 2007.

MINELLA, J. P. G. et al. Identificação e implicações para a conservação do solo das fontes de sedimentos em bacias hidrográficas. **Revista Brasileira de Ciência do Solo**, v. 31, n. 6, p. 1637–1646, dez. 2007.

MINELLA, J. P. G. et al. Estimating suspended sediment concentrations from turbidity measurements and the calibration problem. **Hydrological Processes**, v. 22, n. 12, p. 1819–1830, 15 jun. 2008.

MINELLA, J. P. G. et al. Changing sediment yield as an indicator of improved soil management practices in southern Brazil. **Catena**, v. 79, n. 3, p. 228–236, dez. 2009.

MINELLA, J. P. G.; MERTEN, G. H. Monitoramento de bacias hidrográficas para identificar fontes de sedimentos em suspensão. **Ciência Rural**, v. 41, n. 3, p. 424–432, mar. 2011.

MINELLA, J. P. G.; MERTEN, G. H. Índices topográficos aplicados à modelagem agrícola e ambiental. **Ciência Rural**, v. 42, n. 9, p. 1575–1582, set. 2012.

MINELLA, J. P. G.; MERTEN, G. H.; CLARKE, R. T. Método "fingerprinting" para identificação de fontes de sedimentos em bacia hidrográfica rural. **Revista Brasileira de Engenharia Agrícola e Ambiental**, v. 13, n. 5, p. 633–638, out. 2009.

MINELLA, J. P. G.; MERTEN, G. H.; MAGNAGO, P. F. Análise qualitativa e quantitativa da histerese entre vazão e concentração de sedimentos durante eventos hidrológicos. **Revista Brasileira de Engenharia Agrícola e Ambiental**, v. 15, n. 12, p. 1306–1313, dez. 2011.

MINELLA, J. P. G.; MERTEN, G. H.; RUHOFF, A. L. Utilização de métodos de representação espacial para cálculo do fator topográfico na equação universal de perda de solo revisada em bacias hidrográficas. **Revista Brasileira de Ciência do Solo**, v. 34, n. 4, p. 1455–1462, ago. 2010.

MINELLA, J. P. G.; WALLING, D. E.; MERTEN, G. H. Combining sediment source tracing techniques with traditional monitoring to assess the impact of improved land management on catchment sediment yields. **Journal of Hydrology**, v. 348, n. 3-4, p. 546–563, jan. 2008.

MINELLA, J. P. G.; WALLING, D. E.; MERTEN, G. H. Establishing a sediment budget for a small agricultural catchment in southern Brazil, to support the development of effective sediment management strategies. **Journal of Hydrology**, v. 519, p. 2189–2201, nov. 2014.

MOGES, A.; HOLDEN, N. M. Farmers' perceptions of soil erosion and soil fertility loss in Southern Ethiopia. **Land Degradation & Development**, v. 18, n. 5, p. 543–554, set. 2007.

MOREIRA, V. S. **Territorialidades rurais em Júlio de Castilhos-RS: da pecuária extensiva a agricultura familiar (Rural territorialities in Júlio de Castilhos-RS: from extensive cattle ranching to family farm)**. [s.l.] 2008. 132 f. Master Dissertation (Master in Geography) – Universidade Federal de Santa Maria, Santa Maria, 2008.

MORO, M. **Avaliação do modelo LISEM na simulação dos processos hidrossedimentológicos de uma pequena bacia rural nas encostas basálticas do RS (Evaluation of the lisem model for the simulation of hydrosedimentologic processes in a small rural catchment on the basal**. [s.l.] 2011. 133 f. Thesis (PhD in Water Resources and Sanitation) – Universidade Federal do Rio Grande do Sul, Porto Alegre, 2011.

MUGGLER, C. C.; PAPE, T.; BUURMAN, P. Laser grain-size determination in soil genetic studies 2. Clay content, clay formation, and aggregation in some Brazilian oxisols. **Soil Science**, v. 162, n. 3, p. 219–228, mar. 1997.

MUKUNDAN, R. et al. Sediment Source Fingerprinting: Transforming From a Research Tool to a Management Tool 1. **JAWRA Journal of the American Water Resources Association**, v. 48, n. 6, p. 1241–1257, 17 dez. 2012.

NAVRATIL, O. et al. Temporal variability of suspended sediment sources in an alpine catchment combining river/rainfall monitoring and sediment fingerprinting. **Earth Surface Processes and Landforms**, v. 37, n. 8, p. 828–846, 30 jun. 2012.

NAZARI SAMANI, A.; WASSON, R. J.; MALEKIAN, A. Application of multiple sediment fingerprinting techniques to determine the sediment source contribution of gully erosion: Review and case study from Boushehr province, southwestern Iran. **Progress in Physical Geography**, v. 35, n. 3, p. 375–391, 5 maio 2011.

NOSRATI, K. et al. An exploratory study on the use of enzyme activities as sediment tracers: biochemical fingerprints? **International Journal of Sediment Research**, v. 26, n. 2, p. 136–151, jun. 2011.

NOSRATI, K. et al. A mixing model to incorporate uncertainty in sediment fingerprinting. **Geoderma**, v. 217-218, p. 173–180, abr. 2014.

NRIAGU, J. O. A global assessment of natural sources of atmospheric trace metals. **Nature**, v. 338, n. 6210, p. 47–49, 2 mar. 1989.

OLIVEIRA, F. P. DE. **Modelagem do escoamento supercial e da erosão hídrica em bacia rural em Arvorezinha, RS, utilizando o WEPP (Evaluation of the lisem model for the simulation of hydrosedimentologic processes in a small rural catchment on the basalt slopes of Rio Grande do**. [s.l.] 2010. 173 f. Thesis (PhD in Water Resources and Sanitation) – Universidade Federal do Rio Grande do Sul, Porto Alegre, 2010.

OLIVEIRA, F. P. DE et al. Fatores relacionados à suscetibilidade da erosão em entressulcos sob condições de uso e manejo do solo. **Revista Brasileira de Engenharia Agrícola e Ambiental**, v. 16, n. 4, p. 337–346, abr. 2012.

OLLEY, J. et al. The application of fallout radionuclides to determine the dominant erosion process in water supply catchments of subtropical South-east Queensland, Australia. **Hydrological Processes**, v. 27, n. 6, p. 885–895, 15 mar. 2013.

OSMAN, A. M.; THORNE, C. R. Riverbank Stability Analysis. I: Theory. **Journal of Hydraulic Engineering**, v. 114, n. 2, p. 134–150, fev. 1988.

OVERBECK, G. et al. Brazil's neglected biome: The South Brazilian Campos. **Perspectives in Plant Ecology, Evolution and Systematics**, v. 9, n. 2, p. 101–116, 11 dez. 2007.

PELEGRINI, G. et al. **Agroecologia: realidade sociohistórica e perspectivas para agricultura familiar**. [s.l.] URI, 2012. p. 155

PELLEGRINI, A. **Índices de desempenho ambiental e comportamento hidrossedimentológico em duas bacias hidrográficas rurais (Indexes of environmental performance and hydrosedimentological behavior in two rural watersheds)**. [s.l.] 2013. 108 f. Thesis (PhD in Soil Science) – Universidade Federal de Santa Maria, Santa Maria, 2013.

PELLEGRINI, J. B. R. et al. Impacts of anthropic pressures on soil phosphorus availability, concentration, and phosphorus forms in sediments in a Southern Brazilian watershed. **Journal of Soils and Sediments**, v. 10, n. 3, p. 451–460, 20 ago. 2010.

PELLEGRINI, J. B. R. **Planejamento do uso do solo em unidades de produçãofamiliar produtoras de fumo: limites e possibilidades para asuperação de conflitos agroambientais (Land use planning in family production units of tobacco: limits and possibilities for overcoming the agro**. [s.l.] 2011. 128 f. Thesis (PhD in Soil Science) – Universidade Federal de Santa Maria, Santa Maria, 2011.

PHILLIPS, J. M.; RUSSELL, M. A.; WALLING, D. E. Time-integrated sampling of fluvial suspended sediment: a simple methodology for small catchments. **Hydrological Processes**, v. 14, n. 14, p. 2589–2602, 15 out. 2000.

PILS, J. R. V.; KARATHANASIS, A. D.; MUELLER, T. G. Concentration and Distribution of Six Trace Metals in Northern Kentucky Soils. **Soil and Sediment Contamination: An International Journal**, v. 13, n. 1, p. 37–51, 10 ago. 2004.

PIMENTEL, D. et al. Environmental and economic costs of soil erosion and conservation benefits. **Science (New York, N.Y.)**, v. 267, n. 5201, p. 1117–23, 24 fev. 1995.

PIMENTEL, D. Soil Erosion: A Food and Environmental Threat. **Environment, Development and Sustainability**, v. 8, n. 1, p. 119–137, fev. 2006.

POLETO, C.; MERTEN, G. H.; MINELLA, J. P. The identification of sediment sources in a small urban watershed in southern Brazil: an application of sediment fingerprinting. **Environmental technology**, v. 30, n. 11, p. 1145–53, out. 2009.

PORTO, P.; WALLING, D. E.; CALLEGARI, G. Using 137 Cs and 210 Pb ex measurements to investigate the sediment budget of a small forested catchment in southern Italy. **Hydrological Processes**, v. 27, n. 6, p. 795–806, 15 mar. 2013.

POULENARD, J. et al. Infrared spectroscopy tracing of sediment sources in a small rural watershed (French Alps). **The Science of the Total Environment**, v. 407, n. 8, p. 2808–19, 1 abr. 2009.

POULENARD, J. et al. Tracing sediment sources during floods using Diffuse Reflectance Infrared Fourier Transform Spectrometry (DRIFTS): A case study in a highly erosive

mountainous catchment (Southern French Alps). **Journal of Hydrology**, v. 414-415, p. 452–462, jan. 2012.

POULENARD, J.; DORIOZ, J.-M.; ELSASS, F. Analytical Electron-Microscopy Fractionation of Fine and Colloidal Particulate-Phosphorus in Riverbed and Suspended Sediments. **Aquatic Geochemistry**, v. 14, n. 3, p. 193–210, 6 maio 2008.

PRIZOMWALA, S. P.; BHATT, N.; BASAVAIAH, N. Provenance discrimination and Source-to-Sink studies from a dryland fluvial regime: An example from Kachchh, western India. **International Journal of Sediment Research**, v. 29, n. 1, p. 99–109, mar. 2014.

PULLEY, S.; FOSTER, I.; ANTUNES, P. The uncertainties associated with sediment fingerprinting suspended and recently deposited fluvial sediment in the Nene river basin. **Geomorphology**, v. 228, p. 303–319, jan. 2015.

QUARANTA, A et al. Ion Beam Induced Luminescence capabilities for the analysis of coarse-grained river sediments. **Spectrochimica acta. Part A, Molecular and biomolecular spectroscopy**, v. 121, p. 1–8, jan. 2014.

QUINTON, J. N. et al. The impact of agricultural soil erosion on biogeochemical cycling. **Nature Geoscience**, v. 3, n. 5, p. 311–314, 18 abr. 2010.

RAVAIOLI, M.; ALVISI, F.; VITTURI, L. M. Dolomite as a tracer for sediment transport and deposition on the northwestern Adriatic continental shelf (Adriatic Sea, Italy). **Continental Shelf Research**, v. 23, n. 14-15, p. 1359–1377, set. 2003.

RECIO-VAZQUEZ, L. et al. Multivariate statistical assessment of functional relationships between soil physical descriptors and structural features of soil organic matter in Mediterranean ecosystems. **Geoderma**, v. 230-231, p. 95–107, out. 2014.

RIJSDIJK, A.; SAMPURNO BRUIJNZEEL, L. A.; SUTOTO, C. K. Runoff and sediment yield from rural roads, trails and settlements in the upper Konto catchment, East Java, Indonesia. **Geomorphology**, v. 87, n. 1-2, p. 28–37, jun. 2007.

RITCHIE, J. C. et al. Soil and soil organic carbon redistribution on the landscape. **Geomorphology**, v. 89, n. 1-2, p. 163–171, set. 2007.

RITCHIE, J. C.; MCCARTY, G. W. 137Cesium and soil carbon in a small agricultural watershed. **Soil and Tillage Research**, v. 69, n. 1-2, p. 45–51, fev. 2003.

ROSSATO, M. S. **Os climas do Rio Grande do Sul: variabilidade, tendências e tipologia (The climates of Rio Grande do Sul: variability, trends and typology)**. [s.l.] 2011. 240 f. Thesis (PhD in Geography) – Universidade Federal do Rio Grande do Sul, Porto Alegre, 2011.

SANTOS, D. S. DOS; SPAROVEK, G. Retenção de sedimentos removidos de área de lavoura pela mata ciliar, em Goiatuba (GO). **Revista Brasileira de Ciência do Solo**, v. 35, n. 5, p. 1811–1818, out. 2011.

SCHEINOST, A. C. Use and Limitations of Second-Derivative Diffuse Reflectance Spectroscopy in the Visible to Near-Infrared Range to Identify and Quantify Fe Oxide Minerals in Soils. **Clays and Clay Minerals**, v. 46, n. 5, p. 528–536, 1998.

SCHULLER, P. et al. Using (137)Cs and (210)Pbex and other sediment source fingerprints to document suspended sediment sources in small forested catchments in south-central Chile. **Journal of environmental radioactivity**, v. 124, p. 147–59, out. 2013.

SCOTTO, M. A. L. **Fluxos de fósforo, carbono e sedimentos de em uma bacia hidrográfica sob cultivo intensivo no sul do Brasil**. [s.l.] 2014. f. Master Dissertation (Master in Soil Science) – Universidade Federal de Santa Maria, Santa Maria, 2014.

SEPASKHAH, A. R.; TAFTEH, A. Pedotransfer function for estimation of soil-specific surface area using soil fractal dimension of improved particle-size distribution. **Archives of Agronomy and Soil Science**, v. 59, n. 1, p. 93–103, jan. 2013.

SETTIMIO, L. et al. Fate and lability of silver in soils: effect of ageing. **Environmental pollution**, v. 191, p. 151–7, ago. 2014.

SHARROW, S. H. Soil compaction by grazing livestock in silvopastures as evidenced by changes in soil physical properties. **Agroforestry Systems**, v. 71, n. 3, p. 215–223, 4 jul. 2007.

SMITH, H. G.; BLAKE, W. H. Sediment fingerprinting in agricultural catchments: A critical re-examination of source discrimination and data corrections. **Geomorphology**, v. 204, p. 177–191, jan. 2014.

SPERATTI, A. et al. Conservation Agriculture in Latin America. In: FAROOQ, M.; SIDDIQUE, K. H. M. (Eds.). . **Conservation Agriculture**. Cham: Springer International Publishing, 2015. p. 391–415.

STENBERG, B. Visible and Near Infrared Spectroscopy in Soil Science. **Advances in Agronomy**, v. 107, n. 10, p. 163–215, 2010.

STONE, M. et al. The use of composite fingerprints to quantify sediment sources in a wildfire impacted landscape, Alberta, Canada. **The Science of the total environment**, v. 473-474, p. 642–50, 1 mar. 2014.

STRAHLER, A. N. Quantitative analysis of watershed geomorphology. **Transactions, American Geophysical Union**, v. 38, n. 6, p. 913, 1957.

TELLES, T. S.; GUIMARÃES, M. D. F.; DECHEN, S. C. F. The costs of soil erosion. **Revista Brasileira de Ciência do Solo**, v. 35, n. 2, p. 287–298, abr. 2011.

TERRA, F. DA S. **Espectroscopia de reflectância do visível ao infravermelho médio aplicada aos estudos qualitativos e quantitativos de solos (Reflectance spectroscopy from visible to mid-infrared applied for qualitative and quantitative studies of soils)**. [s.l.] 2011. 375 f. Thesis (PhD in Soil Science) – Universidade de São Paulo Escola Superior de Agricultura " Luiz de Queiroz ", Piracicaba, São Paulo, 2011.

THOMAZ, E. L.; VESTENA, L. R.; RAMOS SCHARRÓN, C. E. The effects of unpaved roads on suspended sediment concentration at varying spatial scales - a case study from Southern Brazil. **Water and Environment Journal**, v. 28, n. 4, p. 547–555, 21 dez. 2014.

TIECHER, T. et al. Forms of inorganic phosphorus in soil under different long term soil tillage systems and winter crops. **Revista Brasileira de Ciência do Solo**, v. 36, n. 1, p. 271–282, fev. 2012.

TIECHER, T. et al. Contribuição das fontes de sedimentos em uma bacia hidrográfica agrícola sob plantio direto. **Revista Brasileira de Ciência do Solo**, v. 38, n. 2, p. 639–649, abr. 2014.

TIECHER, T.; DOS SANTOS, D. R.; CALEGARI, A. Soil organic phosphorus forms under different soil management systems and winter crops, in a long term experiment. **Soil and Tillage Research**, v. 124, p. 57–67, ago. 2012.

UDO, E. J.; OGUNWALE, J. A.; FAGBAMI, A. A. The profile distribution of total and extractable copper in selected Nigerian soils. **Communications in Soil Science and Plant Analysis**, v. 10, n. 11, p. 1385–1397, 11 nov. 2008.

UZEIKA, T. **Aplicabilidade do modelo SWAT (Soil and Water Assessment Tool) na simulação da produção de sedimentos em uma pequena bacia hidrográfica rural**. [s.l.] 2009. 144 f. Master Dissertation (Master in Water Resources and Sanitation) – Universidade Federal do Rio Grande do Sul, Porto Alegre, 2009.

UZEIKA, T. et al. Use of the swat model for hydro-sedimentologic simulation in a small rural watershed. **Revista Brasileira de Ciência do Solo**, v. 36, n. 2, p. 557–565, abr. 2012.

VAN OOST, K. et al. The impact of agricultural soil erosion on the global carbon cycle. **Science (New York, N.Y.)**, v. 318, n. 5850, p. 626–9, 26 out. 2007.

VERHEYEN, D. et al. The use of visible and near-infrared reflectance measurements for identifying the source of suspended sediment in rivers and comparison with geochemical fingerprinting. **Journal of Soils and Sediments**, v. 14, n. 11, p. 1869–1885, 10 ago. 2014.

VISCARRA ROSSEL, R. A. **ColoSol. Executable software to perform colour space model transformation for soil colour**. Disponível em: <http://www.usyd.edu.au/agric/acpa/people/rvrossel/soft02.htm>.

VISCARRA ROSSEL, R. A. et al. Visible, near infrared, mid infrared or combined diffuse reflectance spectroscopy for simultaneous assessment of various soil properties. **Geoderma**, v. 131, n. 1-2, p. 59–75, mar. 2006a.

VISCARRA ROSSEL, R. A. et al. Colour space models for soil science. **Geoderma**, v. 133, n. 3-4, p. 320–337, ago. 2006b.

VISCARRA ROSSEL, R. A. et al. In situ measurements of soil colour, mineral composition and clay content by vis–NIR spectroscopy. **Geoderma**, v. 150, n. 3-4, p. 253–266, maio 2009.

VISCARRA ROSSEL, R. A.; BEHRENS, T. Using data mining to model and interpret soil diffuse reflectance spectra. **Geoderma**, v. 158, n. 1-2, p. 46–54, ago. 2010.

VISCARRA ROSSEL, R. A.; MCGLYNN, R. N.; MCBRATNEY, A. B. Determining the composition of mineral-organic mixes using UV–vis–NIR diffuse reflectance spectroscopy. **Geoderma**, v. 137, n. 1-2, p. 70–82, dez. 2006.

WAINER, H. Robust Statistics: A Survey and Some Prescriptions. **Journal of Educational Statistics**, v. 1, n. 4, p. 285, 1976.

WALKLEY, A.; BLACK, I. A. An examination of the Degtjareff method for determining soil organic matter, and a proposed modification of the chromic acid titration method. **Soil Science**, v. 37, n. 1, p. 29–38, jan. 1934.

WALLING, D. E. Tracing suspended sediment sources in catchments and river systems. **The Science of the Total Eenvironment**, v. 344, n. 1-3, p. 159–84, 15 maio 2005.

WALLING, D. E. Beryllium-7: The Cinderella of fallout radionuclide sediment tracers? **Hydrological Processes**, v. 27, n. 6, p. 830–844, 15 mar. 2013a.

WALLING, D. E. The evolution of sediment source fingerprinting investigations in fluvial systems. **Journal of Soils and Sediments**, v. 13, n. 10, p. 1658–1675, 27 ago. 2013b.

WALLING, D. E.; COLLINS, A. L. The catchment sediment budget as a management tool. **Environmental Science & Policy**, v. 11, n. 2, p. 136–143, abr. 2008.

WALLING, D. E.; OWENS, P. N.; LEEKS, G. J. L. Fingerprinting suspended sediment sources in the catchment of the River Ouse , Yorkshire , UK. **Hydrological Processes**, v. 975, n. 13, p. 955–975, 1999.

WALLING, D. E.; WOODWARD, J. C. Tracing sources of suspended sediment in river basins: a case study of the River Culm, Devon, UK. **Marine and Freshwater Research**, v. 46, n. 1, p. 327–336, 1995.

WALSH, L. M.; SUMNER, M. E.; KEENEY, D. R. Occurrence and Distribution of Arsenic in Soils and Plants. **Environmental Health Perspectives**, v. 19, n. August, p. 67–71, 1977.

WILKINSON, S. N. et al. Using sediment tracing to assess processes and spatial patterns of erosion in grazed rangelands, Burdekin River basin, Australia. **Agriculture, Ecosystems & Environment**, v. 180, p. 90–102, nov. 2013.

WOJDYR, M. **Fityk 0.8.2 free software**, 2007.

WYNN, T. Streambank retreat: a primer. Watershed Update, January-March 2006. **American Water Resources Association, Hydrology and Watershed Management Technical Committee**, v. 4, n. 1, p. 1–14, 2006.

YAHIA, D.; ELSHARKAWY, E. E. Multi pesticide and PCB residues in Nile tilapia and catfish in Assiut city, Egypt. **The Science of the total environment**, v. 466-467, p. 306–14, 1 jan. 2014.

YANG, D. et al. Global potential soil erosion with reference to land use and climate changes. **Hydrological Processes**, v. 17, n. 14, p. 2913–2928, 15 out. 2003.

YANG, H.; MOUAZEN, A. M. Vis/near and mid-infrared spectroscopy for predicting soil N and C at a farm scale. In: THEOPHANIDES, T. (Ed.). . **Infrared Spectroscopy-Life and Biomedical Sciences**. Rijeka, Croatia: Intech Press, 2012. p. 185–210.

YAO, S. et al. The effects of vegetation on restoration of physical stability of a severely degraded soil in China. **Ecological Engineering**, v. 5, p. 723–734, 2009.

YU, L.; OLDFIELD, F. A multivariate mixing model for identifying sediment source from magnetic measurements. **Quaternary Research**, v. 32, n. 2, p. 168–181, set. 1989.

ZEBRACKI, M. et al. Tracing the origin of suspended sediment in a large Mediterranean river by combining continuous river monitoring and measurement of artificial and natural radionuclides. **The Science of the total environment**, v. 502, p. 122–32, 1 jan. 2015.

ZHANG, B.; YANG, Y.; ZEPP, H. Effect of vegetation restoration on soil and water erosion and nutrient losses of a severely eroded clayey Plinthudult in southeastern China. **CATENA**, v. 57, n. 1, p. 77–90, jun. 2004.

ZIEGLER, A. D.; GIAMBELLUCA, T. W. Importance of rural roads as source areas for runoff in mountainous areas of northern Thailand. **Journal of Hydrology**, v. 196, n. 1-4, p. 204–229, set. 1997.

PUBLICATION ARISING FROM THIS THESIS

Until the defense of this thesis, some components of the research have been published, are in press, or have been submitted for publication. Some of them are listed below:

i) Tiecher, T., Minella, J.P.G., Miguel, P., Rashe, J.W.A., Pellegrini, A., Capoane, V., Ciotti, L.H., Schaefer, G.L., Rheinheimer, D.S. (2014) Contribuição das fontes de sedimentos em uma bacia hidrográfica agrícola sob plantio direto (The contribution of sediment sources in a rural catchment under no-tillage). Article in Portuguese with English abstract. *Revista Brasileira de Ciência do Solo*, v.38, n.2, p.639–649. Available online at: http://dx.doi.org/10.1590/S0100-06832014000200028. **(Appendix 3)**

ii) Tiecher, T., Caner, L., Minella, J.P.G., Rheinheimer, D.S. (2015) Combining visible-based-colour parameters and geochemical tracers to improve sediment source discrimination and apportionment. *Science of the Total Environment*, v.527–528, p.135–149. Available online to authorized users at: doi:10.1016/j.scitotenv.2015.04.103. **(Appendix 4)**

iii) Tiecher, T., Caner, L., Minella, J.P.G., Bender, M.A., Rheinheimer, D.S. (2015) Tracing sediment sources in a subtropical rural catchment of southern Brazil by using geochemical tracers and near-infrared spectroscopy. Article in press at *Soil and Tillage Research*. Available online to authorized users at: http://dx.doi.org/10.1016/j.still.2015.03.001. **(Appendix 5)**

APPENDIX 1

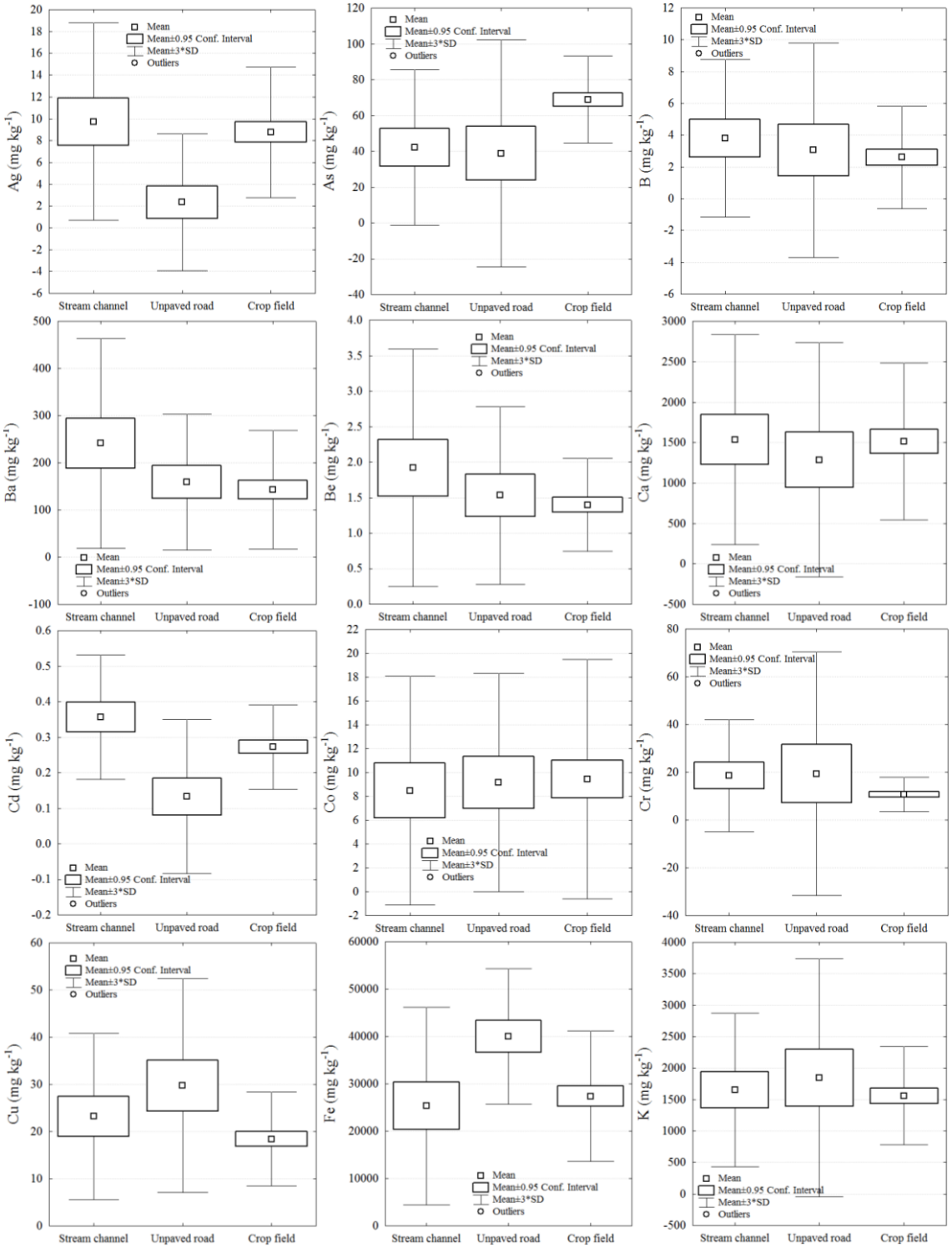

Box-plot of geochemical tracer concentrations in sediment sources of Arvorezinha catchment indicating the mean, the 95% confidence interval, and the non-outliers range (mean concentration plus three standard deviation).

APPENDIX 1 (continuation)

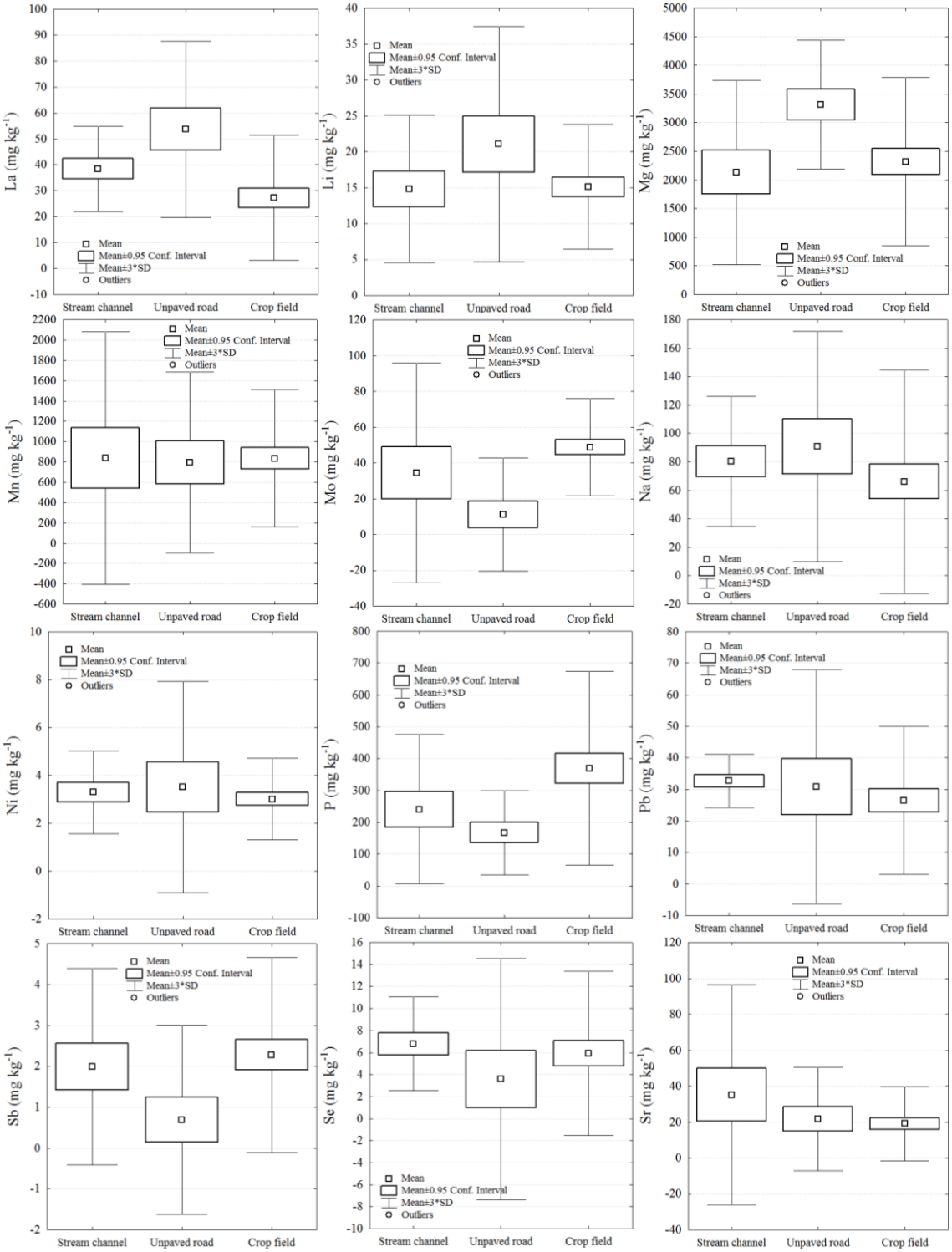

Box-plot of geochemical tracer concentrations in sediment sources of Arvorezinha catchment indicating the mean, the 95% confidence interval, and the non-outliers range (mean concentration plus three standard deviation).

APPENDIX 1 (continuation)

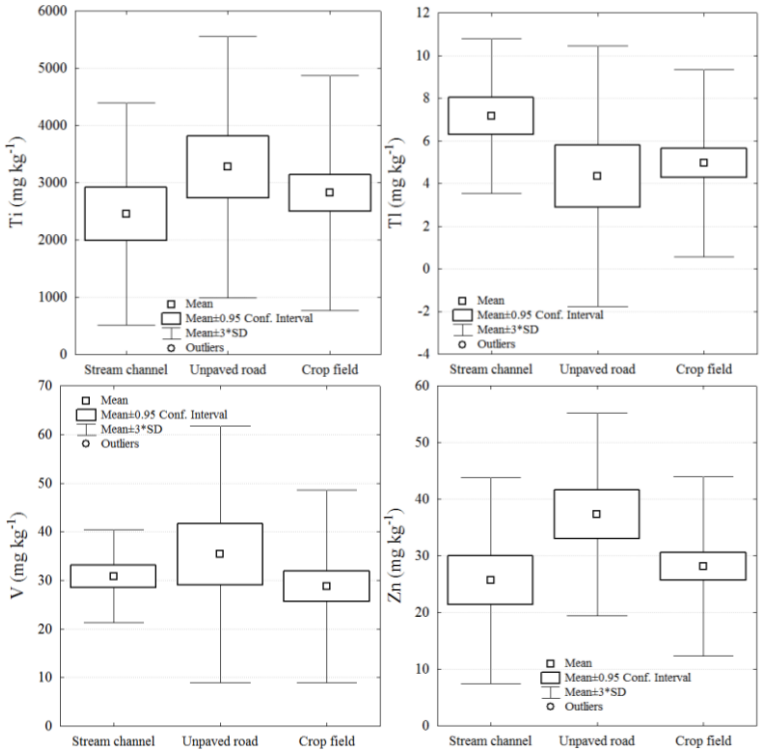

Box-plot of geochemical tracer concentrations in sediment sources of Arvorezinha catchment indicating the mean, the 95% confidence interval, and the non-outliers range (mean concentration plus three standard deviation).

APPENDIX 2

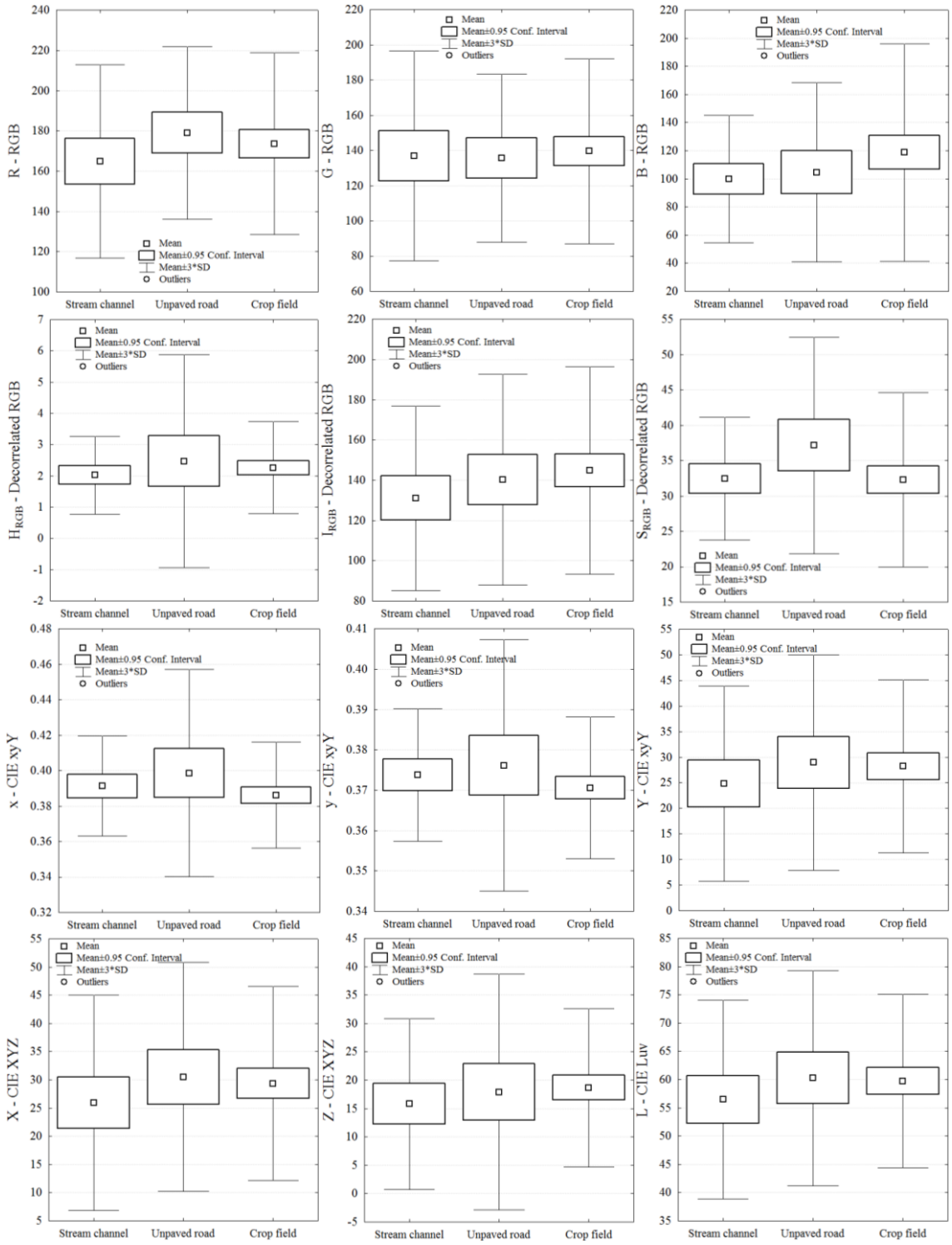

Box-plot of VIS-based-colour parameters values in sediment sources of Arvorezinha catchment indicating the mean, the 95% confidence interval, and the non-outliers range (mean concentration plus three standard deviation).

APPENDIX 2 (continuation)

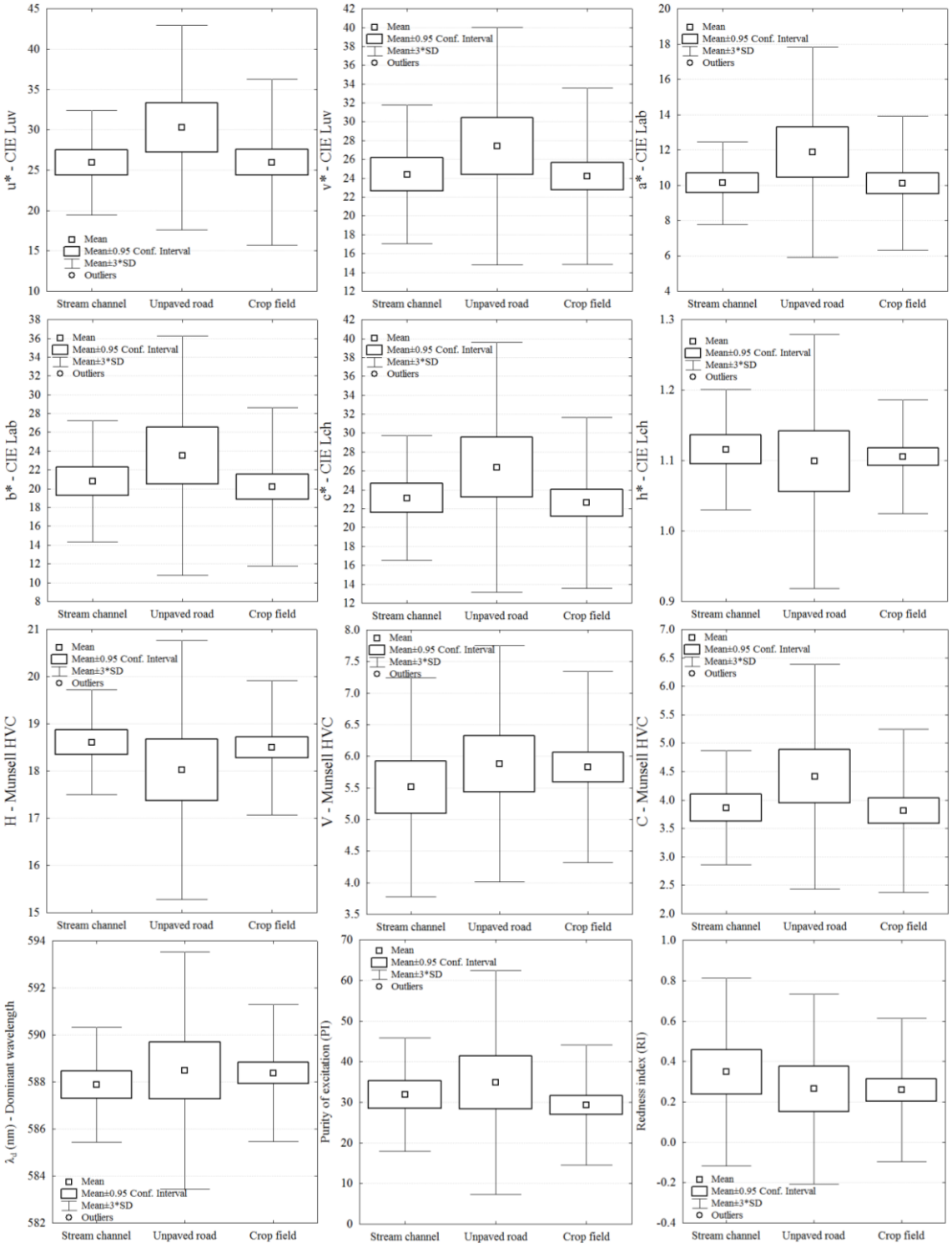

Box-plot of VIS-based-colour parameters values in sediment sources of Arvorezinha catchment indicating the mean, the 95% confidence interval, and the non-outliers range (mean concentration plus three standard deviation).

APPENDIX 3

CONTRIBUIÇÃO DAS FONTES DE SEDIMENTOS EM UMA BACIA HIDROGRÁFICA AGRÍCOLA SOB PLANTIO DIRETO[1]

Tales Tiecher[2], Jean Paolo Gomes Minella[3], Pablo Miguel[4], Jimmy Walter Rasche Alvarez[5], André Pellegrini[2], Viviane Capoane[6], Lucas Henrique Ciotti[7], Gilmar Luiz Schaefer[7] & Danilo Rheinheimer dos Santos[3]

RESUMO

O conhecimento das principais fontes difusas de produção de sedimento pode aumentar a eficiência de utilização dos recursos públicos, investidos em estratégias de gestão em bacias hidrográficas, que visem mitigar a transferência de sedimentos aos cursos d'água. Objetivou-se com este trabalho avaliar as fontes de sedimentos numa bacia hidrográfica rural de cabeceira com predomínio de cultivos anuais sob plantio direto e com intensa e inadequada exploração dos recursos naturais, por meio da quantificação da contribuição relativa das estradas e das lavouras na produção global de sedimentos. A bacia hidrográfica está localizada no município de Júlio de Castilhos, Rio Grande do Sul. O período de estudo foi de maio de 2009 a abril de 2011. Para a identificação das fontes, foi utilizado o método *fingerprinting*, que compara os solos de diferentes fontes e os sedimentos que são encontrados em suspensão no canal de drenagem, usando elementos traçadores. O manejo inadequado do solo nas áreas de lavoura, a falta de planejamento das vias de acesso e a ausência de práticas de controle do escoamento superficial, que sejam compatíveis com a fragilidade condicionada pelos solos e pelo relevo da bacia hidrográfica, têm provocado o surgimento de processos erosivos acelerados com efeitos negativos ao agricultor e à sociedade. As estradas apresentam alta porcentagem de contribuição na transferência de sedimentos, mas a contribuição das áreas de lavoura aumenta em precipitações pluviais de alta magnitude. Isso evidencia que a magnitude dos eventos de chuva

[1] Recebido para publicação em 22 de julho de 2013 e aprovado em 19 de novembro de 2013.

[2] Doutorando em Ciência do Solo, Universidade Federal de Santa Maria - UFSM. Av. Roraima, 1000, Bairro Camobi. CEP 97105-900 Santa Maria (RS). Bolsista CAPES. E-mail: tales.t@mail.ufsm.br, andre.pellegrini@yahoo.com.br

[3] Professor do Departamento de Solos, UFSM. Bolsista do CNPq. E-mail: jminella@gmail.com, daniloesaf@gmail.com

[4] Professor Auxiliar do Departamento de Solos, Faculdade de Agronomia Eliseu Maciel, Universidade Federal de Pelotas. Campus Universitário, s/n. Caixa Postal 354. CEP 96010-900 Pelotas (RS). E-mail: tchemiguel@yahoo.com.br

[5] Doutorando em Ciência do Solo, UFSM. Bolsista CNPq. E-mail: jwrasche@yahoo.com.ar

[6] Doutoranda em Geografia, Universidade Federal do Paraná. Rua XV de Novembro, 1299, Bairro Centro. CEP 80060-000 Curitiba (PR). Bolsista CAPES. E-mail: capoane@gmail.com

[7] Aluno do Curso de Agronomia, UFSM. Bolsista CNPq. E-mail: lucasciotti@hotmail.com, gilmarschaefer2007@yahoo.com.br

APPENDIX 4

Science of the Total Environment 527–528 (2015) 135–149

Contents lists available at ScienceDirect

Science of the Total Environment

journal homepage: www.elsevier.com/locate/scitotenv

Combining visible-based-color parameters and geochemical tracers to improve sediment source discrimination and apportionment

Tales Tiecher [a,b,*], Laurent Caner [b], Jean Paolo Gomes Minella [a], Danilo Rheinheimer dos Santos [a]

[a] Universidade Federal de Santa Maria, Department of Soils, 1000 Roraima Avenue, 97105-900 Santa Maria, RS, Brazil
[b] Université de Poitiers, IC2MP-HydrASA UMR 7285, 7 rue Albert Turpain, B35 TSA 51106, 86073 Poitiers, France

HIGHLIGHTS

- This is the first attempt to combine geochemical tracers and VIS-color parameters.
- Geochemical and VIS-color properties together improved source discrimination.
- Prediction error decreased using both geochemical and color tracers.

GRAPHICAL ABSTRACT

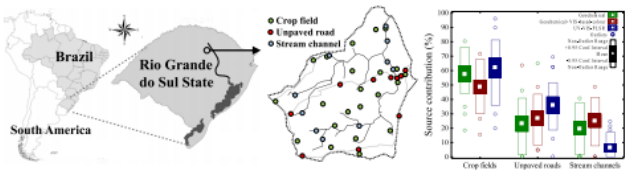

ARTICLE INFO

Article history:
Received 6 February 2015
Received in revised form 27 April 2015
Accepted 27 April 2015
Available online xxxx

Editor: D. Barcelo

Keywords:
Soil erosion
Modeling
Alternative fingerprints
Fingerprinting approach

ABSTRACT

Parameter selection in fingerprinting studies are often time-consuming and costly because successful fingerprint properties are generally highly site-specific. Recently, spectroscopy has been applied to trace sediment origin as a rapid, less expensive, non-destructive and straightforward alternative. We show in this study the first attempt to combine both geochemical tracers and color parameters derived from the visible (VIS) spectrum in a single estimate of sediment source contribution. Moreover, we compared the discrimination power and source apportionment using VIS-based-color parameters and using the whole ultra-violet–visible (UV–VIS) spectrum in partial last square regression (PLSR) models. This study was carried out in a small (1.19 km^2) rural catchment from southern Brazil. The sediment sources evaluated were crop fields, unpaved roads, and stream channels. Color parameters were only able to discriminate unpaved roads from the other sources, disabling its use to fingerprint sediment sources itself. Nonetheless, there was a great improvement in source discrimination combining geochemical tracers and color parameters. Unlike VIS-based-color parameters, the distances between sediment sources were always significantly different using the whole UV–VIS-spectrum. It indicates a loss of information and, consequently, loss of discriminating power when using VIS-based-color parameters instead of the whole UV–VIS spectrum. Overall, there was good agreement in source ascription obtained with geochemical tracers alone, geochemical tracers coupled with color parameters, and UV–VIS-PLSR models, and all of them indicate clearly that the main sediment source was the crop fields, corresponding to 57 ± 14, 48 ± 13, and 62 ± 18%, respectively. Prediction errors for UV–VIS-PLSR models (6.6 ± 1.1%) were very similar to those generated in a mixed linear model using geochemical tracers alone (6.4 ± 3.6%), but the combination of color parameters and geochemical tracers decreases the prediction error (5.4 ± 2.0%). Therefore, the use of VIS-based-color parameters combined to geochemical tracers can be a rapid and inexpensive way to improve source discrimination and precision of sediment source apportionment.

* Corresponding author at: Universidade Federal de Santa Maria, Department of Soils, 1000 Roraima Avenue, 97105-900, Santa Maria, RS, Brazil.
E-mail address: tales.t@hotmail.com.br (T. Tiecher).

http://dx.doi.org/10.1016/j.scitotenv.2015.04.103
0048-9697/

APPENDIX 5

Soil & Tillage Research xxx (2015) xxx–xxx

Contents lists available at ScienceDirect

Soil & Tillage Research

journal homepage: www.elsevier.com/locate/still

Tracing sediment sources in a subtropical rural catchment of southern Brazil by using geochemical tracers and near-infrared spectroscopy

Tales Tiecher [a,b,*], Laurent Caner [b], Jean Paolo Gomes Minella [a], Marcos Antonio Bender [a], Danilo Rheinheimer dos Santos [a]

[a] Universidade Federal de Santa Maria, Department of Soil Science, 1000 Roraima Avenue, 97105-900 Santa Maria, RS, Brazil
[b] Université de Poitiers, UMR 7285 IC2MP-HydrASA, TSA 51106, 5 rue Albert Turpain, 86073 Poitiers Cedex 9, France

ARTICLE INFO

Article history:
Received 6 November 2014
Received in revised form 28 February 2015
Accepted 2 March 2015

Keywords:
Erosion
Modeling
Suspended sediment
Fingerprinting approach

ABSTRACT

Conventional fingerprinting methods based on geochemical composition still require a time-consuming and critical preliminary sample preparation. Thus, fingerprinting characteristics that can be measured in a rapid and cheap way requiring a minimal sample preparation, such as spectroscopy methods, can be a good choice for this purpose. The present study aimed to evaluate the sediment sources contribution in a rural catchment by using conventional method based on geochemical composition and an alternative method based on near-infrared diffuse reflectance (NIR) spectroscopy. This study was carried out in a rural catchment with an area of 1.19 km^2 located in southern Brazil. The sediment sources evaluated were crop fields, unpaved roads and stream channels. Twenty nine suspended sediment samples were collected from nine significant storm runoff events between October 2009 and July 2011. NIR spectra of the sources and the suspended sediment samples were very similar. Nevertheless, the alternative method used to trace suspended sediment based on NIR spectroscopy was sensitive enough to detect differences in mineralogical composition of the sources materials, which were confirmed by X-ray diffraction analyses. Both conventional and alternative methods were able to discriminate the sediment sources and, despite the lack of correlation between the two methods, provided very close source ascription. The differences in the final results obtained by conventional and alternative methods are due to the nature of the variables used in each case, which are not mandatorily correlated. Efforts should be taken to try to combine both geochemical composition and near-infrared spectroscopy information on a single estimative of the sediment sources contribution in order to provide results with an even higher accuracy.

1. Introduction

Soil erosion is a well-known problem that generates both on-site and off-site effects. On-sites problems are related to the decrease of soil fertility and water holding capacity which have direct effects on crops productivity. Off-sites problems are related to the dams, reservoirs and canals siltation, as well as the degradation of aquatic environments caused by the transport of nutrients and pollutants to the water bodies. The connectivity between the origin of soil erosion and its impacts on the watercourses is not straightforward, as it is governed by complex mechanisms resulting from hydrosedimentological behavior of each river catchment (Minella and Merten, 2011). Therefore, a major limitation of most studies of sediment transfer, whether quantitative or qualitative, is the lack of information about the origin of the sediments (Walling et al., 2013). The knowledge of the spatial pattern of the main diffuse sources of pollution, such as sediment, can increase the efficiency of use of resources invested in management strategies aiming to mitigate the transfer of sediment and adsorbed pollutant to the watercourses. Recently there has been a growing interest in studies aiming to understand spatial patterns of suspended sediment sources in order to have a better description of the connection processes between sediment source and sink as well as the planning of natural resources (Walling, 2013).

The contribution of sediment sources can be estimated by direct and indirect methods. The most common methods are indirect, involving either visual observations (e.g., analysis of aerial photos, Day et al., 2013) or measures of erosive activity (e.g., plots of erosion, Anh et al., 2014). Direct methods for estimating the contribution of sediment sources based on the fact that the physical and chemical characteristics of eroded sediments are

* Corresponding author at: Universidade Federal de Santa Maria, Department of Soil Science, 1000 Roraima Avenue, 97105-900 Santa Maria, Brazil.
Tel.: +55 55 32208108; fax: +55 55 32208256.
E-mail address: tales.t@hotmail.com (T. Tiecher).

http://dx.doi.org/10.1016/j.still.2015.03.001
0167-1987/

VITAE

Tales Tiecher, filho de Ernani Luiz Pavlak Tiecher e Singlair Terezinha Dal Sotto Tiecher, nasceu dia 13 de fevereiro de 1987, em Independência, Rio Grande do Sul (RS). Estudou na Escola Estadual de Educação Básica Amélio Fagundes de Independência – RS dos 5 aos 17 anos de idade (1992 a 2004), desde o jardim de infância até a conclusão do ensino médio. Durante o ensino médio cursou concomitantemente o curso Técnico em Agropecuária na Sociedade Educacional Três de Maio de 2003 a 2004.

Em março de 2005 ingressou no Curso de Agronomia da Universidade Federal de Santa Maria (UFSM). Trabalhou como estagiário voluntário no Laboratório de Química e Fertilidade dos Solos a partir de julho do mesmo ano. Foi bolsista do Programa Institucional de Bolsas de Iniciação Científica (PIBIC) sob orientação do professor Danilo Rheinheimer dos Santos de agosto de 2006 até a conclusão do curso de Agronomia, em julho de 2009.

Realizou o curso de Mestrado em Ciência do Solo (agosto 2009 a fevereiro 2011) no Programa de Pós-Graduação em Ciência do Solo (PPGCS) da UFSM sob orientação do professor Danilo Rheinheimer dos Santos (título da dissertação: *Dinâmica do fósforo em um solo muito argiloso sob diferentes preparos de solo e culturas de inverno*).

Em março de 2011 começou o Doutorado no Programa de Pós-Graduação em Ciência do Solo da UFSM, também sob orientação do professor Danilo Rheinheimer dos Santos, onde obteve em março de 2015 o grau de Doutor em Ciência do Solo. Na UFSM fez o doutorado presencialmente em dois anos e meio de um total de quatro exigidos pela universidade (março 2011 a março 2013, e de setembro de 2014 a fevereiro de 2015).

A partir do segundo semestre de 2012 começou também o Doutorado na *Université de Poitiers*, França, sob orientação do professor Laurent Caner onde obteve o grau de Doutor em "*Sciences de la Terre et de l'Univers, Espace, Secteur de Recherche Terre Solide et Enveloppes Superficielles*" com maior grau de distinção (menção "*très honorable*"). Na Université de Poitiers, França, cursou um ano e meio presencialmente (de abril de 2013 a agosto de 2014), de um total de três anos exigidos pela universidade.

Desde outubro de 2014 é professor do curso superior de Tecnologia em Agropecuária da Universidade Regional Integrada do Alto Uruguai e das Missões (URI), Câmpus de Frederico Westphalen e responsável técnico do Laboratório de Análise de Solos e Tecido Vegetal da URI-FW.